Cytokinin Metabolite Distribution at Tissue- and Cell-Specific Levels

Ioanna Antoniadi

Imperial College London
Department of Life Sciences,

A thesis submitted for the degree of Doctor of Philosophy and the Diploma of Imperial College London

To my Dad

'Στους γονείς μου οφείλω το ζην και στον δάσκαλο μου το ευ ζην'

Μέγας Αλέξανδρος για τον Αριστοτέλη

'To my parents I owe my being and to my teacher, my well-being.'

Alexander the Great for Aristotelis

ABSTRACT

Cytokinins are pivotal plant hormones regulating the cell cycle and many components of development. They also transduce environmental signals such as nutrient deficiency and drought. The significance of cytokinin genes in agriculture has been highlighted by several reports, which associate them with improved crop performance. The aim of this study is to gain a better understanding of cytokinin metabolite distribution, in order to shed light on cytokinin transport, biochemistry and its function.

Cytokinin metabolite levels were shown to vary amongst pea tissues and vascular saps, and across developmental stages. Detection was pushed to new limits by performing cytokinin measurements in distinct cell populations. For the first time, heterogeneous distribution was demonstrated within the *Arabidopsis* root apex and between the intra- and extra-cellular compartments.

A cytokinin gradient was revealed within the *Arabidopsis* root tip with maximal concentration in the columella, root cap, initials and QC cells. Cell-specific analysis of the *TCSn:GFP* cytokinin signaling reporter line indicated tZ as the only bioactive cytokinin related to intra-cellular cytokinin signaling. This result, coupled with identification of active cytokinins in the apoplast, indicates a significant role for cytokinin receptors at the plasma membrane. Cytokinin glucosides were largely intra-cellular, with their prevalence in cytokinin responsive cells indicating a role in cytokinin signaling. The riboside cZR was identified as a major transported cytokinin form while tZ-cytokinins were predominantly shoot compounds. The lateral root zone was also identified as a candidate site for cytokinin loading into the xylem.

Comprehensive analysis of cytokinin's distribution was also examined, particularly in response to strigolactone effects, another plant hormone which regulates branching. Strigolactone inhibited cytokinin degradative enzymes in root apices, thus acting as a local positive regulator of cytokinins. Furthermore, an *RMS2*-dependent mechanism regulating cytokinin homeostasis in the shoots was identified. In conclusion, this research provides new insights into the importance of cytokinin spatial distribution for understanding its roles in cell and developmental biology.

ACKNOWLEDGMENTS

This is the only part of my PhD Thesis that I wish I could have written in Greek, my mother language, because what is written below truly comes from my heart.

I owe my deepest gratitude to my supervisor **Dr Colin Turnbull**. Without his continuous advice, guidance and endless support this work would have been difficult to complete. Dr Colin Turnbull was next to me every step of the way throughout the experiments and the writing. Although he was busy as the Principal Investigator, leading the research of our laboratory, he was available whenever I needed his help either – whether that was in his office or via email from the other side of this planet! He would always find the time to discuss the ongoing experiments or to comment on my writing for travel grant applications or reports – for this, I am forever indebted. His enthusiasm and respect for good research was highly inspiring and will always stay with me. Through him, I've been introduced to a world of positive collaborations - this is something invaluable in our field. Dr Turnbull taught me that good research is not only that which leads to a publishable article in a high impact factor journal, but also that which cannot be immediately explained.

I would also like to deeply thank my supervisor for the opportunity he gave me to travel and collaborate with other laboratories. By showing me the way to apply for travel grants, he has helped me to secure the next step in my career and it is thanks to him that I had the confidence and experience to apply and obtain a Post-doc Fellowship before the end of my PhD. I was fortunate to have total freedom in my research, with a supervisor who let me make my own mistakes and learn from them, without ever feeling as if I had failed. His optimism and support during these years made this PhD a pleasure even during the highly stressed periods. Above everything, Dr Turnbull taught me that failure should also be embraced, that controversial results can still be exciting, that collaborators are friends and that research is not more important than family. For all these reasons and many more I will never be able to thank him enough. I can only hope to make him proud throughout my next carrier steps.

I would also like to thank Prof. **Karin Ljung** for giving me the opportunity to collaborate with her and the Umea Plant Science Center (UPSC) laboratory. This was an invaluable experience for me, not only because I learnt new techniques and had access to incredible equipment and facilities, but also because I truly became part of her lab, even for the periods when I

was back in London. I'm thankful for her advice, guidance and support throughout this period. I would also like to acknowledge Dr **Ondřej Novák** for these excellent collaborations with UPSC. His help and advice was crucial to the completion of projects, which were a big part of my PhD thesis. I am grateful for the indispensable technical assistance of **Roger Granbom**. Without him the endless sowings for all the sorting experiments would have been unbearable! Also I would like to acknowledge Dr **Aleš Pencík** for his assistance with LC-MS handling and help in the lab. I am also thankful to all the people that made these collaborative projects possible and successful: **Lenka Plačková,** Dr **Biljana Simonovik** and Dr **Karel Doležal.**

Special thanks also to our collaborator Dr **Vaclav Motyka** from IEB, Prague, Czech Republic who conducted the CKX enzymatic experiments and was always helpful in discussions for future experiments.

I would like to extend my gratitude to colleagues in the laboratory of Imperial College; Dr **Mark Bennett** who trusted me to handle the LC-MS and supported me throughout my learning process. To Dr **Rosa Lopez-Cobollo,** for being our lab manager and taking care of so many things which made my life in the lab much easier, giving me more time to spend of my research and, above all, for her friendship. Thanks to my examiner Dr **Thostern Hamman** during most of my post-graduate years, particularly for his useful advice and our discussions. Dr **Sadia Kashif** for our friendship and help in the lab, I am very grateful. And to Dr **Joseph McKenna,** Dr **Edward Langton and** Dr **David Charles** for our scientific and general discussions – thank you too. To students **Victor Jones, Kenny Yeung, Nicolas Kral, William Pelton, and Nicolas Ortiz Vaquerizas** for all their help in the lab over the past few years. Finally, special thanks to **Martin Selby** and **Katie Murray** for taking care of my big pea cultures for seed amplifications (without them I wouldn't have material to work on!).

This thesis would not have been possible without the endless support of my family in Greece. Aside from providing me with the opportunity to pursue my postgraduate studies, the encouragement from my parents and sisters throughout these years have been invaluable. They were, and always are, next to me – whether we're in the same house or in different countries. Words cannot express the value of their support, particularly during the tougher time of this research while I was away from my country. I would like to especially thank them for the last 6 months when I moved back home to write my thesis. I would like to individually thank my father, **Giannis Antoniadis**, to whom I have dedicated this work, for always being there to help - making macros for my time-consuming calculations, giving a

digital substance to my complicated, hand-drawn hormone pathways (which I often thought impossible), but most of all for spending sleepless nights just to keep me company whilst I was battling with deadlines. And, of course, for taking care of my young son during the weekends, every morning before going to work and every night before putting him to bed so I could focus on my work these last 6 months! I am also grateful to my mother, **Aristea Manousaki**, who managed to make my thesis writing period as comfortable as possible. She took care of EVERYTHING that could possibly have distracted me from writing during these 6 months, including her grandson, and she made the environment that I was living in beautiful with her love and care. She also typed parts of the thesis that I had written in paper when my eyes got tired of the computer screen. I would like to deeply thank my sister, **Mariana Antoniadi**, for spending what should have been the most carefree summer by taking care of her nephew, so I could focus on my writing, and even bringing me little snacks to keep me going. Finally, I would also like to thank my sister **Chrysanthi Antoniadi** for her solace and support and for entertaining her nephew several afternoons so I could work. Words cannot express the depth of my gratitude. If it wasn't for them I could never have achieved my goals – both in my career and in life. 'Σας αγαπάω πολύ'.

I would also like to thank my new family; **Philip Vain** and **Thomas Vain**. To my 10 month-old amazing little boy, Philip, who kept me company during my last experiments by giving me some motivating kicks to remind me that I have to finish lab work before he arrives in the world. More than anyone, he made my PhD writing time efficient and productive so that I could finish quickly and spend time with him. He also gave me great training in sleepless nights so that when it was needed for the thesis-writing, it was 'a piece of cake' for me. This little 'γκρινιαρης' brought light to the tough times of writing just with his little beautiful smile. I would like to thank 'τον αγαπημενο μου', Thomas, for his help during my thesis completion. His love and enthusiasm for research was highly inspiring and our scientific discussions during the latest stages of my experiments and also during my writing time were indispensable. His advice, guidance and help in confocal microscopy and statistics were also highly important. Finally, I am grateful for his support and understanding during the completion of my thesis and for being part of our beautiful little family.

I owe my deepest gratitude to my family in London; My uncle **Dimitris Antoniadis** who, apart from motivating and advising me with my PhD studies, was always present to help me with several house-movings and anything I needed while I was living in London. To my aunt **Mary Antoniadis** for having me as a guest in her house for periods of times during my

studies, but never making me feel like a guest but as a real part of the family. To my little cousin **Cathryn Antoniadis** for allowing me to use her room as my own whilst I stayed at their place. My 'cousinoula', **Joanna Antoniadis**, who has made available her support in a number of ways. She was always there when I needed assistance with my English writing, even if this meant that she would spend a sleepless night. She was supporting me by working during the evenings through skype when we both had to submit a project. She came to visit me during my first 3 months scientific trip when I was initially feeling lonely. She even tried to help me in the lab ('πολυ αποτυχημένα') some late evenings when I had to cancel our plans for a drink. Several late evenings she came with food at Imperial so I could have dinner and be able to continue with my experiments. I could keep going with this, but I will stop by saying a big thank you to Joanna and to all my family in London, including my amazing cousin 'Μπελίτσα' too, who supported me in various ways during my PhD studies in London and most importantly made sure I never felt alone even though away from my country.

I would like to thank my friends in London **Dr Panagiotis Vorkas, Dr Alexandros Pechlivanis, Dr Konstantina Spaggou, Dr Paul Benton, Elisa Hutinga and Filotheos Bezerianos** not only for making these years of my life more beautiful but also for their help and advice in discussions concerning LC-MS, PCAs, heatmaps and modeling. Also I would like to thank our big '**London-muppet-house-family**' for making these years so special.

Big thanks also to my friends-for-life from Greece, **Maria, Giorgos G., Giorgos M.** and **Niki** who were always supportive and present when I needed them no matter the distance.

Finally, I would like to acknowledge **Development-The Company of Biologists**, **Erasmus** fellowship and **EMBO** for financially supporting my collaborative visits to UPSC. Without their support, this PhD and my experience and expertise in the field would not have been the same.

STATEMENT OF ORIGINALITY

I hereby declare that this thesis is my own work except for some collaborative research data explicitly indicated in specific Figures. To the best of my knowledge, none of the work presented in this thesis has been previously submitted for a qualification either at Imperial College London or at any other institution. It contains no previously published materials. However, some parts of the work were presented in a poster at the 2nd Cytokinin meeting (July 2012) in Berlin, Germany and in a talk at the 'Auxins and Cytokinins in Plant Development' International Symposium (June-July 2014) in Prague, Czech Republic.

COPYRIGHT DECLARATION

Table of Contents

LIST OF TABLES

LIST OF FIGURES

ABBREVIATION LIST

cZ cis-Zeatin

cZ7G cis-Zeatin-7-glucoside

cZ9G cis-Zeatin-9-glucoside

cZOG cis-Zeatin-O-glucoside

cZR cis-Zeatin riboside

cZROG cis-Zeatin-O-glucoside riboside

cZR(M)P cis-Zeatin riboside monophosphate

D(H)Z Dihydrozeatin

D(H)Z7G Dihydrozeatin-7-glucoside

D(H)Z9G Dihydrozeatin-9-glucoside

D(H)ZOG Dihydrozeatin-O-glucoside

D(H)ZR Dihydrozeatin riboside

D(H)ZROG Dihydrozeatin-O-glucoside riboside

D(H)ZR(M)P Dihydrozeatin riboside monophosphate

iP N6-Isopentenyladenine

iP7G N6-Isopentenyladenine-7-glucoside

iP9G N6-Isopentenyladenine-9-glucoside

iPR N6-Isopentenyladenosine

iPR(M)P N6-Isopentenyladenosine monophosphate

iPRDP N6-isopentenyladenosine-50-diphosphate

iPRTP: N6-isopentenyladenosine-50-triphosphate

tZ trans-Zeatin

tZ7G trans-Zeatin-9-glucoside

tZ9G trans-Zeatin-9-glucoside

tZOG trans-Zeatin-O-glucoside

tZR trans-Zeatin riboside

tZR(M)P trans-Zeatin riboside monophosphate

tZRDP trans-Zeatin riboside diphosphate

tZRTP: trans-Zeatin riboside triphosphate

tZROG trans-Zeatin-O-glucoside riboside

ADP, AMP, ATP adenosine 5 ′ phosphates

DMAPP dimethylallyl diphosphate

MEV Methylerythritol phosphate

HMBDP hydroxymethyl- butenyl diphosphate

FAD flavin adenine dinucleotide

UPLC Ultra Performance Liquid Chromatography

HPLC High Performance Liquid Chromatography

LC-MS Liquid Chromatography Mass Spectrometry

MRM multiple reaction monitoring

SPE Solid Phase Extraction

FACS Fluorescence Activated Cell Sorting

LSCM Laser Scanning Confocal Microscopy

MS Murashige and Skoog medium

ANOVA Analysis of variance

FRET Fluorescence Resonance Energy Transfer

DII-VENUS Aux/IAA-based auxin signalling sensor

TILLING Targeting Induced Local Lesions in Genomes

MW Molecular Weight

BAP N6-Benzyladenine

CKX Cytokinin oxidase/dehydrogenase

INCYDE 2-Chloro-6-(3-methoxyphenyl)aminopurine

IAA indole-3-acetic acid

GR24 synthetic strigolactone

Roscovitine 6-benzylamino-2-[1(R)-(hydroxymethyl)pro-pyl]amino-9-isopropylpurine

5DS 5-deoxystrigol

ent-2’-epi-5DS ent-2’-epi-5-deoxystrigol

ABA abscisic acid

EDTA Ethylenediaminetetraacetic acid

DPIP 2,6-dichlorophenol indophenol

MES 2-(N-morpholino)ethanesulfonic acid

BSA Benzenesulfonic acid

DMSO Dimethyl sulfoxide

HCOOH Formic Acid

HNO_3 Nitric Acid

NH_4OH Ammonium hydroxide

NaN_3 Sodium Azide

OxIAA 2-Oxindole-3-Acetic Acid

IPT adenosine phosphate-isopentenyltransferases

CYP735A cytochrome P450 mono-oxygenase

LOG cytokinin-phosphoribohydrolase 'Lonely guy'

CKX cytokinin dehydrogenase

UGT76C, UGT85A Glucosyl-transferase

AHK *Arabidopsis* Histidine Kinases

AHP *Arabidopsis* Histidine Phosphotransfer

CRF Cytokinin Response Factors

ARR *Arabidopsis* Response Regulators

CRE1 Cytokinin Response 1

WOL Wooden Leg

PUP Purine Permease

ENT equilibrative nucleoside transporter

ABCG14 ATP-Binding Cassette (ABC) transporter subfamily G14

RMS/rms RAMOSUS

MAX/max MORE AXILLARY GROWTH

DAD/dad DECREASED APICAL DOMINANCE

D/d DWARF

BRC/brc BRANCHED

TB/tb TEOSINTE BRANCHED

FC/fc FINE CULM

CCD Carotenoid Cleavage Dioxygenase

CYP711A1 class III cytochrome P450 monooxygenase

PDR/pdr PLEIOTROPIC DRUG RESISTANCE

HTD/htd HIGH TILLERING DWARF

SMAX/smax SUPRESSOR OF MAX

SMXL/smxl SMAX-LIKE

KAI/kai KARRIKIN INSENSITIVE

TCSn Two-Component System (new)

AUX1/LAX Auxin influx permease/like AUX1

PIN Pin-formed Polar Auxin Transporter

SCR/scr SCARECROW

GUS β-glucuronidase

GFP Green Fluorescent Protein

CHASE Cyclases/Histidine kinases Associated Sensory Extracellular

HSP Heat Shock Protein

UPS Ubiquitine-Proteasome System

LRR Leucine-rich repeat

SCF Skp/Culin/F-box

PM plasma membrane

ER endoplasmic reticulum

FW tissue Fresh Weight

LR Lateral Root

N&I Node & Internode

QC Quiescent Center

At *Arabidopsis thaliana*

Ps *Pisum sativum*

Ph *Petunia hybrida*

Os *Oryza sativa*

Zm *Zea mays*

cv cultivar

Chapter 1

Introduction

1.1. Importance of the plant hormone cytokinin

Cytokinin's already known functions suggest that it is one of the most crucial hormones for the development and homeostasis of all land plants. They have been shown to regulate crucial developmental processes as described in Table 1.

Cytokinin Function	Reference
cell division and differentiation	Mok & Mok 2001
pathogen resistance	
shoot branching	
chloroplast formation and differentiation	
root proliferation	Werner et al. 2001
apical dominance and axillary meristem initiation	McSteen 2009 Ongaro & Leyser 2008 Tanaka et al. 2006
maintenance of meristem function	Werner et al. 2003 Higuchi et al. 2004 Leibfried et al. 2005 Kurakawa et al. 2007
phyllotaxis	Giulini et al. 2004
seed dormancy and germination	reviewed in Mok 1994
stimulation of leaf expansion	
shoot growth	Kiba et al. 2013
nutrient starvation	Martín et al. 2000 Sakakibara et al. 1999
recovery response	
anthocyanin production	Deikman & Ulrich 1995
reproductive competence	Ashikari et al. 2005
plant transpiration and stomatal opening	Dodd & Beveridge 2006
leaf senescence	Gan & Amasino 1995 Kim et al. 2006
plant response to environmental stress signals	Argueso et al. 2009 Aloni et al. 2005 Sakakibara 2006 Werner et al. 2006 Mayzlish Gati et al. 2012 Yang et al. 2012 Nishiyama et al. 2012
directly linked with increasing crop yield	Ashikari et al. 2005 Zalewski et al. 2010 Ghanem et al. 2011 Rahayu et al. 2005 Rivero et al. 2010 Huynh et al. 2005

Table 1 *Cytokinin roles in plant development.*

Most of the above mentioned processes are vital for all plants, therefore it can be predicted that the activity and/or amount of cytokinins is finely tuned. However, little is known about the regulation of this tuning which is controlled by internal and external factors such as other phytohormones and inorganic nitrogen sources (reviewed in Ha *et al.,* 2012; El Showk *et al.,* 2013 and Sakakibara *et al.,* 2005).

1.2. Cytokinin compounds and their chemistry

Naturally occurring cytokinins (CKs) are N6-substituted adenines carrying either an isoprene-derived side chain (family of isoprenoid cytokinins) or an aromatic one (family of aromatic cytokinins). Zeatin (cis- and trans- zeatin, cZ and tZ respectively) is formed with the hydroxylation of the side chain of N6-(Δ2-isopentenyl)-adenine (IP) while reduction of its isoprene double bond yields dihydrozeatin (DHZ). Initially, these free base (nucleobase) cytokinin forms were considered to be the bioactive cytokinins (Spiess 1975; Schmitz & Skoog 1972; Sakakibara 2006). The chemical structures of the nucleobases and the representative aromatic cytokinin 6-benzyladenine, BAP, are shown in Figure 1. In addition to the nucleobases, cytokinins are also present as ribosides (when a ribose sugar is attached to the N9 position of the purine ring) and nucleotides (when the ribose moiety bears a phosphoryl group). Finally cytokinins can be also found in conjugated forms when a sugar (most commonly glucose or in some cases xylose) is substituted at the N7 or N9 position of the purine ring (7N-, 9N-glucosides) or at the hydroxylated side chain (O-glucosides and O-xylosides) (Sakakibara 2006; Dobrev & Kamínek 2002). The chemical structures of all the isoprenoid cytokinins are summarized in Figure 2 along with the description of cytokinin biosynthetic pathway.

The structural variations of the adenine moiety, the side chain (presence or absence of a hydroxyl group at the end of the prenyl chain) and the stereoisomeric position distinguish each cytokinin molecule. The physiological significance of this remains under study. However this discrimination between the structure of the cytokinin metabolites has been shown to confer differences in their stability and activity in vivo and in vitro (susceptibility to cytokinin oxidases; Kollmer *et al.,* 2014; Galuska *et al.,* 2007; Gadjosova *et al.,* 2011), and in biological activity estimated by measuring affinity to the corresponding receptors and in bioassays (Yamada *et al.,* 2001; Spíchal *et al.,* 2004; Mok *et al.,* 2005; Yonekura-Sakakibara *et al.,*

2004). Cytokinin receptors displayed different affinities with tZ, IP and cZ while cytokinin ribosides were also shown to activate the receptors and to induce cytokinin-related responses in bioassays indicating that they have hormonal activity (Romanov *et al.,* 2006; Schwartzenberg *et al.,* 2007; Spíchal *et al.,* 2004; Yonekura-Sakakibara *et al.,* 2004).

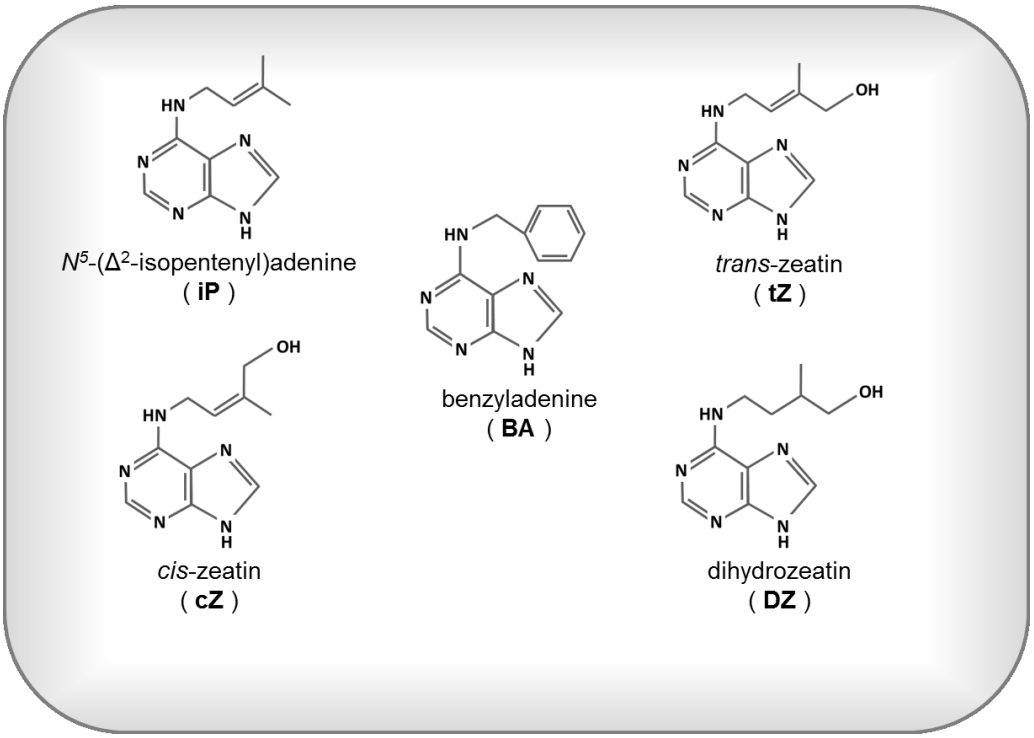

Figure 1 *Structures of representative bioactive cytokinin forms occurring naturally.*

1.3. Cytokinin biosynthesis and homeostasis.

A scheme of the cytokinin biosynthesis and signaling pathway was proposed only lately when the genes involved were cloned and characterized.

1.3.1. Cytokinin precursors

Cytokinin nucleotides, being the firstly biosynthesized cytokinin forms, derive from three independent pathways:

- The main biosynthesis pathway is adenine derived. Adenosine phosphate isopentenyltransferases (IPTs) from higher plants catalyse the reaction of N-prenylation at the N6-terminus of adenosine 5′ phosphates (ADP or ATP) using them as prenyl acceptors and dimethylallyl diphosphate (DMAPP) as prenyl donor producing IPRP (isopentenyl adenine nucleotide, collective term for IPRMP, IPRDP and IPRTP) which is the first cytokinin compound synthesized (Kakimoto 2001; reviewed in Hwang & Sakakibara 2006). DMAPP is a metabolite produced from the Methylerythritol phosphate (MEV) pathway occurring in the cytosol of eukaryotes (Rohmer *et al.,* 1999).

- An IPRP independent pathway is also suggested for de novo biosynthesis of trans-zeatin nucleotide, tZRP (collective term for tZRMP, tZRDP and tZRTP). In Agrobacterium, the production of tZRP was suggested to occur from a hydroxylated side chain transferred from hydroxymethyl- butenyl diphosphate (HMBDP – a metabolite of the MEP pathway occurring in bacteria and plastids (Hecht *et al.,* 2001) to adenosine 5-monophosphates (AMP) (Krall *et al.,* 2002), but this remains to be shown also in plants (Kakimoto *et al.,* 2003). However, inhibition of CYP735A (enzyme responsible for the conversion of IPRP to tZRP in the IPRP dependent pathway) with metyrapone, an inhibitor of cytochrome P450 enzymes, indicated the existence of the IPRMP independent pathway in plants (Åstot *et al.,* 2000). In the same study it was also shown that this pathway requires a metabolite deriving from the MEP pathway, as proposed for bacteria (Åstot *et al.,* 2000). While in vivo labelling experiments confirmed these findings (Åstot *et al.,* 2000; Nordström *et al.,*

2004), aspects of the IPRP independent pathway and its biological significance are poorly understood.

- Finally, the tRNA pathway has been proposed, since a prenylated adenosine adjacent to tRNAs with anticodons complementary to codons beginning with uridine, is released as a cytokinin after the degradation of the tRNA (Skoog *et al.,* 2014; Vreman *et al.,* 1978). In *Arabidopsis*, *IPT2* and *IPT9* were identified to catalyze the tRNA prenylation (Golovko *et al.,* 2002; Kakimoto 2001; Takei *et al.,* 2001.b). The tRNA pathway was confirmed as a source of cZ-type cytokinins when in the *Arabidopsis* double knock out mutant *ipt2ipt9*, no cZ was detected while tZ and IP were found at wild type levels (Miyawaki *et al.,* 2006).

1.3.2. Cytokinin biosynthesis and metabolism

The key genes for cytokinin biosynthesis and metabolism (Figure 2, reviewed by Dobrev and Kamínek 2002, Sakakibara 2006; Hwang and Sakakibara 2006 and Spíchal 2012) are listed below.

- The cytokinin biosynthetic enzyme adenosine-phosphate-isopentenyl transferase (7 *IPT* genes in *Arabidopsis*; (Kakimoto 2001; Takei *et al.,* 2001.b; Sakamoto *et al.,* 2006) catalyses the biosynthesis of IPRP which is the first compound in the biosynthesis pathway. Based on the amino acid sequences of *Arabidopsis IPTs*, 2 genes have been also identified in Pea (*Pisum sativum*, Tanaka *et al.,* 2006) and 8 genes in rice (Sakamoto *et al.,* 2006).

- The tRNA-isopentenyl transferase (2 *tRNA-IPT* genes in *Arabidopsis*; Sakamoto *et al.,* 2006; Miyawaki *et al.,* 2004; 2006) forms cZ ribotides (cZRP). The tRNAs that recognize codons starting with UNN can undertake prenylation at the adenine residue adjacent to the 3'-end of the anticodon by *tRNA-IPT* enzymes (Taller 1994). Then the prenylated tRNA having a cis-hydroxyl group can be further degraded forming cZRP. The rice genome contains also 2 *tRNA-IPT* genes (Sakamoto *et al.,* 2006) while in Physcomitrella all the 7 *IPTs* showed high homology with *Arabidopsis*, were identified as *tRNA-IPTs* (Yevdakova & von Schwartzenberg 2007). Even with only 3 of them being characterized and confirmed to function as *tRNA-IPTs* (Yevdakova & von Schwartzenberg 2007), the functional and evolutionary importance of the tRNA-dependent cytokinin biosynthesis

pathway in moss is indicated (Frébort *et al.,* 2011; Lindner *et al.,* 2014).

- The cytochrome P450 monooxygenase cytokinin trans-hydroxylase catalyzes the hydroxylation of iP-ribotides (IPRP) at the prenyl side chain producing the tZ-ribotides and therefore it can initiate the formation of all the zeatin cytokinin forms (2 *CYP735A* genes in *Arabidopsis*; Takei *et al.,* 2004.a). CYP735As recognize only IPRP as substrate therefore this reaction cannot occur for IP-ribosides or IP. Finally, the hydroxylation catalyzed by these enzymes is stereo specific thus cZRP is also not a substrate for the reaction (Takei *et al.,* 2004.a). The physiological function of cytokinins has been recently shown to be modified by this trans-hydroxylation step since when both *AtCYP735As* were knocked out, a striking impediment of the shoot growth was observed (Kiba *et al.,* 2013).

- The cytokinin riboside 5'-monophosphate phosphoribohydrolase, LONELY GUY (9 *LOG* genes in *Arabidopsis*; Kuroha *et al.,* 2009) directly converts all cytokinin ribotides into their respective free-base active form in a single-step reaction (Kurakawa *et al.,* 2007). The name LOG, abbreviation for Lonely Guy, derives from its respective mutant phenotype in which the shoot apical meristem is deficient and the flowers often have only one 'lonely' stamen (Kurakawa *et al.,* 2007). The phosphoribohydrolase activity of this enzyme releases a ribose 5'-moonophosphate moiety from cytokinin nucleotides IPRP, tZRP, DZRP and cZRP (monophosphates). The respective di- or triphosphate nucleotide forms, the cytokinin ribosides and the nucleobases were not appropriate substrates for the reaction (Kurakawa *et al.,* 2007). *LOG* genes have been identified initially in rice and they are 6 (Kurakawa *et al.,* 2007). However the active cytokinin forms can be also produced without the catalytic activity of the *LOG* enzymes through two gradual steps through a 5'-ribonucleotide phosphohydrolase and an adenosine nucleosidase, respectively (reviewed by Sakakibara 2006). The genes responsible for these two reactions have not been identified yet and therefore the difference between the two pathways of cytokinin activation in terms of biological significance has not been elucidated. However the cytokinin activation step through *LOG* genes has already been shown to be crucial for normal growth and development in *Arabidopsis* (Kuroha *et al.,* 2009).

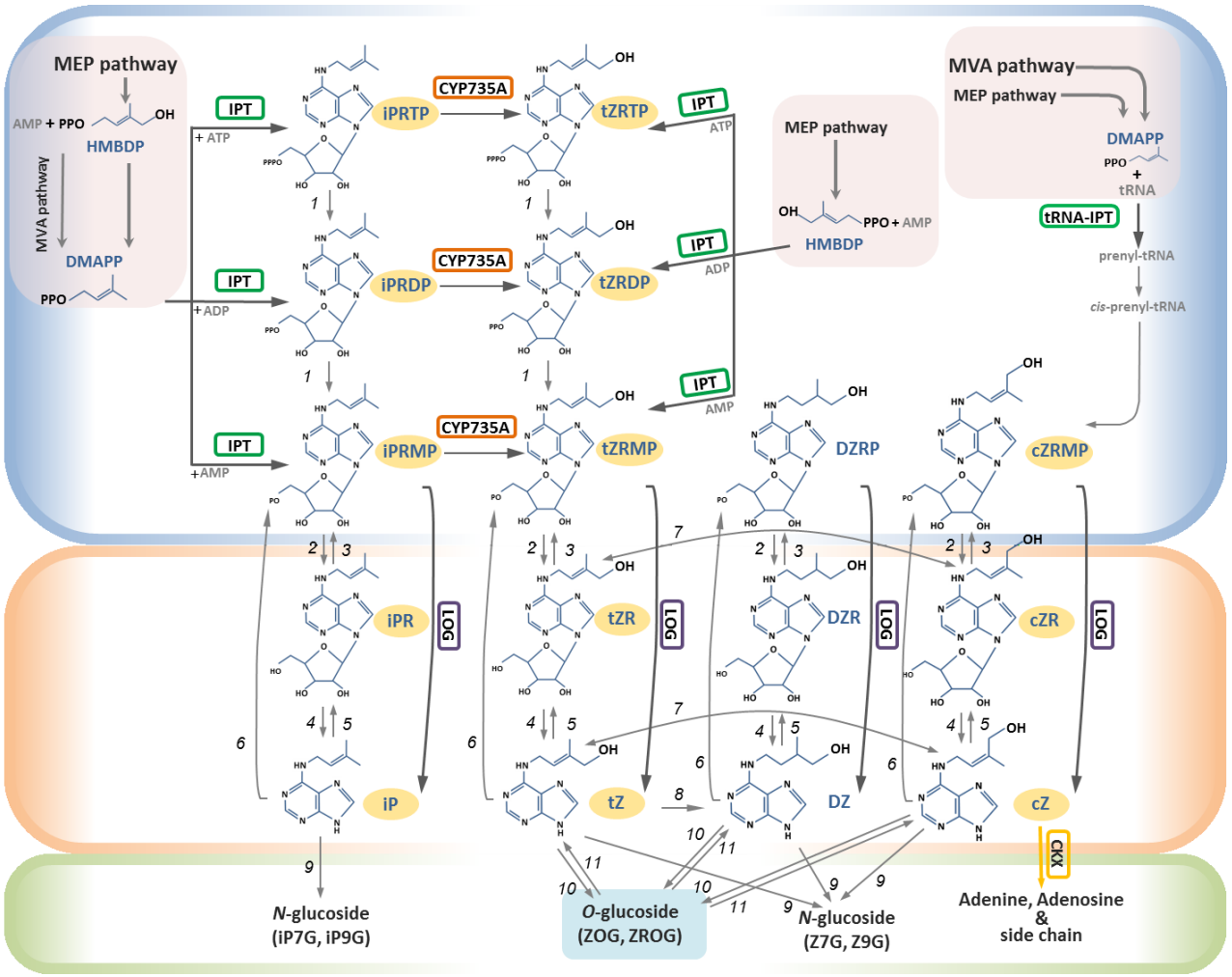

Figure 2 *Scheme of cytokinin biosynthesis, metabolism, conjugation and degradation in plants. The shaded-boxes indicate; blue: cytokinin biosynthesis, orange: bioactive cytokinins (apart from cZR) and green: cytokinin deactivation through either irreversible N-glucosylation or irrevocable CKX degradation. The fully-coloured boxes represent; purple: cytokinin precursors and blue: cytokinin reversible deactivation through O-glucosides. Key enzymes in cytokinin pathway are named and surrounded by boxes with coloured perimeter; green: adenosine phosphate-isopentenyltransferases (IPT genes) utilizing ATP, ADP or AMP as isoprenoid acceptors and forming IPRTP, IPRDP, IPRMP, tZRTP, tZRDP and tZRMP, respectively, also tRNA-specific isopentenyltransferase forming cZRMP, orange: CYP735A genes, cytochrome P450 mono-oxigenase, catalysing the conversion from IP-nucleotides to tZ-nucleotide forms, purple: cytokinin-phosphoribohydrolase 'Lonely guy' (LOG genes) transforming cytokinin nucleotides to nucleobases and yellow: cytokinin dehydrogenase (CKX) irreversibly degrading all compounds indicated by a fully coloured yellow circle into adenine and their respective side-chains. (1) phosphatase,(2)ribonucleotidephosphohydrolase, (3) adenosine kinase, (4) adenosine nucleosidase, (5) purine nucleoside phosphorylase, (6) adenine phosphoribosyltransferase, (7) zeatin isomerase, (8) zeatin reductase, (9) N-glucosyltransferase, (10) zeatin-O-glucosyltransferase, (11) b-glucosidase. All precursors and cytokinin compounds full names as indicated in the texts or in the Abbreviation list.*

1.3.3. Cytokinin homeostasis

Some of the key genes responsible cytokinin homeostasis (Figure 2, reviewed by Sakakibara 2006 and Spíchal 2012) are mentioned below:

- The cytokinin oxidases/dehydrogenases (7 *CKX* genes in *Arabidopsis*) are flavoproteins that catalyze the irreversible degradation of IP, tZ and cZ and their respective ribosides and nucleotides to adenine and adenosine by cleavage of the side chain (Figure 3, Galuszka *et al.,* 2001; 2000; Werner *et al.,* 2006). CKXs act by recognizing the double bond of the isoprenoid side chain which is absent in DZ and its derivatives, O-glycosides conjugates and aromatic cytokinins, making these compounds resistant to degradation by CKX (Galuszka *et al.,* 2000; 2007). However, it has been recently shown that AtCKXs can degrade also aromatic cytokinins but less efficiently than the ones with unsaturated bonds (Galuszka *et al.,* 2007; Kowalska *et al.,* 2010). For many years CKX has been considered as oxidase but more recent studies indicated that other electron acceptors are preferred over oxygene for the reaction (Bilyeu *et al.,* 2001; P Galuszka *et al.,* 2001; Laskey *et al.,* 2003) and therefore the enzyme is now classified as dehydrogenase. In rice 11 *CKX* genes have been identified (Ashikari *et al.,* 2005) while maize, where *CKX* was found for the first time, have 13 sequences of the *CKX* family in its genome (Gu *et al.,* 2010). In Pea 2 *CKX* genes have been found while CKX activity has been confirmed also in vitro (Gaudinová *et al.,* 2005; Vaseva-Gemisheva *et al.,* 2005). Degradation of cytokinin by CKX is a pivotal mechanism for controlling the levels of the hormone in plants and therefore overexpression and deficient *CKX* expression has been excessively used in cytokinin research (Werner *et al.,* 2001; 2003; 2010).

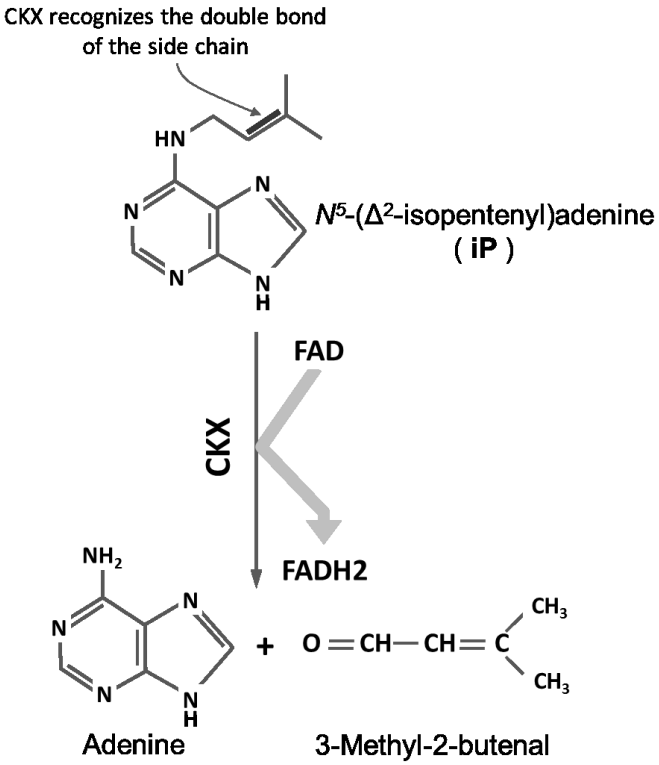

Figure 3 *Example of cytokinin dehydrogenase (CKX) enzymatic reaction for cytokinin degradation using IP as substrate. The side chain of the IP is oxidated by CKX resulting in the production of adenine and 3-Methyl-2-butenal. The reaction requires an electron acceptor which takes two electrons from the flavin cofactor of the enzyme. CKX specifically recognized the double bond indicated in red color and therefore cytokinin molecules like DZ that lack this double bond present resistance to CKX degradation.*

- The cytokinin-N-glucosyltransferase (2 *UGT76C* genes in *Arabidopsis*) glucosylates bioactive cytokinins like IP, tZ, DZ, cZ and BAP. The respective N-glucosides are produced by the glucosylation at the N3, N7 and N9 position of the purine moiety (Hou *et al.,* 2004). The reaction is practically irreversible since N-glucoconjugates are not efficiently cleaved by β-glucosidase – an enzyme catalyzing the deglycosylation (Coutinho *et al.,* 2003; Brzobohaty *et al.,* 1993; Sakakibara 2006). This coupled with the fact that 7-N-glucoside is the major conjugate formed when plants are treated with cytokinin, suggests the involvement of N-glucosylation in detoxification (Hou *et al.,* 2004). Recent in vivo studies in mutants and overexpressors of *AtUGT76C1* and *AtUGT76C2* indicated that the two genes have close physiological roles but to a different level. In accordance with this, *GUS* promoter expression analysis showed that *AtUGT76C1* had weaker expression compared to *AtUGT76C2* but in more distinct tissues (Wang *et al.,* 2013; 2011).

- The cytokinin zeatin-O-glucosyltransferase (*UGT73C1*, *UGT73C2* and *UGT85A1* gene in *Arabidopsis*, they are also called *ZOGTs*; Hou *et al.,* 2004). O- glucosides are produced by glucosylation of cytokinin at the hydroxyl group of the side chains of tZ, cZ and DZ (Dobrev and Kamínek 2002). O-glucosides are resistant to the cleavage by *CKXs* and O-glucosylation is a reversible reaction (Brzobohatý *et al.,* 1993). Since glucosidases can convert these conjugates back into their respective active cytokinin forms their role has been suggested to be stable, inactive local or long-distance travelling storage forms of cytokinin. O-glucosyltransferases have been also isolated from *Phaseolus lunatus* (Martin *et al.,* 1999; 2001.b) and *Zea mays* (Martin *et al.,* 2001.a; Veach *et al.,* 2003) in which further in vivo studies were performed to identify the enzymes that preferentially conjugate cZ or tZ (Martin *et al.,* 2001.a; Pineda Rodo *et al.,* 2008). Therefore the O-glucosyltransferases can be distinguished in *ZOG1, UGT85A1* and in *cis-ZOGT1*, *cis-ZOGT2* transferring the glucose mainly in tZ and cZ, respectively.

1.4 Cytokinin signaling

In summary, cytokinin signaling occurs by a multistep two-component system through a histidine (H) and an aspartate (D) phosphorelay. When cytokinin binds to the transmembrane CHASE domain of the hybrid histidine kinase receptors (AHKs), autophosphorylation is induced on a conserved phospho-accepting H residue within their kinase domain (HK). Then the phosphoryl group is transferred to conserved D residue within the receiver domain of the AHK receptors. The phosphoryl group is then transferred to a conserved H residue on histidine phosphotransfer proteins (AHPs) which are translocated from the cytoplasm to the nucleus and also induce cytokinin response factors (CRFs) translocation from the cytoplasm to the nucleus. Once entering the nucleus the phosphoryl group that AHPs carry, is transferred to a conserved D residue in the receiver domain of response regulators (*ARRs*). B-ARRs, being nuclear transcription factors, are then activated and initiate the transcription of primary cytokinin responsive genes. They also induce the transcription of *A-ARRs* that acting as a negative feedback loop in the cytokinin signaling by inhibiting the transfer of the phosphoryl group from the AHPs to the B-ARRs. Finally, B-ARRs also up regulate the transcription of *CRFs*. The above described signaling mechanism of cytokinin is reviewed by Hwang *et al.,* (2012), Nongpiur *et al.,* (2012) and Spíchal (2012) and is also presented in Figure 4.

The key genes for cytokinin signaling (Figure 4, reviewed by Kakimoto 2003; Heyl & Schmülling 2003; Hwang *et al.,* 2012; Nongpiur *et al.,* 2012 and Spíchal 2012) are listed below.

- The hybrid histidine kinases (3 *AHK* genes in *Arabidopsis*) consist of the transmembrane domain, the ligand-binding CHASE domain, the histidine kinase domain and finally the receiver domain which include a conserved H and D residue, respectively, being key factors for the multistep phosphorelay cascade required for cytokinin signaling (Lomin *et al.,* 2012). The description of the cytokinin receptor domains is also described in Figure 4. The first cytokinin receptor identified in *Arabidopsis* was CRE1/WOL/AHK4 (Inoue *et al.,* 2001; Suzuki *et al.,* 2001; Yamada *et al.,* 2001) while shortly after AtAHK2 and AtAHK3 were also described (Hwang & Sheen, 2001). The induction of *AtAHK4/CRE1* transcript levels as a response to cytokinin treatment, indicates the existence of a positive-feedback loop in cytokinin signaling (Franco-Zorrilla *et al.,* 2002). The affinity that cytokinin receptors bind the different active forms has been shown to vary indicating a specificity in the signaling mechanism within the plant and between different plant species (Romanov *et al.,* 2006; Spíchal *et al.,* 2004; Yonekura-Sakakibara *et al.,* 2004). Although cytokinins were suggested to be perceived at the plasma membrane (Inoue *et al.,* 2001; Ueguchi *et al.,* 2001; Kim *et al.,* 2006) recent findings report the localization of the cytokinin receptors on the endoplasmic reticulum membrane (ER; Lomin *et al.,* 2012; Wulfetange *et al.,* 2011).

- The histidine-containing phosphotransfer (5 *AHP* genes in *Arabidopsis*; Suzuki *et al.,* 1998), having a conserved H residue, function as phosphorelay carriers between the AHK receptors and the downstream nuclear responses caused due to their translocation (Suzuki *et al.,* 2002; Tanaka *et al.,* 2004; Imamura *et al.,* 2001). AtAHP6 contains an aspargine (N) instead of the conserved H residue, thus AHP6 is unable to accept a phosphoryl group. Therefore it is identified as a pseudo-phosphotransferase acting as an inhibitor of cytokinin signaling pathway. However this negative feedback loop has been shown to be involved in crucial physiological processes, like protoxylem differentiation (Mähönen *et al.,* 2006.a). The translocation of AHPs from the cytosol to the nucleus and the opposite, has been recently shown to occur constantly in a phosphorylation- and cytokinin-independent manner (Punwani & Kieber 2010). Finally it has also been shown that CRE1/WOL/AHK4, in the absence of cytokinin can act as a phosphatase dephosphorylating AHPs and thus regulating cytokinin signaling pathway

(Mähönen *et al.,* 2006.b).

- The *ARABIDOPSIS RESPONSE REGULATORS* (*ARR* genes) have a receiver domain with conserved residues (D) that are responsible for accepting phosphoryl groups. There are three types of *ARR* genes, two of which (type *A-ARRs* and type *B-ARRs*, 11 genes in *Arabidopsis* from each type) participate in cytokinin signaling. They are discriminated according to the size of their C-terminal domains with *A-ARRs* having short C-termini and *B-ARRs* having a longer C-termini which acts as DNA binding and stimulation of transcription initiation. Another discrimination factor is that *A-ARRs* are cytokinin-inducible in contrast with *B-ARRs* (Imamura *et al.,* 1999; Kiba *et al.,* 1999). When the phosphorylated AHPs are translocated in the nucleus the phosphoryl group is transferred to both A- and B-ARRs. When B-ARRs receive the phosphoryl group, they become activated and initiate the transcription of cytokinin primary response genes (Argyros *et al.,* 2008; Heyl *et al.,* 2008; Imamura *et al.,* 1999; Ishida *et al.,* 2008; Mason *et al.,* 2005) and thus the pleiotropic cytokinin activities within the plant take place. In addition phosphorylated B-ARRs are also responsible for the transcriptional stimulation of *A-ARRs* (Hwang & Sheen, 2001; Sakai *et al.,* 2001) which then inhibit cytokinin signaling as a negative feedback loop (To *et al.,* 2004). The phosphoryl group that A-ARRs accept from the AHPs entering the nucleus, is responsible for their activation, function and protein stability independently of B-ARRs (To *et al.,* 2007a).

- *CYTOKININ RESPONSE FACTORS* (*CRFs*) are a small subset of transcription factors involved in cytokinin signaling in Tomato and *Arabidopsis* (Cutcliffe *et al.,* 2011; Rashotte & Goertzen, 2010; Rashotte *et al.,* 2006). Rashotte *et al.,* 2006 has described *CRFs* and his findings are mentioned below. Six CRF genes have been identified in *Arabidopsis* and three of them are transcriptionally upregulated by cytokinin. CRFs have been shown to rapidly translocate to the nucleus in response to cytokinin and this effect was AHK- and AHP-dependent but autonomous from ARRs. Microarray data displayed a group of common gene targets for B-ARRs and CRFs while complementation studies of *arr* multiple mutants in *Arabidopsis* by cytokinin-inducible expression of *CRFs* indicated their action downstream of *B-ARRs*. However, the implication of CRFs in other signaling cascades and their activation from other sources than cytokinin has not been excluded (Rashotte *et al.,* 2006).

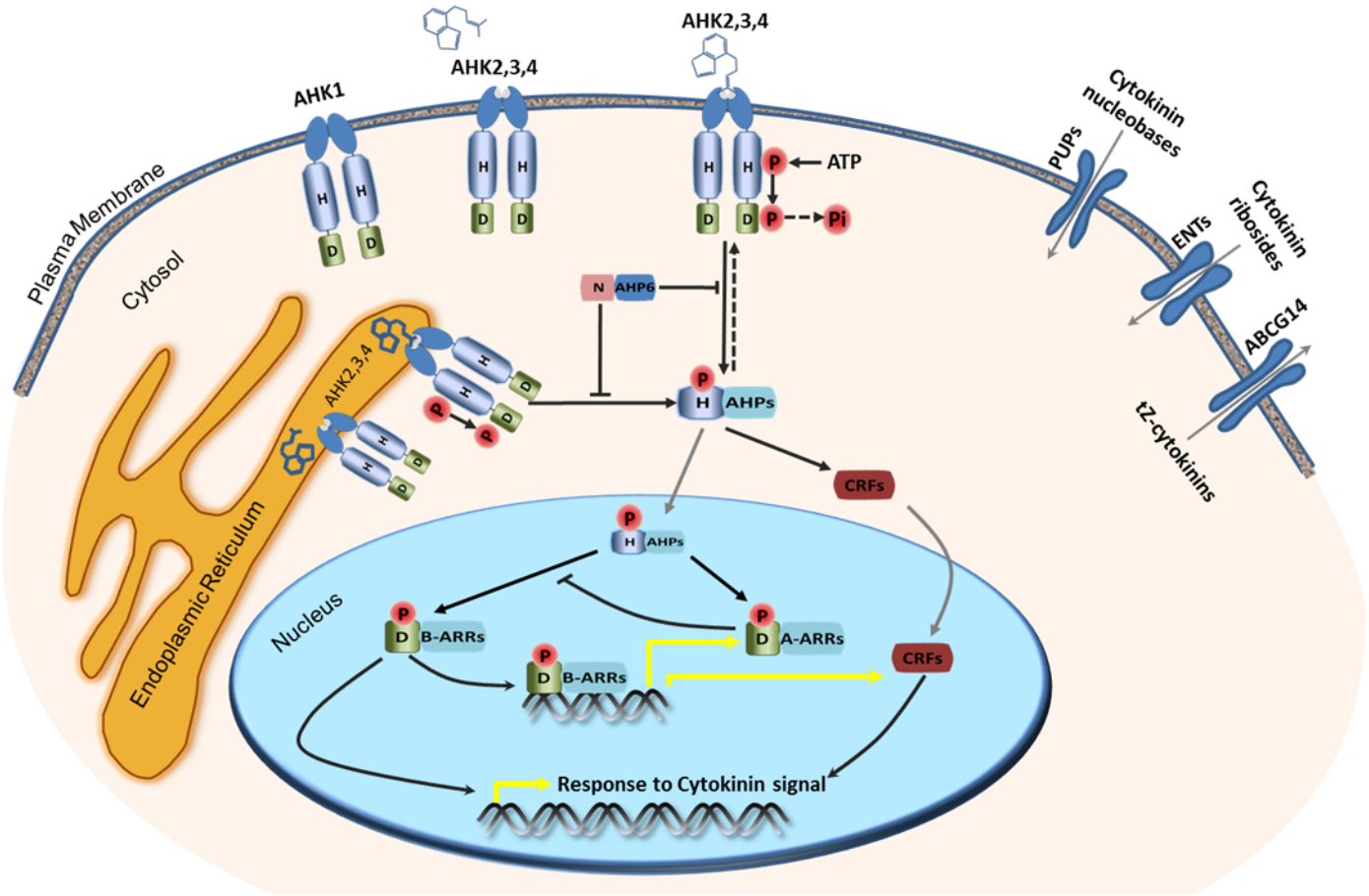

Figure 4 *Model of cytokinin signaling. Cytokinin is perceived by AHK receptors (AHK2, AHK3 and AHK4) localized in the plasma membrane and the endoplasmic reticulum. CKI1 is involved in CK signaling but does not perceive cytokinins. Cytokinin receptors include the transmembrane ligand-binding CHASE domain (blue oval shape), the histidine kinase domain (light blue cylinder) having a conserved histidine residue (H) and the acceptor domain (green cylinder) having a conserved aspartate residue (D). When cytokinin binds to the receptor conformational changes occur and trigger a multistep H-D-H-D phosphorelay. Initially a phosphoryl group is transferred from H to D within the receptor and then it is relayed to the H of phosphoro-transferase proteins (AHPs) which are then translocated from the cytoplasm to the nucleus. There AHPs pass the phosphoryl group to the D of Type A response regulators (A-ARRs) which are then stabilized and to the D of Type B response regulators (B-ARRs). Phosphorylated B-ARRs activate A-ARRs transcription which acts as a negative feedback loop in cytokinin signaling and induce transcription of cytokinin response genes directly or through Cytokinin Response Factors (CRFs) which had been translocated to the nucleus after triggered by the cytoplasmic phosphorylated AHPs. AHP6 is a pseudo-phosphorotransferase containing an aspargine (N) instead of D and thus acting as inhibitor of the phosphorelay.The yellow arrows indicate transcription, the grey arrows represent translocation, the black arrows induction while the cut black arrows inhibition. Cytokinin transporters are also shown on the plasma membrane: purine permease (PUPs), equilibrative nucleoside (ENTs) and ABCGD14 which transfer cytokinin nucleobases, ribosides and tZ-cytokinin forms, respectively.*

1.5. Cytokinin distribution, transport and uptake

1.5.1. Cytokinin distribution

For many years cytokinin was thought to be biosynthesized in the root tip and transported through the xylem to the rest of the plant parts. Only after the discovery of genes participating in the cytokinin biosynthesis (*IPT* and *CYP735A* genes: Miyawaki *et al.,* 2004; Takei *et al.,* 2004.a), metabolism (*LOG* genes: Kuroha *et al.,* 2009), degradation (*CKX* genes: Werner *et al.,* 2003), perception (*AHK* genes: Higuchi *et al.,* 2004; Nishimura *et al.,* 2004) and signaling (Type *A*- and *B*- *ARR* genes: D'Agostino *et al.,* 2000; Kiba *et al.,* 2002; 2003; To *et al.,* 2004; Tajima *et al.,* 2004; Mason *et al.,* 2004) it was proved that this was not the case.

An overview of the expression pattern of cytokinin related genes in *Arabidopsis* is presented in Figure 5. The spatial expression patterns of the transcriptional and/or translational fusions with reporter genes in transgenic *Arabidopsis* lines, confirmed for most of the cases with actual transcript levels, indicated that cytokinins can be locally biosynthesized, act as short or long-distance signals through the xylem and the phloem saps and be degraded at local or distant sites regulating in that way its distribution and building up its concentration gradients within the tissues (Hirose *et al.,* 2008; Kudo *et al.,* 2010).

The expression patterns of *AtIPT3, AtABCG14* and *AtCKX6* genes in the vasculature supports the existence of cytokinin in the plant long-distance travelling network (Miyawaki *et al.,* 2004; Werner *et al.,* 2003). Likewise, the sites of expression of *AtIPT* genes (Miyawaki *et al.,* 2004) does not always match with those of cytokinin degradation (Werner *et al.,* 2003), and/or of cytokinin nucleobases formation represented by the *AtLOG* genes (Kuroha *et al.,* 2009), and/or cytokinin signaling genes (D'Agostino *et al.,* 2000; Ferreira & Kieber, 2005; Kiba *et al.,* 2003, 2002; Tajima *et al.,* 2004; To *et al.,* 2004; Yokoyama *et al.,* 2007). For example, as presented in Figure 5, *AtIPT4* and *AtIPT8* expression in seeds-embryos did not coincide with any *AtCKX*, *AtLOG* and *AtARR* gene expression. However only the expression of *AtUGT76C1* and *AtUGT76C2* coincided with this of *AtIPT4* and *AtIPT8* indicating the conjugation of the cytokinins synthesized at this site (Wang *et al.,* 2013; Wang & Irving, 2011). Similarly, in *Arabidopsis* root hair where *AtLOG2* was expressed no respective patterns for *AtCKX* or *AtIPT* expression was detected (Kuroha *et al.,* 2009; Miyawaki *et al.,* 2004; Werner *et al.,* 2003). Yet, fluorescence of the synthetic cytokinin reporter line *TCSn:GFP* was detected in *Arabidopsis* root hair (Zürcher *et al.,* 2013). Combination of these data could imply that

cytokinins nucleotides transported in root hair are converted to the bioactive nucleobases through *AtLOG2* to initiate the signaling cascade required for cytokinin-dependent inhibition of root hair growth (Mock 1994). Finally, *AtENT6* (cytokinin nucleoside transporter analyzed in Chapter 1.5.4.) expression across the plant vascular tissue proposed its association with the transport of the shoot-root travelling nucleosides (Hirose *et al.,* 2008).

On the other hand, in *Arabidopsis* meristematic tissues like the shoot apical meristem the expression overlaps for *tRNA-AtIPT2, AtCYP735A2, AtCKX1, AtCKX2,* all three cytokinin receptors, 7 *B-ARRs* and 2 *A-ARRs*. Similar patterns are shown in Figure 5 for the leaf and root vasculature, leading to the proposal that cytokinin acts as an autocrine or a paracrine signal at these sites. Local function of cytokinin is also indicated in zones containing endoreduplication events like trichome (overlaid expression of *AtIPT7, AtCKX4* and 3 *B-ARRs*) and stipule (overlaid expression of *AtIPT5* and *AtCKX2*). Finally cytokinin biosynthesis (*AtIPT* genes), rapid cytokinin activation (*AtLOG* genes) but tight regulation (*AtCKX* genes) is displayed in zones with high rates of cell division like axillary buds, lateral root primordium and root procambium (Figure 5).

Tissue expression studies concerning cytokinin receptors through promoter expression studies and RNA gel plot hybridizations showed that *AtAHK4* expression predominated in the root tissue while *AtAHK3* RNA was mainly detected in the rosette leaves (Nishimura *et al.,* 2004; Higuchi *et al.,* 2004). These results were also supported by the physiological roles of *AtAHK4* and *AtAHK3* concerning root vasculature development (Mähönen *et al.,* 2000) and leaf development and longevity (Kim *et al.,* 2006; Riefler *et al.,* 2006), respectively. A hypothesis for the implication of the two receptors in perceiving long-distance travelling cytokinins through the phloem and xylem was also formed. This hypothesis was further endorsed by a comparative study between the hormone-binding characteristics of the two receptors using a live-cell based binding assay in transgenic bacteria (Romanov *et al.,* 2005) which heterologously expressed *AtAHK3* and *AtAHK4* (Romanov *et al.,* 2006). *AtAHK4* displayed an almost 10 fold higher affinity to IP than *AtAHK3* (Romanov *et al.,* 2006), a trend which is conserved also in maize (Yonekura-Sakakibara *et al.,* 2004). Combining all the above mentioned results with data supporting that IP-compounds are mainly transported through the phloem while tZ-compounds through the xylem (analyzed in Chapter 1.5.2, Hirose *et al.,* 2008), the preference of IP from *AtAHK4* could be interpreted as phloem derived cytokinins are preferentially perceived in the root tissue. More experiments are required to provide direct evidence for such a preferential involvement of cytokinin receptors in the xylem and phloem derived cytokinins.

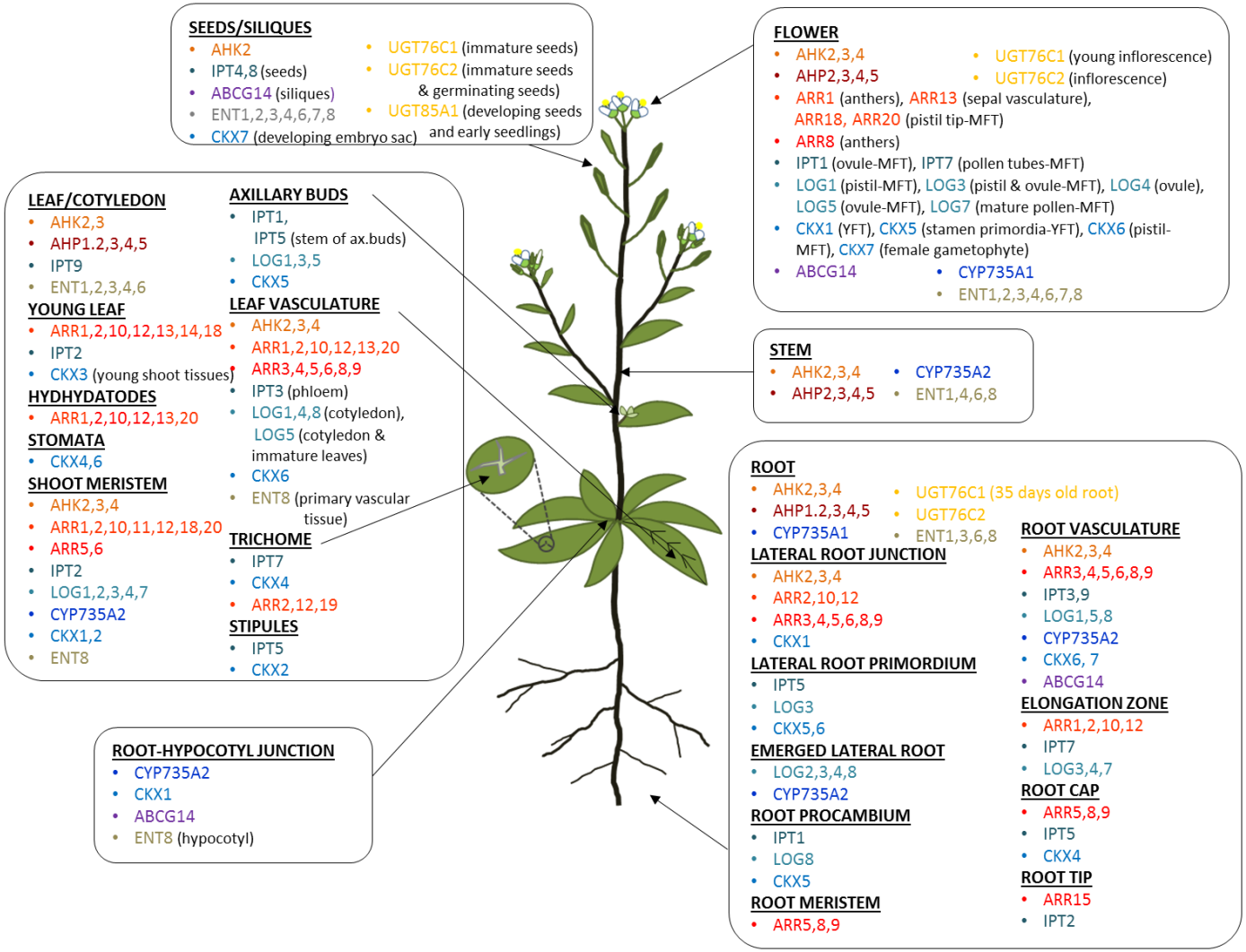

Figure 5 *Overview of tissue-specific distribution of cytokinin related genes expression in Arabidopsis. The data derive from Nothern analysis data for AHPs (Tanaka et al. 2004) and from transcriptional and/or translational GUS and/or GFP fusions for IPTs* (Miyawaki *et al.,* 2004; Takei *et al.,* 2004.b)*, for CYP735A2* (Kiba *et al.,* 2013; Takei *et al.,* 2004.a)*, for LOGs* (Kuroha *et al.,* 2009)*, for CKXs* (Werner *et al.,* 2006; Werner *et al.,* 2003; Kollmer *et al.,* 2014)*, for AHKs* (Nishimura *et al.* 2004; Higuchi *et al.* 2004)*, for type-A ARRs* (D'Agostino *et al.,* 2000; Ferreira & Kieber, 2005; Kiba *et al.,* 2003, 2002; To *et al.,* 2004b, 2007b)*, for type-B ARRs* (Tajima *et al.* 2004; Mason *et al.* 2004)*, for UGTs (Jin et al., 2013; Wang et al., 2011; 2013), for ENTs (Li et al., 2003; Sun et al., 2005) and for ABCG14 (Zhang et al., 2014.a; Ko et al., 2014).*

1.5.2. Cytokinin as a long-distance signal

Several lines of evidence, including grafting experiments, demonstrate cytokinin movement in the xylem and phloem sap suggesting a bidirectional mechanism of long-distance transport through the vasculature (Bangerth, 1994; Beveridge *et al.,* 1994; Corbesier *et al.,* 2003; Hirose *et al.,* 2008; Ishikawa *et al.,* 2005; Kuroha *et al.,* 2002; Matsumoto-Kitano *et al.,* 2008; Morris *et al.,* 2001; Napoli 1996; Stirnberg *et al.,* 2002; Turnbull *et al.,* 1997).

Cytokinins are travelling inside the plant basipetally, through the phloem sap, and acropetally, through the xylem sap. Detection of cytokinin compounds in the xylem (Kuroha *et al.,* 2002; Morris *et al.,* 2001; Takei *et al.,* 2001.a; Hirose *et al.,* 2008; Lejeune *et al.,* 2006) and in the phloem sap (Hirose *et al.,* 2008; Corbesier *et al.,* 2003; Lejeune *et al.,*2006) support this model. Recent grafting experiments in *Arabidopsis*, using cytokinin defective mutants (atIPT1;3;5;7 mutant, in which the content of both iP-type and tZ-type cytokinins decreased in comparison with wild-type plants (Miyawaki *et al.,* 2006), revealed that iP-type cytokinins are the most common type transported basipetally and tZ-type CKs are transported acropetally (Matsumoto-Kitano *et al.,* 2008; Corbesier *et al.,* 2003; reviewed by Kudo *et al.,* 2010; Müller & Leyser 2011). The fact that tZ-type cytokinins are travelling from root to shoot is further supported by the experiments of Takei *et al.,* (2004a) who showed that the expression of both *AtCYP735A* genes, converting IPRP to tZRP, is high in the roots. Supporting evidence for cytokinin movement through the phloem sap was presented when visualized radiolabelled cytokinins were shown in planta to travel through symplastic connections in the phloem (Bishopp *et al.,* 2011.b).

Physiological roles of these long-distance travelling cytokinins confirmed their significance in plant development and adaptation. The role of xylem cytokinin in regulating shoot branching has been well studied in highly branching mutants displaying low cytokinin levels in the xylem sap. These characteristics were both restored when wild type scion was grafted to the mutant rootstock revealing the existence of a basipetal signal regulating xylem cytokinin and therefore branching (Beveridge *et al.,* 1997.b; Foo *et al.,* 2007). The chemical nature of this signal is still not clear but it seems crucial for unravelling the branching regulatory mechanism and the exact role of xylem cytokinin in this. *RMS2* in Pea is the only gene, identified until today, regulating this basipetal signal (Foo *et al.,* 2005). Another physiological role for xylem cytokinin was implicated when cytokinin translocation and accumulation followed respective alterations in nitrogen availability (Samuelson and Larsson, 1993; Takei *et al.,* 2001.a). More specifically NO_3^- stimulated tZ enrichment in the roots (Takei *et al.,* 2001.a; Takei *et al.,* 2002; Takei *et al.,*

2004.b) and this increase of cytokinin concentration was later shown to induced leaf growth (Rahayu *et al.,* 2005). Finally, this regulation was also supported by cytokinin-related gene expression studies since it was shown that cytokinin biosynthesis through *AtIPT3* is responsible for rapid alterations in the NO_3^- status (Takei *et al.,* 2004.b). Finally, a combination of grafting experiments and disruption of the phloem flow by induced callose synthesis revealed that phloem derived cytokinin was responsible for the maintenance of the vascular patterns in *Arabidopsis* root tip (Bishopp *et al.,* 2011.b).

1.5.3. Cytokinin as a local signal

As mentioned in Chapter 1.5.1., nitrogen deprivation increases xylem cytokinin (Rahayu *et al.,* 2005; Takei *et al.,* 2001.a) and that this might be involved in the coordinating response of leaf growth under these conditions (Rahayu *et al.,* 2005). However the expression patterns of *AtIPT3* showed that nitrogen dependent cytokinin synthesis occurs both in roots and leaves (Takei *et al.,* 2004.b). In addition, leaves exposed to atmospheric ammonia revealed that local nitrogen levels could change cytokinin concentration in the leaves (Collier *et al.,* 2003). Therefore it can be also suggested that local cytokinin synthesized in the leaves is important as a response to nutritional status. The contradictory results of Rahayu *et al.,* (2005) and Dodd *et al.,* (2004) concerning the relationship between local and/or long-distance cytokinin and leaf expansion as a response to nitrogen status are discussed by Dodd & Beveridge 2006.

Further implications for cytokinin function as a paracrine signal occurred by experiments with radioactive cytokinins applied to leaves showed that only a small proportion was transported to other plant parts while the rest remained at the treated site (reviewed by Kudo *et al.,* 2010). Faiss *et al.,* (1997) suggested that local production of cytokinin is more important for the activation of axillary buds than xylem cytokinin using reciprocal grafting in tobacco plants overexpressing a bacterial *IPT* gene. The active cytokinin forms were found to promote axillary buds outgrowth when they were applied directly to them and increased cytokinin levels were observed in and around axillary buds during growth initiation (Foo *et al.,* 2007; Turnbull *et al.,* 1997). Cytokinin action as a local signal was also supported by the upregulation of *PsIPT1* and *PsIPT2* genes in Pea nodal stem following decapitation (Tanaka *et al.,* 2006). This effect is attributed to the decreased concentrations of auxin moving basipetally from the decapitated site (Shimizu-Sato & Mori, 2001) and is indicating that bud outgrowth following decapitation was due to the locally produced nodal cytokinin.

1.5.4. Cytokinin transporters

However recent data showing variation of cytokinin responses in different cell types (analyzed in Chapter 1.4) suggest that there are additional routes of cytokinin transport. Cell to cell transport occurs through the apoplastic and symplastic pathways (through cell wall and cytoplasm respectively) and through trans-membrane protein channels or transporters. The PIN-based polar auxin transport stream has been shown to occur through the apoplastic/symplastic movement (Cambridge & Morris 1996).

IAA transport also occurs through its famous influx transporters, (*AUX1/LAX* family of PM permeases) and efflux carriers (*PIN* family and ATP-binding cassette (*ABC*) superfamily of transporters; Zazímalová *et al.,* 2010).

While diffusion might also play a role, evidence from *Arabidopsis* cell cultures indicates that cytokinins are also actively taken up by the plant cells (Cedzich *et al.,* 2008). Further research concerning cytokinin translocation across the plasma membrane, suggests two gene families as candidates for cytokinin transporters. Members of the *Arabidopsis* purine permease (*PUP*) gene family have been shown to mediate the uptake of cytokinin compounds and adenine in a common proton-coupled high affinity purine transport system (Bürkle *et al.,* 2003; Gillissen *et al.,* 2000). Series of experiments in *Arabidopsis* cell cultures and in yeast by heterologous expression of *AtPUPs* and transport competition assays revealed that *AtPUP1* could transport caffeine, adenine, cytosine, tZ, IP, tZR and adenosine while *AtPUP2* was involved in the uptake of adenine, IP, tZ, cZ, kinetin, BAP and tZR (Bürkle *et al.,* 2003; Gillissen *et al.,* 2000). Therefore PUPs have been proposed as candidate transporters for cytokinin energy-dependent cell to cell movement. However, evidence in planta is still expected to confirm this suggestion.

Another gene family suggested as cytokinin transporter is the equilibrative nucleoside transporter (*ENT*) gene family. AtENT1 was the first functional characterized nucleoside transporter in plants (Möhlmann *et al.,* 2001). AtENT4, AtENT6 and AtENT7 indicated transport of pyrimidine and purine nucleosides, deoxynucleosides and to a smaller extent nucleobases (Wormit *et al.,* 2004). The same was also shown for AtENT3 and additionally nucleotides (ATP and ADP) revealed some inhibitory effect in competition assays with transport of radiolabelled adenosine (Li *et al.,* 2003). The first proof that ENTs can actually transport cytokinin compounds was found in rice when *OsENT2*, expressed in yeast cells, was shown to mediate the uptake of radiolabelled IPR and with less efficiency tZR (Hirose *et al.,* 2005). The same result was confirmed a bit later concerning *AtENT6* (Hirose *et al.,* 2008). Finally the desired identification of ENT cytokinin transporters in planta came with

the characterization of the *AtENT8* and *AtENT3* loss-of-function mutants which displayed reduced sensitivity to IPR and tZR but not to the nucleobases IP and tZ (Sun *et al.,* 2005). In accordance with these findings transgenic *Arabidopsis* lines overexpressing *AtENT8* were hypersensitive to IPR but not to IP while the uptake efficiency of radiolabelled IPR in *atent3* and *atent8* mutants was significantly reduced (Sun *et al.,* 2005).

Even though PUPs and ENTs could participate in cytokinin transport, their broad substrate specificity and weak mutant phenotypes indicates that there might be other cytokinin transporters responsible for the major regulation of cytokinin-related plant development. Indeed, only in 2014, an ATP-binding cassette (ABC) transporter subfamily G14 (*AtABCG14*) was identified in *Arabidopsis* by two research groups as a key regulator of the acropetal cytokinin transport (Ko *et al.,* 2014; Zhang *et al.,* 2014.a). The *atabcg14* mutant displayed a serious shoot growth delay which was rescued by exogenously supplied tZ. Cytokinin concentration in the mutant shoots was found reduced while the opposite trend was shown in the shoots. This trend in the mutant was also supported by expression studies in *A-ARR* genes. Consistently with the above mentioned findings, the actual cytokinin levels in the xylem sap of *atabcg14* were dramatically reduced while the grafting of *atabcg14* scion to wild-type rootstock restored the mutant phenotype, an effect that was not observed with the opposite graft combination. Finally, in planta feeding experiments using labelled tZ revealed that *AtABCG14* functions as an efflux pump required for the transport of the fed cytokinin (Ko *et al.,* 2014; Zhang *et al.,* 2014.a).

1.6. Cytokinin distribution in cell-specific level

1.6.1. Cytokinin response in specific cell types

Other indirect methods of assessing cytokinin distribution, including expression studies of various cytokinin promoters driving the expression of β-glucuronidase (*GUS*) or green fluorescent protein (*GFP*) markers, suggest that specific cell types play an important role.

The expression of *AHP6* (*Arabidopsis* Histidine Phosphotranfer protein 6 involved in inhibiting of cytokinin signaling) expands through the vascular bundle in genetic backgrounds with decreased cytokinin signaling suggesting that it specifies the spatial domain of *AtAHP6* expression (Mähönen *et al.,* 2000). Werner *et al.,* showed that the *cytokinin oxidase 6* (*CKX6*) in *Arabidopsis* wild type plants was expanded from the vascular strands acropetally into the

stele initials when treated with BAP revealing a prominent ectopic *GUS* activity (Werner *et al.,* 2006). Cytokinin responsiveness of *ARR15:GUS* and *ARR16:GUS* was reduced in *Arabidopsis* roots to the stele containing the vasculature and the endodermis, respectively (Kiba *et al.,* 2002; 2004; Heyl & Schmülling 2003). However wild type *Arabidopsis* plants of the same developmental stage and treatment showed an ubiquitous activation of the cytokinin reporter *ARR5:GUS* which suggests that all cells are competent to react to cytokinin treatment (D'Agostino *et al.,* 2000; Romanov *et al.,* 2002). Taken together these results indicated that the specific combination of elements that are necessary for the cytokinin signaling chain are present in only the responsive cells (Werner *et al.,* 2006; Heyl & Schmülling 2003). Consistently, in situ hybridization of post embryonic roots showed that while *AtARR15* expression in *Arabidopsis* wild type roots was detected to the intervening procambial cells adjacent to the xylem axis, in *atahp6* mutant it broadened radially to occupy the protoxylem position (Bishopp *et al.,* 2011.a; Mähönen *et al.,* 2006.a). This indicates that *AtAHP6* acts to facilitate protoxylem specification by downregulating cytokinin signaling in a spatial specific manner. Recently results deriving from a transgenic line overexpressing *AtCKX7* suggested that the cellular localization/compartmentalization of cytokinin degradation in combination with substrate specificity of CKX isoforms are significant restrictions specifying cytokinin activities (Köllmer *et al.,* 2014).

1.6.2. Subcellular localization of cytokinin-related genes

An overview of the subcellular localization of the gene products related with cytokinin biosynthesis, metabolism, homeostasis, signaling and transport provides an insight in cytokinin distribution in cell-specific level and is summarized in Figure 6.

Plastids were shown to be a major subcellular compartment for the first step of cytokinin biosynthesis *AtIPT1, AtIPT3, AtIPT5* and *AtIPT8* expression was found in the chloroplasts while *AtIPT7* in the mitochondria. Finally, *AtIPT4* and *tRNA-AtIPT2* in the cytosol (Kasahara *et al.,* 2004; Miyawaki *et al.,* 2004; Takei *et al.,* 2004.b) indicating that cZRP production is cytosolic. The subcellular localization of the IPRP hydroxylation for tZRP production catalyzed by *AtCYP735A* enzymes is still unknown along with *AtIPT6* and *tRNA-AtIPT9*. Cytokinin metabolism through *LOG* enzymes catalyzing the conversion of all cytokinin nucleotides to bioactive free bases displayed both nuclear and cytosolic localization (Kuroha *et al.,* 2009). This spatial intra-cellular distribution of cytokinin biosynthetic and metabolic

genes indicates the presence of a transport mechanism facilitating the translocation of cytokinin nucleotides to the cytosol or the nucleus.

This kind of mechanism is further broadened to the vacuole and apoplast concerning this time also cytokinin ribosides and free bases. This is implied by the vacuolar localization of *AtCKX1* and *AtCKX3* and the apoplastic one of *AtCKX2* (Werner *et al.,* 2003) and the predicted secretion of *AtCKX4, AtCKX5* and *AtCKX6*. These consist cytokinin degradation enzymes and only one of them, *AtCKX7* exhibited expression in the cytoplasm (Köllmer *et al.,* 2014). Cytokinin nucleobases conjugation through the O-glucosyltransferase *AtUGT85A1* was suggested to take place in the cytoplasm and nucleus (Jin *et al.,* 2013) while the *AtUGT73C1* and *AtUGT73C5* were predicted to have chloroplastic localization.

The bioactive cytokinin nucleobases and the IPR and tZR ribosides that displayed efficient binding with cytokinin receptors (Romanov *et al.,* 2006; Spíchal *et al.,* 2004; Stolz *et al.,* 2011; Yonekura-Sakakibara *et al.,* 2004) were also indicated to efficiently translocate inside the endoplasmic reticulum lumen since cytokinin receptors have been shown to sense cytokinins at this site (Wulfetange *et al.,* 2011; Lomin *et al.,* 2012; Caesar *et al.,* 2011) but also to the apoplast since the presence of a subset of cytokinin receptors at the plasma membrane is still believed (Higuchi *et al.,* 2004; Inoue *et al.,* 2001; Kim *et al.,* 2006).

The transport of cytokinin ribosides and nucleobases through the cell membrane has been shown to occur through AtENT and AtPUP transporters respectively which exhibited localization on the plasma membrane (Bürkle *et al.,* 2003; Li *et al.,* 2003; Wormit *et al.,* 2004) and through *AtABCG14* which was also localized at the same site and has been suggested to export tZ-type cytokinins out of the cell (Ko *et al.,* 2014; Zhang *et al.,* 2014.a). The transport system of the hormone concerning the exit of compounds from chloroplasts and mitochondria and their respective entrance in the endoplasmic reticulum, vacuole, nucleus or chloroplasts again is still unknown.

After cytokinin is perceived by the receptors located either in the plasma membrane or in the endoplasmic reticulum the signaling cascade of the hormone is triggered. This is described in Chapter 1.4 and the respective scheme is presented in Figure 6. However the subcellular localization of the genes involved in cytokinin signaling is also shown in Figure 4 to keep an overview of all cytokinin-related genes compartmentalization.

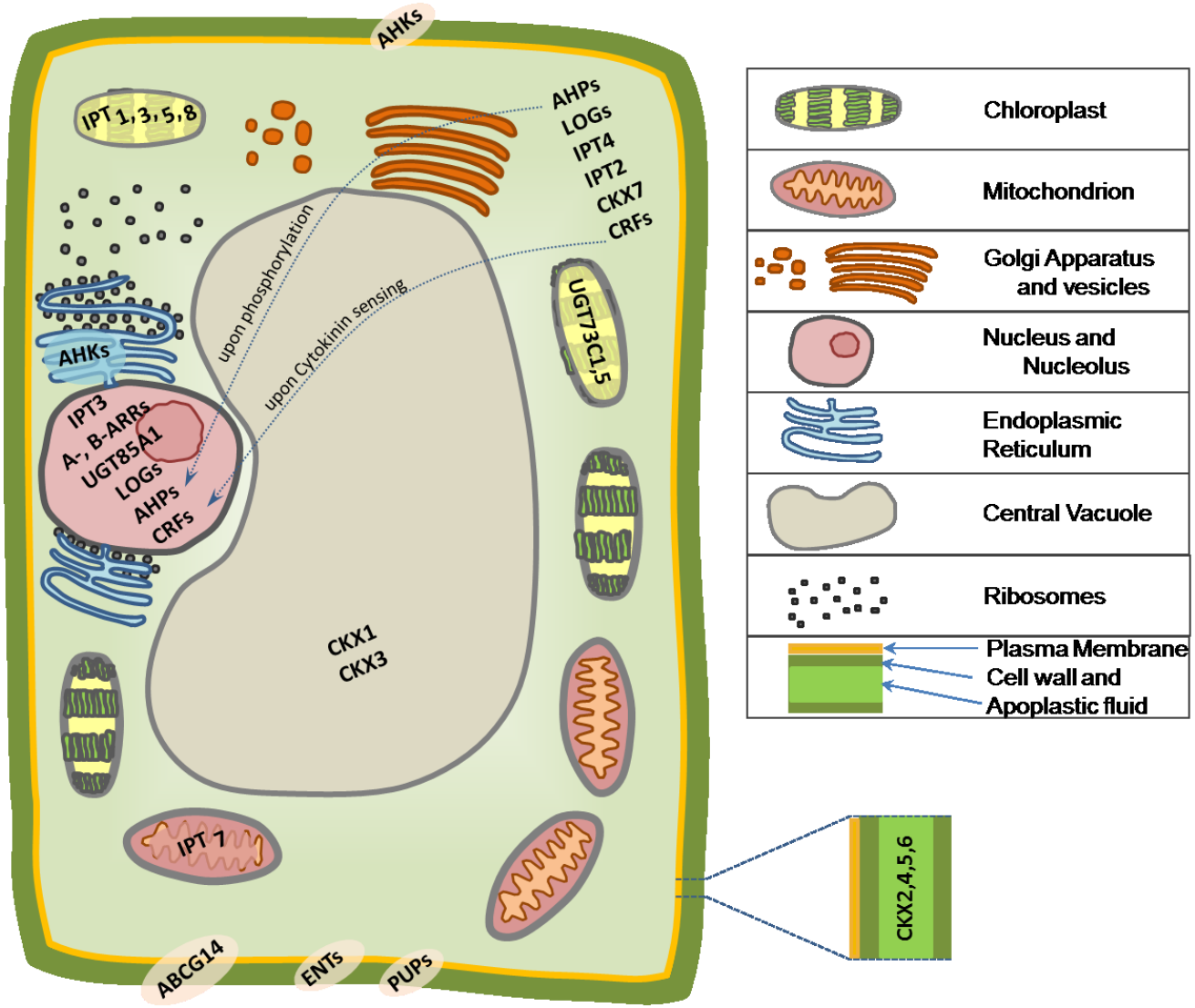

Figure 6 *Subcellular localization of cytokinin-related genes. The data derive from transcriptional and/or translational GFP fusions or bioinformatic predictions according to the gene sequence when mentioned below. Localization of IPTs was described by Kasahara et al., 2004; Miyawaki et al., 2004 and Takei et al., 2004.b, of LOGs by Kuroha et al., 2009, of CKXs by Werner et al., 2003 and Kollmer et al., 2014 (CKX4, CKX5 and CKX6 are predicted to be secreted) and of UGT85A1 by Jin et al., 2013 (UGT73C5 and UGT73C1 are predicted to localize in the chloroplasts). Cytokinin receptors have been predicted and shown to localize to the plasma membrane (Inoue et al., 2001; Ueguchi et al., 2001; Kim et al., 2006) but were also indicated to localize to the endoplasmic reticulum (Caesar et al., 2011; Wulfetange et al., 2011; Lomin et al., 2012). For the rest of the cytokinin signaling components localised mainly either in the cytoplasm and/or in the nucleus as indicated, respective references are given in Chapter 1.4. The localization of IPT6, IPT9, CYP735As, UGT76Cs, AHP6, ARR3, ARR4, ARR5, ARR8, ARR9, ARR17 have not been determined while ARR11, ARR13, ARR14, ARR20 and ARR21 compartmentalization to the nucleus is only predicted.*

1.7 Strigolactone effects on cytokinin

Branching mutants in *Arabidopsis* and pea display severely reduced xylem cytokinin levels. This effect was identified in all *max* (*MORE AXILLARY GROWTH*) mutants in *Arabidopsis* and in all *rms* (*RAMOSUS*) mutants in pea, apart from *rms2* (Morris *et al.,* 2001; Foo *et al.,* 2007; Beveridge *et al.,* 1994; Beveridge *et al.,* 1997.a; 1997.b). These branching mutants were later identified to be involved in the biosynthesis and signaling pathway of a novel hormone, strigolactone (Gomez-Roldan *et al.,* 2008; Umehara *et al.,* 2008).

Grafting studies revealed that the reduction of xylem cytokinin levels found in the SL mutants is mediated by the shoot. Wild type rootstocks suppressed the branching phenotype and restored the reduced xylem cytokinin levels in *rms1, rms5* and *rms2* scions suggesting that root-derived strigolactones suppress branching and xylem cytokinin levels. In contrast, wild type rootstocks could not rescue these defects when grafted to *rms3, rms4* and *max2* (Foo *et al.,* 2007; Beveridge *et al.,* 1997.b). This outcome brings evidence for the existence of a basipetal signal which affects xylem cytokinin levels in strigolactone mutants (Beveridge *et al.,* 2000; Foo *et al.,* 2007).

The mutant *rms2* is the only strigolactone mutant presenting neither decreased xylem cytokinin levels (Beveridge *et al.,* 1994; Foo *et al.,* 2007) nor upregulation of *RMS1* and *RMS5* transcripts that is observed in all other *rms* mutants (Foo *et al.,* 2005). Moreover, *RMS2* was required for the full suppression of xylem cytokinin in *rms1, rms4 and rms5* mutants as their levels remain elevated in double mutants with *rms2*. (Beveridge *et al.,* 1997.a; 1997.b; Foo *et al.,* 2007) *DAD1,* being an homolog of *MAX4* (Table 2), was also upregulated in the stems of *dad* mutants (Snowden *et al.,* 2005) while the same effect was detected in *Arabidopsis* using *pMAX4:GUS fusion* (but not for the hypocotyls of *max2* mutants) (Bainbridge *et al.,* 2005). These findings suggest that the basipetal signal mentioned above induces transcription of strigolactone biosynthetic genes and therefore it has been described as a feedback signal. Even though the *RMS2* gene has not been yet cloned and characterized, it is suggested to be tightly linked with the basipetal feedback signal affecting xylem cytokinin levels and strigolactone biosynthetic genes (Dun *et al.,* 2012).

In addition, antagonistic interaction between cytokinin and strigolactone has been reported on bud outgrowth. The strigolactone defective mutant *rms1* displayed a hypersensitive bud

growth response when cytokinin was applied either directly to the bud or supplied via the vascular stream (Dun *et al.,* 2012). In the same work Dun *et al.,* (2012) showed that common application of cytokinin and synthetic strigolactone (GR24) resulted in decreased cytokinin-effect on *rms1* branching but not on *rms4* indicating that strigolactone effect on cytokinin is *RMS4*-dependent. The opposite actions of strigolactone and cytokinin in bud outgrowth regulation have been proposed to converge on the TCP transcription factor *BRC1/TB1* expression in buds (Minakuchi *et al.,* 2010; Dun *et al.,* 2012; Braun *et al.,* 2012). *AtBRC1* has been previously shown to negatively affect bud outgrowth (Aguilar-Martínez *et al.,* 2007). Inhibition of *PsBRC1* expression through cytokinin and respective induction through strigolactone was displayed in pea (Braun *et al.,* 2012) while in maize strigolactone caused no alteration in *TB1* expression (Guan *et al.,* 2012; Minakuchi *et al.,* 2010). However, strigolactone application could not restore the increased bud outgrowth in *brc1* mutants in *Arabidopsis*, maize and pea (Minakuchi *et al.,* 2010; Brewer *et al.,* 2009; Braun *et al.,* 2012) implying that strigolactone signaling is *BRC1*-dependent.

1.7.1 Strigolactone Chemistry and Functions

The molecular identity of the orthologs *MAX (MORE AXILLARY BRANCHING), DAD (DECREASED APICAL DOMINANCE), D (DWARF), and RMS (RAMOSUS)* genes in *Arabidopsis* (*At-Arabidopsis thaliana*), Petunia (*Ph-Petunia hybrida*), rice (*Os-Oryza sativa*) and pea (*Ps-Pisum sativum*) respectively, supports their predicted function in the conserved linear single-pathway of strigolactone (Umehara *et al.,* 2008; Gomez-Roldan *et al.,* 2008).

Strigolactones derive from carotenoids and contain both a tricyclic lactone (ABC-ring) and a butenolide (D-ring) which are connected by an enol bridge (Xie *et al.,* 2010). Naturally occurring strigolactones can be distinguished into two categories with identical stereochemistry but opposite C-ring orientation. The two categories include the strigol-type group and the orobanchol-type group, presented in Figure 7 (Zhang *et al.,* 2014.b; Xie *et al.,* 2013; Zwanenburg and Pospísil 2013). These two groups have been suggested to derive from 5-deoxystrigol (5DS) and ent-2'-epi-5-deoxystrigol (ent-2'-epi-5DS), respectively (Rani *et al.,* 2008; Xie *et al.,* 2010; Zhang *et al.,* 2014.b).

Strigolactones affect various aspects of plant growth and development. They were initially identified at root exudates promoting symbiotic relationships with arbuscular mycorrhizal

fungi and parasitic seed germination (Akiyama and Hayashi 2006). Strigolactones were also found to affect leaf senescence (Woo *et al.,* 2001; Snowden *et al.,* 2005). Their inhibitory role in axillary bud outgrowth was the one that led to the discovery of strigolactones as a novel hormone (Umehara *et al.,* 2008; Gomez-Roldan *et al.,* 2008). Since then,, they have been extensively studied and roles in adventitious root formation (Rasmussen *et al.,* 2012), root architecture (Kapulnik *et al.,* 2011; Ruyter-Spira *et al.,* 2011) and secondary growth (Agusti *et al.,* 2011) have also been revealed.

1.7.2 Strigolactones Biosynthesis and Transport

The strigolactone biosynthetic pathway is presented in Figure 7 and the key genes catalyzing the respective reactions are displayed in Table 2.a for four plant species. *OsD27*, being a β-carotene-9-isomerase/iron-binding protein, has been proposed to catalyze the reaction from all-trans-β-carotene to 9-cis-β-carotene (Adrian *et al.,* 2012; Lin *et al.,* 2009; Brewer *et al.,* 2012) while the orthologs *AtMAX3/OsD17/PsRMS5/PhDAD3* encode a member of the carotenoid cleavage dioxygenase family, CCD7 (Booker *et al.,* 2004; Drummond *et al.,* 2009; Morris *et al.,* 2001; Johnson *et al.,* 2006; Simons *et al.,* 2007; Zou *et al.,* 2006). CCD7 is proposed to cleave 9-cis-β-carotenone into trans-b-apo-10´-carotenal which is then further shortened to carlactone by CCD8 (Adrian *et al.,* 2012) *encoded by the* orthologous genes *AtMAX4/OsD10/PhDAD1/PsRMS1* (Arite *et al.,* 2007; Sorefan *et al.,* 2003; Snowden *et al.,* 2005). Carlactone has been proposed as the key strigolactone precursor form exhibiting activity in bioassays; it impeded tiller outgrowth in rice and induced germination of parasitic seeds germination in a strigolactone-type manner. Also exogenous supply of carlactone influenced leaf morphogenesis and shoot branching in a *MAX1*-dependent manner (Seto *et al.,* 2012; Adrian *et al.,* 2012). Further oxidation of carlactone has been implied to occur though AtMAX1, a monooxygenase of class III cytochrome P450 (CYP711A1) which acts downstream of AtMAX3 and AtMAX4 on a mobile substrate (Booker *et al.,* 2005; Seto *et al.,* 2012; Adrian *et al.,* 2012). Recently, *Os01g0700900*, an homolog of *AtMAX1* in rice, was identified as a carlactone oxidase and shown to catalyze the formation of ent-2'-epi-5DS (Zhang *et al.,* 2014.b). In the same study, Zhang *et al.,* (2014) characterized another rice *AtMAX1* homolog, *Os01g0701400*, as an ent-2'-epi-5DS-4-hydroxylase producing orobanchol-type strigolactones.

Recently, an ATP-binding cassette (ABC) transporter, *PDR1* was identified to be responsible for strigolactone export from cells (Kretzschmar *et al.,* 2012) of *Petunia hybrida*.

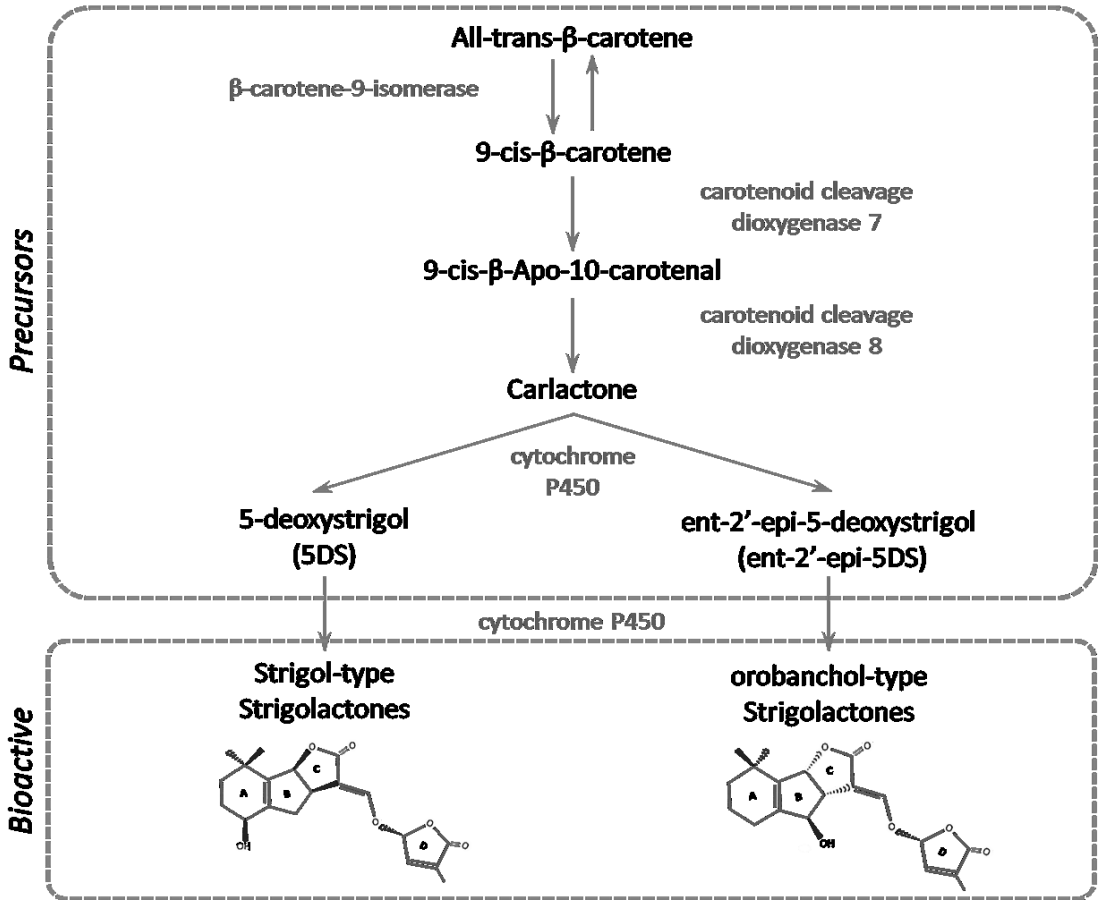

Figure 7 *Strigolactones biosynthetic pathway. The enzyme β-carotene-9-isomerase converts all trans-β-carotene to 9-cis-β-carotene which is the cleaved by the carotenoid cleavage dioxygenase 7 (CCD7) to form 9-cis-β-Apo-10-carotenal. CCD8 catalyzes then the generation of carlactone, the key strigolactone precursor form. Bioactive strigolactones are classified in two groups: strigol-type and orobanchol types and are shown along with their respective chemical structures. The two respective immediate precursors of the bioactive molecules are 5-deoxystrigol (5DS) and ent-2'-epi-5-deoxystrigol (ent-2'-epi-5DS) which initially derive from carlactone. Both these metabolic reactions are catalyzed by a cytochrome P450. Written in black strigolactone bioactive compounds and their respective precursors are shown while the enzymes catalyzing the metabolic reaction steps are written in blue.*

Role	Protein Function		Plant species in which respective genes have been identified/cloned				
			Arabidopsis	Pea	Rice	Petunia	References
(a) Biosynthesis	β-carotene-isomerase		AtD27 [1]	PsD27 [2]	D27 [1, 3]		1. Waters et al,. 2012a 2. de St Germain et al,. 2013 3. Lin et al,. 2009
	Carotenoid Cleavage Dioxygenase	7	MAX3 [1]	RM55 [2, 3]	D17/HTD1 [4]	DAD3 [5, 6]	1. Booker et al,. 2004 4. Zou et al,. 2006 2. Morris et al,. 2001 5. Simons et al,. 2005 3. Johnson et al,. 2006 6. Drummond et al,. 2009
		8	MAX4 [1]	RM51 [1]	D10 [2]	DAD1 [3]	1. Soferan et al,. 2003 2. Ante et al,. 2007 3. Snowden et al,. 2005
	Cytochrome P450		MAX1 (?) [1, 2]	2xPsMAX1 (?) [3]	Os01g0700900 [4] Os01g0701400 [4]	PhMAX1 (?) [5]	1. Booker et al,. 2005 4. Zhang et al,. 2014 2. Strinberg et al,. 2001 5. Drummond et al,. 2011 3.de St Germain et al,. 2013
(b) Transport	ABC transporter					PDR1 [1]	1. Kohlen et al,. 2012
(c) Perception and Signaling	α/β hydrolase	strigolactone perception	AtD14 [1]		D14/D88/HTD2 [1,2,3,4,5]	DAD2 [6]	1. Waters et al,. 2012b 4. Lin et al,. 2009 2. Nakamura et al,. 2013 5. Gao et al,. 2009 3. Arite et al,. 2009 6. Hamiaux et al,. 2012
		Karrikin perception	KAI2 [1, 2]		D14L [3]		1. Guo et al,. 2013 2. Zhao et al,. 2013 3. Kagiyama et al,. 2013
	F - box	Common for strigolactone and Karrikin	MAX2 [1, 2, 3]	RM54 [4, 5]	D3 [6, 7]	PhMAX2A-B [8]	1. Stirnberg et al,. 2002 5. Johnson et al,. 2006 2. Stirnberg et al,. 2007 6. Yan et al,. 2007 3. Nelson et al,. 2011 7. Zhao et al,. 2014 4. Beveridge et al,. 1997b 8. Hamiaux et al,. 2012
	Class I Clp ATPase (HSP101 Chaperon like proteign)	Target of strigolactone signaling	SMXL6 SMXL7 SMXL8 [1]		D53 [2, 3]		1. Stanga et al,. 2013 2. Jiang et al,. 2013 3. Zhou et al,. 2013
		Target of Karrikin signaling	SMAX1 [1]		Os08g15231 [2]		1. Stanga et al,. 2013 2. Bennet et al,. 2013
(d) Transcriptional regulators	TCP Transcription Factor		BRC1 BRC2 [1]	PsBRC1 [2]	FC1/OsTB1 [3]		1. Aguillar-Martinez et al,. 2007 2. Braun et al,. 2012 3. Minacuchi et al,. 2010

Table 2 *Classification of genes involved in strigolactone* ***a.*** *biosynthesis,* ***b.*** *transport,* ***c.*** *perception and signaling and* ***d.*** *transcriptional regulators in Arabidopsis, pea, rice and petunia.* ***c.*** *Genes involved in karrikins signaling are mentioned too. Gaps do not indicate absence of genes in species. References for identification and cloning of the genes presented are shown in the last column.*

1.7.3 Strigolactones Perception and Signaling Pathway

The major role of the ubiquitin-proteasome system (UPS) in plant hormones signaling is well known for auxin, gibberellins and jasmonate (reviewed by Santner and Estelle, 2009). Recent identification of the components of strigolactone perception and signaling, including an α/β hydrolase fold protein, a Leucine-rich repeat (LRR) F-box protein and a Clp protease family protein (analyzed below), revealed that strigolactone also shares this targeted protein turnover though UPS signaling. However, the required enzymatic activity of the α/β hydrolase in parallel with its function as strigolactone receptor for the activation of the hormone transduction pathway is a novel mechanism (de Saint Germain *et al.,* 2013). A schematic representation of the strigolactone signaling pathway is displayed in Figure 8 while the genes involved are presented in Table 2.c.

The *OsD14/PhDAD2/AtD14* gene has been characterized as an α/β-fold hydrolase that recognizes strigolactones (Arite *et al.,* 2009; Hamiaux *et al.,* 2012; Nelson *et al.,* 2012) and interacts with *AtMAX2/OsD3/PhMAX2/PsRMS4* encoding for a member of the F-box *LRR* family (Beveridge *et al.,* 1997.b; Hamiaux *et al.,* 2012; Johnson *et al.,* 2006; Stirnberg *et al.,* 2007; Stirnberg *et al.,* 2002; Yan *et al.,* 2007; Zhao *et al.,* 2014). The F-box protein confers substrate specificity, acting as an adapter between the core subunits of the SCF (*Cullin* and *Skp*) complex and the target protein. The complex of OsD14 and OsD3 was recently shown to be completed with the identification of OsD53*,* a class I Clp ATPase protein, which acts as a repressor of strigolactone signaling (Zhou *et al.,* 2013). The strigolactone-induced degradation of OsD53 by the proteasome is a molecular link between perception of the hormone and its responses (Zhou *et al.,* 2013). The *Arabidopsis* orthologs were also identified; *AtSMXL6, AtSMXL7* and *AtSMLX8* (Stanga *et al.,* 2013). Finally, *AtBRC1, AtBRC2/OsFC1/PsBRC1* has been characterized as a plant-specific TCP transcription factor which acts as an integrator of hormonal signals, including strigolactones and cytokinins, controlling shoot branching (Braun *et al.,* 2012; Aguilar-Martínez *et al.,* 2007; Minakuchi *et al.,* 2010).

Karrikins are smoke-derived seed germination stimulants that have been shown to stimulate effects on seed germination and seedling photomorphogenesis, similar to strigolactones, in a *MAX2*-dependent manner (Nelson *et al.,* 2011). However, unlike strigolactones, karrikins do not impede axillary bud outgrowth in pea or *Arabidopsis*,

suggesting that *MAX2* has dual roles in the signaling of the two molecules (Nelson *et al.,* 2011). Even though karrikins and strigolactones share the same F-box protein in their signaling pathways, they have been shown to be perceived by a different α/β-fold hydrolase, AtKAI2/OsD14L (KARRIKIN- INSENSITIVE 2/ DWARF14-LIKE) in *Arabidopsis* and rice (Kagiyama *et al.,* 2013; Guo *et al.,* 2013; Zhao *et al.,* 2013). Karrikin signalling includes degradation of a class I Clp ATPase, similarly to strigolactone, which was recently identified to be encoded by *AtSMAX1* and *Os08g15230* in *Arabidopsis* and rice, respectively (Stanga *et al.,* 2013; Bennett and Leyser 2014).

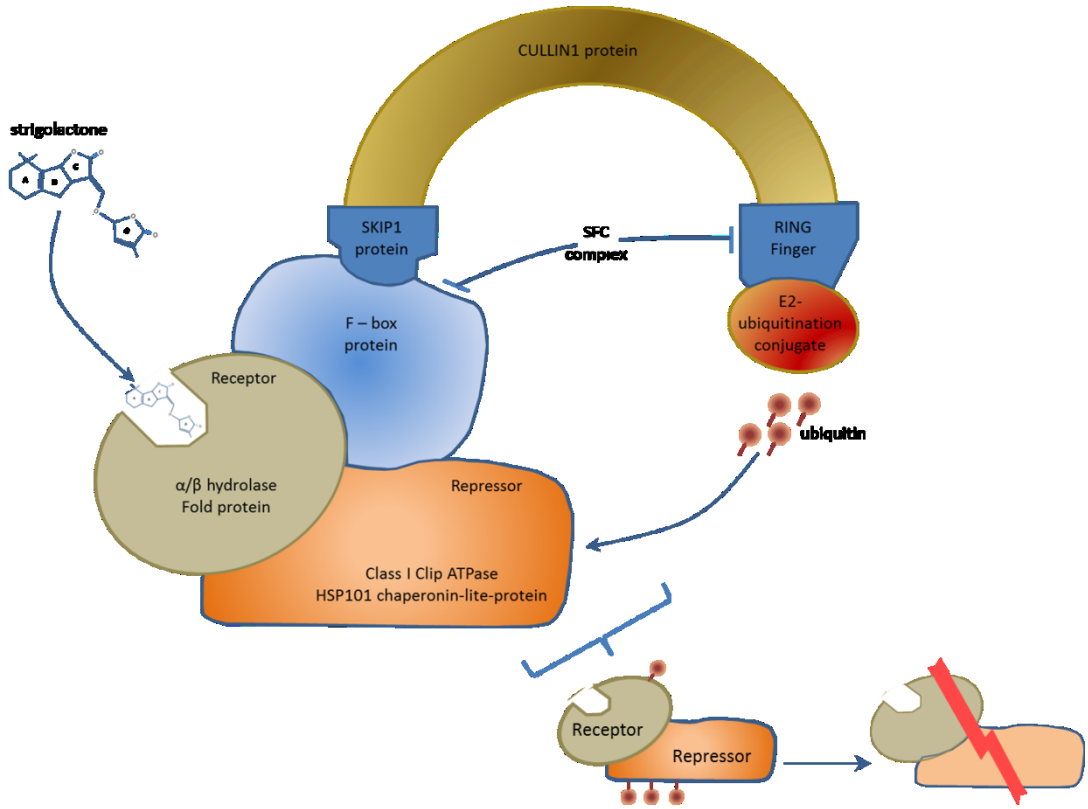

Figure 8 *Strigolactone signaling pathway. Strigolactone is perceived by an α/β hydrolase which then interacts with an F-box protein. The F-box protein then triggers the formation of a complex between SCF (SKIP1-CULLIN1-F-box) and the target protein which belongs to the Class I Clp ATPase family and it is a repressor of strigolactone signaling. The E2-ubiquitination conjugate then proceeds to the ubiquitination of the target protein and degradation by the proteasome. Once the repressor is degraded strigolactone signaling-mediated transcription can initiate.*

Chapter 2

Materials and Methods

2.1. Plant Materials and Growth Conditions

2.1.1 *Arabidopsis thaliana*

Seeds of wild-type *Arabidopsis thaliana* Col-0 and the *GFP* lines used in this study, *pWOODEN LEG: GFP (pWOL: GFP), pSCARECROW:GFP (pSCR:GFP), J2812:GFP, M0028:GFP* and *TCSn:GFP,* presented in Table 3, were surface-sterilized using 20% (v/v) bleach and 0.1% Tween for 5 min (2×2.5 min) and then rinsed five times with sterile distilled water. The sterilized seeds were then plated on solid Murashige and Skoog (MS) medium (0.44% MS medium [Duchefa], 1% Sucrose, 0.05% MES and 1% agar [Merck], pH 5.7 adjusted with KOH).

Transgenic Plant Line	GFP expression pattern	Reference	Source
M0028:GFP	Root cap, Columella, Initials and QC	Swarup et al., 2005	Karin Ljung
J2812:GFP	Epidermis and Cortex	www.plantsci.cam.ac.uk/Haseloff/	Karin Ljung
pSCR:GFP	Endodermis	Birnbaum et al., 2003	Philip Benfey
pWOL:GFP	Stele	Birnbaum et al., 2003	Philip Benfey
TCSn:GFP	Root Cap, Columella, Initials, QC and Stele	Zürcher et al., 2013	Bruno Müller

Table 3 *Transgenic Arabidopsis GFP lines used. Their expression patterns, the reference and the source of the seeds are also presented.*

For the collection of larger amounts of root material for cell sorting and apoplastic fluid collection, seeds were sown at high density (100 seeds per row) on a sterilized nylon mesh (Sefar Nitex, 03-110/47) placed on the solid MS medium. After vernalization at 4°C for 3 to 4 days, the plates were placed vertically under 150 mE light in long day conditions (16 h of light, 8 h of darkness) at 22°C and grown for 8 days before harvesting.

2.1.2 *Pisum sativum*

The wild-type cultivars Parvus (L77) and Térèse provided by Colin Turnbull and Catherine Rameau respectively were grown in 100% well-wetted vermiculite for 7 to 12 days, as mentioned for each experiment. Thus the seedlings were developed utilizing the nutrients provided by the cotyledons while the root remained clean from soil and therefore could be rinsed and used in experiments. 20 seeds were placed each 20×20 cm square pot in 2-3 cm below the surface. When plants were grown for 3 weeks, as stated in the respective experiment of xylem and phloem extraction, two seeds were placed in each 10×10 cm square pot filled in 3/4 with a mix of soil and vermiculite (1:4) and the top 1/4 of the pot with 100% vermiculite to maintain the epicotyl area clean for xylem extraction. All cultivars were grown at 23°C/15°C, 16 h light/8 h dark photoperiod, under a light intensity of 300 *mmol/m^2s.*

2.2. Fluorescence Activated Cell Sorting (FACS)

Flow cytometry is the only method with which single cells can be assessed, categorized according to the desired criteria (size, fluorescence and granularity) and sorted into single-cell units or in our case in homogeneous groups. The system can be distinguished in three sequential parts: Fluidics, optics and detectors.

The fluidic system is responsible for the flow of the sample in the instrument which is achieved by hydrodynamic focusing. The crucial role that they come to play is when sheath fluid and sample arrive to the flow cell where they merge, centered into a pressurized stream and pass through a single cell-sized 100 µM nozzle (flow tip). At the same time, a piezoelectric actuator attached to the flow cell induces droplet formation, as a result of surface tension. Finally, an electrical charge is applied to the stream at the exact point when the forming droplet detaches from the main stream. The charged droplets meeting the criteria set by the user end up in the appropriate collection tube as they pass by an electrostatic field generated by deflection plates which attract or repulse it.

The advantage of setting criteria in order to collect a homogeneous population is due to the optics and detectors part of the system. The charged droplets coming out of the flow cell are then arrested by an intense light source (optics). The FACSAria instrument used provides three lasers, a 405 nm (violet), a 488 nm (blue) and a 633 nm (red). For sorting of *GFP* lines

only the blue laser was required. Since the cells are able to absorb and scatter light, they are at this point interrogated and according to their forward and side scatters (axial and perpendicular light scatter to the laser beam, FSC and SSC) their relative size and complexity or granularity are defined respectively. Also at this interrogation point the cells' endogenous fluorochromes and/or the ones that have been transgenically imported (*GFP*) emit fluorescent signal.

The scattered light and/or the emitted fluorescence are then gathered and directed individually for each laser to photomultipliers (PMT). This occurs by special filters of the PMTs that are able to separate the photons of the excitation light in accordance with their energy and allocate them to the respective photodetectors. The detectors convert the photons into electrons which are then interpreted and recorded by the computer as a digital value.

A schematic representation of FACS is presented in Figure 9.

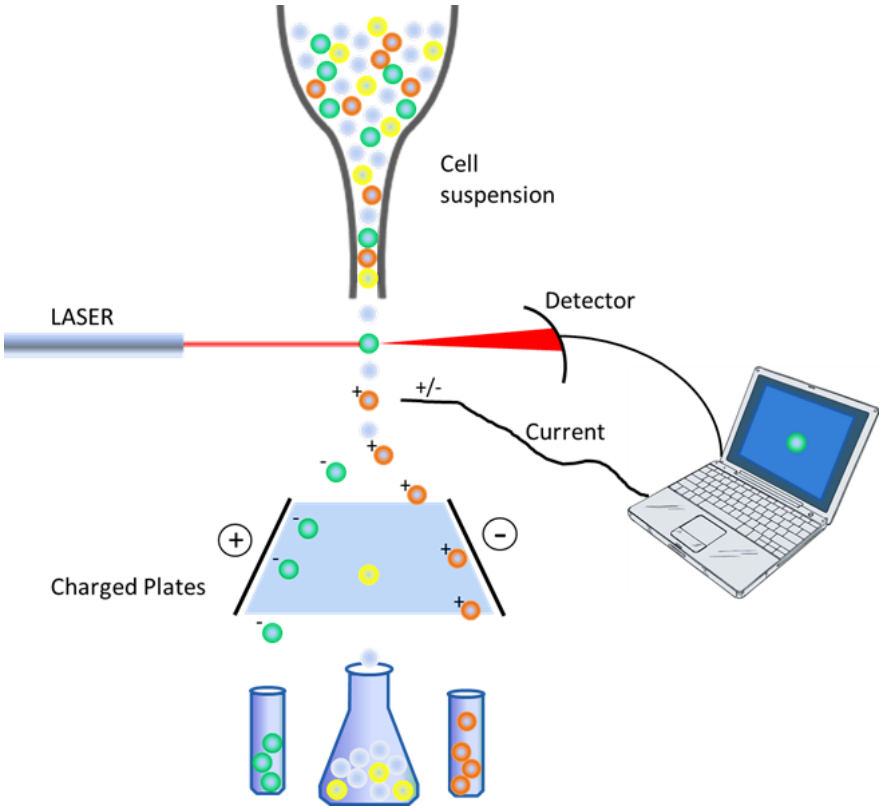

Figure 9 *Schematic representation of how Fluorescent Activated Cell Sorting (FACS) works. Cells are loaded into the flow cytometer. They are forced to pass one by one cell from an interogaion point where their light emision is triggered by lazers. The excitation of each cell according to its fluoresence and forward and side scatter are perceived by detectors and the information is sent to the computer. The computer classifies the information according to the desired criteria that have been initially set and sends a respective current to the cells that need to be collected (blue and red cells). The ionised cells pass through an electric field created by two oppositely charged plates and the positive and negative cells are respectively collected into different tubes. The cells not fitting with the criteria set are not being charged and therefore result in the waste (white and yellow cells).*

2.3. Cytokinin Quantification

Extracts from plant tissue constitute a complicated mixture of many components. The presence of cytokinins in this mixture occurs in minute amounts (less than 50 pmol/g FW). Therefore the quantification of the endogenous levels of the hormone requires intensive extraction and purification of the hormone resulting in chemical background reduction, as well as sensitive and sufficiently selective analytical tools. Research in plant hormone quantification field has established liquid chromatography combined with mass spectrometry as the best method for cytokinin quantification (van Rhijn *et al.,* 2001; Novák *et al.,* 2003; Dobrev and Kamínek 2002).

2.3.1 Cytokinin Extraction from plant tissues

The tissue was quickly weighed on 0.0001g balance and snap frozen in liquid N_2. The frozen tissue was grinded to powder using liquid N_2. Then 10 ml/g of tissue fresh weight (FW) of cold (4°C) extraction solvent (HPLC grade methanol /formic acid/water; 60:5:35 and 35 mg/L 5'AMP; Sigma A2252) along with 10 ng/g of FW deuterium-labeled cytokinin internal standards ($[^2H_5]$Z, $[^2H_5]$ZR, $[^2H_5]$ZRP, $[^2H_3]$DHZ, $[^2H_3]$DHZR, $[^2H_6]$iP, $[^2H_6]$iPR, $[^2H_6]$iPRP, $[^2H_5]$tZ9G, $[^2H_3]$DHZ9G and $[^2H_6]$IP9G; OlChemIm) were added and mixed in the sample. The samples were transferred into 15 ml falcon tubes and centrifuged at 10,000×g for 20 min at 4^{o}C. The collected supernatant-extract was passed through 5 ml "Sep Pak C18" cartridges ("Vac 500 mg 6 ml"; Waters) which have been previously washed with 5 ml HPLC grade methanol. These cartridges have high hydrolytic activity and are used for the solid-phase extraction on the basis of reversed-phase interactions and thus they attach hydrophobic compounds such as lipids and pigments. After passing through the cartridge the sample was collected in 10 ml glass tubes.

2.3.2 Cytokinin Purification

The samples after the extraction step described above were evaporated up to 1 ml in order to remove the organic constituent from the extract which would cause washing of the polar cytokinins. Then, 4 ml of 1M formic (pH 1.4) was added causing positive ionization of the cytokinin metabolites. The samples were then washed through ''Oasis MCX 150 mg 30 μm" cartridges (Waters p/n 186000256) which have been previously washed with 5 ml 1 M formic

acid. These columns have a mixed character of both reverse-phase and cation-exchange so the ionized cytokinins were retained in the cartridge. The cartridge was washed again with 5 ml 1M formic acid to secure the charge. A second wash of the column with 5 ml HPLC grade methanol removes the neutral hydrophobic compounds, like IAA and ABA. The cytokinin nucleotides are retained to the column because of electrostatic forces. Finally, cytokinins were eluted with the addition of 5 ml 0.35 M ammonium hydroxide in 60% HPLC grade methanol. The solution drastically increased the pH to 11 establishing favorable conditions for elution of cytokinins which were collected in 10 ml glass tubes.

2.3.3 Preparation of the purified cytokinins for LC-MS/MS analysis

The eluates containing the purified cytokinins were fully evaporated and redissolved in 100 µl HPLC grade methanol in which all cytokinins were dissolved efficiently and transferred into an Eppendorf tube. The samples were centrifuged at full speed for 10 min at room temperature, the collected supernatant was filtered through 0.45µm×4mm diameter syringe filter and finally collected into auto-sampler vial suitable for LC-MS (12x32 mm with 300 µl fused glass insert, silicone/PTFE septum, screw cap with injection hole e.g. Chromacol vial Cat 3-FISV with Cat 9-SC(B)-ST1 cap). The syringe filter was rinsed with 100 µl HPLC grade methanol to collect any remaining cytokinins which was then added to the sample vial. After complete evaporation, the dried samples were re-dissolved in 200 µl of 10mM ammonium acetate buffer (pH 3.3) with 5% acetonitrile which was the mobile phase buffer for the respective LC-MS/MS analysis.

2.4. Liquid Chromatography Mass Spectrometry (LC-MS/MS)

Quantitative analysis of natural isoprenoid cytokinins in Pea tissue and extracted saps was achieved by coupled an Agilent 1100 Binary LC system and an Applied Biosystems Q-Trap hybrid mass spectrometer (MS) fitted with a TurboIonspray (electrospray). LC-MS/MS analysis was performed as described by Foo *et al.,* (2007) utilizing a solvent gradient of acetonitrile in 10 mM ammonium acetate, (pH 3.4) (mobile phase/solvent A: 5% acetonitrile in 10 mM ammonium acetate, solvent B as 95% acetonitrile in water with 0.1% formic acid for a solvent program (A): initially 5% for 4 min, ascending to 14% at 20 min and finally rising

to 32% at 25 min (respectively solvent program B: 0%, then 15% and finally 35%); Flow rate was at 200 µL/min. The chromatography column used in the HPLC system was a 32 Phenomenex 3 µm C18 Luna 100 x 2-mm column with guard column heated to 40^{o}C. Source operation was in positive ion multiple reaction monitoring (MRM) mode with dwell time 30 mins for each MS-MS ion pair. The injected volume ranged from 10 – 80 µl depending on cytokinin levels. Scheduled scan mode where each MRM signal is scanned only for a 2 or 4 minute window centered on the expected retention time of the target compound, facilitated enhancement of signal to noise ratio. Cytokinin transitions representing mass-to-charge ratio and retention times are described in Table 4.a. The d-standard corresponding in each cytokinin compound for calculations is presented in Table 4.b

a.		Expected Positive Ion		Retention Time
Name	MW	Parent	Daughter	~min
cZ	219	220	136	9.23
d-tZ	224	225	136	9.43
tZ	219	220	136	9.75
d-DZ	224	225	136	10.21
DZ	221	222	136	10.59
d-Z9G	386	387	225	11.51
Z9G	381	382	220	12.08
d-ZRP	436	437	225	12.01
d-DZ9G	386	387	225	12.18
ZRP	431	432	220	12.21
DZRP	433	434	222	12.27
DZ9G	383	384	222	12.33
cZRP	431	432	220	13.37
d-tZR	356	357	225	16.81
tZR	351	352	220	16.95
d-DZR	356	357	225	17.24
DZR	353	354	222	17.26
cZR	351	352	220	17.91
d-IP	209	210	136	21.24
IP	203	204	136	21.48
d-IP9G	371	372	210	21.79
IP9G	365	366	204	22.01
d-IPRP	421	422	210	22.51
IPRP	415	416	204	22.75
d-IPR	341	342	210	26.28
IPR	335	336	204	26.37

b. Correspondence between cytokinin d-standards and respective compounds	
Endogenous Compound	Labelled Compound
cZ	d-tZ
cZR	d-tZR
cZRP	d-ZRP
DZ	d-DZ
DZR	d-DZR
DZRP	d-ZRP
IP	d-IP
IPR	d-IPR
IPRP	d-IPRP
tZ	d-TZ
tZR	d-tZR
ZRP	d-ZRP
DZ9G	d-DZ9G
IP9G	d-IP9G
Z9G	d-Z9G

Table 4 a. *Labelled and endogenous cytokinin compounds identified through LC-MS/MS. The respective molecular weight (MW), expected parent and daughter positive ions and retention time (min) are also displayed.* ***b****. Correspondance between the endogenous cytokinin compounds detected and the labelled d-standards for calculation of the cytokinin concentration.*

2.5. Statistics

Statistical analysis has been performed using R 3.1.1 (http://www.R-project.org/). Different statistical tests have been used depending of the analysis: (i) the Student t-test have been used to compare either two independent samples with different treatments or paired samples as indicated in each Figure (star display: p-value <0,05 *; p-value <0,01 ** ; p-value <0,001 ***) (ii) ANOVA followed by the post-oc test Tukeys (pairwise comparison of mean) have been used when more than two samples per analysis were considered (letter display: 5% level of confidence).

Chapter 3

Detailed analysis of local and long-distance transported cytokinin metabolites in tissues and vascular saps of Pisum sativum ecotypes.

3.1 Introduction

The natural cytokinins can be distinguished in two main groups: the isoprenoid cytokinins, being highly abundant in plants, and the aromatic cytokinins present at much lower concentrations (reviewed in Zalabák *et al.,* 2011). Therefore in the current study only isoprenoid cytokinins were examined as the main representatives of this phytohormone.

Cytokinin metabolism is finely tuned as mentioned in Chapter 1.3.2. Briefly, cytokinins can be divided into three main groups according to the metabolic step that they represent: the firstly biosynthesized nucleotides (IPRP, tZRP, DZRP and cZRP) representing cytokinin precursor forms, the ribosides following after the respective dephosphorylation step (IPR, tZR, DZR and cZR) and the cytokinin nucleobases (IP, tZ, DZ, cZ) produced either from dephosphorylated ribosides or directly from nucleotides as a result of catalysis by LOG enzymes. The cytokinin ribosides tZR and IPR and all the nucleobases have been used in studies and shown to bind to cytokinin receptors with different affinities (Romanov *et al.,* 2006; Spíchal *et al.,* 2004; Stolz *et al.,* 2011; Yonekura-Sakakibara *et al.,* 2004). Therefore they are considered as bioactive cytokinin forms. Cytokinin glucosyl-conjugates, which were also quantified in the current work, are categorized in two groups, the O- and N- glucosides, and they have both displayed no activity in receptor binding assays. However, while the N-glucosides are irreversibly inactive forms of cytokinin, the O-glucosides can be reconverted to the bioactive cytokinin nucleobases. Another way to group/categorize cytokinin

metabolites is according to the differences in their isoprenoid chain: IP-, tZ-, DHZ- and cZ-compounds.

The cytokinin forms predominant in most plant material analysis are tZ- and IP-types and their respective nucleobases tZ and IP are the ones also presenting the highest affinities to the cytokinin receptors (Stolz *et al.,* 2011). IP- and tZ- cytokinins have been also suggested to be transported through phloem and xylem, respectively (Hirose *et al.,* 2008; Matsumoto-Kitano *et al.,* 2008). However, studies in maize and pea have shown important roles of DZ and cZ at particular developmental stages and/or processes (Quesnelle and Emery, 2007; Zalabak-Galuska unpublished, reviewed in Zalabák *et al.,* 2011). For example xylem-derived tZR was found to negatively regulate adventitious root formation in cucumber (Kuroha *et al.,* 2002).

For the above mentioned reasons, it is difficult to consider only one representative compound when talking about cytokinins, as can be done with IAA as the main active auxin form. To conclude, cytokinin metabolism is highly interconnected, compound homeostasis is rapidly and highly adjusted by several enzymatic processes to maintain their right concentration related to their roles and/or activity as indicated in Figure 2 (Chapter 1.3.2.)

In this Chapter endogenous cytokinin levels are presented in the form of a detailed tissue map of pea (*Pisum sativum*) to provide basic knowledge on the distribution of cytokinin metabolites within the plant. The reason why this study was done in Pea is not only because it is a legume crop and therefore it is economically important, but also because molecular tools are now available in pea. A detailed genetic map with several genetic markers is available, high throughput forward and reverse genetic tools in pea have been constructed recently with a TILLING population available combined with a database with the respective information of the phenotype and sequence of the mutant genes (Dalmais *et al.,* 2008) and its transcriptome sequence has been recently completed (http://www.biomedcentral.com/1471-2164/13/104). Finally but most importantly for this study, pea is the only plant species until now that has been reported to have *RMS2*, a gene controlling feedback signal regulation of long-distance transported cytokinins (Foo *et al.,* 2007).

This study can be further used as the basis for understanding specific functions of the hormone in these individual tissues analysed. Until now assumptions about cytokinin distribution have been based mainly on gene expression studies (reviewed by Hirose *et al.,* 2008) but here the actual concentration of the hormone metabolites is presented.

3.2 Aims

The aim of this Chapter was to examine if and how the distribution of cytokinin metabolites varies between specific tissue parts and fluids of pea. This information is important because specific cytokinin compounds have been suggested to be linked with particular biological functions.

3.3 Materials and Methods

3.3.1. Plant materials

All the experiments performed in this Chapter concerned the two cultivars of Pea, cv. Parvus and cv. Térèse. Cv. Parvus was used for most of the experiments being the main cultivar under study. Cv. Térèse was used additionally in some similar experiments to distinguish between general trends of cytokinin compounds among tissues in pea and trends that concerned the specific variety. More information concerning the plant material used in this Chapter is described in Chapter 2.1.2

3.3.2. Growing conditions

For the tissue experiments, seedlings were harvested either 7 or 12 days after sowing (as indicated for individual experiments in 3.4). Therefore they were only planted in 100% vermiculite which provides great advantages when working with Pea. Until that age peas supply their needs for nutrients from the cotyledons so soil and composts can be avoided. This feature facilitated the harvesting of clean root tissue without the need of media and sterile conditions like with *Arabidopsis*. Only when cv Parvus was grown during three weeks for xylem and phloem sap collection the seeds were planted in soil in order to develop a bigger root and shoot system which would result in higher volumes of xylem and phloem sap collected, respectively. The seeds for this sap isolation experiment were placed on a mixture of F2s Levington compost:vermiculite (4:1) which filled ¾ of the pot and then covered the remaining ¼ of the pot with vermiculite to maintain the epicotyl area as clean as possible for xylem collection procedure.

All plants were grown in Fitotron controlled environment cabinets (Weiss-Gallenkamp, Loughborough, UK), with photoperiod 16h/8h day/night (the light was provided by cool white fluorescent tubes supplemented with incandescent lamps, providing total PAR of approximately 300 µmol/m^2s) , temperature23°C/15°C and relative humidity of 55%/60%.

3.3.3. Tissues isolation

For isolating specific tissue samples the process mentioned below was followed. The entire plants were extracted from the vermiculite, gently washed under running water to get rid of any remaining vermiculite and placed in glass-beaker containing MilliQ water. The plants were then dried from the excess of water by transferring them onto absorbent paper. By using a scalpel the desired tissue was excised, weighed, wrapped in aluminum foil and frozen in liquid nitrogen. To isolate mm of root segments, roots of Parvus were aligned and cut with a tool which had five razor blades with specific adjustable width in between them. The segments collected included the cellular division zone (0-6 mm), continuing with 6-16 mm root segment that could correspond to the elongation zone, 16-26 mm, 26-36 mm and 36-46 mm as the cellular maturation zone and two more segments 0-10 mm above the first emerged lateral root and 10-20 mm above the first lateral root including more mature lateral roots. A schematic representation is presented in Figure 10.

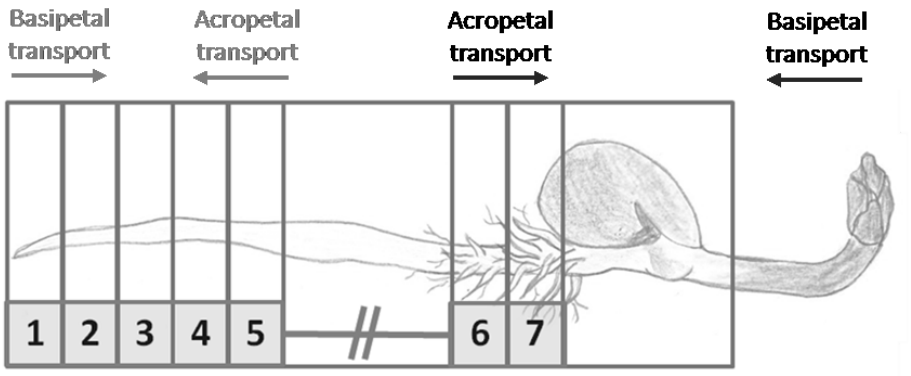

Figure 10 *Root segments as isolated from 7 days old Parvus seedlings. The cell populations present in these root segments are the epidermis, the cortex and the stele. The latter one includes the endodermis, the pericycle, the proto- and meta-xylem, the proto- and meta-phloem and the (pro)cambium.* ***1.*** *0-6 mm root segment: Root tip including cellular division zone and part of cellular elongation zone. Additional cell populations in the root tip are the root cap, columella, initials and QC.* ***2.*** *6-16 mm root segment: Cellular elongation zone,* ***3.*** *16-26 mm root segment: Cellular maturation zone,* ***4.*** *26-36 mm root segment: Cellular maturation zone,* ***5.*** *36-46 mm root segment: Cellular maturation zone ,* ***6.*** *0-10 mm above the first lateral root segment: immature lateral root zone,* ***7.*** *10-20 mm above the first lateral root segment: mature lateral root zone and end of the root tissue. The root parts between 5 and 6 were not examined.*

3.3.4 Xylem sap isolation

Xylem was isolated with the syringe-suction method as described in Beveridge *et al.,* (1997.a) with some modifications. The evening prior to xylem sap collection the plants were thoroughly watered to ensure maximum volumes of vascular sap. Pea stems were cut off with a razor blade at the epicotyl site. The section was rinsed with distilled water to avoid contamination by sap deriving from damaged cells. A flexible silicon tube attached to a 2 ml syringe was applied to the decapitated plant which was still rooted. The diameter of the tube varied according to the epicotyl diameter. To ensure an airtight connection the tube was also tied strongly in place. The syringe plunger was then gently pulled out and held at position to create vacuum in the syringe for 2 h. The procedure took place in normal growth conditions for pea described in Chapter 2.1.2. The extracted xylem sap was then transferred into an Eppendorf tube which was frozen in liquid nitrogen and stored at −80°C.

3.3.5. Phloem sap isolation

For phloem exudates isolation the pea stems, having been detached to facilitate xylem sap collection described in Chapter 3.3.4., were used. The method followed was slightly modified from Marentes and Grusak, (1998). The excised shoots (3-4 per sample), including all aerial pea parts above the epicotyl, were placed for 5 min to a 15 ml falcon tube containing 10 ml of exudation solution (10 mM Na_2EDTA, pH 8.0) to allow initial exudation and rinsing avoiding contamination deriving from damaged cells. The stems were then transferred in clean falcon tubes filled with 10 ml of the exudation solution and placed in transparent closed box to maintain high humidity levels and low transpiration rates. The boxes were placed back in the growth chamber of peas for 12 h. The shoots were then removed from the falcon tubes and the exudates were closed and frozen in liquid nitrogen and stored at −80°C.

3.3.6. Cytokinin purification and quantification through LC-MS/MS

Cytokinin extraction, purification for the isolated tissue samples (Chapter 3.3.3) was done as described in Chapters 2.3.1 and 2.3.2. Cytokinins deriving from the isolated samples from phloem and xylem sap had no need for extraction or even purification since the exudates were much cleaner samples than the plant tissue ones.

Each extracted xylem sap sample derived from a pool of at least three plants. The mixture of d-standard cytokinins (5 ng of each labelled compound) was added to each xylem sap sample which was then passed through a syringe-filter (0.45 μm × 4 mm), collected in an autosampler vial suitable for LC-MS/MS analysis and proceeded for cytokinin quantification.

Each phloem exudate sample derived from at least three plants and undergone through a process described below to get rid of EDTA since it can cause technical problems in the LC-MS/MS analysis. Therefore, C-18 cartridges were prepared by washing with 5ml methanol and then 5 ml of milliQ water. The phloem exudates, after the addition of cytokinin standards mixture (5 ng of each labelled compound), were passed through the column. The cartridges were washed again with 5 ml of milliQ water and phloem cytokinins were finally eluted with 5 ml of 70% methanol. The eluates followed the preparation for LC-MS/MS procedure as described in Chapter 2.3.3.

Quantification of cytokinins derived from tissue samples and saps was performed as described in Chapter 2.3.3 and 2.4. For all experiments three biological replicates were examined. The concentration of cytokinin was calculated in pmol/g of tissue fresh weight for the tissue samples and in pmol/number of plants for the vascular sap samples.

3.3.7. CKX enzymatic activity measurements

The samples derived from the sectioning of pea root described in Chapter 3.3.3., Figure 10, were also checked for CKX enzymatic activity using [^{3}H]iP as substrate. The enzymatic assay was performed kindly by our collaborator Dr. Vaclav Motyka in IEB Prague (institute of experimental botany). The substrate used was 2 μM [^{3}H]iP, the equivalent enzyme per assay was 15 mg and the reaction buffer was TAPS-NaOH + DPIP (pH 8.5). The reaction was incubated for 1 hour and the separation of iP from adenine was done by HPLC (Petr Dobrev). The results were calculated as nmol of Adenine produced per g of tissue fresh weight per hour of reaction.

3.4 Results

In this section quantification of cytokinin metabolites in distinct tissue parts and saps of Pea is presented. The aim was to create a basic level of understanding of the distribution of cytokinins across the plant.

3.4.1 Long-distance transported cytokinins

As mentioned in Chapter 1.5.2 and 1.5.3 cytokinins can act as local or long-distance signals. Basipetally and acropetally moving cytokinins derived from the same plants were quantified by isolating phloem and xylem sap, respectively, from cv. Parvus.

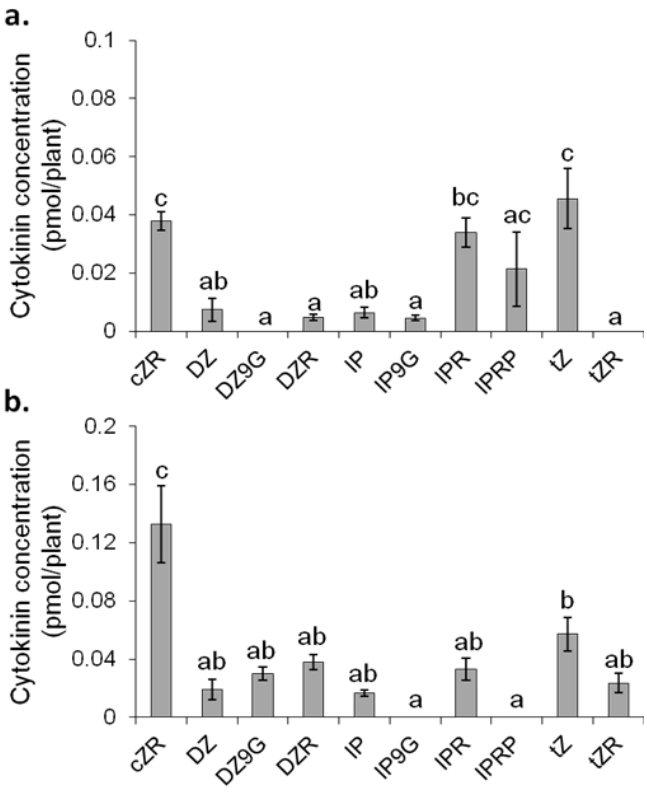

Figure 11 *Quantification of* ***a.*** *Phloem and* ***b.*** *Xylem cytokinins of 3 weeks old cv. Parvus. Each sample derived from a pool of at least 3 plants and 3 biological replicates were analyzed. The error bars indicate the standard error (n=3). The xylem and the respective phloem were extracted from the same pool of plants. The concentration of cytokinin was calculated in pmol and normalized to the number of plants used. Statistical analysis was performed using ANOVA and Tukey's test.*

As shown in Figure 11, most of the cytokinin compounds were present in both the xylem and phloem sap of cv. Parvus. The ribosides cZR, IPR and the nucleobase tZ predominated in cv. Parvus phloem followed by IP and DZ. In the respective xylem sap samples, cZR was the main cytokinin form followed by tZ. While IP9G and IPRP were below the detection limit in the xylem, the same was the case for DZ9G and tZR in the corresponding phloem samples.

Xylem and Phloem cytokinins were also quantified in 12 days old seedling of cv. Térèse in order to identify common features between the two saps regardless the Pea cultivar.

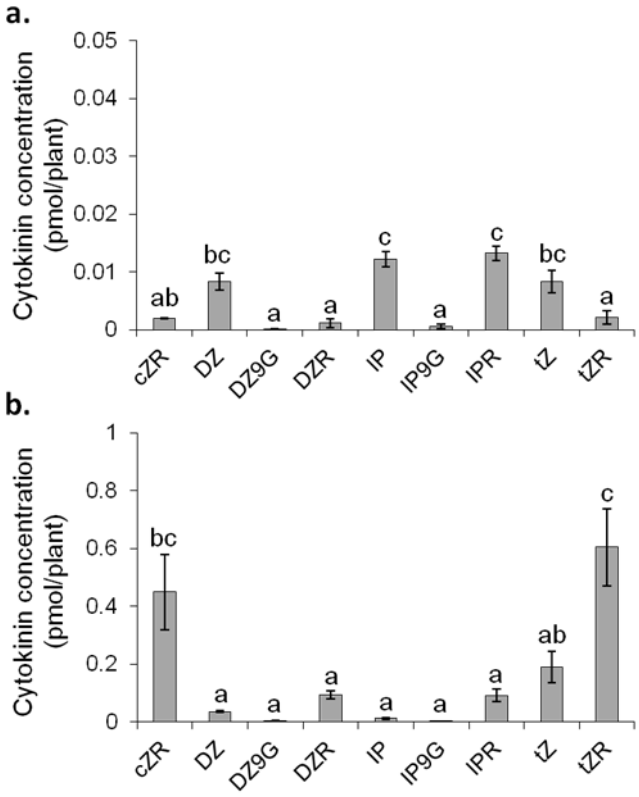

Figure 12 *Quantification of* ***a.*** *Phloem and* ***b.*** *Xylem sap cytokinins in 12 days old cv. Terese seedling. Each sample derived from at least 3 plants and 3 biological replicates were analyzed. The error bars indicate the standard error (n=3). The xylem and the respective phloem were extracted from the same pool of plants. The concentration of cytokinin was calculated in pmol and normalized to the number of plants used. Statistical analysis was performed using ANOVA and Tukey's test.*

As displayed in Figure 12, the cytokinin glucoside DZ9G was below the detection limit only in the phloem sap while IP9G was not detected in the xylem, in agreement with the results in cv. Parvus. IP and IPR followed by tZ, DZ and finally cZR were the principal forms in cv. Térèse phloem sap (Figure 12.a.) while in the xylem sap tZR was mainly enriched followed by cZR and less by tZ.

Common trends between cv. Parvus and cv. Térèse concerning the prevalent basipetally transported cytokinins were identified for the ribosides IPR and cZR and for the nucleobases tZ and DZ. Respectively, for the acropetally moving cytokinin forms similar tendencies were observed for cZR and tZ potent presence.

3.4.2 Cytokinin metabolites quantification in sequential tissue parts along the plant.

Quantification of cytokinin metabolites was performed in sequential distinct parts of Pea to understand the distribution of the hormone scanning from shoot to the root. Cytokinin quantification has been performed on shoot, junction and root. Tissues were isolated from 12 days old cv. Parvus and cv. Térèse (Figures 13 and 14 respectively). The results deriving from these experiments were organized in graphs according to compounds concentration levels and when possible to their role in cytokinin metabolism. For example the graphs **a**., **b**., and **c**., in both Figures 13 and 14 represent IP- and tZ-nucleotides, ribosides and nucleobases, respectively.

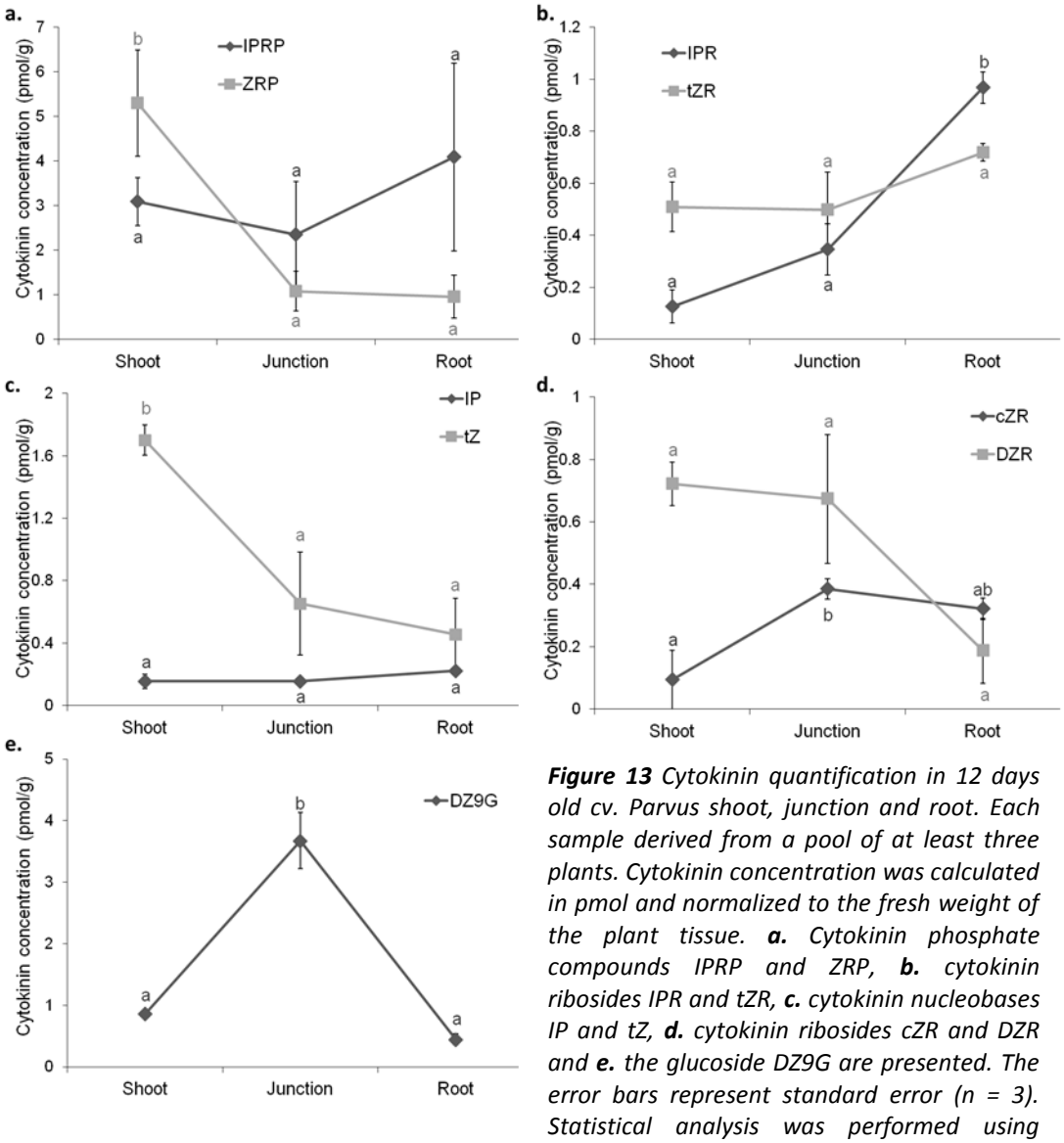

Figure 13 *Cytokinin quantification in 12 days old cv. Parvus shoot, junction and root. Each sample derived from a pool of at least three plants. Cytokinin concentration was calculated in pmol and normalized to the fresh weight of the plant tissue.* ***a.*** *Cytokinin phosphate compounds IPRP and ZRP,* ***b.*** *cytokinin ribosides IPR and tZR,* ***c.*** *cytokinin nucleobases IP and tZ,* ***d.*** *cytokinin ribosides cZR and DZR and* ***e.*** *the glucoside DZ9G are presented. The error bars represent standard error (n = 3). Statistical analysis was performed using ANOVA and Tukey's test.*

In the cv. Parvus, the predominant forms identified per tissue were IPRP in the root, DZ9G in the junction and tZRP in the shoot (Figure 13.a and 13.e). tZRP was also found in all tissues but its abundance was significantly lower in the junction and root compared to the shoot (Figure 13.a). Surprisingly, IPRP and IP didn't show any difference among the different tissues when IPR was identified as an increasing gradient from shoot to root. Unlike tZR which has been measured with a similar concentration in the different tissues, tZRP and tZ displayed an opposite trend with IPR with and increasing gradient from root to shoot (Figure 13.b and 13.c). DZR concentration showed a trend of reduction towards the root while cZR was increased in the junction compared to the shoot as it can be seen in Figure 13.d. DZ9G, being the only glucoside detected well in cv. Parvus, displayed a significant Peak at the junction tissue (Figure 13.e).

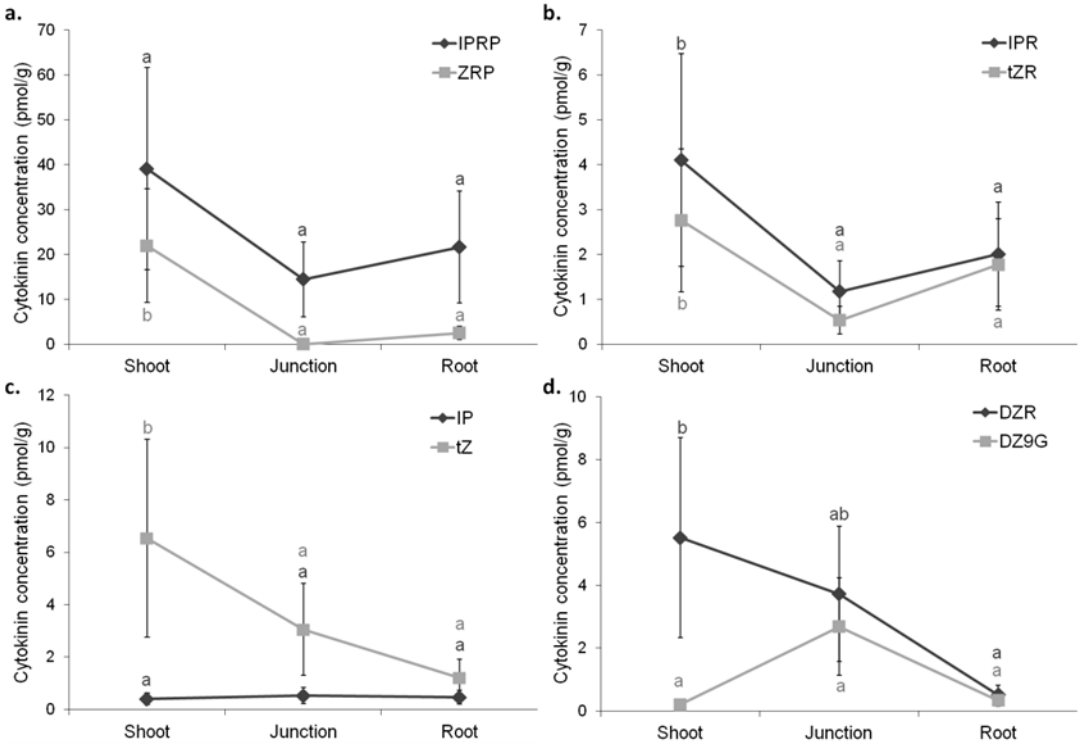

Figure 14 *Cytokinin quantification in 12 days old cv. Terese shoot, junction and root. Each sample derived from a pool of at least three plants. Cytokinin concentration was calculated in pmol and normalized to the fresh weight of the plant tissue.* ***a.*** *Cytokinin phosphate compounds IPRP and ZRP,* ***b.*** *cytokinin ribosides IPR and tZR,* ***c.*** *cytokinin nucleobases IP and tZ and* ***d.*** *the cytokinin riboside DZR and the glucoside DZ9G are presented. The error bars represent standard error (n = 3). Statistical analysis was performed using ANOVA and Tukey's test.*

Compared with cv. Parvus, cytokinin distribution of IPRP, IP, tZRP, tZ and DZ9G showed similar trends in the same tissues of cv. Térèse, as presented in Figure 14. In cv. Térèse, IPRP was consistently the most abundant compound across the plant while tZRP levels were high in the shoot but lower towards the junction and root tissues (Figure 14.a). Interestingly, IPR and tZR followed similar trends by having increased levels in the shoot (Figure 14.b) which is, compare to cv. Parvus a completely opposite distribution of these metabolites. tZ was measured with a higher concentration in the shoot and IP was found equally distributed between the tissue as observed in cv. Parvus (Figure 14.c). DZR displayed a gradual and significant reduction of its levels from shoot to root as observed only as a tendency in the cv. Parvus. Such as in the cv. Parvus, the highest concentration of DZ9G was retrieved in the junction but it showed no significant difference was observed when compared to the other tissues of the cv. Térèse (Figure 14.d).

Among the tissues analysed, cytokinin metabolites have been found equally or unequally distributed in the previous experiment (Figure 13 and 14). Some compounds displayed predominant trends in specific tissues. This is why next a more detailed analysis was performed including the sequential tissues of shoot, first node and internode, epicotyl, hypocotyl and root, isolated from cv. Parvus 12 days after sowing (Figure 15).

As presented in Figure 15.a IPRP was the predominant cytokinin form in most tissues but showed reduced concentration in the tissues of epicotyl and hypocotyl. tZRP showed few variations among the tissues but were not significant. tZR have been indeed preferentially found into the root when IPR was mainly found into the hypocotyl and the root. IP displayed elevated levels in the tissues of first node and internode and root showing similar trend to IPRP. The concentration of the nucleobase tZ presented significant difference among the tissues with high levels in the shoot tissue, significantly decreasing in the first node and internode and epicotyls. A strong concentration has been measured in the hypocotyl and a lower level in the shoot (Figure 15.c). It is also observed that IPRP and tZRP follow similar distribution into the cv. Parvus. Subsequently, IPR and tZR also follow the same distribution with a preference in the root tissues. However IP and tZ the bioactive forms display a different distribution compare to their direct precursor IPR and tZR. Especially tZ showed a strong concentration in the shoot (Figure 15.c). The riboside cZR was stably present along the plant tissues while DZR displayed a significant peak in the shoot (Figure 15.d). cZR and especially DZR presented an antagonistic distribution compared to the other riboside forms, IPR and tZR. As previously observed DZ9G presented high concentration in the hypocotyl

where DZ levels were at the lowest concentration. DZR and DZ appeared to be correlated being abundant in the shoot and then significantly reduced in all the other tissues analysed.

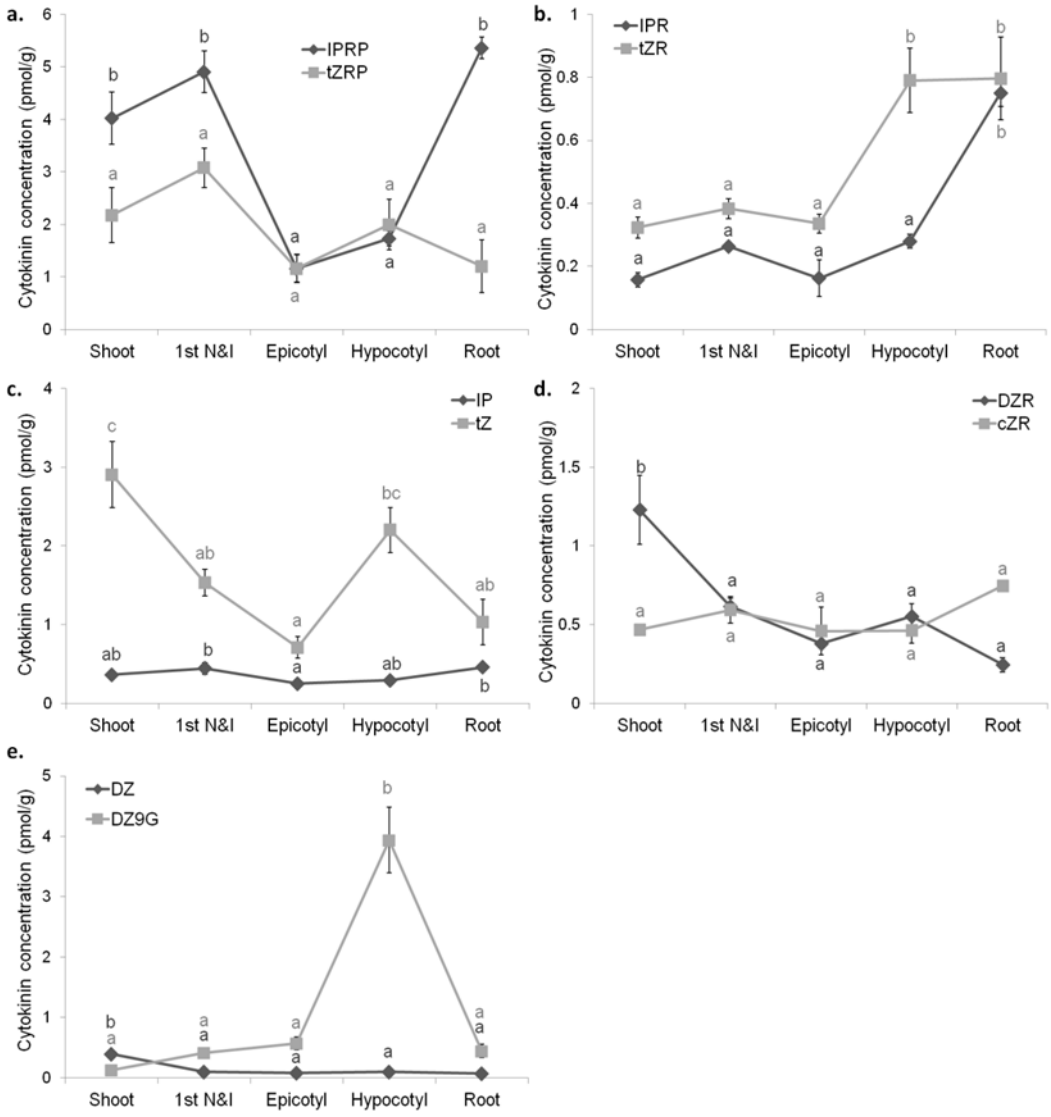

Figure 15 *Cytokinin quantification in 12 days old cv. Parvus shoot, first node and internode (1st N&I), epicotyl, hypocotyl and root.* ***a.*** *cytokinin phosphate compounds IPRP and ZRP,* ***b.*** *cytokinin ribosides IPR and tZR,* ***c.*** *cytokinin nucleobases IP and tZ,* ***d.*** *cytokinin ribosides cZR and DZR and* ***e.*** *the glucoside DZ9G and the nucleobases DZ are presented. Each sample derived from a pool of at least 3 plants. Cytokinin concentration was calculated in pmol and normalized to the fresh weight of the plant tissue. The error bars represent standard error (n = 3). Statistical analysis was performed using ANOVA and Tukey's test.*

3.4.3 Detailed analysis of cytokinin distribution along the root tissue

As described in the previous chapter, cytokinin metabolites distribution appeared to be tightly dependent on the tissue analyzed (e.g. DZ9G in the hypocotyl). It might also be dependent of the differentiation stage of the tissue. For example, distribution as a gradient along the tissues was observed as a decrease of concentration of tZ and DZR between the shoot and the node and first internode. In order to measure these gradients of metabolites having samples from the same tissue in different differentiation stage a simpler model has been chosen: the root. Therefore, cytokinin metabolites were examined in a detailed sequential sectioning of the root of cv. Parvus. The particular interest in the root tissue occurred from the fact that the primary root has a relatively simple structure which is common among plants. Also the loading of the xylem sap -and consequently the xylem cytokinins- presummaby takes place in the root, so this analysis also aimed to discover whether a specific part of the root was linked with the acropetally moving cytokinins.

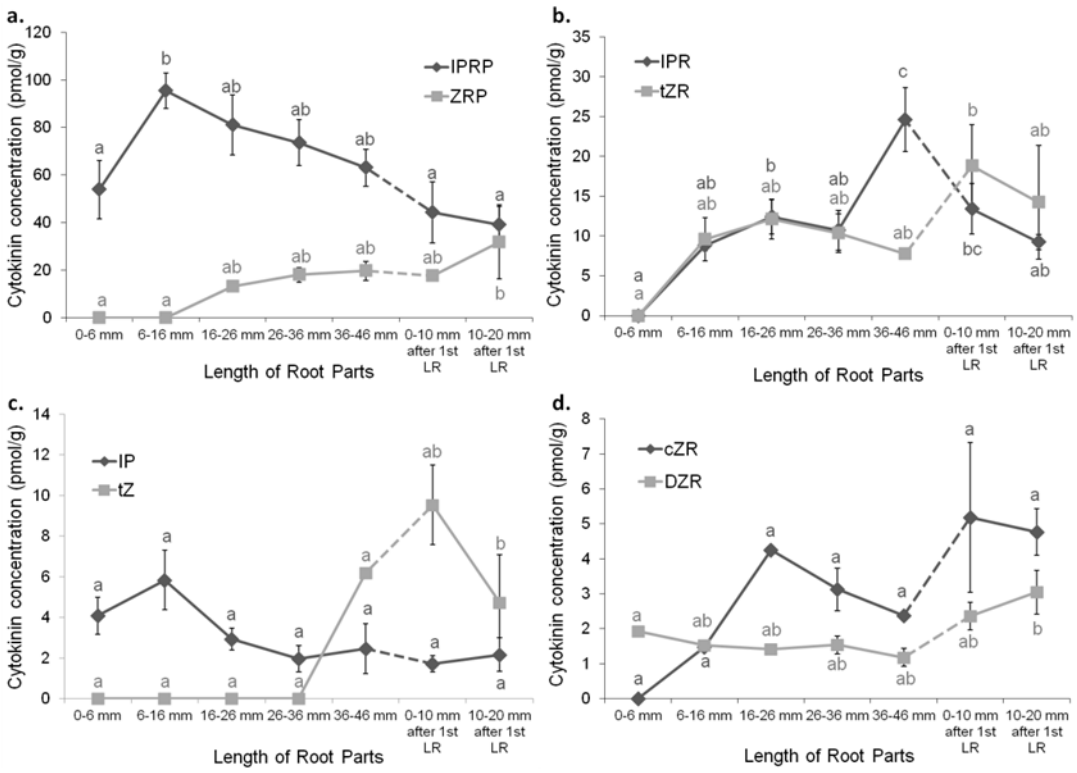

Figure 16 *Cytokinin quantification in root segments of 7 days old cv. Parvus seedlings. The 0 mm represents the root cap of the primary root. The root part above 46 mm until the first lateral root was not examined, as described in Chapter 3.3.3, Figure 10.* ***a.*** *cytokinin phosphate compounds IPRP and ZRP,* ***b.*** *cytokinin ribosides IPR and tZR,* ***c.*** *cytokinin nucleobases IP and tZ and* ***d.*** *cytokinin ribosides cZR and DZR are presented. Each sample derived from a pool of 30-50 plants. Cytokinin concentration was calculated in pmol and normalized to the fresh weight of the plant tissue. The error bars represent standard error (n = 3). Statistical analysis was performed using ANOVA and Tukey's test.*

Cv. Parvus seedlings were grown for 7 days when their root was harvested, sectioned in sequential parts (mm) and processed for cytokinin analysis as described in Chapter 3.3.3 and 3.3.6. As shown in Figure 16.a, IPRP being the most abundant compound across the root parts analysed, displayed accumulated levels at the root part 6-16mm above the root tip. IP showed the same trend. This was not the case for the respective riboside IPR which was below the detection limits in the root tip and showed a significant peak 36-46 mm above the root tip. tZRP was also below the detection limits at the root tip and showed a significant increase at the lateral root zone. Approximately similar trends were followed by cZR, tZR and tZ. DZR displayed an increase of its concentration in the mature lateral root zone but in contrast it was detected in the root tip and in equivalent amount from 0 to 46 mm.

To complement the data analysis described above, the root parts isolated for cytokinin quantification were also examined for CKX activity as an in vitro indication of the degradation rates of the hormone.

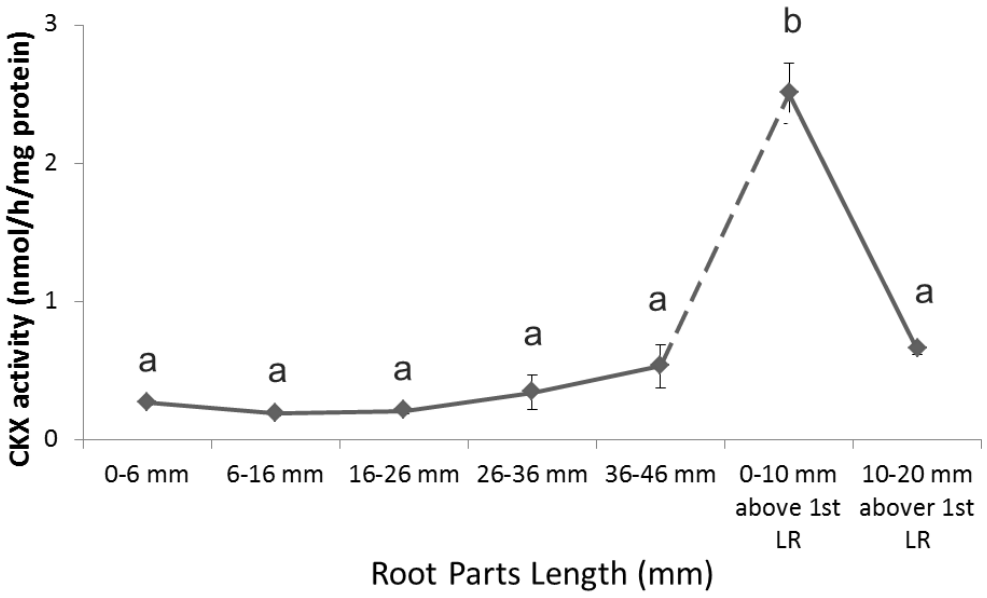

Figure 17 *CKX enzymatic activity measured in root segments of 7 days old cv. Parvus seedlings using IP as substrate. Each sample was a pool of 30-50 plants and 3 biological replicates per sample were examined. The CKX activity was calculated in nmol of enzyme per hour and normalized to the mg of respective protein. The error bars represent standard error (n=3). Statistical analysis was performed using ANOVA and Tukey's test. The CKX enzymatic activity measurements were performed by Dr Vaclav Motyka as described in Chapter 3.3.7.*

As shown in Figure 17, CKX activity was stable across the root tissue analysed indicating that cytokinin degradation occurs throughout the root tissue at similar rates. However, a significant increase of the enzymatic activity was observed at the immature lateral root zone site.

3.5 Discussion

Differences in cytokinin metabolite distribution along the plant axis, due to long-distance transport or steady state net content which could be local biosynthesis against local degradation, has been mentioned several times based on cytokinin-related gene expression studies. However absolute quantification of the endogenous cytokinin levels has not been performed across the whole plant in such detail. Research on regulation of axillary bud outgrowth resulted in several detailed cytokinin studies but concerning mainly the bud and corresponding stem tissues or xylem exudates (Chatfield *et al.,* 2000; Faiss *et al.,* 1997; Wickson and Thimann, 1958). Here cytokinin profile in distinct tissues and saps throughout pea plants is presented. Such analysis provides a basis for better understanding of different cytokinin functions.

More and more ways are available for obtaining hormone concentration changes. Mass spectrometry has been now a well-established method for absolute quantification of hormones. However novel techniques which allow hormonal quantification in vivo are now evolving. Examples of recent advances towards this direction are the FRET-based reporters for abscisic acid measurements (Waadt *et al.,* 2014) and the DII-VENUS sensor to map auxin distribution (Brunoud *et al.,* 2012). However cytokinins have been proven more challenging for the development of such a tool because of the lack of one main representative compound of the hormone. Recently, Tian *et al.,* (2014) developed a *ZmCKX1*-based cytokinin microbiosensor (Tian *et al.,* 2014) in an attempt to rapidly determine cytokinin concentrations in vitro. Although this is a promising approach for rapid sensing of cytokinin content, it provides no specificity to the individual compound levels which as it has been proven in this Chapter varies greatly between tissues. Another problem with this biosensor is that members of the *CKX* family preferentially cleave some bioactive compounds than others (Gajdosová *et al.,* 2011; Galuszka *et al.,* 2007; Köllmer *et al.,* 2014). Therefore even though this kind of tools are promising, LC-MS/MS still remains the “golden standard” method for cytokinin quantification.

3.5.1 Long-distance cytokinin movement

Cytokinin has been shown to act as a local or long-distance signal. The metabolites of the hormone have been shown to translocate acropetally through the transpiration stream in several plant species such as bean, chickpea, petunia, *Arabidopsis*, pea and rice (Bangerth, 1994; Beveridge *et al.,* 1994; Ishikawa *et al.,* 2005; Kuroha *et al.,* 2002; Morris *et al.,* 2001; Napoli *et al.,* 1996; Stirnberg *et al.,* 2002; Takei *et al.,* 2001.a; Turnbull *et al.,* 1997). Xylem cytokinin was extracted and quantified as part of the investigation of this study for cytokinin distribution within pea seedlings. As in most of the experiments in this Chapter, the quantification of the hormone was performed in cv. Térèse and cv. Parvus to identify general trends of cytokinin distribution in Pea.

In both ecotypes examined the glucoside DZ9G was detected exclusively in the xylem while the predominant acropetally transported cytokinins were cZR and tZ followed by tZR. This coincides with previous findings suggesting that the main cytokinins in the xylem sap are the zeatin forms (Beveridge *et al.,* 1997.a; 1997.b; Faiss *et al.,* 1997)and that upregulation of IPT genes in the roots led to export of zeatin ribosides export in the xylem sap (Faiss *et al.,* 1997). Understanding xylem cytokinins better is also important since they seem to be a crucial part of the homeostatic mechanism of the hormone (Foo *et al.,* 2007).

Long-distance transport of cytokinins has been implied to be also mediated by the phloem translocation system along with the delivery of photosynthetic compounds throughout the plant. Corbesier *et al.,* (2003) showed that IP compounds in *Arabidopsis* phloem exudates from leaves increase according to the floral transition. Also, Hirose *et al.,* (2008) measured cytokinins in *Arabidopsis* phloem sap. Here we present for the first time cytokinin metabolites quantification in phloem exudates from the whole stems of Pea. Most of the isoprenoid cytokinins were well detected in the pea phloem with tZ, IPR, IP, DZ and cZR prevailing. Also, the nucleotide IPRP and the glucoside IP9G were exclusively found in the pea phloem sap since in the respective xylem sap these compounds were below the detection limit.

Phloem and xylem saps were extracted from the same plants. Therefore the dissimilar cytokinin profiles occurring from the two saps indicated that there was no cross-contamination -at least not above the set threshold of the detection limit.

Our findings cannot clearly support the suggestion that IP-types are the only cytokinin forms predominant in the phloem while tZ-types are the ones in the xylem (reviewed in Hirose *et al.,* 2008; Kudo *et al.,* 2010; Müller and Leyser, 2011).

IP and IPR were indeed between the prevalent compounds in pea phloem but zeatin forms of cytokinin were also found in high abundance. Since this suggestion was based on results in *Arabidopsis* phloem exudates from leaves it could be possible that the difference derives from diversity between plant species or from the fact that all the published cytokinin measurements in phloem come from leave exudates while the ones presented here were from the whole stem. However, Corbesier *et al.,* (2003) had also detected several zeatin compounds in the phloem sap. Hirose *et al.,* (2008) used a different normalization method for xylem and phloem cytokinins therefore a direct comparison may not be so conclusive. The results coming from Matsumoto-Kitano *et al.,* 2008 by using grafting combinations between the quadruple *atipt1;3;5;7* mutant and the wild-type, were the ones clearly indicating iP-cytokinins as basipetal messengers and tZ-cytokinins as acropetal ones. However, respective experiments have not been performed in other plant species. Similarly our findings in the xylem sap suggested that not only tZ-cytokinins are acropetally transported. The riboside cZR was also a prevalent compound in both xylem and phloem sap of both pea cultivars examined suggesting that this compound is a major transport cytokinin form.

3.5.2 Cytokinin metabolite quantification in sequential tissue parts across the plant.

A detailed analysis of cytokinin metabolites was performed in sequential tissue parts in cv. Parvus and cv. Térèse. The aim was to establish robust conclusions about cytokinin compound profiles within distinct tissues in pea. The same distribution was also examined within the same tissue (pea root) in a more thorough study. Cytokinin compounds profiles varied between different tissues of pea seedlings or even within different developmental stages of the same tissue represented by root segments. Some compounds interestingly displayed high tissue-specificity while the concentration of others remained stable across the plant body. Here the results of the individual experiments of Chapters 3.4.2. and 3.4.3. are discussed as an overview for each cytokinin compound.

IPRP, being the precursor of almost all cytokinins, predominated in all tissues compared to the rest of cytokinin compounds, apart from Parvus hypocotyl where DZ9G and tZ were more abundant (Figures 13, 14 and 15). The high concentration of IPRP in both shoots and roots of pea is also in accordance with the spatial expression pattern of cytokinin biosynthetic enzymes in the respective tissues. In the root *AtIPT5* is expressed in lateral root primordia*, AtIPT7* in the elongation zone, *AtIPT1* in the root procambium and *AtIPT3* in the root vasculature while in the shoot the expression of *AtIPT5* is detected in the stipules and stems of axillary buds, of *AtIPT7* in the trichome of leaves, of *AtIPT1* in the axillary buds and of *AtIPT3* in the phloem (Miyawaki *et al.,* 2004; Figure 2 Chapter 1.3.2). The accumulation of IPRP in the first 6-16mm of the root tip of pea, supported by *AtIPT7* expression detected in the root elongation zone corresponding to this root segment (Miyawaki *et al.,* 2004), implies high rates of cytokinin biosynthesis there and could possibly explain the appearance of tZRP, IPR, tZR and even cZR which were below the detection limit until this root segment (Figure 16). This is in accordance with the main cytokinin biosynthesis pathway, (Figure 2, Chapter 1.3.2) in which IPRP is required for the generation of most cytokinin forms. The reduction of IPRP concentration in the tissues of hypocotyl (Figure 15) and epicotyl is in agreement with the *IPT* genes expression patterns in *Arabidopsis* absent from hypocotyl of *Arabidopsis* (Miyawaki *et al.,* 2004; Figure 5 Chapter 1.5). This is also supported by the gradual reduction of IPRP from the pea root tip towards the shoot-root junction displayed in Figure 16.

tZRP was interestingly identified as a shoot specific compound in pea (Figures 13, 14, 15). This contradicts the suggestion that zeatin compounds are produced almost exclusively in the root and translocated through the xylem to the shoot (Hirose *et al.,* 2008). Since tZRP is the first biosynthesized zeatin form and was not transported through the xylem sap (Figures 11 and 12), its prevalence in the shoot suggests zeatin biosynthesis in the aerial parts of pea. This is also in agreement with *AtCYP735A2* expression profiles, converting IPRP to tZRP, which displayed similar transcript levels in the root as in the stems (Takei *et al.,* 2004.a). The lower concentrations of tZRP found in the pea root, were mainly attributed to its accumulation towards the hypocotyl. tZRP was below the detection limits in the first 16mm of the root tip and its concentration gradual rise became significant only at the mature lateral root segment (Figure 16). This is confirmed by *GUS* driven promoter expression studies on *AtCYP735A2* showing that while expression in the root tip concerns only a few columella cells, the expression was undetectable in the elongation and differentiation zone but appeared eventually with maturation with highest root expression taking place at the mature lateral root zone (Kiba *et al.,* 2013).

IPR and tZR were the only cytokinin compounds that exhibited different trends between cv. Térèse and cv. Parvus. Both compounds were shoot-specific in cv. Térèse (Figure 14) but root specific in cv. Parvus (Figure 13). Therefore it is indicated the gradients and tissue specificity of these ribosides could be responsible for the phenotypic alterations between the two cultivars under study. For example IPR and tZR differential profiles in cv. Parvus and cv. Térèse could be linked with the dwarf phenotype of cv. Térèse and the tall phenotype of cv. Parvus respectively. One of the seven characteristics that Mendel studied in pea concerned plant height and it was linked to the *LE* gene. Follow up research revealed that the *LE* gene encodes for a GIBBERELLIN 3-OXIDASE1 and regulates the levels of the bioactive GA_1 which is abundant in the tall wild type peas. The dwarf *le-1* mutants are deficient in the conversion of the inactive precursor GA_{20} to the GA_1 resulting in lower levels of bioactive gibberellins and therefore to dwarf phenotype (reviewed by Reid and Ross, 2011).

The bioactive nucleobase IP was one of the most stably detected compounds in pea tissues in all analyses (Figures 13.c and 14.c). Tissue specificity was only displayed in the root and first node and internode (Figure 15.c) but when it was measured in root segments its concentration exhibited no shift across Parvus root (Figure 16.c). This could be possibly attributed to the tight control of IP levels by CKX enzymes since this compound is found to be the best substrate for CKX enzymes (Gajdosová *et al.,* 2011).

Another cytokinin compound that displayed shoot specificity in pea was tZ (Figures 13.c, 14.c and 15.c). This could be attributed to the accumulation of tZ in pea shoots since it was one of the major cytokinin forms transported through the xylem and/or to the prevalence of tZRP in the pea shoot. tZ-type cytokinins were found also in 10 days old *Arabidopsis* to be more abundant in the shoot than in the root tissue in accordance with pea (Zhang *et al.,* 2014.a) while in 14 days old *Arabidopsis* seedlings tZ-type cytokinins shoot levels were the similar with the ones at the roots (Ko *et al.,* 2014). Since in both these studies cytokinin concentrations were summed as a group of tZ-forms and therefore included results for tZRP, tZR and tZ levels, possible alterations in tZR levels for example according to the different age of the plants could alter the final conclusion.

DZ and DZR were also identified as shoot specific compounds in pea (Figures 13.d, 14.d and 15.d and 15.e) and since neither DZR nor DZ was one of the prevalent xylem cytokinins (Figures 11.b and 12.b), this could be attributed to the high shoot tZRP which is the precursor of all DZ-forms.

The glucoside DZ9G was the only glucoside well-detected in pea tissues and it was found accumulated in the junction tissue (Figures 13.e and 14.d) which was further defined to be the hypocotyl (Figure 15.e). One possible explanation of this high DZ glucosylation activity in the hypocotyl could that DZ, transported from shoot to root through the phloem (Figures 11.a and 12.a), is deactivated in the hypocotyl tissue to result in lower concentrations in the root since DZ and DZR were both found reduced in the root tissue compared to the shoot (Figures 13.d, 14.d, 15.d and 15.e). DZ9G was also found predominant (more than 3 times fold increase) in the shoot than in the root of 10 days old *Arabidopsis* seedlings but since this was not a tissue detailed analysis it can be only assumed that this increase corresponds to the hypocotyl tissue observed also in pea.

In general, the shoot and root tissues presented differences in their cytokinin content which could be expected since they are sites of high rates of cytokinin biosynthesis and metabolism according to the respective gene expression profiles (Figure 5, Chapter 1.5). Also, the shoot and root tissue are both sinks of the long-distance transported cytokinins through the xylem and phloem respectively. A tissue of particular interest was the hypocotyl which presented accumulation of specific cytokinin compounds like tZ and DZ9G while the neighboring tissue of epicotyl had the least concentration of cytokinins compared to the other tissues analysed (Figure 15).

3.5.3. Cytokinin metabolite distribution varies along the primary root axis.

The pea root was chosen as a simple model tissue with distinct differentiation stages presenting similar organization in most plant species. Therefore pea root was dissected in tissue parts starting from the apical root tip including the cellular division zone (0-6 mm), continuing with 6-16 mm root segment that could correspond to the elongation zone, 16-26 mm, 26-36 mm and 36-46 mm as the cellular maturation zone and two more segments 0-10mm above the first emerged lateral root and 10-20 mm above the first lateral root including more mature lateral roots (Figure 10). Cytokinin metabolites were quantified in these root segments to examine if cytokinin distribution is shifted according to the differentiation stage. Another reason of the specific interest in the root tissue was also because the loading of the xylem is believed to occur there.

The gradients of IPRP, tZRP and IP within the root tissue of pea were already discussed in the overview of Chapter 3.5.2. IPRP trend across the root tissue matched that of IP but not IPR

(Figure 16) implying the action of the *LOG* genes, enzymes catalyzing direct conversion of IPRP to IP, especially in the root tip were IPR was below the detection limits. Indeed, *AtLOG3, AtLOG4* and *AtLOG8* expression is detected in the root tip (Kuroha *et al.,* 2009). The nucleobase tZ and the riboside tZR followed ZPR increased concentrations in the lateral root zone (Figure 16) suggesting that their metabolism in this tissue part is presumably not catalyzed - at least not exclusively - by *LOG* genes which would convert tZRP directly to tZ. This is also supported by *LOG* genes expression pattern in the root (Kuroha *et al.,* 2009) since *AtLOG2, AtLOG3, AtLOG4* and *AtLOG7* are expressed in the emerged lateral root zones or lateral root primordia but only *AtLOG1* and *AtLOG8* expression are detected also in the mature primary root.

All zeatin compounds, apart from DZR, were below the detection limits at the root tip (Figure 16). cZR also followed tZ-compound trends and this could be partially because of the interconversions that can occur between tZR and cZR through zeatin isomerase, as shown in Figure 2 (Chapter 1.3.2). As previously mentioned the expression of *AtCYP735A2*, being the enzyme catalyzing the hydroxylation of the main precursor of all zeatin forms, tZRP, is detected in a few columella cells while its highest expression in the root concerns the maturation zone (Kiba *et al.,* 2013). This indicates that xylem loading is unlikely to occur in the root tip since none of the cytokinin compounds found abundant in the xylem sap (Figures 11.a and 12.a) were detected at this root segment (Figure 16). In agreement with this, the suggested transporter of cytokinins into the xylem *AtABCG14* displayed no expression in the root tip (Ko *et al.,* 2014).

Instead, accumulation of tZ, tZRP, IPR, tZR, DZR and cZR was exhibited in the lateral root zone (Figure 16) where both *AtCYP735A2* and *AtABCG14* showed high expression levels (Kiba *et al.,* 2013; Ko *et al.,* 2014). This coupled with the result that most of these compounds are common with the ones predominating in the xylem sap (Figures 11.b and 12.b) sets this root part as a candidate for cytokinin xylem loading. In agreement with this hypothesis, tZR and tZ increased levels in the hypocotyl (Figure 15.b and 15and.c) could possibly represent more the loaded xylem compounds than the locally present forms in this tissue.

Bielach *et al.,* 2012 performed a similar analysis in *Arabidopsis* concerning dissection of 7 days old seedlings in 6mm root parts starting from the root apex corresponding also to the different developmental stages concerning the lateral root development. tZ and all ribosides apart from cZR displayed stable levels across the root. IP levels were increased only in the first zone (0-6mm) while cZR concentration gradually reduced from the root apex towards

the hypocotyl. Comparing our results with this experiment conserved trends between *Arabidopsis* and Pea were identified for IP and DZR compounds. In contrast, tZ and the rest of the ribosides were below the detection limit in the root tip (0-6mm) while their concentration increased gradually towards the hypocotyl. Finally, Svačinová *et al.,* (2012) measured cytokinin concentration in the apical part (0-5mm) of 8 days old *Arabidopsis* root. IPR and tZR were also detected in *Arabidopsis* root tip which was not the case for Pea. Concerning the bioactive nucleobases, IP was 10 times lower than tZ in *Arabidopsis* while in Pea the reverse trend was indicated. The non-conserved cytokinin concentration trends in similar tissues between pea and *Arabidopsis* could be attributed to the size difference between the two plants. A root part of 5 mm or 6 mm in *Arabidopsis* would be equivalent of a root segment of approximately 50 mm or 60 mm of pea, respectively. Comparison between pea and *Arabidopsis* cytokinin concentration in similar root developmental stages would require sectioning of *Arabidopsis* root in 1 mm-scale.

To further investigate the control of cytokinin distribution in the root parts of pea under study, the activity of the cytokinin degradative enzymes, CKX, was measured. CKX enzymes were stably active in the first apical 46 mm of the root tip (Figure 17) indicating that cytokinin degradation occurs in this root area. This is in agreement with the stable presence of the IP compound in this root area (Figure 16.c) which was used as substrate in the enzymatic assay, even though its levels could be also controlled by glycosyltransferases and other enzymes affecting its metabolism. An accumulation of CKX enzymatic activity was observed at the lateral root emergence zone (Figure 17; 0-10 mm above the first lateral root). This peak did not correspond to an IP or even IPR peak in this root part. However IPR displayed significantly higher concentration levels compared to the rest of the root segments at the 36-46 mm root part which were not retrieved anymore at the lateral root emergence zone (Figure 16.b). Since the next sequential root parts (above 46mm, Figure 10) were not examined for cytokinin levels and CKX activity, it can only be speculated that IPR concentration was reduced because CKXs were highly activated 0-10 mm above the first lateral root. In terms of biological significance, it can be hypothesized that CKX activity showed increased degradation of cytokinins in the lateral root zone since the hormone plays a pivotal role in inhibition of lateral root formation. Lowered cytokinin concentrations in the roots result in enhanced root systems (Werner *et al.,* 2010) while cytokinin receptor mutant displayed induced lateral root formation (Riefler *et al.,* 2006). Also targeted expression of *AtIPT* and *AtCKX* in the pericycle, where lateral root initiation takes place, exhibited reduced and enhanced lateral root density respectively (Laplaze *et al.,* 2007a). To test this

hypothesis, CKX activity and lateral root density could be measured in seedlings treated with exogenously applied cytokinin. The overlapping functions in *CKX* genes restrict the genetic studies through the respective mutants and a multiple *CKX* mutant phenotype has not been published yet.

3.6 Conclusions

- IP-cytokinins prevail in the phloem sap and tZ-forms predominate in the xylem sap of pea. However there are additional abundant compounds, such as cZR in the systemic transport pathways.
- tZRP, tZ and DZR were identified as shoot-specific compounds in pea while IP and IPRP were stably detected in almost all tissues of pea with the latter being the most abundant cytokinin.
- The gradients of the ribosides IPR and tZR within pea seedlings could be related to the different height of pea cultivars under study.
- N-glucosylation of DZ was found to be hypocotyl specific.
- The lateral root zone but not the root tip was indicated as the possible xylem loading site for cytokinins.
- Concentrations of most cytokinin compounds vary between sequential tissues and between different developmental stages of the same tissue.

Chapter 4

High-resolution cell-specific analysis of cytokinin compounds distribution in the Arabidopsis root apex.

The results of this Chapter derived from collaboration between Imperial College London and Umea Plant Science Center (UPSC, Umea, Sweden). The people contributing, to this work were Ioanna Antoniadi Lenka Plačková, Biljana Simonovik, Karel Doležal, Colin Turnbull, Karin Ljung and Ondřej Novák. Specific contributions are stated in the Figure legends.

Ioanna Antoniadi and Biljana Simonovik conducted and optimized all sowing, protoplast isolation and cell-sorting procedures. Lenka Plačková and Ondřej Novák optimized the cytokinin purification and LC-MS/MS methods. Ioanna Antoniadi conducted the control experiments. Ioanna Antoniadi, Lenka Plačková, Karel Doležal, Colin Turnbull, Karin Ljung and Ondřej Novák discussed planning, progress and data interpretation throughout the project.

4.1 Introduction

In Chapter 3 it was suggested that cytokinin metabolite distribution is altered in distinctive tissues, even between sequential-10 mm root parts. The challenge of this chapter is taking innovative leading edge approaches to push the limits of detection and examine cytokinin metabolite distribution in cell-specific populations. Such a detailed hormonal analysis in plants has been done only for auxin (Petersson *et al.,* 2009) which is present in significantly higher concentrations in plants than cytokinins and can be represented only by one compound, IAA.

Several attempts to examine cytokinin functions have used divergent methods such as radiolabelled cytokinins (Mader *et al.,* 2003), cytokinin immunolocalization against tZR (Castiglione 1998; Rijavec *et al.,* 2011) and cytokinin-responsive promoter driven constructs with β-glucuronidase (GUS), luciferase or green fluorescent protein (*GFP*) (Bielach *et al.,* 2012; Zürcher *et al.,* 2013). Here, we demonstrate quantification of at least 15 cytokinin metabolites in specific cell types of the *Arabidopsis* apical root using a combination of Fluorescence Activated Cell-Sorting (FACS) and ultra-sensitive mass spectrometry (LC-MS/MS). This study, along with the one previously mentioned done for auxin, complements the similar transcriptional work that has performed at the cell level in *Arabidopsis* root apex (Birnbaum *et al.,* 2003, 2005; Brady *et al.,* 2007) bringing us a step closer to unravelling the details of gene-hormone regulation taking part in the root apex.

The root tissue was chosen as a model system for this kind of study, including the one described here, firstly because of its importance in agriculture and secondly because of its relatively simple cell and tissue organization which is conserved among plant species. The different root zones can be distinguished sequentially starting from the root apex into the meristematic, the elongation and the differentiation zone. The last of these zones extends up to the appearance of root hairs. The organization and amount of cells are exceptionally consistent between roots. All the different cell types derive from the initials bordering the quiescent center and are organized in distinctive cell files which are also well conserved. These are the protoderm, establishing the initials, root cap and endodermis, the periderm, creating the cortex and epidermis and the plerome which forms the stele (Dolan *et al.,* 1993).

Arabidopsis was used in the experiments described in this Chapter because of the variety of *GFP* transgenic lines developed. By combining the lines *J2812* which is expressed in

epidermal and cortex cells of the root (www.plantsci.cam.ac.uk/Haseloff/), *pSCR:GFP* which is expressed in the endodermis and QC (Swarup *et al.,* 2005), *pWOL:GFP* which is expressed in the stele (Birnbaum *et al.,* 2003) and *M0028* which is localized in the root cap, columella, initials, and QC (Birnbaum *et al.,* 2003) a detailed fluorescent map of the *Arabidopsis* distinctive cell types of the root apex can be generated. This fluorescent map was translated into a cytokinin map after developing the method balancing the least amount of tissue required and the maximum recovery from cytokinin purification and detection in the mass spectrometer.

Here, the quantification of cytokinin metabolites is presented for the first time in the *Arabidopsis* root apex at cell-specific resolution. This study will provide a substantial tool for future research in cytokinin metabolism, distribution and functions.

4.2 Aims

The aims of this Chapter were to develop a method for cytokinin analysis in cell-specific populations and then to examine the possible presence of a cytokinin gradient within the *Arabidopsis thaliana* root tip. Substantial improvement of the resolution of mapping cytokinin pools will facilitate a better understanding of the biochemistry and functions of the hormone since sites of biosynthesis do not necessarily represent sites of maximal hormone accumulation and signaling.

4.3 Materials and Methods

4.3.1. Plant Material and Growth Conditions

The transgenic *Arabidopsis thaliana GFP* lines *pWOODEN LEG:GFP [pWOL:GFP], pSCARECROW:GFP [pSCR:GFP], J2812:GFP and M0028:GFP* and Col-0 wild-type for the control experiments were sterilized using 20% (v/v) bleach and 0.1% Tween for 5 min (2×2.5 min) and then rinsed five times with sterile water. All seeds were sown in 3 rows (~100 seeds/row) on square Petri dishes containing standard MS media (1× concentration Murashige and Skoog salt mixture: 4.4 g/L, 1% sucrose, 0.5 g/L MES, 1% agar and adjusted to

pH 5.7 with KOH) covered with sterile mesh squares. All plated seeds were vernalized for 3 days in darkness and at 4°C before being transferred in 23°C and long-day conditions (16 h light and 8 h darkness) where they were placed vertically and remained for 8 days. One standard cell-sorting experiment required 30-40 Petri dishes meaning approximately 9000 seedlings.

4.3.2 Protoplast isolation

The apical part of the nine days old seedlings' root (~1/3 of the root) was harvested and rinsed with distilled water. The collected root part was further chopped and added to 100 ml flasks containing 25 ml of protoplast isolation buffer (600 mM mannitol, 2 mM $MgCl_2$, 10 mM KCl, 2 mM $CaCl_2$, 2 mM MES, 0.1% BSA, pH 5.7. Cell wall dissolution occurred by the addition of 0.3u/ml pectolyase and 45u/ml cellulysin in the isolation buffer. The solution was then incubated for 2 h at 22°C in darkness and with stirring at 125 rpm (gentle manual stirring also occurred every 20 min). The protoplasts were separated from the undigested root tissue using a 40 mm cell filter, centrifuged for 3 min at 1000 rpm at 4°C and the supernatant was discarded.

4.3.3 Cell Sorting

In order to separate the *GFP*$^+$ from the *GFP*$^-$ protoplasts, cell sorting was performed using a BD FACS Aria I flow cytometer (BD Biosciences) as described in Petersson *et al.,* (2009) and Pencik *et al.,* (2013). The protoplasts were resuspended in 1 ml of sorting buffer (0.7% NaCl), loaded in the cell sorter (4°C) and passed individually through a 100 µm nozzle. The undamaged protoplasts were selected according to their forward and side scatter light absorption while the fluorescent ones were distinguished by their *GFP* excitation (488 nm laser) and using as a control their autofluorescence. The isolated cell populations were frozen immediately after sorting in liquid N_2 and stored at -80°C until purification. The software used for the data processing was FACSDiva 6.1.2. Two samples of 200.000 *GFP*+ and *GFP*- protoplasts were collected at the end of each sorting (2 technical replicates) and 6-9 sortings were performed (6-9 biological replicates) as mentioned in the respective Figure ledgent. The cytokinin concentration in the *GFP*+ cells was normalized according to the respectively collected *GFP*- protoplasts.

4.3.4 Control Experiments

Treatments of protoplasts: Root protoplasts were isolated as described in Chapter 4.3.2 from Col-0 wild-type roots while treated with 10 µM INCYDE (Zatloukal *et al.,* 2008; Aremu *et al.,* 2012), 100 µM adenine, 3 mM NaN_3 or the DMSO control by adding the chemical in the protoplast isolation buffer. The isolated protoplasts were collected by centrifugation and resuspended in 200 µl of sorting buffer. The cytokinins were then purified using MCX columns and their content was measured through LC-MS/MS as described in Chapter 4.3.5 and 4.3.6, respectively.

Leakage tests: Isolated root protoplasts from Col-0 wild-type roots were resuspended in 1 ml of cold sorting buffer and kept on ice for 180min imitating the sorting procedure/technique. After 0, 90 and 180 min respectively, the protoplasts were centrifuged for 3 min at 1000 rpm at 4°C, and the pellet and the respective supernatant were separated and processed for cytokinin quantification following the same process as the above control experiments.

4.3.5 Cytokinin Purification Protocols

Aliquots of around 200,000 protoplasts in 0.7% NaCl (ca 1 ml) were diluted with water at a ratio of 3:1 (v/v) and adjusted to pH 2.7 with 1 M HCl. Prior to extraction, 0.1 pmol of isotope-labelled cytokinin standards was added to each sample. Two SPE (Solid Phase Extraction) protocols were tested according to previously published purification methods with some modifications (Dobrev and Kamínek, 2002; Svačinová *et al.,* 2012). The first method utilized Oasis® MCX cartridges (1cc/30 mg; Waters) conditioned with 1 ml of 100% methanol and water, equilibrated with 1 ml of 50% (v/v) nitric acid, 1 ml of water and 1 ml of 1M HCOOH. After sample application onto Oasis® MCX column, non-retained compounds were removed by a wash step using 1 ml of 1M HCOOH and pre-concentrated analytes were eluted by two-step elution using 1 ml of 0.35 M NH_4OH aqueous solution and 2 m of 0.35 M NH_4OH in 60% (v/v) methanol solution. The second method utilized the in-tip microSPE based on the StageTips technology (Rappsilber *et al.,* 2003). Final optimized microSPE protocol is shown in Figure 21. Briefly, combined multi-StageTips (containing C18/SDB-RPSS/Cation-SR layers) were activated with 50 µl of acetone/methanol/water/50% (v/v) nitric acid/water (by centrifugation at 2,000 rpm, 15 min, 4°C). After application of the sample (200 µl, 2,500 rpm, 30 min, 4 °C), the microcolumns were washed with 50 µl of water/methanol (2,200 rpm, 20 min, 4°C), and elution of samples was performed with 50 µl

of 0.5 M NH_4OH in 60% (v/v) methanol (2,200 rpm, 20 min, 4°C). All eluates were collected and evaporated to dryness using a Speed-Vac concentrator, and dissolved in 40 µl of 10% methanol. Ten microliters of each sample were analysed using UHPLC-MS/MS, according to the method described by Svačinová *et al.,* (2012) with minor modifications.

4.3.6 UHPLC-MS/MS Method

Separation and determination of samples were performed by 1290 Infinity Binary LC System coupled to the 6490 Triple Quad LC/MS System with Jet Stream and Dual Ion Funnel technologies in positive mode (Agilent Technologies). The samples were injected onto a reversed-phase column (Acquity UPLC® CSH C18 1.7 µm, 2.1 x 150 mm, Waters) and separated using a 30 min linear gradient containing system of methanol (A) and 15mM ammonium formate (pH 3.95, B) at a flow rate of 0.25 ml/min. Column temperature was set to 40°C and sample temperature to 4°C. The following binary gradient was used: 0 min, 10:90 (A:B) – 13.0 min, 23:77 (A:B) – 19.0 min, 36:64 (A:B) – 25.0 min, 70:30 (A:B). At the end of the gradient the column was washed with 100% methanol and re-equilibrated to initial conditions (5 min). Determination of endogenous cytokinins in protoplasts was performed by multiple reaction monitoring (MRM) of the protonated precursor and appropriate product ions. The MRM transitions, optimized instruments setting, retention times and detection limits are shown in the Supplemental Table 1. The MassHunter software (Version B.05.02, Agilent Technologies) was used to determinate the concentrations of cytokinins using stable isotope dilution.

4.4 Results

4.4.1 Method development for quantify cytokinins at cell level

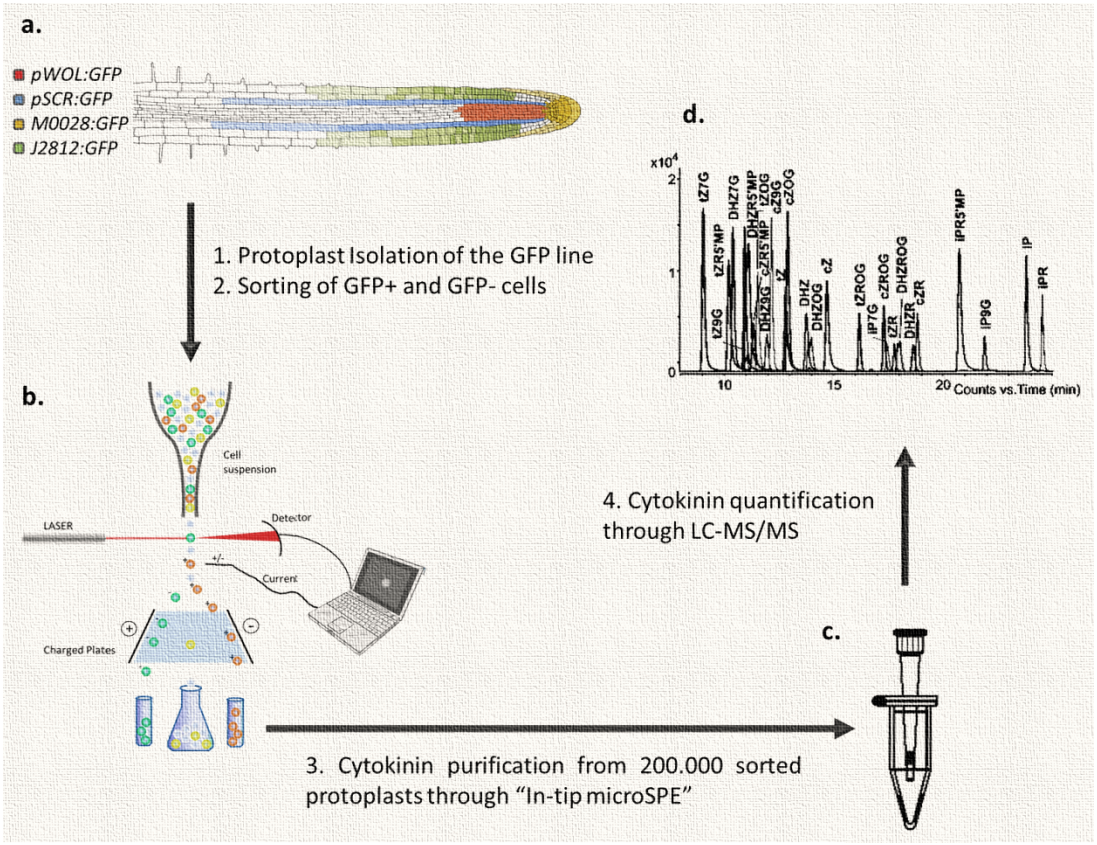

Figure 18 *Scheme of method followed to quantify cytokinins in cell-specific populations. Protoplasts were isolated from each GFP line overviewed in* ***a.*** *where a scheme of Arabidopsis root represents in color code the different GFP lines from which the* GFP+ *populations derived. J2812:GFP signal is displayed in red color, pWOL:GFP in red, pSCR:GFP in blue and M0028:GFP in yellow. Then the isolated protoplasts were sorted through FACS as indicated in* ***b.*** *Cytokinins deriving from the sorted cell populations of approximately 200.000 protoplasts per replicate, were purified using the "In-tip microSPE" represented in* ***c.*** *Finally cytokinin metabolites were quantified through LC-MS/MS. A representative cytokinin chromatogram is shown in* ***d.*** *The Figure contains parts drawn by Ondřej Novák and Ioanna Antoniadi.*

Following the outline of the method developed in Figure 18, protoplasts were isolated from root tissue of 8-day-old *Arabidopsis thaliana* seedlings expressing *GFP* in specific cell types of the root tip. Four well-characterized *GFP*-expressing lines *J2812:GFP, pWOODEN LEG:GFP (pWOL:GFP), pSCARECROW:GFP (pSCR:GFP),* and *M0028:GFP* were chosen so that all cell types in the root apex (epidermis, cortex, stele, endodermis, root cap, columella, columella initials, and QC; Figure 18.a) were covered (Petterson *et al.,* 2009). The isolated protoplasts were sorted using FACS into *GFP*-expressing (GFP^+) and non-*GFP* expressing (GFP^-)

protoplasts, thus enabling the use of a specific reference population for each biological replicate (Figure 18.b). Cytokinins deriving from the isolated cell populations were then purified through the optimised In-tip microSPE process (Figure 18.c.), as described below, and they were finally quantified through UHPLC-MS/MS (Figure 18.d.), as described in 4.3.6.

4.4.1.A. Protoplast isolation and cell sorting

The seedlings were vertically grown for 8 days in square Petri dishes covered with mesh to facilitate the harvesting of the apical part of the primary root. The collected root parts were further dissected and added to the protoplast isolation buffer which contained enzymes promoting cell wall digestion. After incubation the protoplasts were selected from the undigested material through filtering, isolated by low speed centrifugation and kept on ice until initiating the cell sorting procedure.

For three of the transgenic lines analysed, two samples of 200.000 *GFP*+ and *GFP*– cells were collected during each sorting procedure (2 technical replicates) and at least 6 cell-sorting experiments were performed for each *Arabidopsis* line (6-10 biological replicates). For the M0028:*GFP* line, a total of 20,000 to 100,000 isolated protoplasts were collected for each biological and technical replicate (for both the *GFP*+ and *GFP*– cell populations). Commercial sorting buffers with unknown composition were replaced by 0.7% sodium chloride (NaCl) solution to minimize the sample matrix. Moreover, known composition of the sorting buffer was also usable during further optimization of a subsequent purification step.

4.4.1.B. Optimization of the cytokinin purification process for isolated protoplasts

To accomplish purifying and quantifying cytokinins in cell-specific level the high selectivity, affinity and capacity of the multi-StageTip sorbents (C18, SDB-RPS and Cation-SR), presented by Svacinova *et al.,* (2012) was used. The micro-purification step has been further optimised as a novel powerful one-step high-throughput approach for complex cytokinin analysis in isolated cell populations of *Arabidopsis* root apex.

Initially, the purification process using the commercially available mixed-mode cation-exchange phase (Oasis MCX column) was compared with the extraction capacity of multi-Stage Tip micro-columns packed with one- (×1), two- (×2) and three- (×3) layers of each sorbent. As displayed in Figure 19 both purification protocols showed similarly high cytokinin extraction efficiencies, indicating that cytokinins might be enriched by in-tip microSPE. However cytokinin nucleotides exhibited higher efficiency with increasing amount and

surface area of sorbent multilayers. Altogether, total extraction recoveries (76 ± 15%, 82 ± 12%, 81 ± 9% for one, two and three-layers of each sorbent, respectively) were in good agreement with excellent recovery, high reproducibility and robustness of commonly used MCX purification method (82 ± 6%).

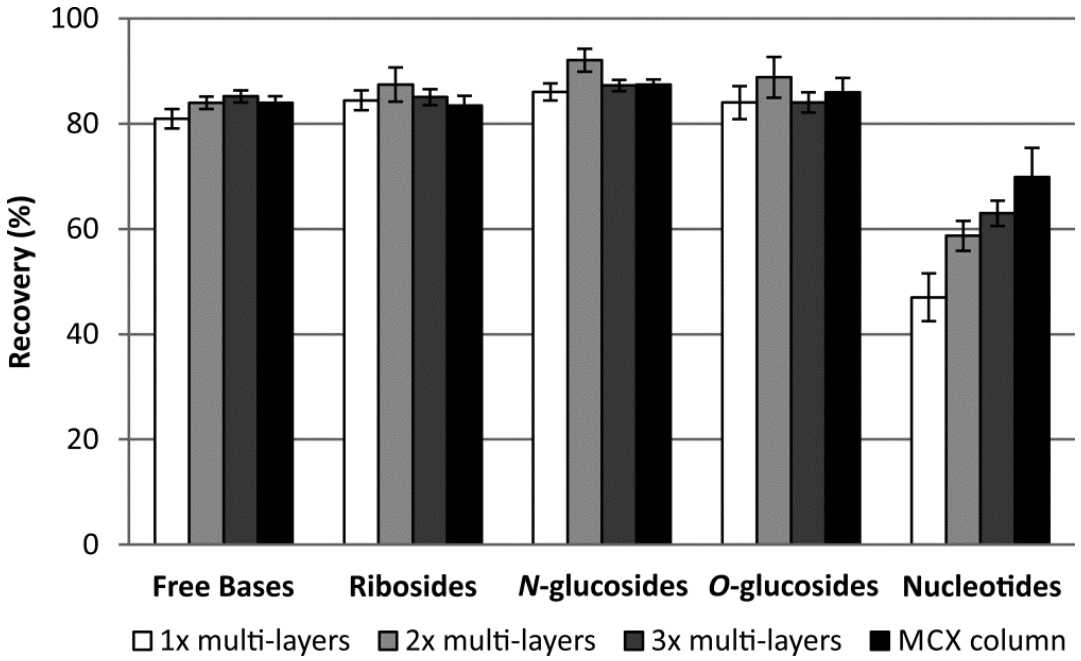

Figure 19 *Recovery (%) of Different Cytokinin Groups in Relation to Number of Sorbent Multi-layers (C18/SDB-RPS/Cation-SR) using in-Tip microSPE Purification Procedure. A number of sorbent multi-layers were tested using a mixture of twenty-six CK standards (0.1 pmol of each). In-tip micro SPE compared with commonly used MCX purification method indicates usefulness of this tool for purification, enrichment, and selective compound isolation. The error bars represent standard error (n=3). Data were generated by Lenka Plačková and the Figure was drawn by Ondřej Novák.*

Since the sorted cell populations were suspended in 0.7% NaCl (sorting buffer), the cytokinin purification process required further optimisation for maximum recovery of the hormone metabolites. This was because high concentrations of chloride anions impede the binding sites of the stationary phase, resulting in impaired cytokinin recovery. Another problem caused by using NaCl is that the large excess of sodium ions will result in the formation of metal adduct ion species, limiting ionization efficiency and thus providing a lower sensitivity of LC-MS method. Therefore, the sorbent activation/equilibration and the sample loading processes were improved.

This was accomplished by examining stronger acidic solutions than 1M formic acid, used in the published microSPE protocol (Svačinová *et al.,* 2012) for activation of C18/SDB-RPS/Cation exchange-SR layers. The results presented in Figure 20.A exhibited higher

process efficiency with nitric acid than formic acid and therefore this was chosen for the new optimised purification protocol. In parallel, it was tested if the detrimental effects of NaCl in the cytokinin purification and LC-MS method could be limited by dilution of the loaded NaCl to the microSPEs. As shown in Figure 20.B the 3:1 dilution of NaCl with water exhibited the highest process efficiency and therefore it was incorporated in the optimised protocol. The samples were acidified using 1M hydrochloric acid (pH 2.7) prior the loading to the in-tip microSPE.

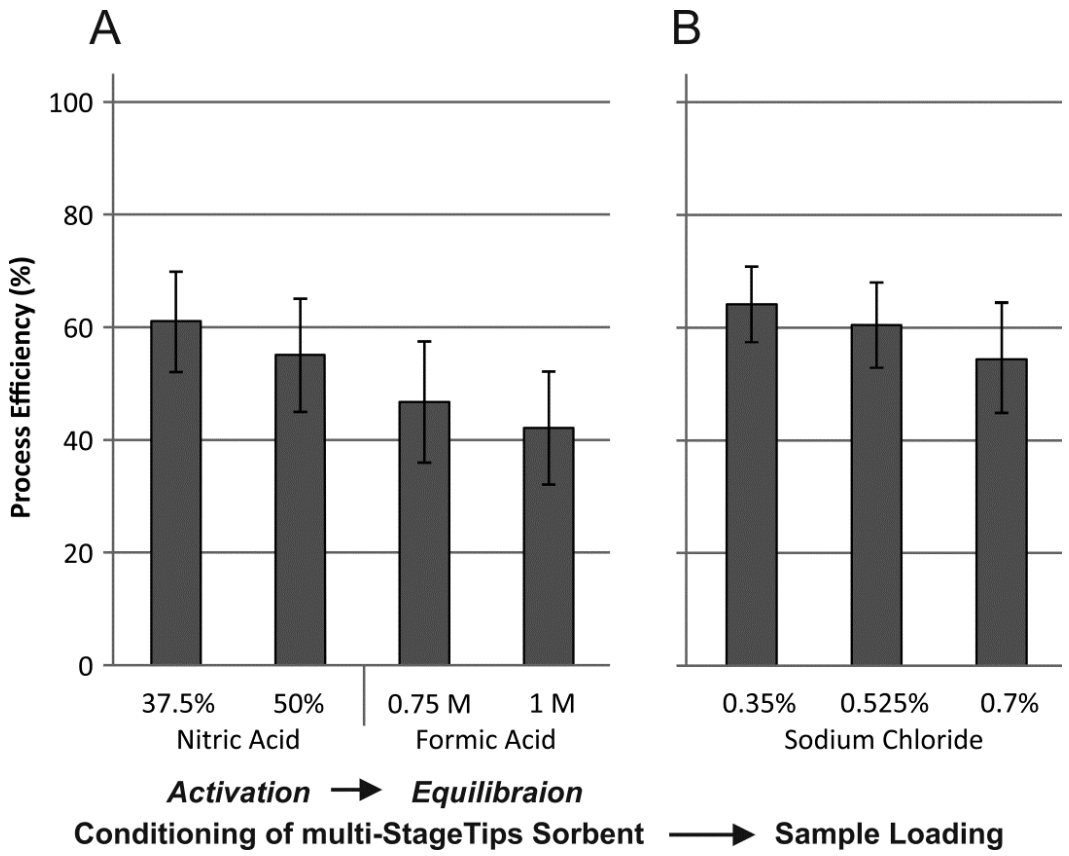

Figure 20 Process Efficiency (%) of in-Tip microSPE Protocol. **(A)** The comparison of two types of acids for conditioning (activation steps) using formic acid and nitric acid. **(B)** Dilution of 0.7% NaCl solution with different content of water (v/v). 3x multi-layers in-tip microSPE (C18/SDB-RP/Cation-SR) was applied to purification of isolated protoplasts. Conditions of activation were optimized to obtain higher yields for all analytes detected. Elution CK fraction was evaporated to dryness and dissolved in 40 µL of 10% methanol for UHPLC-MS/MS analysis. The error bars represent standard error (n=3). *Data generated by Lenka Plačková and the Figure drawn by Ondřej Novák.*

The optimized protocol for cytokinin purification in isolated cell populations is presented in Figure 21.

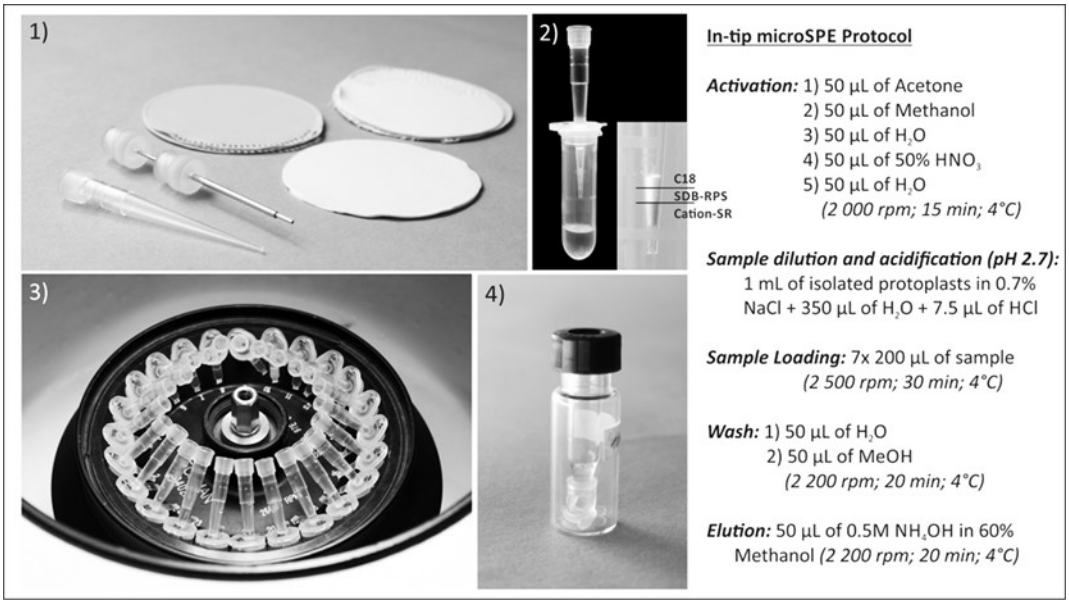

Figure 21 *Optimized in-Tip microSPE Protocol. 1) Preparation of multi-layer in-tip microSPE, 2) Presentation of ready multi-layer in-tip microSPE (C18/SDB-RP/Cation-SR in zoom) attached in an eppendorf tube to facilitate collection of waste or elution sample 3) The washing and elution steps were performed with a centrifuge 4) After the purification process the samples were transferred to an LC-MS vial for quantification. The description of the optimized protocol is presented at the right-side of the Figure. Activation step was optimized to obtain higher yields of each analyte measured. Final cytokinin -enriched fraction was evaporated to dryness and dissolved in 40 µL of 10% methanol for LC-MS/MS analysis. The Figure was drawn by Ondřej Novák.*

Cytokinin metabolites, deriving from the purified samples were then measured through ultra-high performance liquid chromatography–tandem mass spectrometry (UHPLC-MS/MS) in both the GFP^+ and GFP^- samples as described in Chapter 4.3.6. The hormone concentration in the GFP^+ cells of each line was normalized according to the respective GFP^- reference population.

4.4.1.C. Control Experiments

The processes of protoplast isolation and cell sorting being required techniques for achieving the isolation of specific cell populations are drastic procedures that might change the endogenous cytokinin levels. Therefore cytokinin concentration was examined in both procedures, as control experiments of the method, to test whether the levels of the hormone can still represent the endogenous ones after the procedures of protoplasting and cell sorting.

Initially, the effects of the protoplast isolation process on cytokinin levels were investigated. To fulfil this aim, several treatments were performed during the 2 h of enzymatic dissolution of the cell walls. The chemicals used included INCYDE (2-chloro-6-(3-methoxyphenyl)aminopurine) as a cytokinin oxidase inhibitor (Aremu *et al.,* 2012; Zatloukal *et al.,* 2008), adenine as cytokinin transport antagonist (Bürkle *et al.,* 2003; Cedzich *et al.,* 2008) and sodium azide (NaN_3) as inhibitor of ATP-dependent metabolic and membrane transport processes (Tucker, 1993; Petersson *et al.,* 2009).

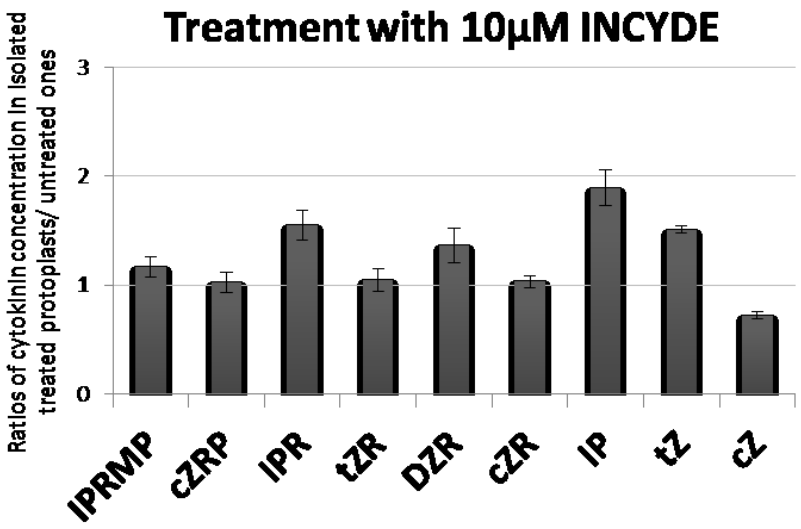

Figure 22 *Ratios of cytokinin concentration in isolated INCYDE-treated protoplasts to the respective untreated samples. The protoplasts were treated for 2 h by adding 10 µM INCYDE to the protoplast isolation buffer. The concentration of the detected metabolites was calculated as pmol/100.000 protoplasts and the respective ratios were then determined. Three biological replicates were performed and each was a pool of at least 1500 roots. Error bars indicate standard error (n=3).*

As shown in Figure 22, the compounds IP, tZ, DZR and IPR were affected by the INCYDE treatment showing elevated levels. However the maximum shift obtained was a 2-fold increase of IP levels. The concentration of cZ was slightly reduced while the rest of the cytokinin metabolites did not respond to the treatment.

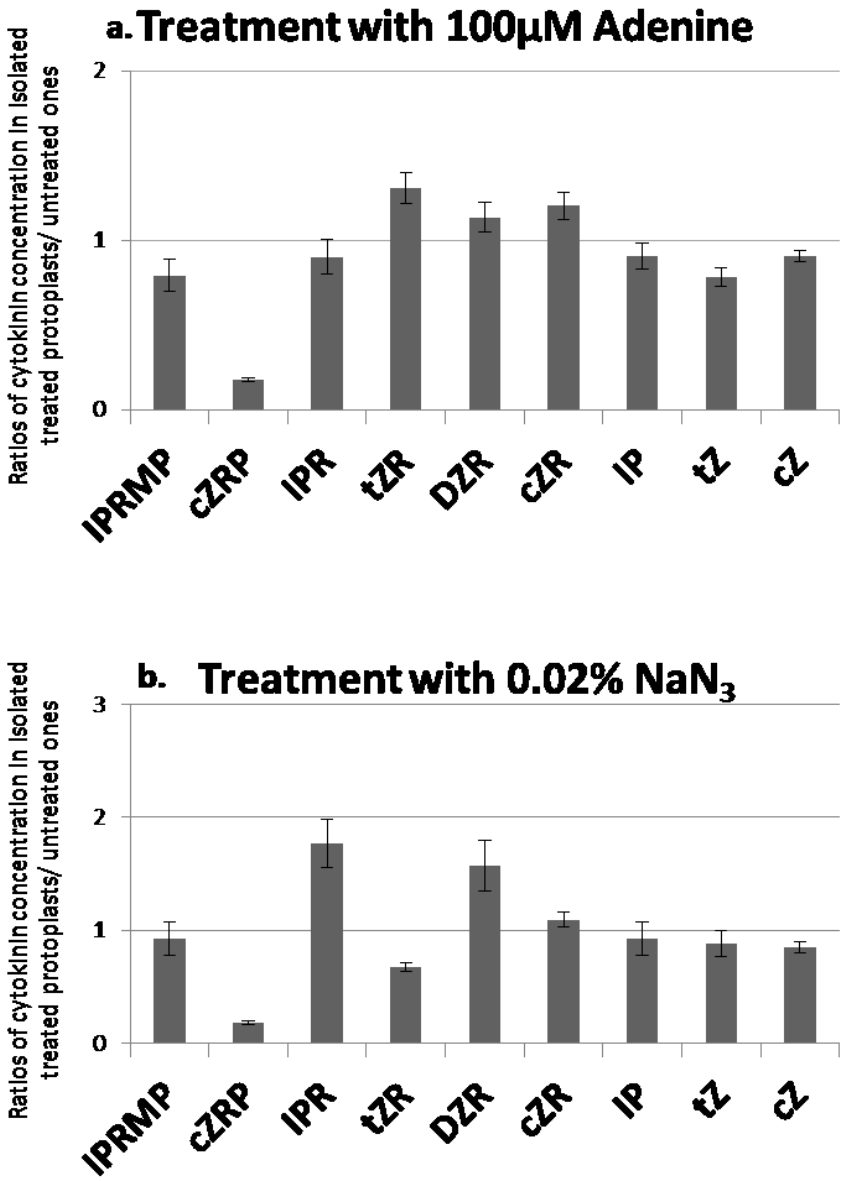

Figure 23 *Ratios of cytokinin concentration in isolated treated protoplasts to the respective untreated ones. The protoplasts were treated for 2 h by adding* ***a.*** *100 µM Adenine and* ***b.*** *3 mM Sodium azide (NaN_3) to the protoplast isolation buffer. The concentration of the detected metabolites was calculated as pmol/100.000 protoplasts and the respective ratios were then determined. Three biological replicates were performed and each was a pool of at least 1500 roots. Error bars indicate standard error (n=3).*

As presented in Figure 23, most cytokinin metabolites exhibited less than two-fold changes in concentration as a response to the treatments. Treatment with sodium azide caused small increases of IPR and DZR while it had the opposite effect on tZR. Levels cZRMP was reduced by both adenine and sodium azide.

Finally, the effect of the cell sorting procedure was examined on cytokinin endogenous levels. Protoplasts were isolated, resuspended in 0.7% NaCl (sorting buffer) and kept at 4°C for 180 min, imitating the sorting process. Samples were centrifuged after 0 min, 90 min and 180 min and the cytokinin metabolites were quantified in the protoplast pellet and the supernatants to check the hormone metabolism and possible leakage.

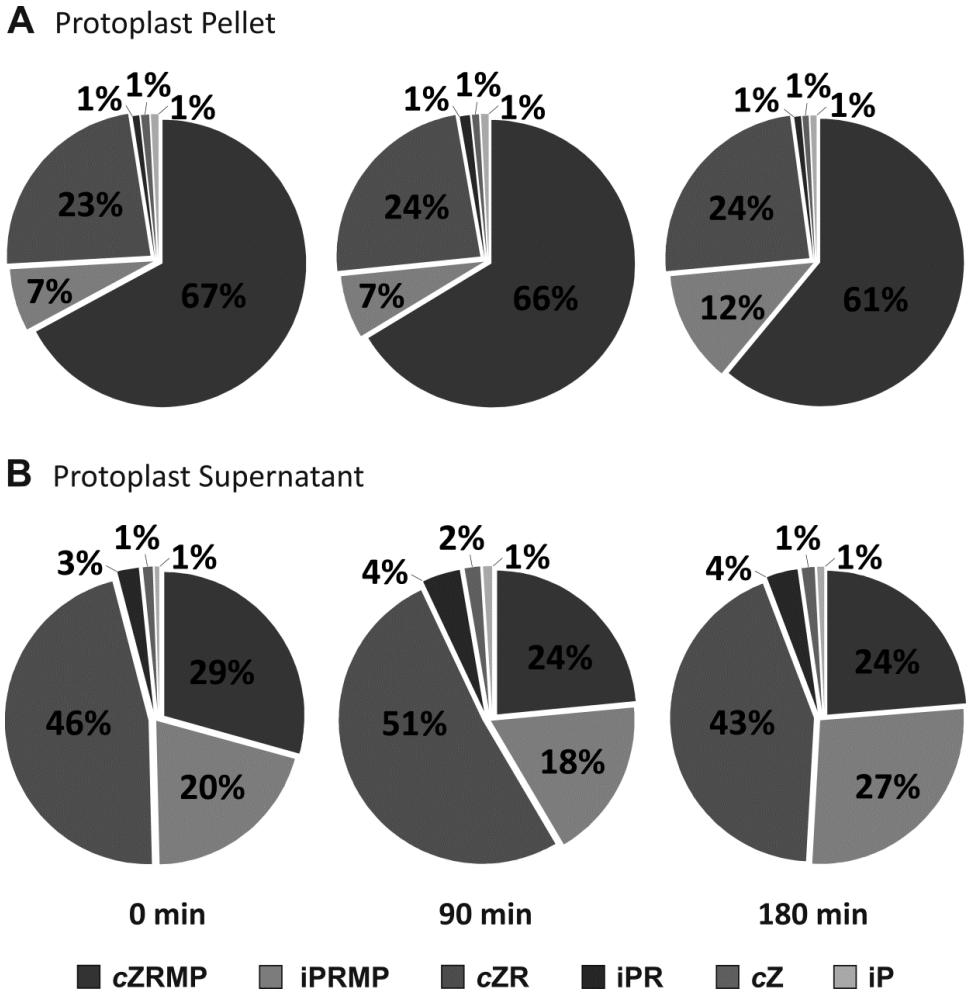

Figure 24 *Distribution of IP- and cZ-compounds of cytokinin (%) during 180 min in* ***A.*** *Protoplast Pellet and* ***B.*** *Protoplast respective supernatant. Isolated protoplasts were suspended in sorting buffer and left on ice. Samples were collected every 90 min, centrifuged and processed for analysis of the cytokinin content in the protoplast pellet and supernatant, respectively. Cytokinin metabolites were quantified in pmol/100.000 protoplasts and the percentages of their distribution were calculated from the sum of the compounds presented. For each time point 3 biological replicates were assessed and every replicate derived from a pool of at least 1500 roots.*

The distribution of cytokinin metabolites in the protoplast pellets and supernatants, presented in Figure 24, remained mostly stable during the 3 hours of incubation at 4°C. These data suggest that cytokinins are not greatly metabolized or leaking from protoplasts kept at 4°C, the same temperature used for cell sorting.

4.4.2 Cytokinin concentration in distinctive cell-types of *Arabidopsis* root apex

After optimization and testing of all the necessary steps, the quantification of cytokinin metabolites in the apical root cell-types under study was finally achieved. In Figure 25, the mean of total cytokinins in each cell population is presented.

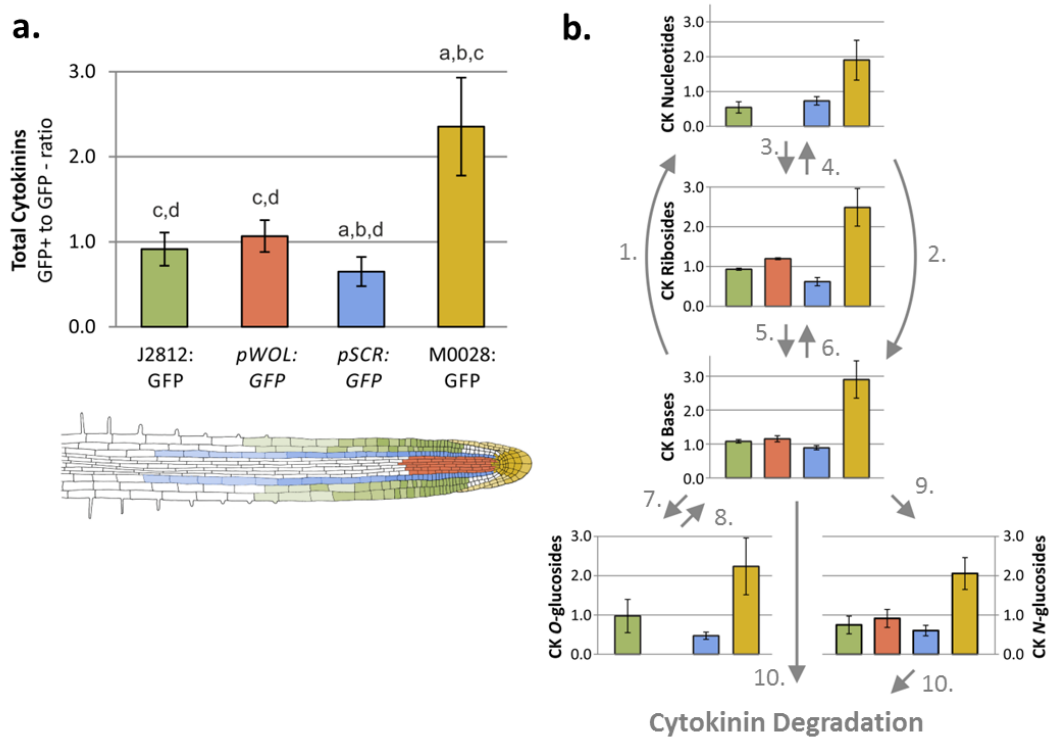

Figure 25 *Cytokinin levels in four different cell types isolated from the Arabidopsis root apex.* ***a****.Total cytokinins levels calculated as mean of the* GFP+ *to* GFP- *ratio of all CK metabolites quantified. A scheme of Arabidopsis root represents in color code the different GFP lines from which the* GFP+ *populations derived. J2812:GFP signal is displayed in red color, pWOL:GFP in red, pSCR:GFP in blue and M0028:GFP in yellow.* ***b.*** *Scheme of CK metabolism for different CK metabolite groups. The metabolites were quantified in pmol/100.000 isolated protoplasts and the respective ratios were computed in each of the sorted transgenic lines J2812:GFP, pWOL:GFP, pSCR:GFP and M0028:GFP. Error bars indicate standard error (n=6-9). The results occurred from 6 biological replicates and for each 2 technical replicates were performed. The error bars indicate standard error and the statistics presented in a. were performed using ANOVA. The numbers in b. represent enzymes involved in cytokinin metabolism as listed below: 1. adenine phosphoribosyltransferase, 2. Cytokinin phosphoribohydrolase 'Lonely guy' (LOG), 3. ribonucleotidephosphohydrolase, 4. adenosine kinase, 5. adenosine nucleosidase, 6. purine nucleoside phosphorylase, 7. zeatin-O-glucosyltransferase, 8. b-glucosidase, 9. N-glucosyl transferase, 10. cytokinin oxidase/dehydrogenase (CKX). Data generated by Ioanna Antoniadi Lenka Plačková, Biljana Simonovik, Karel Doležal, Colin Turnbull, Karin Ljung and Ondřej Novák and the Figure is adapted from Ondřej Novák.*

Thirteen cytokinin metabolites were successfully quantified in the sorted cell populations. These were the phosphates IPRP and cZRP, the ribosides IPR and cZR, the nucleobases IP, cZ and tZ and the glucoside conjugates IP7G, IP9G, tZ7G, tZ9G, cZ9G, tZOG and cZOG, as shown

in Supplementary Figure 3. tZRMP and tZR were not found in either the positive or the negative cells. All the ribosides, apart from tZR, nucleobases and 7-glucosides detected were present in all cell types under study (Supplementary Figure 3, Appendix). On the other hand some cell populations lacked some phosphate forms, O- and 9-glucosides (Supplementary Figure 3, Appendix). In general, all cytokinin metabolites showed the same trend concerning their cell-specific distribution and therefore they were presented as a mean of total cytokinin content (Figure 25.a). Then it became even clearer that cytokinins were accumulated in the root cap, initials, columella and QC (line *M0028*).

4.4.3 Cytokinin-related genes expression in distinctive cell-types of the *Arabidopsis* root apex

In order to get a more complete idea about cytokinin distribution in the root apex, four published datasets on cell-type specific transcriptional and translational signatures (Birnbaum *et al.,* 2003; Brady *et al.,* 2007; Dinneny *et al.,* 2008; Petricka *et al.,* 2012) were screened for 107 cytokinin-related genes shown in Table 5. Data were then combined with published *GFP* and GUS assays that show cell-specific resolution concerning these genes (Kuroha *et al.,* 2009; Mähönen *et al.,* 2006.a; Werner *et al.,* 2003; Zhang *et al.,* 2014.a; Zürcher *et al.,* 2013).

a.

Biosynthesis - Metabolism	
IPT1	At1g68460
IPT2	At2g27760
IPT3	At3g63110
IPT4	At4g24650
IPT5	At5g19040
IPT6	At1g25410
IPT7	At3g23630
IPT8	At3g19160
IPT9	At5g20040
CYP735A1	At5g38450
CYP735A2	At1g67110
LOG1	At2g28305
LOG2	At2g35990
LOG3	At2g37210
LOG4	At3g53450
LOG5	At4g35190
LOG6	At5g03270
LOG7	At5g06300
LOG8	At5g11950
LOG9	At5g26140
AK1	At3g09820
AK2	At5g03300
APRT1	At1g27450
APRT2	At1g80050
APRT3	At4g22570
APRT4	At4g12440
APRT5	At5g11160

b.

Degradation-Conjugation	
CKX1	At2g41510
CKX2	At2g19500
CKX3	At5g56970
CKX4	At4g29740
CKX5	At1g75450
CKX6	At3g63440
CKX7	At5g21482
UGT76C1	At5g05870
UGT76C2	At5g05860
UGT73C1	At2g36750
UGT73C5	At2g36800
UGT85A1	At1g22400

c.

Perception - Signaling	
AHK2	At5g35750
AHK3	At1g27320
CRE1/AHK4	At2g01830
AHP1	AT3g21510
AHP2	AT3g29350
AHP3	AT5g39340
AHP4	AT3g16360
AHP5	At1g03430
ARR1	At3g16857
ARR2	At4g16110
ARR10	At4g31920
ARR11	At1g67710
ARR12	At2g25180
ARR13	At2g27070
ARR14	At2g01760
ARR18	At5g58080
ARR19	At1g49190
ARR20	At3g62670
ARR21	At5g07210
ARR3	At1g59940
ARR4	At1g10470
ARR5	At3g48100
ARR6	At5g62920
ARR7	At1g19050
ARR8	At2g41310
ARR9	At3g57040
ARR15	At1g74890
ARR16	At2g40670
ARR17	At3g56380
ARR22	At3g04280
CRF1	AT4G11140
CRF2	AT4G23750
CRF3	AT5G53290
CRF4	AT4G27950
CRF5	AT2G46310
CRF6	AT3G61630
CRF7	AT1G71130
CRF8	AT1G22985

d.

Transport	
ENT1	At1g70330
ENT2	At3g09990
ENT3	At4g05120
ENT4	At4g05130
ENT5	At4g05140
ENT6	At4g05110
ENT7	At1g61630
ENT8	At1g02630
PUP1	AT1G28230
PUP2	AT2G33750
PUP3	AT1G28220
PUP4	AT1G30840
PUP5	AT2G24220
PUP6	AT4G18190
PUP7	AT4G18197
PUP8	AT4G18195
PUP9	AT1G18220
PUP10	AT4G18210
PUP11	AT1G44750
PUP12	AT5G41160
PUP13	AT4G08700
PUP14	AT1G19770
PUP15	AT1G75470
PUP16	AT1G09860
PUP17	AT1G57943
PUP18	AT1G57990
PUP19	AT1G47603
PUP20	AT1G47603
ABCG14	AT1G31770

Table 5 *List of 107 cytokinin-related genes indicated with their published name and their corresponding accession number. The genes have been categorized according to their role in cytokinin pathway as* ***a.*** *Biosynthesis and Metabolism genes,* ***b.*** *degradation and Conjugation genes,* ***c.*** *Perception and Signaling genes and* ***d.*** *(Candidate) Transport genes.*

Out of 107 genes examined, 32 were identified to be enriched in one or more cell populations of the *WOL:GFP, M0028:GFP, SCR:GFP* and *J2812:GFP* lines and are shown in Table 6.

a. *pWOL:GFP* : Stele	
Miyakaki 2004-Plant Journal	IPT3
Brandy 07-Science	
Brandy 07-Science	IPT5
Brandy 07-Science	IPT7
Brandy 07-Science	LOG1
Petrica 2012-PNAS	LOG3
Birnbaum 03-Science	
Kuroha 2009-The Plant Cell	
Dinneny 2008 Science	
Brandy 07-Science	
Birnbaum 03-Science	LOG4
Kuroha 2009-The Plant Cell	
Brandy 07-Science	LOG5
Kuroha 2009-The Plant Cell	
Kuroha 2009-The Plant Cell	LOG8
Werner 2003-The Plant Cell	CKX5
Brandy 07-Science	CKX6
Werner 2003-The Plant Cell	
Birnbaum 03-Science	UGT85A1
Petrica 2012-PNAS	APT3
Dinneny 2008 Science	
Birnbaum 03-Science	
Birnbaum 03-Science	AtAHK4/CRE1/WOL
Brandy 07-Science	AHK2
Brandy 07-Science	AHP4
Mähönen 2006-Science	AHP6
Petrica 2012-PNAS	ARR21
Brandy 07-Science	PUP4
Brandy 07-Science	PUP18
Brandy 07-Science	CRF1
Dinneny 2008 Science	ABCG14
Birnbaum 03-Science	
Zhang 2014-Nature Communications	
Brandy 07-Science	
Zürcher 2013-Plant Physiology	B-ARRs (TCSn:GFP)

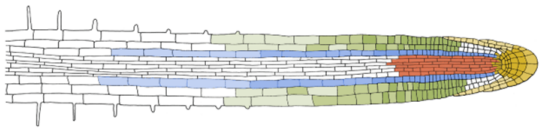

b. *M0028:GFP* : Root cap, Columella, Initials, QC	
Kiba 2013-Developmental cell	CYP735A2
Petrica 2012-PNAS	LOG1
Dinneny 2008 Science	
Kuroha 2009-The Plant Cell	LOG8
Petrica 2012-PNAS	APT1
Dinneny 2008 Science	UGT76C2
Petrica 2012-PNAS	
Brandy 07-Science	UGT85A1
Dinneny 2008 Science	
Petrica 2012-PNAS	
Petrica 2012-PNAS	CKX4
Werner 2003-The Plant Cell	
Werner 2003-The Plant Cell	CKX5
Petrica 2012-PNAS	CRF6
Dinneny 2008 Science	
Zürcher 2013-Plant Physiology	B-ARRs (TCSn:GFP)
Zhang 2014-Nature Communi	ABCG14

c. *pSCR:GFP* : Endodermis&QC	
Dinneny 2008 Science	LOG1
Petrica 2012-PNAS	
Birnbaum 03-Science	LOG4
Kuroha 2009-The Plant Cell	
Birnbaum 03-Science	CRF6
Birnbaum 03-Science	CRF2
Birnbaum 03-Science	ABCG14

d. *J2812:GFP* : Epidermis&Cortex	
Birnbaum 03-Science	LOG4
Petrica 2012-PNAS	LOG7
Dinneny 2008 Science	
Birnbaum 03-Science	
Kuroha 2009-The Plant Cell	
Birnbaum 03-Science	LOG8
Birnbaum 03-Science	UGT85A1
Petrica 2012-PNAS	APT4
Dinneny 2008 Science	
Birnbaum 03-Science	CRF3
Birnbaum 03-Science	CRF2
Birnbaum 03-Science	ABCG14
Petrica 2012-PNAS	ARR8
Dinneny 2008 Science	

Table 6 *Gene expression enriched in* ***a.*** *Stele,* ***b.*** *Root cap, Columella, Initials and QC,* ***c.*** *Endodermis and QC and* ***d.*** *Epidermis and Cortex. The data derive from analytical GUS and GFP assays and from four studies in the transcriptome and proteome of cell-specific populations of the root.*

The largest number of cytokinin genes with enhanced expression (22/32) were identified in the root vasculature (Table 6.a) with the least in the endodermis (5/32; Table 6.c). In the root cap, initials, columella and QC 11 genes were enriched and nine in epidermis and cortex. Cytokinin biosynthesis (*AtIPT*), perception (*AtAHK2, AtAHK4/CRE1/WOL*) and cytokinin influx (*AtPUP*) were exclusively detected in the stele. Cytokinin metabolism through the *AtLOG* and *APT* genes was shown to be active in all cell populations of the root apex. The same conclusion was drawn for cytokinin signaling genes (*AtCRF* and *AtARR*) and efflux transport through *AtABCG14* being identified in all four *GFP* lines under study.

4.5 Discussion

In this Chapter a novel method for quantifying cytokinins at high resolution, at the cell specific level, was developed and validated. The optimised method was then used to investigate the distribution of cytokinin metabolites in specific cell populations of the *Arabidopsis* root apex and identify how the hormone builds its gradients within this site.

4.5.1. Method development

A method to quantify IAA and its catabolite OxIAA in cell populations was recently developed (Pencík *et al.,* 2013; Petersson *et al.,* 2009). However, a more sensitve method was required for cytokinin quantification since its concentration is much lower than IAA within the plant. The method required four steps, as shown in Figure 18, including 1. protoplast isolation of the desired *GFP* trangenic line, 2. collection of the *GFP*+ and *GFP*- cells through fluorescence-activated cell sorting, 3. cytokinin compounds purification and 4. quantification of the hormone using LC-MS/MS. All the four steps were adapted and optimised as discussed below.

The step 3. of the procedure concerned the cytokinin purification process which has been optimised from Svacinova *et al.,* (2012) to one-step micro-purification using in-tip microSPE packed with three layers of each of the sorbents C18/SDB-RPS/Cation SR (Figure 19). In addition, further optimisation steps took place to eliminate disadvantageous effects that the sorting buffer (0.7% NaCl), in which sorted protoplasts were suspended, had on the purification and quantification processes. Initially 3:1 dilution of NaCl loaded in the microSPE, along with the isolated cell populations, was used since it increased the process

efficiency (Figure 20.B). Also, for the activation step of the sorbents packed in the microSPE, nitric acid was showed to be more efficient than the previously used formic acid (Figure 20.A). Therefore the purification protocol was optimised accordingly to these findings and is presented in Figure 21.

Importantly, the steps 1. and 2. of the procedure were tested for alterations in cytokinin metabolism and for leakage of the hormone from the protoplasts. Cytokinin metabolites levels showed no striking difference as a response to the treatments performed during protoplasting as analysed below.

As displayed in Figure 22, inhibiting cytokinin irreversible degradation with the specific CKX inhibitor, INCYDE (Zatloukal *et al.,* 2008) resulted in elevated levels of the nucleobases IP and tZ and the riboside IPR, compounds known to be highly degraded from CKXs (Gajdosová *et al.,* 2011; Köllmer *et al.,* 2014). The fact that the maximum alteration caused by the treatment was only a 2-fold increase of IP concentration suggests maintenance of the representative endogenous cytokinin levels during protoplast isolation.

Treatments with adenine (Figure 23.a), used before as cytokinin transport antagonist (Cedzich *et al.,* 2008; Bürkle *et al.,* 2003), caused not even 2-fold alterations in cytokinin metabolites concentration. The slight response that was observed concerned decrease of all cytokinin nucleobases detected and increased levels of all ribosides. This is in accordance with the common transport H^+-coupled high affinity purine transport system that nucleobase cytokinins and adenine share based on their structural similarities. Similarly with the results presented here, competition studies with adenine and tZ and zeatin ribosides, dispayed that only tZ uptake was inhibited due to adenine presence while the zeatin robosides uptake was increased (Bürkle *et al.,* 2003).

When sodium azide was added to the protoplast isolation buffer (Figure 23.b), as inhibitor of ATP-dependent metabolic and membrane transport processes (Tucker 1993), DZR and IPR levels were elevated while tZR concentration was reduced. The levels of the affected compounds again did not display a more than a 2-fold change indicating that endogenous levels of cytokinin can still be representative even after protoplast isolation. The opposite trends in the alterations observed mainly in the cytokinin ribosides in response to sodium azide could not fully explained. This is due to the fact that this chemical is not only cytokinin related and apart from ATP generating respration inhibition (Drake 1979) it also causes other changes in plant cells like Ca^{2+} levels increase (Gilroy *et al.,* 1989) and reduction of the pH

(Spanswick and Miller 1977) which can interact with cytokinin compounds chemistry. For example CKX enzymes activity is highly pH-dependent (Galuszka *et al.,* 2007).

Conclusively the data deriving from these chemical treatments, suggest that during protoplast isolation cytokinin metabolism is still active and functional but at sufficiently low levels so estimation of the endogenous concentrations of the hormone can still be allowed.

Finally, the examination of cytokinin leakage from the isolated protoplasts during cell sorting demonstrated similar results, as exhibited in Figure 24. Cytokinin analysis of the protoplast pellets indicated that the enzymes responsible for cytokinin metabolism were mainly inactive and that there was no significant leakage for the 3h period required for sorting at 4°C. The cytokinin levels detected in the respective supernatant samples could possibly derive from damaged protoplasts and undigested cell walls occurred during the protoplasting. However the negligible alterations in the cytokinin compound distribution over time also demonstrate no leakage or modification of the hormone metabolism at 4°C during cell sorting.

4.5.2 Cytokinin gene expression and metabolite distribution in the *Arabidopsis* root apex

Cytokinins are present in plant tissues in minute amounts (pmol/g FW) which makes their quantification challenging. However, the rapid improvement of analytical methods such as mass spectrometry during the last 15 years has allowed the detection and analysis of the hormone from gram to milligrams (50mg) of fesh weight tissue (Liu *et al.,* 2012; Müller and Munné-Bosch, 2011; Novák *et al.,* 2008; van Rhijn *et al.,* 2001; Zhang *et al.,* 2001). By using the technique developed in this Chapter, cell-specific cytokinin quantification from transgenic lines with *GFP* expression was for the first time possible in the equivalent of less than 50 cells per root (*M0028* line; Swarup *et al.,* 2005).

In this work, four transgenic *Arabidopsis* lines were chosen due to the combination of their fluoresent signals together covering all the cell populations of the root apex (Figure 18.a). The cytokinin concentration of the *GFP*+ cells of each line was normalized to the concentration of the respective *GFP*- cells to avoid misinterpretation of any shifts in cytokinin levels because of other factors such as slight differences in growth conditions. It should also be noted that any absence of metabolite detection observed in both *GFP*+ and

GFP- cells was interpreted either as a problem of detection or as a complete absence of the compound in the apical part of the root.

The first cell-specific cytokinin map of *Arabidopsis* root apex was finally constructed and it suggests that there is a gradient of cytokinins in the apical part of the *Arabidopsis* primary root including the specific cell types of root cap, columella, initials and QC (Figure 25). Petersson *et al.,* (2009) showed that columella was one of the *Arabidopsis* cell populations accumulating the lowest IAA concentration compared to the surrounding cell types. This, in combination with the highest cytokinin concentration also at the columella presented here is in agreement with the concept of antagonistic crosstalk between auxin and cytokinin controlling several aspects of development and organogenesis. Examples include root meristem size determination (Dello Ioio *et al.,* 2007; Dello Ioio *et al.,* 2008), lateral root priomordia formation (Moreira *et al.,* 2013), lateral root initiation (Laplaze *et al.,* 2007b) and embryonic stem cell niche specification (Müller and Sheen, 2008). In *Arabidopsis* root tips, it was also shown that while the auxin signaling reporter DR5 expression displayed its maximum signal in the central columella cells, the *TCSn*-monitored cytokinin output exhibited its highest enrichment in the outer columella cells surrounding the *DR5* territory (Bielach *et al.,* 2012).

In a complementary approach, a cell-specific analysis of the *Arabidopsis* root apex concerning the expression of cytokinin-related genes was created (Table 6). The data derived from four individual microarray studies in distinctive cell populations of the root (Birnbaum *et al.,* 2003; Brady *et al.,* 2007; Dinneny *et al.,* 2008; Petricka *et al.,* 2012). With the aim of comparing the cell-specific gene expression of cytokinin-related genes with the cytokinin map described above, the data were clasified in four categories corresponding to the cell type populations that *M0028:GFP, J2812:GFP, pWOL:GFP* and *pSCR:GFP* are expressed. The dataset (Table 6) was then augmented by studies concerning *GUS* and/or *GFP* promoter driven expression of cytokinin-related genes (Kiba *et al.,* 2013; Kuroha *et al.,* 2009; Mähönen *et al.,* 2006.a; Miyawaki *et al.,* 2004; Werner *et al.,* 2003; Zhang *et al.,* 2014.a; Zürcher *et al.,* 2013).

The cytokinin gene expression cell-specific analysis of *Arabidopsis* root apex indicated that out of the 11 cytokinin-related genes enriched in the cell types of root cap, columella, QC and initials (*M0028:GFP*) where cytokinin maxima was determined, two belonged to the *AtCKX* family and another two to the *AtUGT* family (Table 6.b). Both these enzymes deactivate cytokinins. It has been previously shown that enhanced CKX activity corresponds

to high concentrations of cytokinin (Gaudinová *et al.,* 2005; Motyka *et al.,* 1994). In accordance, the *ugt76c2* mutant had reduced levels for most of the cytokinin metabolites (Wang *et al.,* 2013). The above mentioned findings are in agreement with the cytokinin increased concentration in the *GFP*+ cells of *M0028* line and with the high expression of genes inactivating cytokinins (*AtCKXs* and *AtUGTs*). The role of these increased levels of cytokinins in the root cap could be speculated to be involved with cytokinin effect in gravitropism (Aloni *et al.,* 2004). Finally, *TCSn:GFP* representing the transcriptional output of cytokinin is also differentially expressed in root cap, confirming our gradient results (Zürcher *et al.,* 2013).

TCSn:GFP also displayed a strong signal in the root vasculature (Zürcher *et al.,* 2013) where maximum expression of most cytokinin-related genes was identified (Table 6.a) compared with the surrounding cell populations of the root apex. It was noticable that cytokinin biosynthesis (*AtIPT* genes) and the receptors of the hormone (*AtAHK* genes) were found to express exclusively in the stele. This was in contrast with the concentration of cytokinins in the stele which showed no induction compared to the average surrounding tissue. An aspect that should be taken into consideration is the presence of apoplastic cytokinins, analysed in Chapter 5.4.4, being excluded from this study due to the cell-sorting procedure. A heterogeneous distribution of the apoplastic cytokinins between different cell populations that could affect the cytokinin distribution in the root apex shown in Figure 25 cannot be excluded. However, such data are unfortunately impossible to get but they could provide a plausible explanation for this contradiction between the cytokinin concentration and gene expression data.

Another possible explanation for these conflicting results is that the enrichment of transporter expression (*AtPUP* and *AtABCG14* genes) in the root vasculature could reallocate cytokinins thus limiting their accumulation at this site. Since the cell populations of root cap, columella, initials and QC where cytokinin metabolites were accumulated also showed the highest expression of four different cytokinin inactivation enzymes, it could be speculated that cytokinins are transported to these cell populations to be inactivated.

Finally the cells of the endodermis displayed reduced cytokinin levels, specifically for cytokinin glucosyl-conjugates and all the cis-zeatin forms. This was not surprising since the number of cytokinin genes expressed in the endodermis was the lowest of all the cell types under study (Table 6). Also the expression of *AtCKXs and AtUGTs* was not enhanced in this cell population, suggesting reduced demand for cytokinin degradation or conjugation.

4.6 Conclusions

- A novel method was developed and presented for cytokinin quantification at high resolution, cell specific levels. This was achieved by a combination of FACS and ultra-sensitive LC-MS/MS which facilitated detection of 15 cytokinin metabolites even in samples as small as 20.000 protoplasts.
- Validation of the method and control experiments showed that the cytokinin content of protoplasts overall changed slightly over the few hours needed to generate and collect the different cell populations, and only small amounts of cytokinins were lost due to protoplast leakage.
- Quantification of cytokinins in a range of *Arabidopsis* root apex *GFP*-marked cells revealed that while cytokinin distribution was similar in three of the cell types under study, it was significantly enriched in the cell populations including root cap, columella, QC and initials.
- A parallel analysis of cytokinin-related gene expression in the cell populations under study showed that in the site of cytokinin maximal concentration, cytokinin-conjugation/degradation genes were predominantly expressed.
- Across the cell populations studied, the majority of cytokinin-related gene expression was found in the stele, with genes related to cytokinin biosynthesis, perception and uptake exclusively detected in this tissue.

Chapter 5

Heterogeneous intra- and extra-cellular distribution of cytokinin metabolites in the Arabidopsis root.

The results of this Chapter derived from collaboration between Imperial College London and Umea Plant Science Center (UPSC, Umea, Sweden). The people contributing to this work were Ioanna Antoniadi, Ondřej Novák, Thomas Vain, Karin Ljung and Colin Turnbull. Specific contributions are stated in the Figure legends.

5.1 Introduction

TCSn:GFP (Two component signal – green fluorescent protein) is a new synthetic promoter fusion which enables reporting of cytokinin transcriptional responses at the cellular level (Zürcher *et al.,* 2013). This reporter has been designed around the native cytokinin receptor-signaling system which is a version of two component – phosphorelay cascade. As shown in Figure 26, *TCSn:GFP* in the primary root tips of *Arabidopsis* shows clear heterogeneous distribution of expression in the primary root of *Arabidopsis* seedlings suggesting a modulation of cytokinin signaling at the cellular level.

In order to understand the biological relevance of the *TCSn:GFP* reporter line, we performed a cell-type specific validation of the reporter. Analytical approaches, such as liquid chromatography - tandem mass spectrometry (LC-MS/MS), can provide accurate quantitative measurements of cytokinin metabolites. Here, the novel method combining Fluorescence Activated Cell Sorting (FACS) with ultra-sensitive LC-MS/MS analysis developed in Chapter 4 was used to quantify cytokinin metabolites in the *GFP*+ and *GFP*- cells of *TCSn:GFP* root tips.

Figure 26 *TCSn:GFP expression pattern in 5 days old Arabidopsis root.*

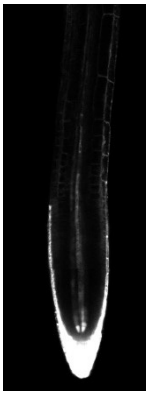

The biological significance of this study is that it provides an essential validation of *TCSn:GFP* as a cytokinin response reporter, relevant to many recent findings where the reporter facilitated discovery of new cytokinin functions (Muller and Sheen 2008; Bencivenga at al., 2012; Marsh-Martinez *et al.,* 2012) and deepened our understanding of existing ones (Leibfried *et al.,* 2005; Gordon *et al.,* 2009; Zhao *et al.,* 2010; Bielach *et al.,* 2012; Chickarmane *et al.,* 2012; Murray *et al.,* 2012).

Finally, the presence of cytokinin metabolites was tested in the extracellular space. The initial reason for this study was to measure cytokinins in the apoplastic space which is excluded in the cell sorting experiments. During the protoplasting process required for FACS, cell walls and apoplastic space are eliminated. The apoplastic space was also an interesting place to look for cytokinins since there are contradictory lines of evidence concerning cytokinin receptors localization.

Until 2011, it was believed that all three cytokinin receptors were localized to the plasma membrane with their cytokinin-binding CHASE domain extracellularly. This conclusion initially derived from the bioinformatic analysis of the AHK protein sequence and from the analogy with sensor His kinase localization in yeast and bacteria (Inoue *et al.,* 2001; Ueguchi *et al.,* 2001). Later it was also experimentally confirmed by the plasma membrane localization of *AtAHK3:GFP* in *Arabidopsis* protoplasts (Kim *et al.,* 2006). It has been proposed that some *CKX*s are secreted to the apoplast in maize, rice and *Arabidopsis* (Bilyeu *et al.,* 2001; Kopecný *et al.,* 2010; Smehilová *et al.,* 2009) suggesting the likely presence of extracellular active cytokinins . On the other hand, more recent results, including cytokinin binding assays with isolated membrane fractions and fluorescence-labelled constructs, suggest that cytokinin sensing predominantly occurs in the endoplasmic reticulum (ER) lumen (Wulfetange *et al.,* 2011; Lomin *et al.,* 2012). This is also supported by data showing that optimal cytokinin-binding activity is at pH 6.5 which is characteristic for ER (Romanov *et al.,* 2006) but not for the apoplast (pH 5.5, J. Li *et al.,* 2005).

5.2 Aims

The aim of this Chapter was to examine whether cytokinin metabolites are enriched in *TCSn:GFP* positive cells, and to discover which are the predominant compounds in the cell populations representing sites of cytokinin response. Such information would provide a clear insight into spatial cytokinin perception and signaling and would reveal a link between fluorescence of *TCSn:GFP* and specific cytokinin metabolites . An additional aim was to investigate whether cytokinins are heterogeneously distributed between intra- and extra-cellular space. This would allow identification of cytokinin metabolites that are excluded in the FACS-related experiments and complete the 'picture' of cytokinin distribution in *Arabidopsis* root apex.

5.3 Materials and Methods

5.3.1 Plant Material, Growth Conditions, Protoplast isolation, Cell Sorting, Cytokinin purification and LC-MS/MS analysis.

The transgenic *Arabidopsis thaliana TCSn:GFP* line (Zürcher *et al.,* 2013) was surface sterilized, sown and grown as described in 4.3.1. When the seedlings were 8 days old they were harvested and processed for protoplast isolation and cell sorting as mentioned in Chapters 4.3.2 and 4.3.3. Cytokinin metabolites were purified from the sorted cells and quantified through LC-MS/MS using the method developed in Chapters 4.3.5 and 4.3.6.

5.3.2 Apoplastic and Symplastic Fluid Extraction

Roots of 8 days old Col-0 seedlings, grown as described above, were harvested, weighted and positioned in a 1ml syringe (without plunger). The syringe containing the sample roots was placed in a 25ml falcon which was then centrifuged at 900×g for 20min at 4°C. The apoplastic fluid was collected from the bottom of the falcon tube and transferred to a clean Eppendorf . The syringe containing the remaining root tissue was snap-frozen in liquid nitrogen and let to thaw at room temperature. Finally, the syringe was placed in a clean 25ml falcon in which the symplastic fluid was collected after a 15 min centrifugation at 2500×g at 4°C. Three biological replicates were analysed and each was a pool of at least 1500 seedlings.

5.3.3 Confocal microscopy

Five days old *TCSn:GFP* seedlings grown as described above, were transferred into liquid MS media supplemented with 10 µM INCYDE - (2-chloro-6-(3-methoxyphenyl)aminopurine - (Zatloukal *et al.,* 2008; Aremu *et al.,* 2012), BAP (6-benzylaminopurine) and Roscovitine - (6-benzylamino-2-[1(R)-(hydroxymethyl)pro- pyl]amino-9-isopropylpurine - (Aremu *et al.,* 2012) for 6 hours. Confocal Laser Scanning Microscopy was then performed using Zeiss LSM 780. The *GFP* signal from at least 10 roots per treatment was analyzed.

5.3.4 Feeding *Arabidopsis* root protoplasts with labelled cytokinins

Protoplasts were isolated following the protocol mentioned in Chapter 4.3.2 from roots of 8 days old *Arabidopsis* seedlings that have been sown and grown as described in Chapter 4.3.1. Isolated protoplasts from 150 Petri dishes (45000 seedlings) were resuspended in protoplast buffer (600 mM mannitol, 2 mM $MgCl_2$, 10 mM KCl, 2 mM $CaCl_2$, 2 mM MES, 0.1% BSA, pH 5.7) and distributed in 7 samples containing equal volumes of protoplast buffer and presumably similar amount of protoplasts. In each sample 1µM of [$^{13}C_5$]tZ or [$^{13}C_5$]cZ was added. The 7 samples included a common sample for [$^{13}C_5$]tZ and [$^{13}C_5$]cZ at 0 min and two samples for each timepoint (30, 60 and 90 min of incubation) for [$^{13}C_5$]tZ and [$^{13}C_5$]cZ. After adding the labelled compounds in the corresponding samples they were further divided in three samples of equal volumes representing the three replicates per sample. The protoplasts were incubated in the dark at RT during continuous mixing (126 rpm) and after the corresponding time of 0, 30, 60 and 90 min the protoplasts were centrifuged at 1000×g for 3 min at 4°C, frozen in liquid nitrogen and stored at -80°C for cytokinin purification and quantification as described in Chapters 4.3.5 (MCX Oasis cartridges were used instead of microSPE columns) and 4.3.6. By pooling and dividing the samples in equal volumes it was attempted to have the data normalized per sample and therefore the cytokinin content was calculated in pmol/sample.

5.3.5.Quantification of the *GFP* signal using Image J software.

ImageJ was used to quantify the fluorescence intensity of the *GFP* in the root. Raw image have been converted in 8-bits. Fluorescence profiles of the stele and the full root have been extracted in grey value which represents the pixel intensity between 0 (black) and 255 (white). Each grey value represents the average pixel intensity of a transversal line crossing the whole root (100 pixels) or just the stele (10 pixels). Plot profiles are the result of the quantification from 10 roots per treatment.

5.4 Results

5.4.1 Quantification of cytokinin metabolites in the *GFP*+ and - cells of *TCSn:GFP*.

TCSn:GFP is widely used as a cytokinin signaling reporter line. Since in Chapter 4 a method for measuring cytokinins at cell-specific levels was developed, the examination of which cytokinin metabolites are enriched in the *TCSn:GFP* positive cells was now possible. Root protoplasts of 8 day old TSCn:*GFP* seedlings were isolated, sorted and analysed as described in Chapter 4. The concentration of cytokinins was quantified in the *GFP*+ and – cells. Finally, the ratio of the cytokinin concentration in *GFP*+/*GFP*- cells was calculated and is presented in Figure 27.

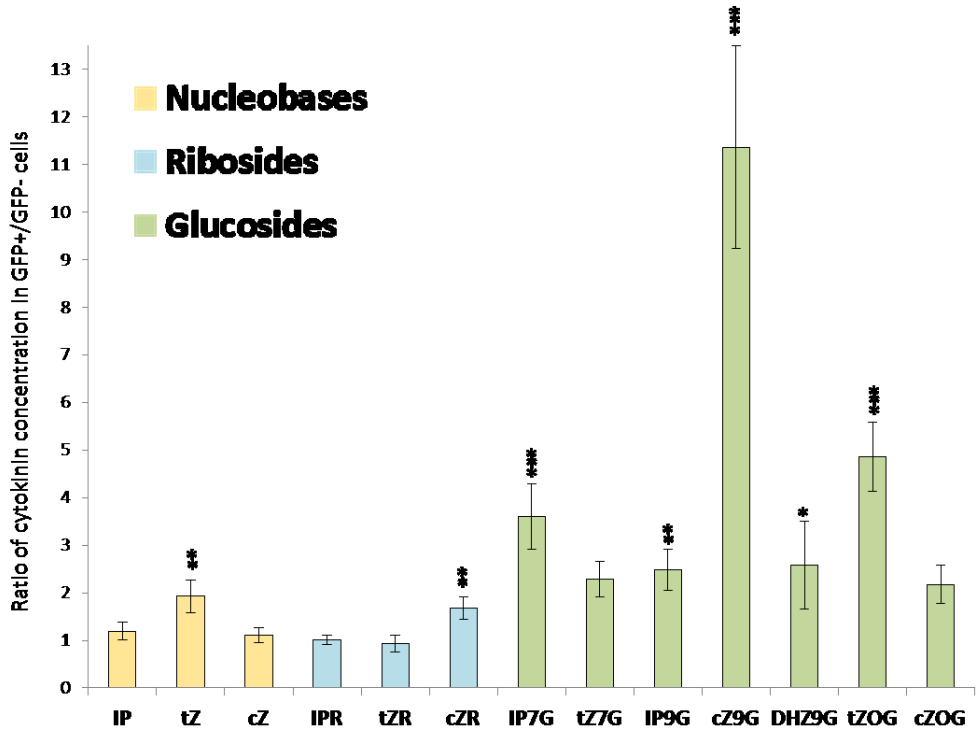

Figure 27 *Ratios of cytokinin concentration of GFP +/*GFP- *root cells of 8 days old TCSn:GFP root apex. The metabolites were quantified in pmol/100.000 protoplasts and the respective ratios were computed. Error bars indicate standard error (n=9). The results represent 9 biological replicates and for each 2 technical replicates were performed. The color of the bars represents different cytokinin metabolite groups; Yellow; cytokinin nucleobases, Blue; cytokinin ribosides and Green; cytokinin glucosyl-conjugates. The stars indicate statistically significant differences of cytokinin concentration between GFP negative and positive cells of TCSn:GFP by paired sample Student's t-test.*

All the nucleobases and ribosides, apart from tZ and cZR which showed a two-fold enrichment in *GFP*+/*GFP*- cells of *TCSn:GFP,* were equally abundant in *GFP*+ and - cells of

TCSn:GFP. The cytokinin glucosyl-conjugates, DHZ9G, cZ9G, iP9G, iP7G and tZOG, were the predominant forms significantly enriched (>4 fold) in the *GFP*+ cells.

5.4.2 Metabolism of [$^{13}C_5$]tZ and [$^{13}C_5$]cZ in *Arabidopsis* root protoplasts.

Since cytokinin glucosides were identified as the predominant forms in the cytokinin-responsive (*TCSn:GFP*+) cells of *Arabidopsis* roots, a root protoplast feeding experiment was performed. The aim was to observe the metabolism and conjugation of cytokinin nucleobases, to explore the possibility that glucoside abundance in the cytokinin responsive cells was due to rapid conjugation of nucleobases. Labelled cZ and tZ were used as fed cytokinins since tZOG and cZ9G were among the predominant glucosides in the *TCSn:GFP*+ cells as shown in Figure 27. [$^{13}C_5$]tZ and [$^{13}C_5$]cZ were added to isolated protoplasts of the transgenic line and cytokinin endogenous and labelled compounds were analyzed after 30, 60 and 90min of incubation, as shown in Figure 28.

As presented in Figures 28.a and 28.b, the predominant metabolites occurred from both applied [$^{13}C_5$]tZ and [$^{13}C_5$]cZ were the tZRP and cZRP nucleotides, respectively. The high yield of cZRMP was accompanied by lower levels of the glucoside cZ7G and the riboside cZR while when labelled tZ was applied, tZR and tZOG were the next most abundant labelled metabolites after tZRMP. The rest of the labelled compounds measured, tZROG, tZ9G, cZROG and cZ9G rspectively were close to baseline levels. The concentration of all compounds produced from [$^{13}C_5$]cZ displayed increases during the first hour of incubation and declined thereafter, while the relative concentrations of [$^{13}C_5$]tZ metabolites showed no trend of reduction up to 90 min of incubation.

Levels of almost all the endogenous cytokinin compounds, presented in Figure 28.c and 28.d, displayed reductions especially within the first 30 min. The endogenous levels of cZ and tZ and their corresponding nucleotides, exhibited reductions over time, with the greater responses showed by tZ-types. Other endogenous compounds that decreased in levels were tZROG, tZ7G and cZR respectively.

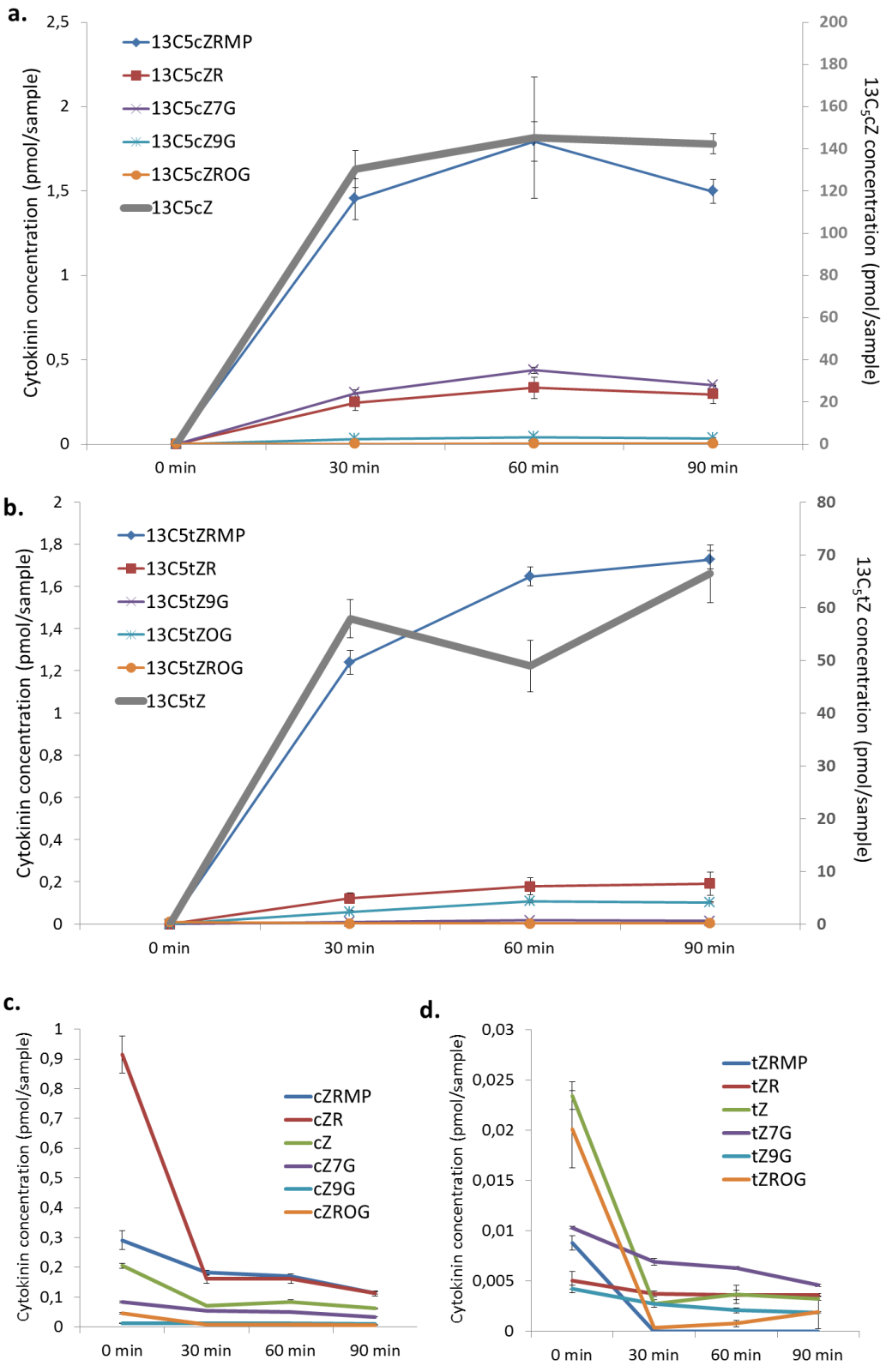

Figure 28 *Cytokinin concentration of* ***a. & b.*** *[$^{13}C_5$] labelled compounds and* ***c. & d.*** *endogenous compounds deriving from of 8 days old Arabidopsis root protoplasts incubated for 30, 60 and 90min with* ***a. & c.*** *[$^{13}C_5$]cZ and* ***b. & d.*** *[$^{13}C_5$]tZ. The concentration was calculated in pmol/sample for all compounds presented. The concentration of the exogenously supplied compounds, [$^{13}C_5$]cZ and [$^{13}C_5$]tZ in* ***a.*** *and* ***b.*** *(thick grey line), respectively, corresponds to the right side axis of the charts. The data for each timepoint derive from three biological replicates and each replicate included protoplasts isolated from a pool of 4500 Arabidopsis roots. The experiment was conducted by Ioanna Antoniadi and the LC-MS/MS method was developed with the assistance of Ondřej Novák.*

5.4.3 Cytokinin quantification in *GFP*+ and - cells of the *TCSn:GFP* line treated with INCYDE.

To further validate the results presented in 5.4.1, cytokinin metabolites levels were measured in *TCSn:GFP* protoplasts that had increased *GFP* signal after a range of treatments. The treatments were applied with the aim of identifying a cytokinin-related chemical that would induce the hormone response and therefore the *TCSn:GFP* signal. In that way, this induction could be translated into the increase of cytokinin compounds compared to the untreated experiment presented in Figure 27.

To select the chemical treatment that induced the highest cytokinin response , 5 days old *TCSn:GFP* seedlings were transferred into liquid media containing 10 µM of either INCYDE, an inhibitor of cytokinin oxidase (Aremu *et al.,* 2012; Zatloukal *et al.,* 2008), 6-benzyladenine (BAP), or Roscovitine, an inhibitor of N-glucosylation (Aremu *et al.,* 2012). Ten seedlings from each treatment were collected after 6 hours and the fluorescence in their root apex was examined and compared to the DMSO control using Laser Scanning Confocal Microscopy (LSCM). The *GFP* signal was quantified separately in the stele and in the whole root to facilitate the final choice of most effective chemical, as described below.

The data presented in Figure 29 show that all treatments caused an increase of the *TCSn:GFP* fluorescent signal*,* as predicted from the biochemical function of these molecules, especially in the stele of the apical meristem area (Figure 29.b). The chemical that showed the biggest difference in both the stele and the whole root was INCYDE. INCYDE was thus selected for use in the subsequent *TCSn:GFP* protoplast experiments.

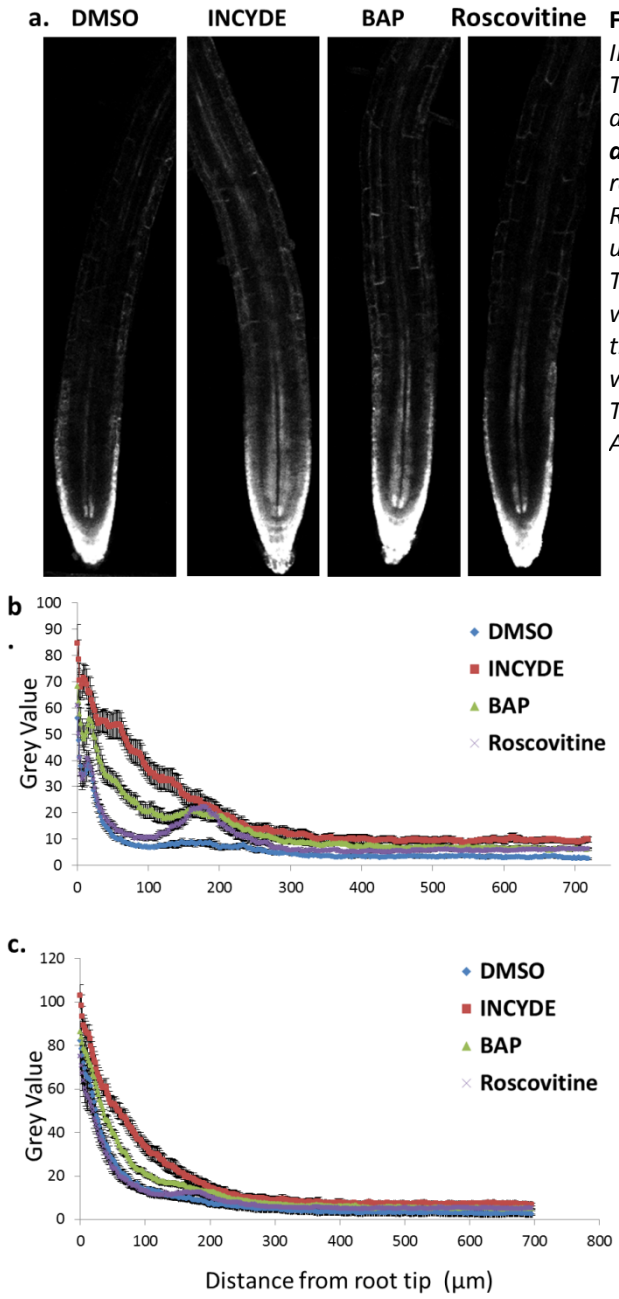

Figure 29 *Treatments of TCSn:GFP with 10 µM INCYDE, BAP and Roscovitine for six hours. The data derived from 10 roots per treatment and 2 individual experiments were performed.* ***a.*** *Representative image of treated TCSn:GFP roots with 10 µM INCYDE, BAP and Roscovitine as indicated. DMSO has been used as control. Quantification of the TCSn:GFP signal in* ***b.*** *the stele and* ***c.*** *the whole root deriving from the photos taken at the confocal microscope. The quantifications were conducted using the program ImageJ. The experiment was conducted by Ioanna Antoniadi with the assistance of Thomas Vain.*

TCSn:GFP roots were treated with 20 µM INCYDE during the 2 h of cell wall digestion for protoplast isolation. The treated protoplasts were then sorted and cytokinin metabolites were quantified in *GFP*+ and *GFP*- cells. The data presented in Figure 27, representing the mock samples, are shown again in Figure 30 in lighter colors (*TCSn:GFP* untreated) so they can be compared with the INCYDE-treated data in the corresponding darker colors. The stars on the top of each bar indicate significant difference in cytokinin concentration between positive and negative cells while the stars on the top of the red brackets denote significant difference in the cytokinin ratio between mock and treated experiment.

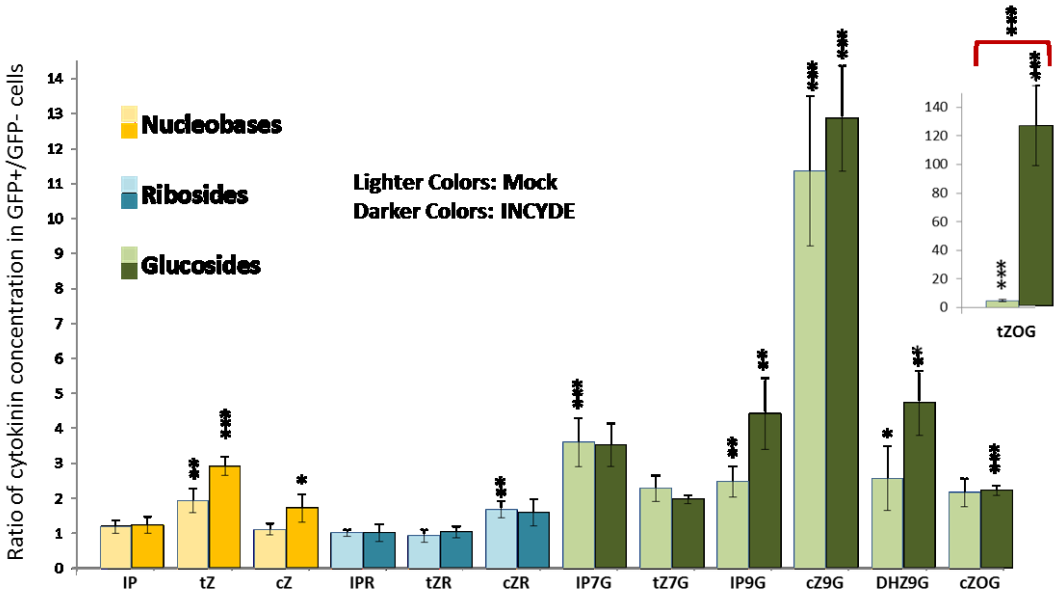

Figure 30 *Ratios of cytokinin concentration in GFP +/*GFP- *root cells of TCSn:GFP line treated or not with 20 μM INCYDE. The metabolites were quantified in pmol/100.000 protoplasts and the respective ratios were computed. The color of the bars represents different cytokinin metabolite groups; The color of the bar representing different cytokinin metabolite groups; Yellow; cytokinin nucleobases, Blue; cytokinin ribosides and Green; cytokinin glucosyl-conjugates. The darker-colored bars concern the results after treatment with INCYDE while the respective lighter-colored ones show the results without treatment (mock) also presented in Figure 27, in order to highlight the response to the treatment. The error bars represent standard error (n=9, for mock and n=6 for treated samples). The stars indicate statistically significant differences of cytokinin concentration between GFP negative and positive cells of TCSn:GFP treated and mock respectively. The starts on the top of the red brackets denote statistically significant difference in the cytokinin ratios between mock and treated experiment. All statistics were performed by paired sample Student's t-test*

As presented in Figure 30, the most enriched cytokinin metabolites in treated *TCSn:GFP* positive cells were the cytokinin glucosides and the nucleobases tZ and cZ. However, only the O-glucoside tZOG responded significantly to INCYDE treatment, with a more than 100 fold increase in the treated *GFP*+ protoplasts compared to the non-treated ones. The respective nucleobase, tZ, also displayed a trend of increase in the *GFP*+ cells of the treated roots.

5.4.4 Cytokinin quantification in the apoplast of *Arabidopsis* roots

As described in 5.4.1 and 5.4.3, the most enriched metabolites detected in the cytokinin responsive *TCSn:GFP* + cells – were the cytokinin glucosides and not the bioactive compounds as expected. Since the cell sorting procedure required discard of the cell walls and apoplastic space, the cytokinins examined were those remaining in the symplastic space. Therefore presence of cytokinin compounds in the root apoplast was tested. The roots of 8 days old seedlings were harvested and processed for apoplastic and symplastic fluid isolation.

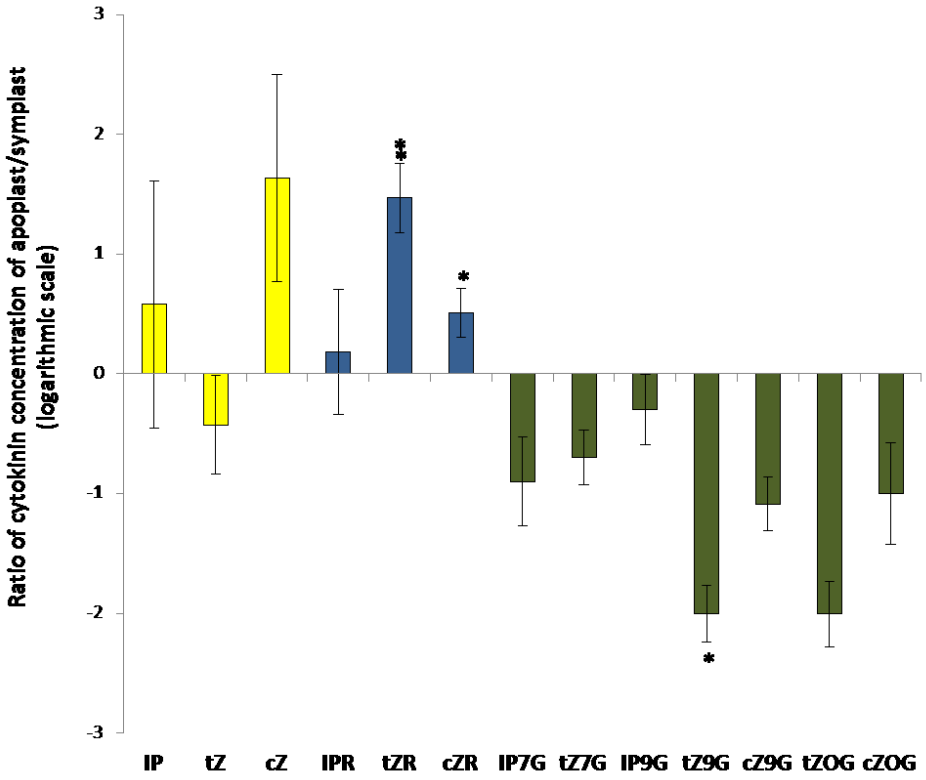

Figure 31 *Ratios of cytokinin concentration in apoplastic/symplastic fluid deriving from 8 days old Arabidopsis wild type roots. The metabolites were quantified in pmol/g of fresh weight (FW) and the respective ratios were computed. Three biological replicates were conducted and each was a pool of at least 1500 roots. The color of the bars represents different cytokinin metabolite groups; Yellow; cytokinin nucleobases, Blue; cytokinin ribosides and Green; cytokinin glucosyl-conjugates. The stars indicate statistically significant differences of cytokinin concentration between symplast and apoplast by paired sample Student's t-test. The results are displayed in log2 scale. See also Supplementary Figure 9.*

As presented in Figure 31, almost all the cytokinin nucleobases and ribosides were either enriched in the apoplastic fluid or equally distributed between symplast and apoplast. The ribosides exhibiting significantly greater abundance in the extracellular space were tZR and cZR. On the other hand all cytokinin glucosides predominated mainly in the symplast. However, of these glucosides only tZ9G was significantly enriched intracellularly.

5.5 Discussion

In this Chapter the method devloped in Chapter 4.4.1 was used to examine if cytokinins are enriched in the *GFP* expressing cells of the *TCSn* line. The biological significance of answering this question is invaluable since this newly published transgenic line is now being widely employed to represent cytokinin signaling outputs. Here it was also demonstrated that cytokinin compounds can be quantified in the apoplastic space of *Arabidopsis* root. Taking together the findings of this Chapter, the intra- and extra-cellular distribution of cytokinin metabolites is unveiled for the first time in *Arabidopsis* roots.

5.5.1 Cytokinin concentration in *GFP*+ cells of TCSn expressive cells

New tools such as *TCSn:GFP* have now been developed (Zürcher *et al.,* 2013) to enable visual reporting of cytokinin signalling at cell-level resolution. Zurcher *et al.,* (2013) showed that *TCSn:GFP* is cytokinin-specific. The main question answered here was whether high *TCSn* signal always corresponds to elevated cellular cytokinin levels (and which specific forms) or whether low TCSn signal (*GFP*- cells) might exist with high cytokinin levels but poor connection to cytokinin signaling. This study can facilitate the description of new cytokinin functions and can add additional dimensions to existing models of cytokinin roles. Therefore, knowledge of which cytokinin metabolites are represented by the *TCSn:GFP* signal is crucial.

Using the method developed in Chapter 4.4.1 specific cell populations were isolated from the roots of the *TCSn:GFP* and the cytokinin metabolites were quantified. Since the transgenic line under study has been designed and proved to report cytokinin signal, the bioactive nucleobases were expected to be most abundant in the *GFP*+ cells. Surprisingly, the predominant metabolites in the cytokinin responsive cells were the glucoside forms of cytokinin, and not the nucleobases or the ribosides which are the main forms that have been shown to bind at the cytokinin receptors (Romanov *et al.,* 2006). The only bioactive nucleobase enriched in the *TCSn:GFP* positive cells was tZ while from the ribosides only cZR was increased (Figure 27). While the difference of the *GFP* signal between + and – cells was substantial, as confirmed by the signal intensity plots derived from FACS (Supplementary Figure 6, Appendix), the bioactive nucleobase tZ and the riboside cZR concentrations were only 2 fold higher in the *GFP*+ cells compared to the *GFP*-. This suggests that *TCSn:GFP* may not be a linear sensor and this is possibly because cytokinin signaling activation requires only

a minute amount of bioactive cytokinins. Consistent with this idea, nucleobase cytokinins are also present at very low abundance compared to their precursors and glucosides.

In addition, the fact that tZ concentration displayed such a small enrichment in the *GFP*+ cells while glucosides like tZOG and cZ9G were 5 and 11 fold increased, respectively (Figure 27), implies that storage (O-glucosides) and deactivation (N-glucosides) of bioactive cytokinins are crucial processes taking place in cytokinin responsive cells probably as a mechanism regulating hormonal output. The detection of high cZOG and tZOG levels in the cytokinin responsive cells indicates that there is substantial storage of the hormone in these cell populations. O-glucoside cytokinins can be interconverted to cytokinin nucleobases through the enzyme beta-glucosidase (Brzobohatý *et al.,* 1993) and therefore are considered a reservoir of cytokinin. The increased levels of N-glucosides indicate that irreversibly inactive cytokinins are accumulated in the *GFP*+ cells of *TCSn:GFP*, since beta-glucosidases do not cleave N-glucosyl-conjugates (Brzobohatý *et al.,* 1993). No activity was observed with AtAHK3 or AtAHK4 in E.coli assays with tZOG, tZROG, tZ7G and tZ9G (Spíchal *et al.,* 2004) supporting their role as biologically inactive cytokinins. However, in an *Arabidopsis* reporter gene assay with *pARR5:GUS* (type *A-ARR gene*), tZOG and tZROG were highly biologically active –close to tZ activity- while tZ7G and tZ9G also triggered a slight expression of the reporter gene, similar to that for DZ and DZR (Spíchal *et al.,* 2004). Therefore a role of these metabolites in cytokinin signaling cannot be excluded.

5.5.2 Cytokinin concentration in *GFP*+ cells of *TCSn* expressive cells following INCYDE treatment

To confirm the novel and surprising findings described above, cytokinins were quantified in *TCSn:GFP*+ cells derived from *Arabidopsis* roots that had undergone chemical treatment triggering enhanced cytokinin response and this was assessed by checking the *TCSn:GFP* signal. The aim was to identify whether the same metabolites that were enriched in cytokinin-responsive cells in Chapter 5.4.1 (Figure 27) were still abundant or even increased following the induction of cytokinin response. The selection of the preferred cytokinin-related chemical was determined by the *TCSn:GFP* signal intensity response . Roscovitine was initially considered the best candidate since it inhibits the formation of cytokinin N-glucosides (Blagoeva *et al.,* 2003), which were highly enriched in the cytokinin responsive cells (Figure 27, Chapter 5.4.1) and also their absolute levels were higher than other cytokinin compounds (Supplementary Figures 5 and 7, Appendix). INCYDE was also tested

since it is known to suppress cytokinin irreversible degradation through *CKX* genes (Zatloukal *et al.,* 2008).

Finally, BAP was also tested as a positive control since Bielach *et al.,* (2012) have shown that *TCSn:GFP* expression was induced by BAP. BAP is more effectively bound to AtAHK3 receptor than to AtAHK4 (Spíchal *et al.,* 2004). Expression profiles of *AHKs* in the *Arabidopsis* root tip revealed that *AtAHK3* was stronger expression at the basal part of the meristem while *AtAHK4* expression was restricted at the root vascular tissues (Nishimura *et al.,* 2004). According to these data, BAP would be expected to trigger cytokinin signaling predominantly in the basal meristem. However this was not the case, since BAP-triggered cytokinin signaling, represented by *TCSn:GFP* signal was induced mainly in the stele (Figure 29; Bielach *et al.,* 2012). A possible explanation for this would be that since *AtAHK3*-mediated signaling through BAP occurs mainly in the basal meristem of the root tip, cytokinin homeostatic mechanisms at this site are able to compensate for BAP excess deriving from exogenous application. In contrast, when high external amounts of BAP are perceived in the vascular tissues of the apical meristem through AtAHK4, a stronger signal of *TCSn:GFP* is observed presumably because the supplementary amounts of BAP cannot be handled and cytokinin signaling is triggered.

Since both chemicals, INCYDE and roscovitine, demonstrated induction of the *TCSn:GFP* signal (Figure 29.a), the levels of fluorescence were quantified to define the regions of increased *GFP* expression. The main difference between the two treatments was in the root vasculature where INCYDE caused the greatest induction (Figure 29.b). An interesting peak of fluorescence was also demonstrated by roscovitine application specifically in stele of the elongation zone of the root (Figure 29). INCYDE was finally chosen for cell sorting experiments because it displayed the strongest and most consistent induction of cytokinin response.

The cytokinins in INCYDE-treated *TCSn:GFP* positive and negative cells showed mainly the same trends as in the untreated controls, with similar compounds enriched in the cytokinin responsive cell populations. The compounds demonstrating increased levels in the *GFP*+ protoplasts in both sorting experiments were the glucosides , while tZ was again significantly increased in the treated *GFP*+ cells compared to the corresponding *GFP*- ones (Figure 30). Interestingly, the compounds that responded to INCYDE treatment were tZ with 1,5-fold increase and tZOG with a striking 24 fold increase compared to the untreated protoplasts. While the tZ response to INCYDE was expected after inhibition of its degradation by *CKX*, the

much stronger reaction of tZOG suggests a rapid metabolic activation of a cytokinin homeostatic mechanism converting the bioactive tZ into the respective storage form. These results also indicate that the main mechanism for tZ homeostasis is via degradation by CKX enzymes. This idea is further supported by complementary data deriving from two studies measuring CKX activity according to substrate specificity (Gajdosová *et al.,* 2011) and cytokinin compound concentrations in *AtCKX* overexpressing lines (Köllmer *et al.,* 2014), and from labeled zeatin metabolism experiments (Gaudinová *et al.,* 2005).

It is also suggested that when cytokinin degradation through *CKX* was inhibited, an alternative cytokinin inactivation process, glucosylation, is employed. The fact that O-glucosides were increased upon INCYDE treatment instead of N-glucosides (Figure 30), could be attributed to the fact that excess of cytokinin is preferentially converted to a reversible storage form. But since irreversible degradation of tZ by *CKX* is the normal mechanism for tZ homeostasis, as discussed above, then cytokinin inactivation through N-glucosylation would be expected to be a more potent backup route upon INCYDE treatment, instead of the production of the reversible O-glucosides. As O-glucosylation appears to be the alternative mechanism of cytokinin detoxification upon INCYDE application, and O-glucosides are resistant to CKX action (A*rms*trong 1994), it is likely that O-glucosides would be the least affected compounds under these conditions.

Cytokinin response to INCYDE application displayed a degree of cell level specificity since *TCSn:GFP* expression was more substantially increased in the stele (Figure 29.b). The stele has been shown to be one of the few tissues where only one receptor (AtAHK4) was able to sense cytokinins (Stolz *et al.,* 2011). The sensing of cytokinins by AtAHK4 in the stele is known to regulate vital plant functions such as cellular differentiation (Mähönen *et al.,* 2000; 2006) or sensing of nutritional alterations (reviewed by Argueso *et al.,* 2009; Werner and Schmülling 2009). The finding that tZ and tZOG are the enhanced compounds in the cytokinin responsive cells (Figure 30) of the stele is in accordance with previous comparisons of receptor sensitivities in E.coli assays showing that AtAHK4 is highly specific for tZ and IP compounds while AtAHK3 perceived a wider range of cytokinins (Spíchal *et al.,* 2004). However IP compounds were neither predominant in the *TCSn:GFP*+ cells nor responded to the INCYDE application (Figure 30) which was surprising since IP is also one of the preferential substrates for CKX enzymes. A comparison of the vacuolar *AtCKX1*, the apoplastic *AtCKX2* and the cytosolic *AtCKX7* in the respective CKX overexpressor lines indicated that maximal IP degradation through CKXs occurred in the apoplast (Köllmer *et al.,* 2014). Even if cytosolic degradation of IP was also shown, it could be hypothesized that

extracellular IP degradation indicates that some cytokinin signaling through IP also occurs through extracellular perception. Since the apoplast is excluded in the sorting experiments, this could be a possible explanation of why IP was not abundantly detected in the *TCSn:GFP*+ cells and did not respond to the INCYDE treatment.

5.5.3 Apoplastic Cytokinins

Finally, cytokinin compounds were detected and quantified in the apoplastic fluid of *Arabidopsis* roots. The aim of these measurements was the completion of the "picture" of cytokinin distribution in the root apex, described in Chapter 4.4.2, since the cell-sorting technique used to provide such kind of data excludes cell walls and therefore the apoplastic space.

The apoplastic fluid was initially extracted under various centrifuge forces and times suggested by different papers (Dannel *et al.,* 1995; Li *et al.,* 2008; Lohaus *et al.,* 2001; Wada *et al.,* 2009; Witzel *et al.,* 2011; Yu *et al.,* 1999) to decide which is the optimum for extracting most of the apoplastic cytokinins while getting the least possible symplastic contamination. As shown in Supplementary Figure 8 (Appendix) there was no significant difference in apoplastic overall cytokinin levels extracted under several centrifuge conditions. Therefore, we used the minimum centrifuge force tested (900×g for 20 min) since it has been shown before that the symplastic contamination under these conditions is minimal (Dannel *et al.,* 1995; López-Millán *et al.,* 2001; Yu *et al.,* 1999).

Interestingly, cytokinins were not only present in the apoplast of the *Arabidopsis* primary root but the most abundant metabolites there were the nucleobase cZ and the ribosides cZR and tZR, while IP and IPR were equally distributed between symplast and apoplast (Figure 31). Consistent with the cytokinin profile from the sum of *GFP*+ and *GFP*- cells from the *TCSn:GFP* sorting experiment (Supplementary Figure 5, Appendix), being equivalent to the root symplast in this case, the cytokinin glycosyl-conjugates were similarly predominant in the symplastic fluid (Figure 31). This provides further strong evidence for the reliability of both the sorting and the apoplastic extraction methods because the methods are completely independent.

The riboside cZR was interestingly found to be a dominant cytokinin in both the apoplast and the symplast (Figures 28 and Supplementary Figure 9, Appendix). It is possible that cZR is metabolized only when there is need for additional active cZ or tZ (through isomerization)

but is mainly kept in the riboside form that lacks activity in both E.coli assays and bioassays (Spíchal *et al.,* 2004).

The bioactive tZ, was the only nucleobase enriched in the *TCSn* expressing cells (Figures 27 and 30) and was not upregulated in the apoplast (Figure 31). The presence of the nucleobases IP and cZ in the apoplast is consistent with the finding that secreted *CKX*s preferentially degrade cytokinin free bases (Galuszka *et al.,* 2007).

It is proposed that the nucleobases and ribosides, apart from cZR, were not enriched in the treated or untreated symplast of *GFP*+ cells of the *TCSn* line because they were mainly present in the apoplast. This hypothesis provides a new perspective to add to the current debate about the localization of cytokinin receptors, in particular that at least some of cytokinin sensing may occur in the apoplast.

Since none of the nucleobases, except possibly tZ, or ribosides, except cZR, were enriched in the symplastic space (Figure 31), the existence of functional receptors and/or transporters in the plasma membrane can be inferred. This is in accordance with the cytokinin compounds that have been shown in vitro to be carried across the plasma membrane by PUPs and ENTs (Bürkle *et al.,* 2003; Gillissen *et al.,* 2000; Hirose *et al.,* 2005), and also by the novel efflux carrier AtABCG14 (Ko *et al.,* 2014; Zhang *et al.,* 2014.a). If cytokinins were perceived in the endoplasmic reticulum (ER) lumen, as recent data suggest (Wulfetange *et al.,* 2011; Lomin *et al.,* 2012; Caesar *et al.,* 2011), then they should be either able to passively penetrate the plasma membrane or be transported across it as well as the ER membrane. While no non-transported mediated movement of cytokinins has been published yet, cytokinin trans-membrane carriers have been identified only in the plasma membrane (Bürkle *et al.,* 2003; Gillissen *et al.,* 2000; Hirose *et al.,* 2005) and not in the ER membrane.

Future relatively simple approaches can directly test for plasma membrane localization of cytokinin receptors. For example, this could include incubation of cZ, tZ and IP attached to sepharose beads with *TCSn:GFP* root protoplasts followed by measurement of the levels of fluorescence. The cytokinins will not be able to penetrate the cell because they are covalently bound to the beads and therefore any increase of the *TCSn* fluorescence would represent cytokinin signaling activation by receptors localized in the plasma membrane.

5.5.4 High levels of O-glucosides could partially represent bioactive nucleobases levels

The surprising predominance of glucosides in the cytokinin responsive cells deriving from either control or INCYDE-treated *TCSn:GFP* roots (Figures 27 and 30) was further investigated by testing whether their presence represents bioactive cytokinin forms which have been conjugated. For this reason, a feeding experiment was performed using [$^{13}C_5$]tZ and [$^{13}C_5$]cZ in *Arabidopsis* root protoplasts. Interestingly, the fed nucleobases were predominantly metabolized to their respective nucleotide forms, tZRP and cZRP (Figures 28.a and 28.b) and not to their respective conjugates. This is in accordance with analogous feeding experiments in tobacco cells and oat leaves (Gajdosová *et al.,* 2011) and with the crucial physiological role of the recently characterized *AtAPT1* gene catalyzing the conversion of cytokinin nucleobases to their corresponding nucleotide forms (Zhang *et al.,* 2013). Additional compounds produced from the application of labeled cZ were cZ7G and cZR (Figure 28.a) while from the labeled tZ, tZR and tZOG were also produced (Figure 28.b).

The applied labelled nucleobases were taken up by the cells within the first 30 min of incubation but their concentration remained mostly stable during the period of 1.5 h. This could mean that the metabolism of the labelled nucleobases was very slow, occurring mainly within the first 30 min of incubation. Since this is perhaps unlikely, another possible explanation for the stable levels of labelled nucleobases is that both the uptake and metabolism take place during the 1.5 h of incubation. However if labelled cytokinin molecules continue to enter the cells, the concentration of the metabolites produced would be expected to increase over time, which was not the case. Since adenine compounds, the main product from CKX-mediated degradation of cytokinins were not measured in this experiment, it can only be assumed that uptake and metabolism of labelled nucleobases occur throughout the 90 min of incubation but degradation through CKX maintains stable cytokinin content. Phosphate compounds, being the prevalent metabolites of the applied labelled nucleobases, have been shown to be efficiently degraded by CKX enzymes and are preferred substrates for the vacuolar AtCKX1 and AtCKX3 (Gajdosová *et al.,* 2011; Galuszka *et al.,* 2007; Kowalska *et al.,* 2010; Köllmer *et al.,* 2014). However neither of these enzymes displayed expression in the root tip (Werner *et al.,* 2003), where the protoplasts derive from. Therefore it is possible that the high concentrations of phosphate cytokinins as the main metabolic products of fed nucleobases are due to lack of their degradation through CKX enzymes at the root tip-derived cells. In contrast, the amounts of ribosides and N-glucosides produced from the applied labelled nucleobases might be underestimated. Cytokinin

ribosides have been shown to be efficiently degraded by the apoplastic AtCKX4 (Gajdosová *et al.,* 2011; Petr Galuszka *et al.,* 2007) and AtCKX5 (Gajdosová *et al.,* 2011) which are highly expressed in the root tip area (Werner *et al.,* 2003) and might therefore being exported to the extracellular space. This was also supported by their prevalence in the root apoplast (Figure 31). *AtCKX*7, expressed in the vasculature of young seedling including the root tissue (Köllmer *et al.,* 2014), preferentially degraded tZ, cZ and cytokinin 9-glucosides (Gajdosová *et al.,* 2011; Galuszka *et al.,* 2007; Kowalska *et al.,* 2010; Köllmer *et al.,* 2014). In contrast, O-glucosides are resistant to CKXs.

It can be concluded that while phosphate compounds were the main forms produced from labelled nucleobases, their stable levels implied possible action of CKX. Combination of CKX enzymes compartmentalization, tissue-specific expression and substrate specificity (Gajdosová *et al.,* 2011; Galuszka *et al.,* 2007; Köllmer *et al.,* 2014; Kowalska *et al.,* 2010; Werner *et al.,* 2003) indicted that cytokinin ribosides and 9-glucosides, also identified as metabolic products of fed nucleobases, are much better substrates for AtCKXs that are expressed in the root tip than cytokinin phosphate forms. It was also implied that cytokinin ribosides are most probably exported extracellularly for degradation which is in accordance with tZR and cZR predominance in the apoplast (Figure 31). Finally, N-glucosides still remain as good candidates for metabolic products derived from the fed nucleobases, because they can be efficiently degraded by the cytosolic AtCKX7 and this could be the reason why they do not accumulated greatly in the feeding experiment (Figures 28.a and 28.b). Future similar feeding experiment should be conducted by including *AtCKX* and *AtAPT* gene expression measurements, labelled adenine quantification and removal of feeding buffer after the first 30 min to prevent uptake after that timepoint.

Since high concentrations of cZ and tZ were applied to the protoplasts causing high production of their endogenous respective glucosides (Figure 28.c and 28.d), it could be hypothesized that the corresponding endogenous compounds will display a reduction, and that was the case. The endogenous concentration of cZR exhibited reduction which could correspond to the produced [$^{13}C_5$]cZR in response to labeled cZ application (Figure 28.c). Degradation through CKX enzymes is possibly responsible for the reduced levels of all these endogenous compounds mentioned above, as a mechanism for maintaining total cytokinin contents within the protoplasts.

5.6 Conclusions

- *TCSn:GFP* positive cells had increased levels of total cytokinins (Supplementary Figure 4, Appendix) and therefore the transgenic line can be now considered validated as a reporter of cytokinin status.
- The bioactive nucleobase representing *TCSn:GFP* transcriptional output seems to be tZ.
- The symplastic fluid of *Arabidopsis* roots is not enriched in cytokinin nucleobases and ribosides. Instead, these compounds were either predominantly in the respective apoplastic fluid or equally distributed between symplast and apoplast.
- The cytokinin glucosyl-conjugates demonstrated increased concentration in the symplast of *Arabidopsis* roots while being also the principal forms of the hormone in the *TCSn*-expressing protoplasts. While high levels of O-glucosides could partially derive from bioactive nucleobases, the origin of the increased N-glucoside levels observed could not be proven by relevant feeding experiments. However, their production from nucleobases could not be excluded.
- Protoplast feeding with labelled tZ or cZ revealed that in both treatments the predominant metabolic products of these nucleobases were their respective phosphate forms.

Chapter 6

Strigolactone effects on cytokinin metabolites distribution

6.1 Introduction

Strigolactone is a plant hormone that has been shown to affect various plant processes like shoot branching, adventitious root formation, secondary growth, root architecture (reviewed by Koltai, 2011; Waldie *et al.,* 2014 and Yoneyama *et al.,* 2009). They also have biological activity as root exudates affecting parasitic seed germination and interactions with arbuscular mycorrhizal fungi (Akiyama and Hayashi 2006).

A strong interaction between the novel plant hormone strigolactone and cytokinin was established when acropetally moving cytokinins were found to be severely reduced in all *rms* strigolactone mutants, (pea mutants displaying increased branching phenotype), apart from *rms2*. The same decrease was also observed in all *max* strigolactone mutants (*Arabidopsis* mutants displaying increased branching phenotype) (Beveridge *et al.,* 2000; 1997; 1994; Dun *et al.,* 2006; Foo *et al.,* 2005; Foo et al., 2007) suggesting a conserved effect of strigolactone on mobile cytokinins. Grafting experiments revealed that strigolactone regulates xylem cytokinins through a basipetally-mobile signal in *Arabidopsis* and Pea (Beveridge *et al.,* 1994; Beveridge *et al.,* 1997.b; Foo *et al.,* 2007; Morris *et al.,* 2001; Beveridge 2000). The same signal was also shown to up-regulate strigolactone biosynthetic genes in *Arabidopsis*, Pea and Petunia (Mashiguchi *et al.,* 2009; Foo *et al.,* 2005; Ongaro and Leyser 2008) and thus it is has been called a feedback signal.

The *rms2* mutant is the only known branching mutant that does not display reduced xylem cytokinin levels and enhanced strigolactone biosynthetic gene expression (Foo *et al.,* 2007; Beveridge *et al.,* 1997.a) implying that *RMS2* controls the proposed basipetal feedback

signal. More direct evidence was provided by the double mutant *rms1rms2*. The reduced xylem cytokinin content in *rms1* is counteracted in *rms1rms2* indicating that *rms2* can inhibit the influence of *rms1* on acropetally moving cytokinins (Foo *et al.,* 2007; Beveridge *et al.,* 1997.a).

In this Chapter strigolactone's effect on xylem cytokinin was used as a tool to investigate two aspects of cytokinin distribution. One was whether the root cytokinin levels in *rms* mutants correlate with their xylem cytokinin content. The second aspect concerned how altered concentrations of root-derived cytokinins affect the concentrations in the aerial parts of pea and in shoot-derived cytokinins. To facilitate investigation of these aspects, two *rms* mutants were selected: the first was the strigolactone-defective mutant *rms1* which has great reduction in its xylem cytokinin content and the second was *rms2* which exhibits increased xylem cytokinin. The opposite effects of these two *rms* mutants in acropetal cytokinin transport would facilitate discrimination of mechanisms of differential cytokinin distribution.

6.2 Aims

The aim of this Chapter was to complement previous findings of this work concerning cytokinin distribution within the plant tissues by further examination of how strigolactone regulates the gradients of the hormone, since its mutants display perturbed root-derived xylem cytokinin contents.

6.3 Materials and Methods

6.3.1 Plant Material

The pea cultivar Parvus was the wild type genotype used in all the experiments of this Chapter. The strigolactone mutant lines *rms1-1* (WL5237) and *rms2-2* (WL5951) being in Parvus genetic background were also used. All three genotypes used are tall and photoperiod-responsive lines (Beveridge *et al.,* 1994; 1997.a).

6.3.2 Growth Conditions

Xylem and phloem saps were harvested from 3 week old plants. A tissue specific experiment including shoot, first node and internode, epicotyl, hypocotyl and root tissues was conducted using 12 day old plants; and for the root segment experiment, 7 day old seedlings were used. Plants were grown as described in Chapter 3.3.2.

6.3.3 Phloem and Xylem isolation and Tissue Harvesting

Tissue harvesting and phloem and xylem isolation techniques are described in Chapters 3.3.3, 3.3.4 and 3.3.5.

6.3.5 Cytokinin purification and measurements

Cytokinin extraction, purification and final quantification through LC-MS/MS was performed as described in Chapter 3.3.6.

6.3.6 Measurements of cytokinin oxidase enzymatic activity

CKX activity was measured as described in Chapter 3.3.7.

6.4 Results

6.4.1 Xylem cytokinins perturbation in *rms* mutants.

Strigolactone mutants in pea (*rms*) and *Arabidopsis* (*max*) have shown a conserved alteration in their cytokinin content (Foo *et al.,* 2007). This was re-examined as an initial step of this Chapter. Xylem cytokinins were measured in *rms1* and *rms2* mutants and the published trends were confirmed as shown in Figure 32.

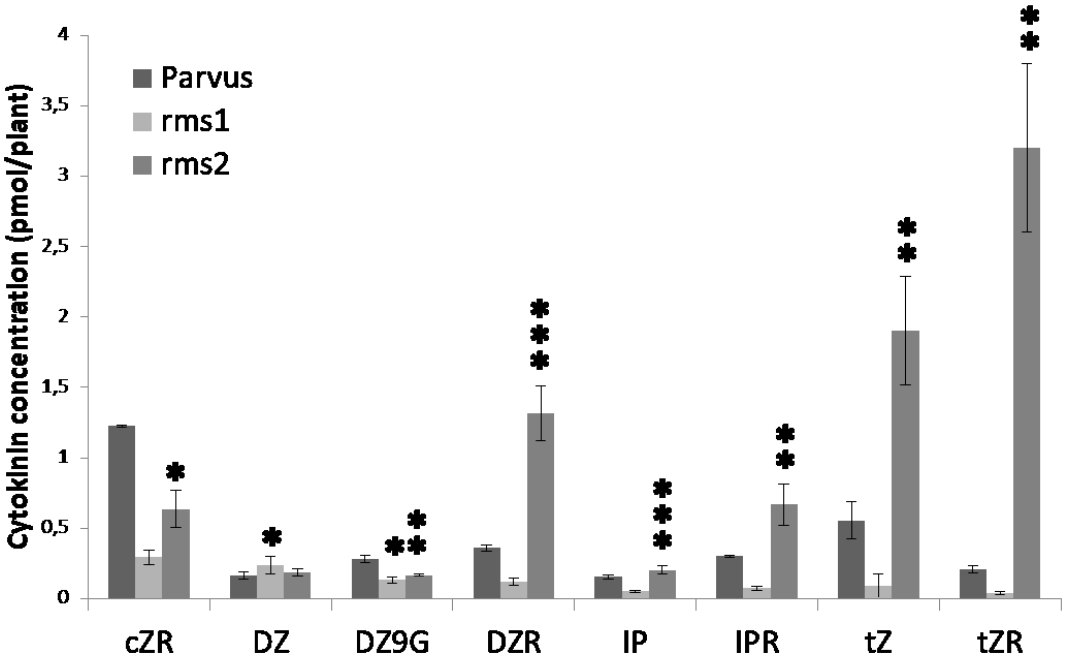

Figure 32 *Quantification of xylem sap cytokinins of 3 weeks old Parvus (wild-type), rms1 and rms2. Each sample derived from a pool of at least 3 plants and 3 biological replicates were analysed. The error bars indicate the standard error (n=3). The concentration of cytokinin was calculated in pmol and normalized to the number of plants used. The stars indicate statistically significant differences of cytokinin concentration between each rms mutant and Parvus by Student's t-test.*

As displayed in Figure 32, xylem-mobile IP- and tZ-cytokinin compounds and DZR exhibited reduced levels in *rms1* and increased levels in *rms2* compared to Parvus wild-type. However cZR and DZ9G concentration was reduced in the xylem sap of both *rms* mutants while DZ exhibited increased levels in *rms1* xylem sap.

6.4.2 Cytokinin quantification in sequential tissues of strigolactone mutant plants

Next, how the differential modification in the cytokinin xylem levels between *rms1* and *rms2* influence cytokinin distribution within the pea tissues was examined. Cytokinins were quantified in sequential tissues of 12 day old *rms1* and *rms2* mutants and compared to the Parvus, wild-type, cytokinins.

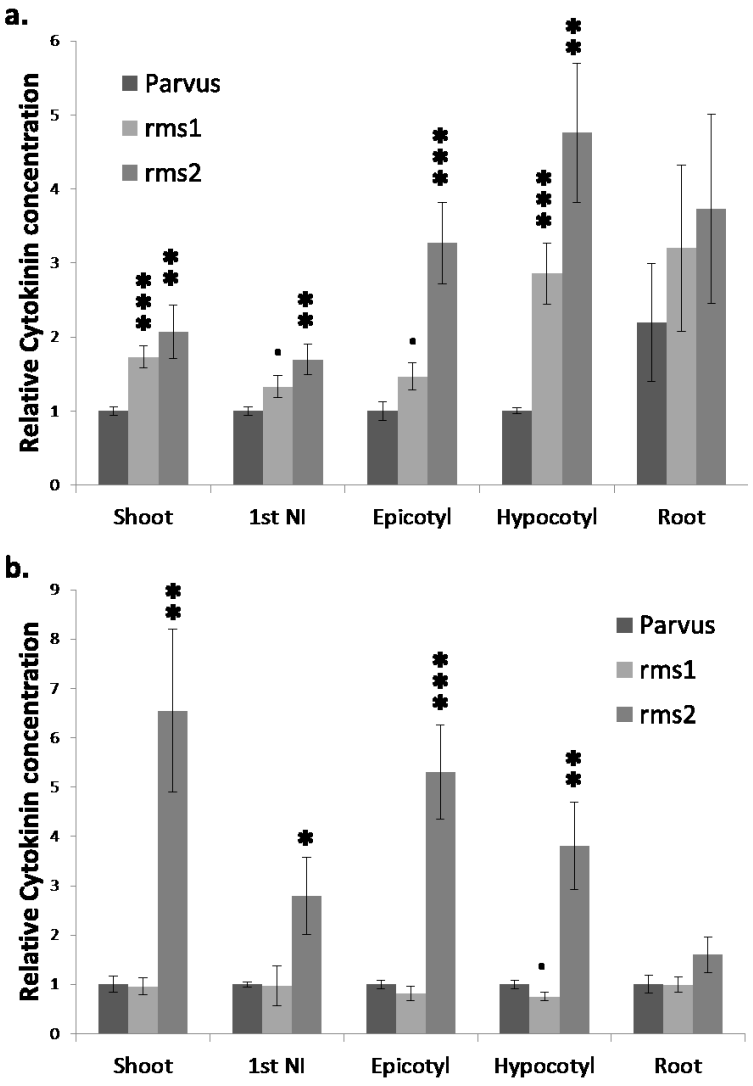

Figure 33 *Cytokinin quantification in Parvus (wild-type), rms1 and rms2 shoot, first node and internode (1st NI), epicotyl, hypocotyl and root.* ***a.*** *IP-cytokinins (mean of IPRP, IPR and IP) and* ***b.*** *tZ-cytokinins (mean of tZRP, tZR and tZ) are presented. Each sample derived from a pool of at least 3 plants. Cytokinin concentration was calculated in pmol and normalized to the fresh weight (FW) of the plant tissue. The data were further normalized to Parvus cytokinin concentration in each tissue. The error bars represent standard error (n = 3). Statistical analysis was performed using Student's t-test comparing cytokinin concentration between each rms mutant and Parvus.*

IP-cytokinins (Figure 33.a) and tZ-types (Figure 33.b) are presented as a mean of IPRP, IPR, IP and tZRP, tZR, tZ, respectively since these compound groups exhibited similar alterations in strigolactone mutants compared to the wild type (Supplementary Figures 10 and 11, Appendix). Root cytokinins remained unaffected by strigolactone mutation. Instead, the aerial parts of *rms1* and *rms2* displayed significant changes in their cytokinin content. IP-cytokinins were increased in the shoot, first node and internode, epicotyl and hypocotyl tissues in both *rms1* and *rms2* mutant compared to Parvus. While tZ-cytokinins displayed

similarly increased levels in the respective tissues of *rms2*, in *rms1* aerial parts levels were unaltered. DZ- and cZ-cytokinins remained mainly unaffected by the mutations in all tissues examined (Supplementary Figures 10 and 11, Appendix).

6.4.3 Cytokinin quantification and cytokinin degradation in sequential root segments of *rms* mutants

Since the loading of the xylem, which had perturbed cytokinin levels as a result of strigolactone mutations, presumably takes place in the root, it was surprising that root tissue cytokinin levels in both *rms1* and *rms2* mutants remained unaffected. Therefore, more detailed cytokinin measurements were performed in sequential root parts of *rms* mutants as displayed in Figures 34 and 35.

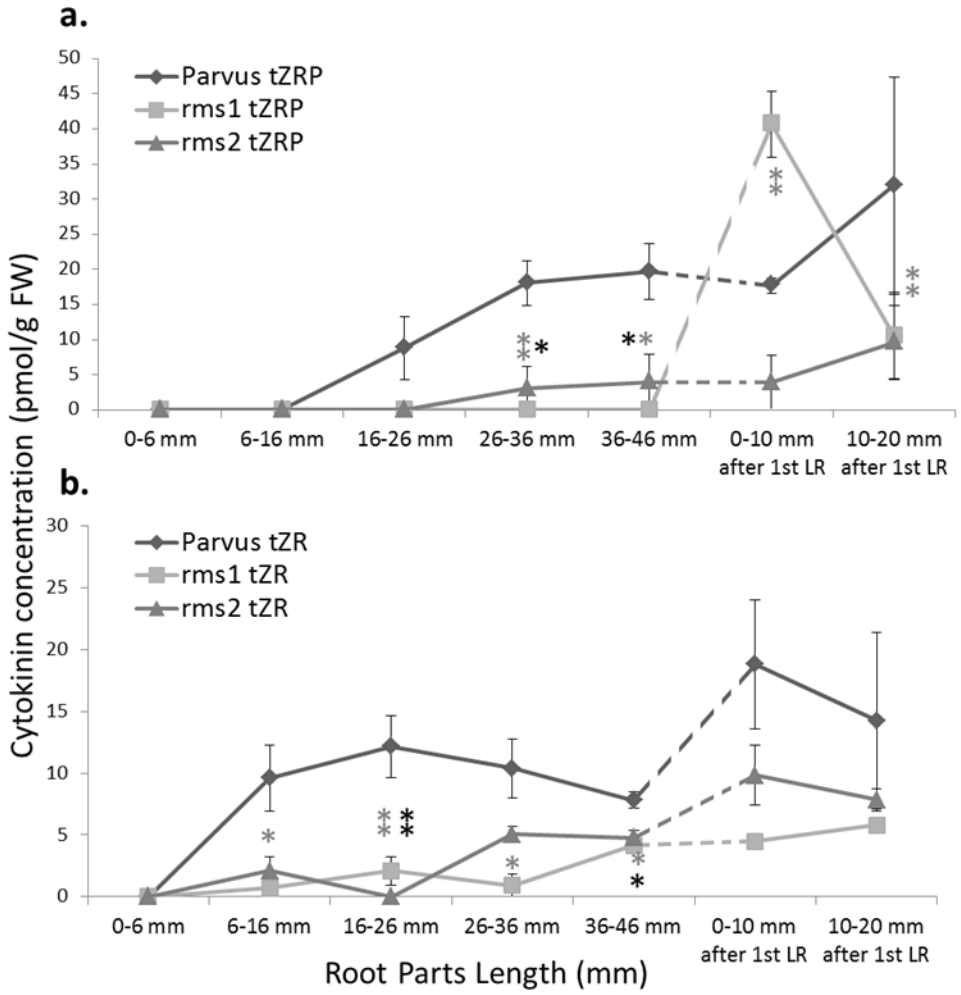

Figure 34 *Cytokinin quantification in root parts of 7 days old Parvus, rms1 and rms2 seedlings The 0 mm represents the root cap of the primary root.* ***a.*** *tZRP concentration,* ***b.*** *tZR concentration. Each sample derived from a pool of 30-50 plants. Cytokinin concentration was calculated in pmol and normalized to the fresh weight (FW) of the plant tissue. The error bars represent standard error (n = 3). The stars indicate statistically significant differences of cytokinin concentration between each rms mutant and Parvus by Student's t-test.*

As shown in Figure 34.a tZRP was reduced in all root segments of *rms2* compared to wild-type. The same was observed for *rms1* apart from the first 10mm above the first lateral root appearance where a striking increase of the compound was exhibited. Similarly, tZR displayed lower levels in all tissue segments in both *rms* mutants with the less strong –non-significant decrease presented in the lateral root zone (0-20mm above the first lateral root, Figure 34.b). Even though tZR is one of the main xylem cytokinin compounds and tZRP is its immediate precursor form, its concentration did not correlate with xylem levels in the *rms* mutants.

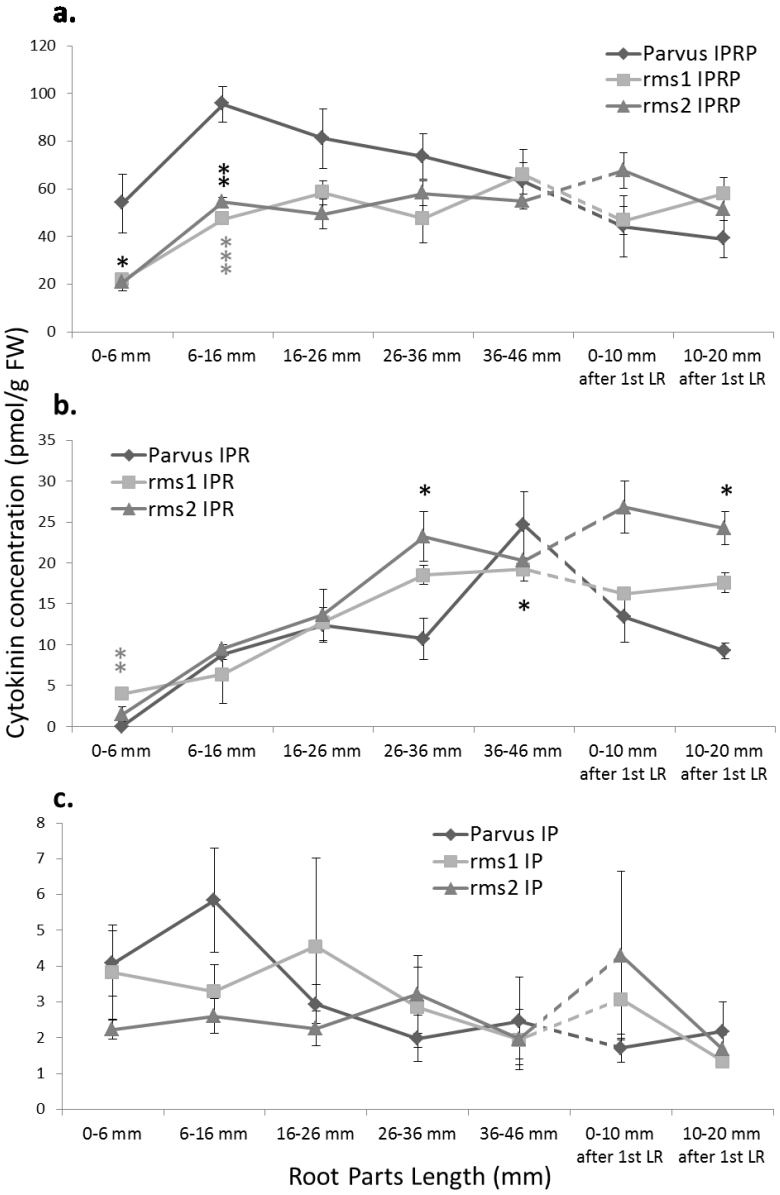

Figure 35 *Cytokinin quantification in root parts of 7 days old Parvus, rms1 and rms2 seedlings The 0 mm represents the root cap of the primary root.* ***a.*** *IPRP,* ***b.*** *IPR and* ***c.*** *IP concentration. Each sample derived from a pool of 30-50 plants. Cytokinin concentration was calculated in pmol and normalized to the fresh weight (FW) of the plant tissue. The error bars represent standard error (n = 3). The stars indicate statistically significant differences of cytokinin concentration between each rms mutant and Parvus by Student's t-test.*

The corresponding results for IP-cytokinins, presented in Figure 35, also did not correlate with the cytokinin levels in the xylem sap of *rms* mutants (Figure 32). IPRP was significantly reduced in both *rms1* and *rms2* in the apical part of the primary root (0-16 mm, Figure 35.a) compared to the wild type while IPR was instead increased in the apical 6 mm (Figure 35.b). Elevated levels of IPR were also displayed by *rms2* at 26-46 mm above the root tip and at 10-20 mm above the first lateral root. In contrast, IP concentration of *rms1* and *rms2* was not significantly different from the wild-type (Figure 35.c). Likewise, no strigolactone-related alteration was observed for cZR and DZR (Supplementary Figure 12, Appendix). Even though this detailed cytokinin analysis within the root tissue did not explain the perturbed xylem cytokinin levels in *rms* mutants, it indicated that there were significant differences between *rms* mutants and wild type in specific root segments that could not be detected by measuring cytokinins in the whole mutant root tissue.

In parallel, to examine whether altered xylem cytokinin concentrations in *rms* mutants were CKX-dependent, the activity of cytokinin oxidase was measured in the same sequential root segments of *rms* mutants.

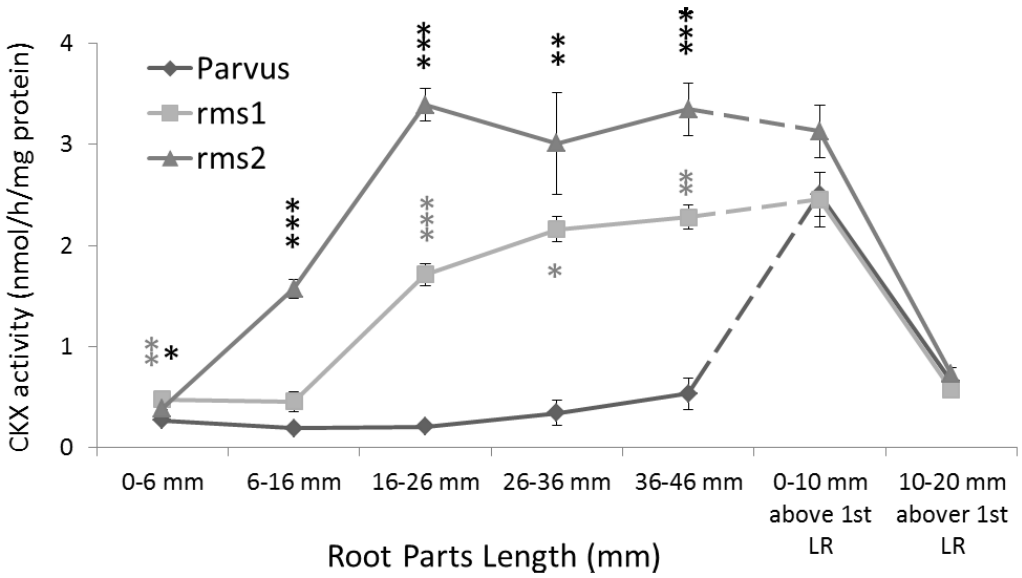

Figure 36 *CKX enzymatic activity measured in sequential root parts of 7 days old Parvus, rms1 and rms2 mutants using IP as substrate. Each sample was a pool of 30-50 plants and 3 biological replicates per sample were examined. The CKX activity was calculated in nmol of enzyme per hour and normalized to the mg of respective protein. The error bars represent standard error (n=3). The stars indicate statistically significant differences of cytokinin concentration between each rms mutant and Parvus by Student's t-test. The CKX enzymatic activity measurements were performed by Dr Vaclav Motyka.*

Figure 36 illustrates that cytokinin degradation was significantly higher in the first 46mm of *rms1* and *rms2* primary roots compared to the wild-type but this trend disappeared in the lateral root zone. Although xylem cytokinin levels in *rms* mutants did not correlate with CKX activity, the enhanced degradation of cytokinin in *rms* mutants was an interesting effect especially since it correlates with reduced levels of some cytokinin compounds in the same root parts.

6.4.4 Basipetally moving cytokinins in *rms* mutants

The reduced cytokinin levels identified in *rms1* xylem (Figure 37), could not be detected in any other tissue of *rms1* examined and most interestingly in the root. So next, phloem cytokinins were measured in *rms* mutants to examine if basipetally moving cytokinins are increased as part of cytokinin homeostatic mechanism thus contributing compensatory amounts of cytokinins in *rms* roots.

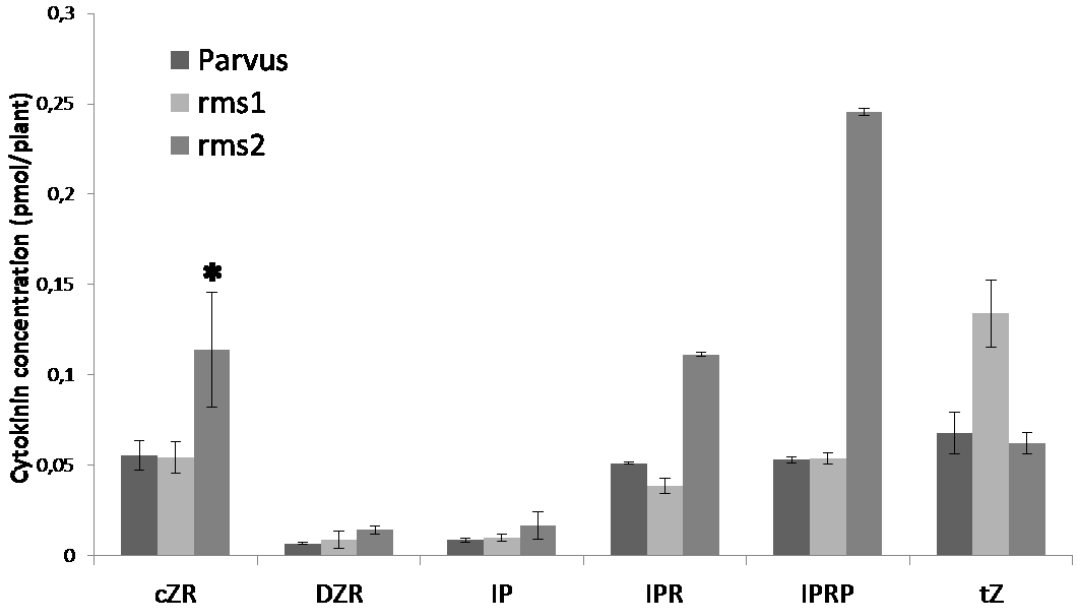

Figure 37 *Quantification of phloem cytokinins of 3 weeks old Parvus, rms1 and rms2. Each sample derived from a pool of at least 3 plants and 3 biological replicates were analysed. The error bars indicate the standard error (n=3). The concentration of cytokinin was calculated in pmol and normalized to the number of plants used. The stars indicate statistically significant differences of cytokinin concentration between each rms mutant and Parvus by Student's t-test.*

As shown in Figure 37, the only compound increased in *rms1* mutant was tZ while all the other compounds had being found reduced in *rms1* xylem were found at wild-type levels. The phloem cytokinins cZR, IPR and IPRP, exhibited enhanced concentrations in *rms2*. However most of these differences were not statistically significant.

6.5 Discussion

6.5.1 Xylem cytokinin perturbation in *rms* mutants does not correlate with root tissue cytokinin concentration.

Strigolactone mutants have been previously shown to have altered xylem cytokinin levels in *Arabidopsis* and Pea (Morris *et al.,* 2001; Foo *et al.,* 2007; Beveridge *et al.,* 1997.a; 1997b). However, in these early studies xylem cytokinin concentration was mainly reported as zeatin ribosides and/or zeatin levels which included all the tZ-, DZ- and cZ-types. Only Foo *et al.,* 2007 showed cytokinin content in xylem sap of *Arabidopsis max* mutants as IPR, tZR and tZ. Figure 32 shows for the first time eight individual xylem cytokinin compounds that were well-detected in the xylem sap of *rms* mutants. While the concentrations of tZ, tZR, IP, IPR and DZR were reduced in *rms1* and increased in *rms2*, in agreement with the previously mentioned studies, cZR and DZ9G were reduced in the xylem sap of both *rms* mutants compared to the wild type. In addition DZ was increased in the xylem sap of *rms1* while this compound was not affected in *rms2*.

It was then hypothesized that these severely perturbed levels of xylem cytokinins in *rms* mutants would be reflected also in the respective root tissue cytokinin profiles, since this is the site where presumably xylem loading occurs. Surprisingly, root cytokinins of *rms* mutants exhibited no significant difference compared with wild type (Figures 33, 34 and 35 and Supplementary Figures 10 and 11, Appendix).

Next a detailed analysis tested whether there is a specific root part(s) that is responsible for the reduced xylem loading in *rms1*, whereas such an effect would not be detected when averaging the whole root tissue.

Strigolactone seems to affect IP-compound metabolism and distribution in root segments and this was also confirmed by the high CKX enzymatic activity detected in the apical 46mm of the root tip of *rms* mutants. However, this effect was diminished in the lateral root zone which had equal CKX activity between *rms* mutants and wild type, implying a tissue-specific regulation of cytokinin turnover by strigolactone.

Overall, tZ-cytokinins were generally reduced in both mutants across most of the root parts examined, while IP-forms were reduced mainly at the apical part of the *rms* primary root but reached wild type or higher levels at the lateral root zone. Most of the differences identified to be significant in the apical regions, were not significant in the lateral root zone, in

agreement with differences in CKX activity. Across all the data, although the cytokinin analysis of root parts of *rms* mutants revealed significant differences between the genotypes, no correlation between the xylem cytokinins and the root cytokinins was identified.

These results suggest that the perturbed xylem cytokinin levels in *rms* mutants are probably due to disrupted loading and not to altered biosynthesis, metabolism and/or degradation of cytokinin in the root of *rms* mutants. Recently AtABCG14 was identified as an efflux pump of cytokinins and suggested to be responsible for acropetally moving cytokinins (Zhang *et al.,* 2014.a; Ko *et al.,* 2014). It is therefore possible that there is a strigolactone-dependent mis-regulation of AtABCG14 causing the depleted xylem cytokinin levels in strigolactone mutants. Future experiments would include identification of the *AtABCG14* homologue in Pea, generation of double mutants between *atabcg14* and strigolactone mutants in *Arabidopsis* and pea, and examination of the respective phenotypes and xylem, shoot and root cytokinin levels. The transcript levels of *AtABCG14* could be also examined in *rms* and *max* mutants.

However, studying cytokinin biosynthesis, metabolism and degradation in strigolactone mutants is still interesting since there are clearly several strigolactone effects on cytokinin even though they may not be directly linked to regulation of xylem cytokinins. Cytokinin degradation, based on CKX activity, was found to be greatly increased in the apical root parts of *rms* primary root zone (0-46mm) while this effect was not apparent in the lateral root zone. This is consistent with cytokinin levels also not being significantly different in the lateral root zone of *rms* mutants and implies a tissue-specific regulation of cytokinin turnover by strigolactone.

In a further attempt to understand the basis of normal cytokinin levels of *rms* roots contrasting with their depleted xylem content, phloem cytokinins were measured in *rms* mutants. The phloem cytokinins in *rms* mutants displayed no significant difference compared to the wild type, apart from increased cZR levels in *rms2* phloem. This indicated that shoot-derived cytokinins were not responsible for the wild type cytokinin levels in the strigolactone mutant roots.

6.5.2 How does perturbed amount of acropetally moving cytokinins in *rms* mutants affects shoot cytokinin levels?

Cytokinin metabolites were quantified in the shoot, first node and internode, epicotyl and hypocotyl of *rms1* and *rms2* mutants to investigate how the reduced and increased levels, respectively, of the two mutants affect cytokinin distribution in these tissues. The tissues of epicotyl and hypocotyl were of particular interest since previous studies in pea and petunia have shown that 5mm of wild-type epicotyl or stem can be sufficient for alteration of the branching phenotype of *rms1* or *dad1*(Foo *et al.,* 2001; Napoli *et al.,* 1996).

Interestingly, IP-cytokinins were up-regulated in both *rms* mutants while tZ-compounds were increased only in *rms2* aerial parts. The rest of the compounds detected exhibited no significant difference between *rms* mutants and wild type for most of the tissues examined (Supplementary Figures 10 and 11, Appendix). Figure 33 summarized the results for cytokinin levels in the shoot parts of *rms* mutants, presented as total IP-and tZ-cytokinins. While IP-forms were significantly increased in most of the aerial parts of *rms1* and *rms2*, tZ-cytokinins were increased in the respective tissues only of *rms2* but not *rms1*. This is the first differential response in cytokinin levels that could possibly correlate to the xylem levels in *rms* mutants. These results agree with similar differential concentration of IP- and tZ-compounds in the stem segments derived from intact *rms1* and *rms2* plants (Young *et al.,* 2014).

The increased IP-type cytokinin levels in *rms1* stem segments were accompanied by *PsIPT1* up-regulation (Young *et al.,* 2014) which has been reported in other strigolactone mutants too (Dun *et al.,* 2012) possibly as a response of cytokinin homeostatic mechanisms to the reduced xylem cytokinins arriving in the shoots of *rms1*. In accordance with this possibility, PsIPTs were not induced in *rms2* stem segments (Young *et al.,* 2014) probably due to the additional systemic supply at this mutant.

The enriched tZ-cytokinins in the aerial parts of *rms2* agreed with the increased tZ-forms arriving from the root. In contrast, wild-type levels of tZ-types in *rms1* aerial parts implied that there is already local compensation probably through *PsIPT1* up-regulation and possibly by further trans-hydroxylation from PsCYP735A. Future experiments would include identification of *PsCYP735A* genes and analysis of their transcript levels in the shoot.

6.6 Conclusion

- Strigolactone effects on cytokinin concentration were shown to be mainly xylem-specific.
- Cytokinin homeostasis rescues shoot cytokinin concentrations in *rms1* but not in *rms2*.
- Perturbed xylem cytokinin levels in strigolactone mutants were not obviously related to cytokinin concentrations in the root tissue where xylem loading presumably occurs.
- Cytokinin analysis of root segments revealed that strigolactone effects in the apical part of the primary root (0-46mm) are different from the lateral root zone and that was also reflected by differential CKX activity.
- Phloem cytokinins were not significantly affected by strigolactone mutations.

Chapter 7

Discussion

7.1 Why study cytokinin and why cytokinin distribution?

Cytokinins regulate crucial aspects of plant development and adaptation. Unravelling cytokinin chemistry, biosynthesis, homeostasis, signaling and distribution will shed light on the very basis of the processes that the hormone controls either individually or more often as a crosstalk with other hormones. This will provide an outstanding advantage to agriculture, horticulture and forestry as it will empower the design of plants with required characteristics for enhanced crop yield or for adaptation in specific environmental conditions. Cytokinins have already been linked with a direct role in controlling such features (Ashikari *et al.,* 2005; Zalewski *et al.,* 2010; Ghanem *et al.,* 2011; Rahayu *et al.,* 2005; Rivero *et al.,* 2010; Huynh *et al.,* 2005; Argueso *et al.,* 2009; Aloni *et al.,* 2005; Sakakibara 2006; Werner *et al.,* 2006; Mayzlish-Gati *et al.,* 2012; Yang *et al.,* 2012; Nishiyama *et al.,* 2012). Thus, fundamental research on cytokinins is exponentially increased.

Roles for aromatic cytokinins are starting to be investigated with the development of new cytokinin quantification methods (Novák *et al.,* 2008) and they are also now included in assays testing binding efficiency to cytokinin receptors (Spíchal *et al.,* 2004). Other recent advances in cytokinin research comprise striking improvements in both cytokinin extraction-purification and sensitivity of LC-MS/MS methods allowing the quantification of the hormone in minute amounts of plant tissue (Svačinová *et al.,* 2012). Novel artificial markers that provide an overview of cytokinin signaling output and degradation rates have been constructed (Zürcher *et al.,* 2013; Tian *et al.,* 2014), simplifying the problems associated with investigating 11 different *B-ARRs* or 7 distinct *CKX*s genes. In the past decade, cytokinin transporters in planta finally made their appearance (Ko *et al.,* 2014; Sun *et al.,* 2005; Zhang *et al.,* 2014.a) while the first crystal structures of cytokinin degradation enzymes, CKX, were published (Bae *et al.,* 2008; Frébortová *et al.,* 2004). Finally, a role for cZ, being considered

as the least active nucleobase, has been elucidated (Kudo *et al.,* 2012; Quesnelle and Emery, 2007).

The above-mentioned findings demonstrate that cytokinin research is rapidly evolving. Variable distribution of cytokinin compounds amongst plant tissues was implicated by the long-distance transport of cytokinins (Kuroha *et al.,* 2002 ; Morris *et al.,* 2001; Takei *et al.,* 2001.a; Hirose *et al.,* 2008; Lejeune *et al.,*2006; Hirose *et al.,* 2008; Corbesier *et al.,* 2003; Lejeune *et al.,*2006). This was also confirmed by grafting experiments and the expression patterns of cytokinin-related genes along the plant (Matsumoto-Kitano *et al.,* 2008 and Figure 5 in Chapter 1.3.2.).However, the understanding of how cytokinins build up their gradients within the plant tissue is a key point that is currently missing, especially concerning the absolute concentration of the different hormone compounds. Therefore the work presented here was focused on investigating cytokinin metabolite distribution by dissecting the plant from tissue to cell level. In Figure 38.a representation of this dissection performed in this work and what it revealed for cytokinin distribution is shown for tZ.

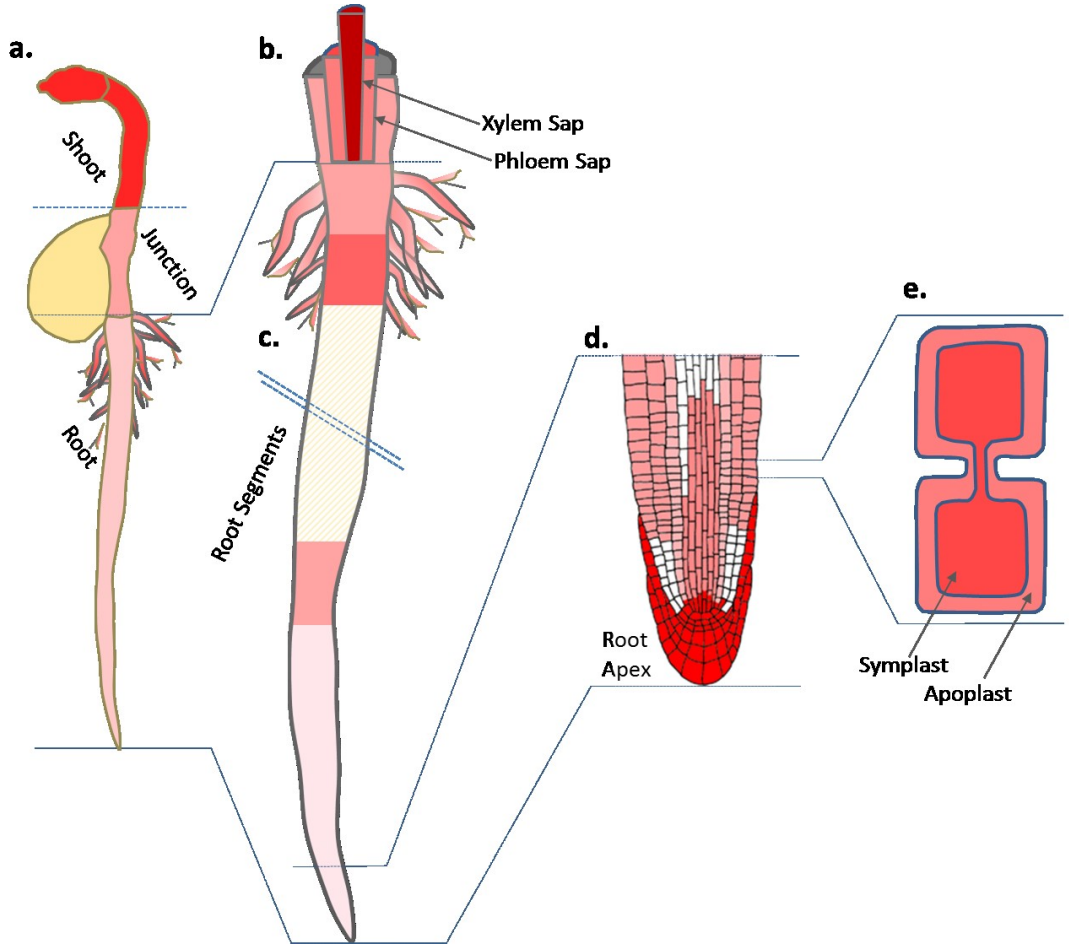

Figure 38 *Schematic representation of tZ distribution whithin* ***a.*** *pea plant body,* ***b.*** *pea moving saps (xylem and phloem),* ***c.*** *pea root,* ***d.*** *Arabidopsis root tip (drawn by Ondřej Novák) and* ***e.*** *intra- and extra-cellular space of Arabidopsis root tip. The increasing intensity of the red colour represents increased cytokinin concentration. The tissue parts and cell populations in white colour were not examined for cytokinin content.*

7.2 A role for long-distance transported cytokinins

The data presented in Chapter 3.4.1 showed that most known cytokinin forms were at detectable levels in both phloem and xylem. The role of these long-distance transported cytokinins is still controversial. Several lines of evidence suggest that phloem and xylem cytokinin act as systemic signals regulating several aspects of plant growth and development such as cambial activity (Matsumoto-Kitano *et al.,* 2008), vascular patterning in the root apex (Bishopp *et al.,* 2011.a; 2011.b), adventitious root formation (Kuroha *et al.,* 2002) and root nodulation in legumes (Sasaki *et al.,* 2014). In this context, root to shoot transported cytokinins have been also suggested to facilitating plant adaptation to environmental stresses like nitrogen availability (Dodd *et al.,* 2004; Rahayu *et al.,* 2005; Samuelson *et al.,* 1992; Takei *et al.,* 2001.a; 2004.b Wagner and Beck, 1993). Recently, Ko *et al.,* (2014) demonstrated that long-distance transport of cytokinins is fundamental for shoot growth.

Other series of data mainly concerning grafting experiments provide further support for the role of long-distance transported cytokinins in maintaining hormone homeostasis throughout the plant. The quadruple *atipt1357* mutant displays severely reduced concentrations of IP- and tZ-cytokinins, but when *atipt1357* roots were grafted to wild type scions, phloem cytokinins were able to restore the concentration of root IP-forms. Likewise, when a wild type rootstock was grafted to a mutant scion the concentration of shoot tZ-cytokinins was rescued (Matsumoto-Kitano *et al.,* 2008).

7.2.1 Xylem and Phloem Cytokinins

The data presented in Chapter 3.4.1 (Figures 11 and 12) suggest that in pea, cZR was a major cytokinin transport form common to both xylem and phloem. Hirose *et al.,* (2008) likewise detected cZR in both phloem and xylem of *Arabidopsis*. In pea xylem, zeatin forms were the predominant cytokinins in accordance with findings in several plant species (Kuroha *et al.,* 2002 ; Morris *et al.,* 2001; Takei *et al.,* 2001.a; Hirose *et al.,* 2008; Lejeune *et al.,*2006). More specifically, cZR, tZ and tZR predominated in the xylem sap of both pea cultivars under study. The most abundant basipetally transported cytokinins were tZ, IPR, IP, DZ and cZR. IP-compounds were the prevalent cytokinins in the phloem sap, in agreement with previously published data (Hirose *et al.,* 2008; Corbesier *et al.,* 2003; Lejeune *et al.,*2006).

Although IP-cytokinins predominated in the phloem while tZ-forms prevailed in the xylem sap of pea, a trend that is now well established (Hirose *et al.,* 2008; Kudo *et al.,* 2010; Matsumoto-Kitano *et al.,* 2008), it was also shown here that tZ was also present in the phloem sap while IP-cytokinins were detectable in the xylem sap. Matsumoto-Kitano *et al.,* (2008) demonstrated this well established trend using grafts between the quadruple *atipt1357*, which has severely reduced cytokinin levels in both roots and shoots (Miyawaki *et al.,* 2006), and wild type. Indeed, when *atipt1357* scions were grafted to wild type rootstocks, tZ-cytokinins, but not of IP-forms, were restored in the shoot. The reciprocal grafting combination was able to restore the concentration of IP-compounds in the root but not tZ-forms, suggesting that tZ-cytokinins are transported through the xylem and IP-cytokinins through the phloem. However this does not prove that only these forms are transported through the vasculature but that xylem tZ-cytokinins and phloem IP-forms are indispensable for the shoot and root cytokinin pools. Also, from these grafting experiments only IPRP, IPR, tZRP and tZR were reported, while the concentrations of cZ- and DZ-cytokinins were not shown.

The prevalence of tZ-cytokinins as xylem transported forms in all species was further supported by data in pea and maize (Beveridge *et al.,* 1997.a; Takei *et al.,* 2001.a). However, in these data sets, measured ZR concentration represented the sum of tZR, cZR and DZR. In addition, some studies propose that *AtCYP735As* expression predominates in the root and therefore generates all tZ-cytokinins in this tissue, a statement that may not be precisely extrapolated to tZ-cytokinins moving only in the xylem sap. Although high expression of these trans-hydroxylases is indeed detected in the root, there are also high expression levels in the shoot (Kiba *et al.,* 2013; Takei *et al.,* 2004.a). Takei *et al.,* (2004.a) demonstrated that *AtCYP735A2* transcript levels were strongly expressed both in root and stem while *AtCYP735A1*, even though significantly lower than *AtCYP735A2*, was detected similarly in the root and flower tissues, but less in the leaves and stem tissues. Overall, it can be concluded that *AtCYP735A* expression is not necessarily predominant in the root. This was also later supported by promoter *GUS* driven expression of *AtCYP735A2* found high in both roots and shoot apical meristem, and also in a part of the hypocotyl (Kiba *et al.,* 2013). Finally, CYP735A enzymes, apart from giving rise to all tZ-cytokinins, can also be responsible for DZ- and cZ-forms through the additional actions of zeatin reductase, and trans-cis isomerase, respectively (Figure 2, Chapter 1.3.2).

Even though IP-cytokinins are suggested to predominate in the phloem, in the grafting experiment mentioned above (Matsumoto-Kitano *et al.,* 2008), measurements for cZ- and

DZ-cytokinins were not presented. Presence of zeatin forms in the phloem sap is also indicated by the partial recovery of tZ-cytokinins in the *atipt1357* rootstocks when grafted to wild type scion. If the main phloem cytokinins were only the IP-types then this partial rescue could not be explained (Matsumoto-Kitano *et al.,* 2008). Hirose *et al.,* (2008) also identified cZR in *Arabidopsis* phloem. Corbesier *et al.,* (2003) presented only the IP-cytokinin levels in leaf phloem exudates but mentioned that zeatin cytokinins were present as well. Finally, Taylor *et al.,* (1990) detected zeatin cytokinins in the phloem of white lupin. In all these studies zeatins are mentioned as one group. It is clearly important to know whether they are actually trans- or cis-forms, especially due to their independent origins. In conclusion, the above-mentioned findings support the results presented in Chapter 3.4.1 (Figures 11.b and 12.b) suggesting that while IP-cytokinins are abundantly detected in the phloem, tZ- and cZ-zeatin forms are also present.

Additionally, the results presented in Chapter 3.4.1 (Figures 11 and 12) indicate unique profiles for some compounds, mentioned below, in the xylem or phloem sap of pea. This helps to confirm the lack of cross-contamination of the two exudates, especially since they were both derived from the same plants. IPRP and IP9G were detected only in phloem while DZ9G was found only in xylem. While the presence of cytokinin nucleotides (IPRP and tZRP) has been reported before in the phloem sap (Corbesier *et al.,* 2003), their detection in xylem sap samples has only been described twice: in *Arabidopsis* (Ko *et al.,* 2014; Supporting information, Figure S6) and in chickpea (Emery *et al.,* 1998). Cytokinin nucleotides transported through the phloem sap indicate they may supplement the locally biosynthesized cytokinin pools in roots. However, the broad spatial distribution of *AtIPT* expression suggests that all tissues can synthesize cytokinins as displayed in Figure 5 (Chapter 1.5.1; Miyawaki *et al.,* 2004). In addition, cytokinin nucleotide concentrations in the wild type rootstock were found at wild type levels even though the grafted *atipt1357* scion and consequently also the phloem deriving from the *atipt1357* scion had severely reduced levels of these compounds (Matsumoto-Kitano *et al.,* 2008). Therefore it seems that phloem derived nucleotides are dispensable for the root.

7.2.2 The xylem loading site of cytokinins following the apoplastic and/or the symplastic pathway

Cytokinin loading into the xylem sap facilitates the acropetal long-distance transport of the hormone and plays a crucial role in the distribution of cytokinins either as part of their homeostatic mechanism or as signal transducer for environmental stresses.

Loading of xylem cytokinins could potentially occur at any part of the root and in Figure 16 (Chapter 3.4.3) it was shown that cytokinin levels vary along the primary root axis of pea. Zeatin forms have been identified as the main forms in the xylem sap in several plant species, as discussed above. There is a concentration gradient of increasing tZRP, precursor of all tZ- and DZ- forms , towards the lateral root zone - represented here by the 20mm root segment above the first lateral root (Figure 16.a) in agreement with high expression of *AtCYP735A2* in the lateral root zone (Kiba *et al.,* 2013). Similar to tZRP, all cytokinin ribosides and the nucleobase tZ were also abundant in the lateral root zone compared to the other primary root segments examined (Figures 14.b, 14.c and 14.d). These results, in combination with previous findings of cZR, tZR and tZ being the prevalent cytokinins in the xylem sap of pea (Figures 11.b and 12.b, Chapter 3.4.1), indicate the lateral root zone as a candidate site for cytokinin loading into the xylem sap. The need for tight cytokinin regulation in this root zone was also implied by the significantly enriched CKX activity above the first lateral root (Figure 17, Chapter 3.4.3).

Another question concerning xylem loading of cytokinins is the cellular route followed. The xylem loading can occur through the apoplast or/and through the symplast. In theory, solutes can reach the xylem either by cell-to-cell movement through plasmodesmata (symplastic route) or by transport through the cell walls and extracellular spaces (apoplastic route). In isolated apoplast and symplast of *Arabidopsis* roots the predominant apoplastic cytokinins were tZR, cZR and cZ (Figure 31, Chapter 5.4.4). These apoplastic cytokinin forms were also found to be enriched in the xylem sap (Figures 11.b and 12.b, Chapter 3.4.1). However tZ which was one of the prevalent xylem cytokinins was not abundant in the apoplast. These data suggest that the loading of cytokinins in the xylem can occur both by the apoplastic and the symplastic pathway. The cytokinins loaded through the apoplastic route would have to face the hydraulic barrier between cortical and stele apoplast known as Casparian bands. The Casparian bands run around the cell wall of the endodermal root cells and are mainly composed of lignin and suberin, acting to prevent non-selective apoplastic bypass of water and solutes to the xylem and consequently to the shoot.

However as reviewed by White (2001), Casparian bands exist in the endodermis throughout the root except for a few millimeters at the extreme root tip. The possibility of the root tip as a loading site of apoplastic cytokinins into the xylem could be discounted from the results showing that all zeatin cytokinins, apart from DZR, were below the detection limit at the first 6 mm of the root tip (Figure 16, Chapter 3.4.3). These conclusions are also supported by the minimal expression of *AtCYP735A2* at the root tip compared to the mature root zone (Kiba *et al.,* 2013). In keeping with this, xylem loading would be unlikely to occur in the apical root zone before protoxylem maturation which has been suggested to coincide (or a bit after) with the simultaneous development of the endodermal Casparian bands (Esau, 1965; Peterson and Lefcourt 1990).

Another site of the root where the apoplastic bypass can freely result in solute entry into the xylem is the lateral root zone, already mentioned above as the best candidate site for xylem loading based on the results presented. The growth of lateral root primordia causes discontinuities in the Casparian bands since they penetrate the endodermis (Ferguson, 1979; Peterson and Moon 1993; White and Broadley, 2003) creating a route between the cortical and stele apoplast. By following this route, apoplastic tZR and cZR could be directly loaded in the xylem without the restriction to selectively pass through the endodermal symplast and possibly activate cytokinin signaling through the endoplasmic reticulum localized receptors (Wulfetange *et al.,* 2011; Lomin *et al.,* 2012; Caesar *et al.,* 2011).

The possibility of plasma membrane localized receptor activation (Inoue *et al.,* 2001; Kim *et al.,* 2006; Ueguchi *et al.,* 2001) by the apoplastically moving ribosides is supported by evidence presented in Chapter 5.4 (Figures 27 and 31) and is discussed below. Stolz *et al.,* (2011) showed that cytokinin signaling specificity is regulated by the combination of the expression patterns of the cytokinin receptors and the different ligand specificities. AtAHK4 displayed lower activity with cytokinin ribosides than did AtAHK3 (Romanov *et al.,* 2006; Spíchal *et al.,* 2004) and it was identified as the main cytokinin receptor in the root vasculature (Stolz *et al.,* 2011). Therefore the apoplastically moving ribosides tZR and cZR could pass through the stele apoplast and load into the xylem with lower probability of triggering cytokinin responses through AtAHK4. It should be noted that cZR showed no activity in E.coli assays expressing *AtAHK3* and *AtAHK4* and in *pAtARR5*:*GUS* gene assay in *Arabidopsis* (Spíchal *et al.,* 2004).

tZ, another of the main xylem cytokinins (Figures 11.b and 12.b, Chapter3.4.1), may activate intracellular cytokinin receptors and signaling since it was the predominant bioactive

intracellular cytokinin in the cytokinin responsive cells of the root (Figure 27, Chapter 5.4.1). However, tZ distribution was not significantly different intra- and extra-cellularly (Figure 31, Chapter 5.4.4), and therefore it could be hypothesized that while symplastic tZ is responsible for intra-cellular cytokinin signaling activation, apoplastic tZ is mainly loaded to the xylem. Abscisic acid has been also suggested to load to the xylem through the apoplastic route (Hartung *et al.,* 2002).

The hypothesis that the cytokinin ribosides tZR and cZR and the nucleobase tZ are loaded through the apoplastic pathway in to the xylem at the lateral root site does not exclude the possibility of an active transport pathway through the symplast. It is conceivable that in addition to the apoplastic route, some ribosides are loaded to the xylem through the symplastic pathway and exported to the apoplast only at the stele. Their presence in *Arabidopsis* apoplast was not exclusive (Figure 31, Chapter 5.4.4) and they have been shown to be actively transported through the plasma membrane by ENT transporters in rice and in *Arabidopsis* (Hirose *et al.,* 2005; Möhlmann *et al.,* 2001; Sun *et al.,* 2005; Wormit *et al.,* 2004). AtENT3 and AtENT6 transporters of cytokinin ribosides have been shown to localize at the plasma membrane but the experiments were performed either in protoplasts or in epidermal onion cells (Li *et al.,* 2003; Wormit *et al.,* 2004). Therefore there is no information about the *GFP* expression of these transporters in different cell types. Later a promoter driven *GUS* study displayed *AtENT3* expression in the vascular tissue including the root (Hirose *et al.,* 2008). Since the endodermis is neighboring tissue to the root vasculature it is not clear from the figures shown whether it is part of the expression domain of *AtENT3* or not.

Finally, AtABCG14 has been recently identified as a key regulator of acropetally transported cytokinins, particularly tZ-types, while its further substrate specificity range remains unclear (Zhang *et al.,* 2014.a). This role is supported by evidence from grafting experiments, reduced xylem cytokinins in the *atabcg14* knockout mutant and feeding experiments (Ko *et al.,* 2014; Zhang *et al.,* 2014.a). AtABCG14 has been shown to affect xylem cytokinin transport. It has been implied as a transporter of cytokinins to the apoplast and thus, according to the discussion above, AtABCG14 could affect xylem cytokinins by regulating their export to the apoplastic route. The expression of the gene in the stele and pericycle cells at almost all sites of the root coincides with the expression of cytokinin biosynthetic genes (*AtIPT3* and *AtCYP735A2*; Kiba *et al.,* 2013; Miyawaki *et al.,* 2004). Therefore cytokinins could enter the xylem following one or more of four candidate routes:

1. Cytokinins produced by different cell types of the lateral root zone are transported through the apoplastic pathway and loaded to the xylem.
2. Cytokinins produced by different cell types across the root are transported through the symplastic pathway and finally exported to the apoplast of xylem parenchyma cells next to the vessels through AtABCG14.
3. Cytokinins produced at different cell types are transported apoplastically and at any site of the root are entering the endodermal symplast through PUP and ENT transporters and then either exported again in the apoplast through ABCG14 at the pericycle and stele cells until loaded to the xylem.
4. Xylem cytokinins originating from cytokinins produced at the pericycle and stele cells by AtIPT3 and AtCYP735A2, are exported to the apoplast through AtABCG14 and loaded to the xylem at any site of the root or specifically at the lateral root zone in agreement with the increased cytokinin levels detected there corresponding to the main xylem forms.

7.3 tZ-cytokinins predominate in the shoot while IP-forms have no tissue specificity

The data presented in Chapter 3.4.2 (Figures 13-15) displayed that tZRP and tZ were predominantly found in the shoots of pea compared to the rest of the tissues. In agreement with this *AtCYP735A2* expression is also detected in the shoot (Kiba *et al.,* 2013; Takei *et al.,* 2004.a) while the phenotypic effects of the double mutant *atcyp735a1a2* were stronger in the shoot than in the root tissue (Kiba *et al.,* 2013). In contrast IPRP and IP did not exhibit abundance in a specific tissue (Chapter 3.4.2, Figures 13-15). These observations can be further supported by the combination of results deriving from three cytokinin deficient plants; the quadruple *atipt1357* that has reduced IPT-dependent cytokinin biosynthesis (Matsumoto-Kitano *et al.,* 2008; Miyawaki *et al.,* 2006), the double mutant *atcyp735a1a2* that has impaired levels of cytokinin trans-hydroxylation (Kiba *et al.,* 2013) and *atabcg14* that has decreased cytokinin transport (Ko *et al.,* 2014; Zhang *et al.,* 2014.a).

Analysis of cytokinin concentration, response and phenotype of these cytokinin mutants indicated that reduced tZ-cytokinins in the mutant shoot caused reduced cytokinin response and as a consequence retarded shoot growth. IP-compounds in the shoots of these mutants did not seem to rescue or affect this phenotypic impairment. This suggests that while tZ-

cytokinins are indispensable for normal shoot growth, IP-forms are not. In agreement *AtAHK3*, being predominantly expressed in the shoot tissues (Nishimura *et al.,* 2004), has been shown to preferentially bind tZ and this is a conserved trend in *Arabidopsis* and maize (Spichal *et al.,* 2004; Yonekura-Sakakibara *et al.,* 2004; Romanov *et al.,* 2006).

However in the mutant roots it can be hypothesized that the synergistic action of IP- and tZ-cytokinins was needed. In the roots of *atipt1357* both tZ- and IP-cytokinins were reduced causing impaired cytokinin response and this resulted in enhanced growth of the root system. Similar root phenotypes have been described by Werner *et al.,* (2010) who showed larger root systems in *CKX* overexpressing lines. In *atcyp735a1a2* mutant roots, IP-cytokinins were reduced but tZ-forms were enhanced maintaining that way total cytokinin levels in the root (Kiba *et al.,* 2013). Also, cytokinin response in root was retained at wild type levels and no severe phenotype was observed in root of *atcyp735a1a2* mutants (Kiba *et al.,* 2013). These results suggest that both tZ- and IP-cytokinins are indispensable for the root tissue. In agreement *AtAHK4*, being prevalently expressed in the root tissues (Nishimura *et al.,* 2004), had similar binding efficiencies for IP and tZ (Spichal *et al.,* 2004; Yonekura-Sakakibara *et al.,* 2004; Romanov *et al.,* 2006). In roots of *atabcg14* mutants both enhanced tZ- and IP-cytokinins concentrations induced additional cytokinin response, resulting in severely impaired root development. This phenotype was described by Zhang *et al.,* (2014) who attributed the dramatic root retardation to reduced meristem activity. Similarly, it has been previously shown either by exogenous application of cytokinin or by overexpression of the bacterial IPT gene that root growth and meristem size were both inhibited (Kuderová *et al.,* 2008; Medford *et al.,* 1989).

The nucleobase IP displayed no tissue-specificity in abundance (Chapter 3.4.2, Figures 13-15), was not significantly increased in the cytokinin responsive cell populations of *TCSn:GFP* (Chapter 5.4, Figures 27 and 30) and was detected equally intra- and extra-cellularly (Chapter 5.4.4, Figure 31). However both IP and tZ, compared to other cytokinin compounds, demonstrated high activity in bioassays, with tZ being mainly the most active between the two (Skoog and Armstrong 1970). They also displayed high binding affinities with cytokinin receptors compared to other cytokinin metabolites, with tZ being preferentially bound by the receptors, especially AtAHK3/ZmHK2 (Romanov *et al.,* 2006; Spíchal *et al.,* 2004; Yonekura-Sakakibara *et al.,* 2004). In accordance, IP and tZ were among the best substrates for CKX enzymes (Kowalska *et al.,* 2010; Köllmer *et al.,* 2014; Galuszka *et al.,* 2007; Gajdosová *et al.,* 2011). Therefore while the importance of both IP- and tZ-cytokinins is firmly established, tZ-forms seem to be more tissue specific and many time appear to be

indispensable (Kiba *et al.,* 2013). Sheen, (2013) gives a possible explanation for differential shoot versus root responses to IP and tZ occurring through complicated interactions of auxin and cytokinin in a molecular level and additional cell-specific signal transduction pathways. This hypothesis was based on the findings that while tZ-cytoknins have a major role in shoot growth the respective levels of auxin are 10 times less in the shoots than in the roots (Kiba *et al.,* 2013).

7.4 cZ-cytokinins; a role in cytokinin transport

cZ-riboside was one of the most predominant cytokinin compounds in both xylem and phloem sap of Pea (Chapter 3.4.1, Figures 11 and 12). This is also a conserved feature in *Arabidopsis* cytokinin bidirectional transport system (Hirose *et al.,* 2008). Therefore it could be suggested that cZR is a major transport CK-form common in xylem and phloem in Pea and *Arabidopsis*. Although xylem derived tZ-cytokinins have been reported to affect shoot growth and systemic nitrogen sensing, a role for cZR has not been further studied. It can be the case either that its role is purely homeostatic by its transport and participation in cytokinin pools of the shoot and root or that it has a physiological role in plant growth and development that is just starting to be unraveled.

Until recently cZ-forms of cytokinin were considered less important than IP and tZ-forms because of their weak responses in some bioassays (Kamínek *et al.,* 1987; Schmitz *et al.,* 1972) but also due to lack of research on them. However, within the last decades cZ was shown to activate cytokinin receptors in *Arabidopsis* and in maize (Inoue *et al.,* 2001; Romanov *et al.,* 2006; Spíchal *et al.,* 2004; Yonekura-Sakakibara *et al.,* 2004) and to be also active in several bioassays (Gajdosová *et al.,* 2011). cZ-cytokinins were also shown to be the main cytokinin form in developing seeds of three chickpea cultivars (Emery *et al.,* 1998), in all tissues of maize (Veach *et al.,* 2003), in the flag leaves of rice (Kojima *et al.,* 2009) and during pea embryogenesis (Quesnelle and Emery 2007). Additional lines of evidence for cZ activity were presented when enzymes responsible for zeatin-O-glucosides production were cloned in maize displaying striking preference in cZ conjugation (Veach *et al.,* 2003). Later, three cZ-O-glucosyltransferases (cZOGT1,2,3) were also identified in rice and they preferentially catalyzed O-glucosylation of cZ and cZR than tZ and tZR (Kudo *et al.,* 2012).

The proposition of cZ physiological effects on plant growth and development was based on evidence that overexpressors of *cZOGTs* in rice displayed deficiencies in crown root numbers, in leaf senescence and in shoot size (Kudo *et al.,* 2012b). In the same work direct impact of cZ activity in root elongation impairment was also shown followed by upregulation of OsRRs cytokinin response genes. Fast accumulation of cZRMP was discovered in maize roots as a response to salinity stress while tZ levels remained stable (Vyroubalová *et al.,* 2009). Similar increases in cZ-cytokinins were also found to follow drought (Havlová *et al.,* 2008), heat (Dobra *et al.,* 2010) and biotic stress (Pertry *et al.,* 2009). Finally, cZ-cytokinins were detected in more than 150 plant species and it was shown that their abundance was associated more with the developmental stage of the plant rather than the evolutionary complexity (Gajdosová *et al.,* 2011). Finally, cZ-cytokinins biological role in the regulation of xylem specification was recently reported when additional protoxylem cell files were observed in the *atipt29* double *tRNA-IPT* mutant but not in *atipt357* (Köllmer *et al.,* 2014). The phenotype of *atipt29*, having undetectable levels of all cZ-cytokinins, apart from cZOG, was mainly chlorotic with reduced primary root length and lateral root formation but no did not displayed any severe retardation in shoot growth like *atipt357* or *atcyp735a1a2* (Miyawaki *et al.,* 2006; Kollmer *et al.,* 2014).

The participation of cZ-compounds in cytokinin homeostatic mechanism was demonstrated by the unanimous increased concentrations of cZ-cytokinins when tZ-cytokinins were deficient , across all *atipt1357, atcyp735a1a2* and *atabcg14* mutants (Kiba *et al.,* 2013; Ko *et al.,* 2014; Matsumoto-Kitano *et al.,* 2008; Zhang *et al.,* 2014.a). Interestingly, cZ-cytokinins rose in the mutants mentioned above following only tZ-types reduction but not IP-types. The identification of cZR as a major transport form of cytokinin could also contribute to maintenance of cytokinin homeostasis in the shoots.

Arabidopsis protoplasts fed with labelled cZ showed that the main metabolites produced were cZRP followed by lower levels of cZR and cZ7G (Figure 28; Chapter 5.4.2). This metabolic route of cZ back to its precursor forms was also shown in maize cultured cells (Yonekura-Sakakibara *et al.,* 2004). No isomerization was observed between tZ- and cZ-ribosides (Chapter 5.4.2, Figures 28a. abd 28.b) and this result was further supported by feeding experiments in rice seedlings, tobacco cells and oat leaves (Gajdosová *et al.,* 2011; Kudo *et al.,* 2012). No isomerization from tZ to cZ was also inferred from absence of detectable cZ, cZR and cZRMP in the atipt29 double mutant which lacks both functional *tRNA-AtIPTs* genes (Miyawaki *et al.,* 2006). These findings imply that cZ-types levels are mainly regulated by de novo cZ-biosynthesis through the tRNA pathway described in

Chapter 1.3.1. Lack of trans-cis isomerization also indicates that the high levels of cZR being transported through the plant body are more likely to have a biological role directly as cZR or cZ rather than contributing to the tZ-cytokinin pools of the sink.

It is also interesting that cZR seems to be almost an inactive cytokinin form when tested in vitro receptor binding assays in *Arabidopsis* and maize (Spíchal *et al.,* 2004; Yonekura-Sakakibara *et al.,* 2004). In agreement with this, cZ-riboside was not able to trigger a cytokinin response in an *pARR5:GUS* bioassay (Spíchal *et al.,* 2004). On the other hand, it was the most effective cytokinin form tested in tobacco callus growth and oat chlorophyll retention bioassays (Gajdosová *et al.,* 2011). These studies indicate that cZR even though being unable to efficiently bind to cytokinin receptors, has great activity in some bioassays probably after its conversion to the bioactive cZ. This characteristic further support the use of cZR as a transport form since the risk of a triggering an unneeded cytokinin response can be avoided.

7.5 Cytokinin *max*ima within *Arabidopsis* root tip are in the columella

Cytokinin gradients within the root apex have already been inferred from promoter-reporter expression studies of cytokinin related genes. The highest expression of *AtCYP735A2* is in the vasculature (Kiba *et al.,* 2013) along with the cytokinin transporter *AtABCG14* (Ko *et al.,* 2014; Zhang *et al.,* 2014.a) while *AtCKX4* is expressed in the root cap. *AtCKX5* and *AtCKX6* expression is detected in the root vasculature with and without reaching the QC, respectively (Werner *et al.,* 2003). However, many cytokinin compounds are mobile and therefore cytokinin-related gene expression analysis does not always represent the sites of hormone production, accumulation and biological function.

To unravel the pattern of cytokinin distribution amongst different cell types, a combination of FACS and LC-MS/MS was used to quantify cytokinins in four *GFP*-marked cell types (Chapter 4.4.1, Figure 18). These marked the endodermal and QC cells, the stele cells, the epidermis and cortex cells and finally the root cap, columella, initials and QC cells resulting in a detailed cell map of the root apex (Chapter 4.4.1, Figure 18.a). The approach followed was previously applied to develop high resolution maps of auxin and OxIAA distribution (Petersson *et al.,* 2009; Pencik *et al.,* 2013). Method validation and control experiments

showed that protoplast isolation and cell-sorting caused only small shifts in cytokinin endogenous content and only slight leakage from protoplasts was observed (Chapter 4.4.1, Figures 22-24). In parallel, the purification method for cytokinins was optimized by using an In-tip microSPE protocol (Chapter 4.4.1, Figures 20 and 19) and ultra-sensitive LCMS protocols were applied to detect and quantify 15 different cytokinins.

The results revealed that while cytokinin distribution was similar across the three of the cell types under study, cytokinin compounds were consistently enhanced in the cell population derived from root cap, columella, initials and QC (Chapter 4.4.2, Figure 25). This is in agreement with TCSn:GFP expression profile (Figure 26, Chapter 5.1; Zurcher *et al.,* 2013) The cytokinin cell map complemented the equivalent map of auxin, notably that the columella was the only site where IAA concentration was found at minimal levels (Petersson *et al.,* 2009), with the exception of the QC. This is in accordance with the well-established antagonistic action of the two major phytohormones within the root regulating lateral root primordia formation (Moreira *et al.,* 2013), root meristem size determination (Dello Ioio *et al.,* 2007; 2008) and embryonic root stem cell niche specification (Müller and Sheen, 2008).

Four studies of microarray data for specific cell types of the *Arabidopsis* root apex (Birnbaum *et al.,* 2003; Brady *et al.,* 2007; Dinneny *et al.,* 2008; Petricka *et al.,* 2012) were examined for cytokinin-related genes and the combined data indicated that cytokinin biosynthesis, metabolism and signaling predominates in the stele cell population compared to the other three cell populations represented by the *GFP* lines used for cytokinin analysis (Chapter4.4.4., Table 6.a). In parallel, in the columella cells that displayed *max*ima of cytokinin concentration, the dominant cytokinin-related genes encoded degradation and conjugation enzymes while this was the only cell population under study where there was no enrichment of expression of cytokinin transporters, apart from ABCG14 (Chapter 4.4.4., Table 6.a). Therefore it could be hypothesized that cytokinins are biosynthesized, metabolized and act mainly in stele cells and they are transported and trapped in the columella cells for inactivation. This hypothesis is further supported by the deficient meristematic activity of *atabcg14* mutant, pointing to the significance of the transporter in cytokinin allocation within different cell types of the root tip (Zhang *et al.,* 2014.a).

7.6 Intra- and extra-cellular cytokinins mediating cytokinin response

As presented in Chapter 5.4.4 (Figure 31), none of the cytokinin nucleobases, apart from tZ, or ribosides were enriched in the symplast of *Arabidopsis* roots. Instead tZR and cZR concentrations, being also the main compounds in the xylem sap, were significantly enhanced in the root apoplast while IP and IPR were equally distributed. The differential distribution of bioactive cytokinins in the intra- and extra-cellular space reported here indicates that cytokinins are passively and/or actively exported in the apoplastic space possibly through transporters like AtABCG14 (Ko *et al.,* 2014; Zhang *et al.,* 2014.a) for degradation and/or transport of the hormone to neighboring cells. Such paracrine transport of cytokinins from the stele cells to the columella where cytokinin *max*ima was detected was suggested in Chapter 7.5. AtCKX2 was shown to degrade cytokinins apoplastically (Werner *et al.,* 2003) while AtCKX4, AtCKX5 and AtCKX6 were also suggested to be secreted according to bioinformatics analysis. The fact that four out of the seven *AtCKX* family members have extra-cellular localization is in agreement with the identification of apoplastic cytokinins. *GFP* fusions for AtCKX7, AtCKX3 and AtCKX1 exhibited intra-cellular localization of these enzymes. More specifically, AtCKX7 is the only cytoplasmic AtCKX (Köllmer *et al.,* 2014) while AtCKX3 and AtCKX1 were localized in the vacuole (Werner *et al.,* 2003). Cytokinin glucosides were the prevalent CKs in the symplast suggesting that cytokinin glucosyltransferases are localized intra-cellularly. This is in agreement with predictions of intracellular localization of AtUGT73C5, AtUGT73C1 and AtUGT85A1 producing tZ- and DZ-O-glucosides (Kieber and Schaller 2014).

In a separate study cytokinins were quantified in *TCSn:GFP* positive root cells , representing the cell populations that are responsible for cytokinin signaling in *Arabidopsis* root. The method for separation of distinct cell populations as protoplasts, developed in Chapter 4.4.1, required the exclusion of the apoplastic fluid from the samples. Therefore the results for cytokinin quantification in the cytokinin responsive cells report only intracellular cytokinins. These results presented in Chapter 5.4.1 (Figure 27) revealed that the only bioactive cytokinin enriched in the *TCSn:GFP* positive cells was tZ. In addition, all cytokinin glucosides were detected abundantly in these cell populations. The compounds that displayed increased levels in the *TCSn*+ cytokinin responsive cells were in striking accordance with those enriched in symplastic samples, while the ones that were abundant in the apoplast showed no enrichment in the positive cells. These results were further supported by

cytokinin quantification in the cytokinin-responsive cells following treatment of the roots with INCYDE which reduced cytokinin degradation and enhanced cytokinin response as shown in Figure 29 (Chapter 5.4.3). Initially the cytokinin forms detected abundantly in the positive cells were in agreement with the non-treated experiment mentioned above, further confirming these results (Figure 30, Chapter 5.4.3). The one cytokinin compound that significantly responded to the treatment, exhibiting 24 times higher enrichment over the non-treated samples, was tZOG. This was in accordance with the increased trend of tZ in the positive cells of the treated *TCSn:GFP* suggesting that cytokinin O-glucosyltransferases intervened to maintain hormone homeostasis, and enable storing of excess tZ in a convertible and non-susceptible to CKX form.

Taken together, these three independent experiments (Figures 27, 30 and 31, Chapter 5.4) are consistent with each other and lead to some novel conclusions concerning cytokinins. The bioactive cytokinin responsible for cytokinin signaling in *Arabidopsis* root tips was shown here to be tZ. This is supported by cytokinin receptor binding assays in which tZ displayed the highest affinity to AtAHK3 and AtAHK4 compared to the other cytokinin compounds tested (Spíchal *et al.,* 2004). Since tZ seems to activate cytokinin signaling intracellularly it can be assumed that this occurs through binding to cytokinin receptors recently shown to be localized in the endoplasmic reticulum (Caesar *et al.,* 2011; Lomin *et al.,* 2012; Wulfetange *et al.,* 2011). In most of *AtCKX* overexpressor transgenic lines tZ was detected at very low levels indicating that is tightly regulated by these enzymes that are responsible for the irreversible degradation of cytokinin.

Another interesting conclusion from the combined data discussed above concerns IP inertia in all these experiments. IP was equally distributed between *GFP* positive and negative cells of both the non-treated and the INCYDE-treated *TCSn:GFP* (Chapter 5.4, Figures 27 and 30) indicating that it is not responsible for intracellular activation of cytokinin signaling cascade. This was surprising not only because IP is known as one of the most active cytokinins in receptor-binding assays and bioassays (Romanov *et al.,* 2006; Spíchal *et al.,* 2004; Stolz *et al.,* 2011; Yonekura-Sakakibara *et al.,* 2004) but also because it has been shown to be one of the best substrates for CKX activity suggesting the importance for control of IP concentration. Its presence in the apoplast (Chapter 5.4.4, Figure 31) combined with its inability to trigger an intracellular *TCSn*-mediated cytokinin response leads to the hypothesis that IP-mediated responses take place in the apoplast by the activation of plasma membrane receptors (Ueguchi *et al.,* 2001; Kim *et al.,* 2006; Inoue *et al.,* 2001). Even though recent findings support cytokinin receptors being localized to the endoplasmic reticulum with the CHASE

cytokinin binding domain exposed to the endoplasmic reticulum lumen (Caesar *et al.,* 2011; Lomin *et al.,* 2012; Wulfetange *et al.,* 2011) the presence of active receptor proteins in the plasma membrane has never been excluded. This hypothesis is further supported by studies concerning the influence of compartmentalization of AtCKX isoforms on their capability to degrade different cytokinin compounds in vitro (Gajdosová *et al.,* 2011; Galuszka *et al.,* 2007; Kowalska *et al.,* 2010). These studies in combination with in vivo data deriving from cytokinin measurements on *AtCKX* overexpressor lines (Köllmer *et al.,* 2014; Werner *et al.,* 2003) suggest that IP and IPR are preferably degraded by the apoplastic AtCKX2, AtCKX4 and AtCKX5 while from the intra-cellularly localized AtCKXs, only the vacuolar AtCKX3 was shown to favor IP-compounds degradation. In contrast, tZ displayed highest activity with the cytosolic AtCKX7 and the vacuolar AtCKX3.

In summary, here it is suggested that cytokinin signaling includes three regulation levels. Two have been already shown. The first concerns the affinities between different cytokinin-types and specific receptors. For example AtAHK3 had lower affinity to IP and IPR than AtAHK4. (Romanov *et al.,* 2006; Spíchal *et al.,* 2004; Stolz *et al.,* 2011; Yonekura-Sakakibara *et al.,* 2004). The second level of cytokinin signaling regulation concerns the tissue- and cell-specific expression of cytokinin receptors (Higuchi *et al.,* 2004; Nishimura *et al.,* 2004; Riefler *et al.,* 2006) and respective distribution of different cytokinin compounds. For example *AtAHK4* expression predominates in the root so IP phloem-derived cytokinins can potentially be perceived. Here a third level of regulation is implied concerning cellular localization of cytokinin receptor and the cytokinin-types that they can perceive. For example symplastic tZ, shown to regulate intracellular cytokinin response, could be possibly perceived by the endoplasmic reticulum cytokinin receptors while IP, and maybe tZR and IPR, that were not responsible for intracellular induction of cytokinin signaling cascade and are similarly present in symplast and apoplast, could possibly be perceived by plasma membrane cytokinin receptors.

7.7 Do cytokinin glucosides have a biological role?

Cytokinin N- and O-glucosides are formed by the attachment of a sugar molecule, usually glucose, at the N^7 or N^9 of the cytokinin purine ring and at the hydroxyl group of zeatin- side chains, respectively. These cytokinin conjugation products are the predominant isoprenoid cytokinin forms found in representative groups of all land plants (Gajdosová *et al.,* 2011).

Cytokinin glucosyl-conjugates were detected abundantly in the columella of the *Arabidopsis* root tip and paralleled the concentration gradients of cytokinin bioactive compounds (Chapter 4.4.2, Figure 25). Glucosides were also highly enriched in the symplast of *Arabidopsis* roots but not in the apoplast (Chapter 5.4.4, Figure 31). They were also highly enriched in the CK-responsive *TCSn:GFP*+ cells of *Arabidopsis* root tips (Chapter 5.4.1, Figure 27). When *TCSn:GFP* protoplasts were treated with INCYDE, inhibiting cytokinin degradation through CKX enzymes, the tZOG increase in the *TCSn:GFP*+ cells represented the strongest response to the treatment (Chapter 5.4.3, Figure 30). These data suggest that cytokinin glucosides are detected mainly at intra-cellular sites where high concentration of bioactive cytokinins was predicted.

However cytokinin glucosides were also detected in very specific sites within the plant, not necessarily following their respective bioactive cytokinins gradients. In the phloem and xylem sap of Pea cytokinin glucosides were found in small amounts, compared to major forms like cZR (Chapter 3.4.1, Figures 11 and 12). Yet, the DZ9G and IP9G, detected as transported cytokinin glucosides, could be defined as “marker-compounds” in the xylem and phloem of Pea respectively since their presence was exclusive in either the acropetal or the basipetal cytokinin translocation, respectively. In addition, DZ9G displayed a significant increase in its concentration in the hypocotyl of both pea cultivars (Chapter 3.4.2, Figures 13-15) indicating that conjugation of DZ in this specific site is required.

This tissue specificity that cytokinin glucosides displayed coupled with their high levels in the symplast of cytokinin responsive cells (Chapter 5.4.4, Figure 31) generates the following question: Do cytokinin glucosides have a direct cytokinin-independent biological role or is their action tightly linked to maintenance of cytokinin homeostasis, therefore only indirectly affecting plant growth?

A feeding experiment in *Arabidopsis* root protoplasts revealed that labelled cZ and tZ could be uptaken by root tip protoplasts and metabolized within 30min. The predominant metabolites occurred by feeding with labelled cZ was cZRP followed by cZR and cZ7G

(Chapter 5.4.3, Figure 28.a). These compounds were not predominant forms in either the symplast of *Arabidopsis* roots or in the cytokinin responsive cells since the major zeatin glucosides identified in these experiments were cZ9G, cZOG, tZ9G and tZOG (Chapter 5.4.1, Figure 27). Similar to cZ metabolic behavior, feeding with labelled tZ resulted in highest levels of tZRP followed by tZR and tZOG (Chapter 5.4.3, Figure 28.b). These data could not prove that high glucoside levels found in the cytokinin responsive cell populations derived necessarily from respectively high levels of cytokinin nucleobases. The glucoside tZOG, that was proposed to play an important storage role in the positive cells of treated *TCSn:GFP* roots (Chapter 5.4.3, Figure 30), was one of the main labelled tZ-metabolites in the feeding experiment (Chapter 5.4.2, Figure 28.b). In addition, O-glucosides apart from being able to reversibly convert to bioactive nucleobases are also resistant to CKX enzymes. It is therefore proposed that O-glucosides can be partially an indicator of bioactive cytokinin pool size while the abundance of N-glucosides could not be proven by this feeding experiment. According to the hypothesis for differential receptor sensing of intra- and extra-cellular cytokinins, discussed in Chapter 6.6, it could be assumed that the increased levels of cZ- and IP-N-glucosides in the cytokinin responsive cells could correspond to high levels of extracellular cZ and IP which are then transferred into the cell for deactivation. This is in accordance with intracellular localization of glucosyltransferases (Kieber and Schaller 2014) and with in vivo and in vitro studies showing that 9-glucosides, being the only suitable glucosides that can acts as CKX substrates, were preferentially degraded by the cytosolic AtCKX7 and the vacuolar AtCKX3 (Gajdosová *et al.,* 2011; Galuszka *et al.,* 2007; Köllmer *et al.,* 2014; Kowalska *et al.,* 2010).

Overexpression of the N-glucosyltransferase *AtUGT76C1* was not accompanied by elevated levels of 7-N-glucosides unless there was cytokinin treatment (Hou *et al.,* 2004). In accordance with this, *AtUGT76C2* knockout mutant and overexpressors had no phenotypic alterations from wild type plants even though N-glucosides, but not IP and tZ, had dramatic changes in their concentration. However, the cytokinin sensitivity in both transgenic lines was highly altered in several physiological responses including root elongation, anthocyanin accumulation, chlorophyll retention and lateral root elongation (Wang *et al.,* 2011). Similar results concerning the lack of phenotype but also the fine modulation of cytokinin sensitivity, were displayed for transgenic lines of *AtUGT76C1* (Wang *et al.,* 2013). N-glucosides showed no activity with cytokinin receptors in E.coli assay (Spíchal *et al.,* 2004) and they are also inactive in most bioassays.

O-glucosides, on the other hand, have a more active role because of their capability to be converted back to cytokinin bioactive forms. Heterologous overexpression of *ZOG1* from Phaseolus lunatus in maize and tobacco exhibited increased concentrations of ZOG followed by alterations in the plant phenotype (Martin *et al.,* 2001.a; 2001.b Pineda Rodo *et al.,* 2008). Even though O-glucosides were biologically active in *Arabidopsis* bioassays, they had no efficiency in cytokinin receptors binding in E.coli assays (Spíchal *et al.,* 2004). These data suggest that O-glucosides are able to affect cytokinin response more strongly than N-glucosides but this feature is also attributed to their function as cytokinin storage forms. In agreement with this, the dramatic increase of tZOG in *TCSn:GFP*+ INCYDE treated cells accompanied a smaller but significant escalation of tZ levels.

Taken together the data of this study and previous research suggest that glucosyltransferases participate in cytokinin responses but this is more possibly due to detoxification and maintenance of cytokinin homeostasis rather than an active independent physiological role in plant development. However future experiments are needed to fully answer this question.

7.8 Strigolactone effect on cytokinin distribution and homeostasis

Strigolactone is a novel plant hormone shown to affect shoot branching (Gomez-Roldan *et al.,* 2008; Umehara *et al.,* 2008) among other crucial developmental plant processes (reviewed by Waldie *et al.,* 2014). The perturbed xylem cytokinin content in *rms* mutants was of particular interest here since it would facilitate further investigation of regulation of cytokinin distribution within plant tissues. The mutants examined were *rms1*, exhibiting low levels of acropetally moving cytokinins, and *rms2*, the only strigolactone mutant displaying increased xylem cytokinin content (Beveridge *et al.,* 1997.a; Beveridge *et al.,* 1994; Foo *et al.,* 2007). It was hypothesized that these oppositely altered trends in xylem cytokinin levels of *rms1* and *rms2* would correlate with differential cytokinin contents in specific tissues and thus allow a better understanding of regulation of cytokinin distribution.

7.8.1 Perturbed xylem cytokinins levels in *rms* mutants did not correlate with root cytokinins.

Interestingly, altered xylem cytokinins in *rms* mutants were not obviously related to root cytokinin profiles, although this tissue is the presumed site of xylem loading (Figures 31-34, Chapters 6.4.1-6.4.3). Therefore, this study did not provide support for the hypothesis that a specific site exists within the primary root where cytokinins are loaded into the xylem (Discussed in Chapter 7.2.1). The results instead indicate that strigolactone may affect xylem cytokinins by influencing their direct export to the xylem, perhaps through regulation of the *ABCG14* transporter in root vasculature (Ko *et al.,* 2014; Zhang *et al.,* 2014.a) and this aspect should be included in future experiments mentioned in Chapter 7.10.

In the context of other functions, strigolactones were recently shown to positively affect secondary growth and this was a conserved effect in pea, *Arabidopsis* and *Eucalyptus globulus* (Agusti *et al.,* 2011). Stem sections of the strigolactone defective mutant *rms1*, used also in this work, had significantly reduced cambium activity compared to the wild type (Agusti *et al.,* 2011). Therefore an alternative hypothesis could be that perturbed xylem cytokinins in strigolactone mutants is a result of altered secondary growth. Future experiments could test this possibility as proposed in Chapter 7.10.

However strigolactone effects on cytokinin were identified in the apical part of pea primary roots (Figures 33 and 34, Chapter 6.4.3). Cytokinin concentration is induced by strigolactone in this specific part of the root, probably through inhibition of *CKX*-dependnt cytokinin degradation. This regulation seems to be local, since it is not obviously related to xylem cytokinin levels in *rms* mutants and not to be affected by the *RMS2*-controlled feedback signal, since cytokinin regulation was similar for both *rms1* and *rms2*.

Another finding was the differential regulation of cytokinins by strigolactone in the apical and lateral root zones, consistent with the variation of cytokinin metabolite distribution along the primary root axis (Figures 16 and 17, Chapter 3.4.3). These findings indicate that different plant functions may be controlled by the interaction of the two hormones in distinct sites of the primary root. For example, the interplay between strigolactone and cytokinin affecting primary root length presumably takes place in the apical part of the root while a different form of crosstalk affecting lateral root development would logically occur at the lateral root zone (reviewed in Rasmussen *et al.,* 2013).

7.8.2 Cytokinin homeostasis seems to be functional in *rms1* aerial parts but not in the ones of *rms2.*

Cytokinin analysis in the aerial parts of *rms* mutants revealed that *rms1* shoots can compensate for reduced xylem cytokinins while in *rms2* the correlation between shoot and xylem cytokinins was strong (Figure 33, Chapter 6.4.2). In particular, IP-type CKs were increased in *rms1* and *rms2* shoot parts while tZ-types showed elevated levels only in *rms2*. This differential behavior of shoot IP- and tZ-cytokinins in *rms1* and *rms2* mutants has been also shown in stem segments of these mutants (Young *et al.,* 2014).

These results strongly suggest cytokinin homeostatic regulation within the shoot. This mechanism seems to be primarily through elevated IP-cytokinin levels, which is in accordance with *PsIPT1* up-regulation in stem segments of *rms1* (Young *et al.,* 2014; Dun *et al.,* 2012). The high IPRP levels in *rms1* aerial parts may be responsible for the wild type levels of tZ-types in the same tissues, through action of *PsCYP735A* hydroxylases. This hypothesis could be tested by identification of *AtCYP735As* homologs in pea and measurements of their expression in *rms1* shoots. On the contrary, in *rms2* aerial parts cytokinins were significantly increased, matching the xylem profile, and thus implying that the compensatory mechanism of the hormone might not be adequate to restore tZ-cytokinins down to normal levels. It has been previously shown that *PsIPT1* transcript levels were not induced in *rms2* stem segments, unlike in *rms1* (Young *et al.,* 2014). However, neither was *PsIPT1* downregulated as would be predicted if it was responsible for homeostatic control of overall CKs.

It was also indicated that the root seems to be the main provider of tZ-cytokinins to the shoot, in agreement with discussions in Chapter 7.2.1. However, xylem tZ-cytokinins were shown to be dispensable for the shoot. This is also supported by grafting experiments showing that tZ-cytokinins were not affected in wild-type scions grafted to *atipt357* triple or to *atcyp735a1a2* double mutant rootstocks (Matsumoto-Kitano *et al.,* 2008; Kiba *et al.,* 2013).

RMS2 has been proposed to regulate a basipetally-moving homeostatic signal which is required for reduced xylem cytokinin export and induction of strigolactone biosynthetic genes in *rms* mutants (Foo *et al.,* 2007; Foo *et al.,* 2005; Beveridge 2000; Beveridge *et al.,* 1994). The additive branching phenotype displayed by *rms1rms2* double mutants (Beveridge *et al.,* 1997.a) also indicated that *RMS1* and *RMS2* genes either control independent pathways or they control signals transmitted in opposite directions along the plant axis

(Beveridge 2000). It has been argued that this novel feedback signal might in fact be auxin, based on the findings that *rms2* shoots have increased IAA levels but wild type IAA transport (Beveridge *et al.,* 2000; Beveridge *et al.,* 1997.a; Beveridge *et al.,* 1994). Regardless of the identity of the *RMS2*-dependent feedback signal, it seems that apart from affecting xylem cytokinin in the roots, it also affects cytokinin homeostasis in the aerial parts of pea.

7.9 Conclusions

The principal conclusions of this work are listed below:

a. Cytokinin compound concentration varies amongst pea tissues and vascular saps moving basipetally and acropetally and even across different developmental stages of the same tissue. While this is in agreement with similar studies in other plant species and with cytokinin-related gene expression profiles, here the detection and specificity were pushed to new limits to facilitate cytokinin quantification at a cell specific level.
b. For the first time heterogeneous cytokinin distribution was demonstrated in different cell populations of the *Arabidopsis* root apex and in intra- and extra-cellular space. A representative scheme for tZ distribution is presented n Figure 38. These detailed studies on cytokinin variation further supported known aspects of the hormone but also revealed novel ones as specified below.
c. Detailed analysis of endogenous cytokinin levels within different segments of pea roots implied the lateral root zone as a candidate loading site for cytokinins into the xylem sap through an apoplastic route.
d. Tissue-specific cytokinin measurements in pea suggested that tZRP and tZ predominate in the shoot. While this is supported by several studies, it is for the first time confirmed by data on the absolute levels of the endogenous compounds.
e. Analysis of cytokinin levels in pea saps derived from the same set of plants showed that the riboside cZR was one of the major transport forms of cytokinin moving both basipetally and acropetally. While this is a conserved trend with *Arabidopsis*, according to Hirose *et al.,* (2008), it has not previously been discussed.
f. The same analysis confirmed previous findings suggesting that tZ-cytokinins predominated in the xylem sap while IP-forms prevailed in the phloem. However it

was also shown that apart from IP-forms, tZ and DZ were also abundant in pea phloem.

g. At a finer spatial scale, FACS technique was combined with a new cytokinin purification method and ultra-sensitive mass spectrometry to achieve measuring cytokinins at the cell-specific level. Several control experiments confirmed that the endogenous levels of the hormone exhibit only small alterations and minimal levels of leakage from isolated protoplasts during the process of generating specific cell populations of the root apex. Therefore the method developed was considered valid for representing cytokinin endogenous levels.

h. Following this newly developed method it was discovered that all cytokinin compounds detected in the *Arabidopsis* root apex consistently showed maximum accumulation in the cell population that includes the columella, root cap, intials and QC. In parallel a re-analysis of published microarray data revealed that the cell population displaying highest expression of several cytokinin-related genes was the stele.

i. Using the same FACS-LCMS method, cytokinins were quantified in *TCSn:GFP*+ cells representing cell populations responsible for the signaling output of the hormone. Interestingly it was implied that tZ was the only bioactive cytokinin compound associated with intra-cellular TCSn/B-ARRs-mediated activation of the hormone signaling in *Arabidopsis* root tips.

j. To further validate these results and because isolation of specific cell populations requires exclusion of cell wall and extracellular spaces, cytokinins were measured in the apoplast and the respective symplast isolated from *Arabidopsis* roots. Several bioactive cytokinin compounds were identified in the root apoplast. This finding, in combination with lack of enrichment of all bioactive cytokinins, apart from tZ, in the symplast of activated intracellular *TCSn*-mediated signaling, implied the presence of active receptors in the plasma membrane.

k. Cytokinin O-glucosides apart from their known role in cytokinin homeostasis were also indicated to have a more active role. This was supported by their predominant presence in cytokinin responsive cell populations of *Arabidopsis* roots and confirmed by their substantial further accumulation in *GFP*+ cells of *TCSn:GFP* roots where cytokinin degradation had been blocked with INCYDE. In agreement with this, tZOG was shown to be one of the metabolites occurring in root protoplasts after feeding with labelled tZ.

l. Cytokinin N-glucosyl-conjugates exhibited interesting profiles in both the tissue- and vascular sap-specific studies in pea. They were also the predominant enriched cytokinins in the symplast and the cytokinin responsive cell populations of *Arabidopsis* root. However, their high abundance does not appear to be explained by rapid conversion from bioactive cytokinins, based on cytokinin feeding experiment.

m. Root cytokinin biosynthesis, metabolism and/or degradation seem to not be responsible for perturbed xylem cytokinin content in *rms* mutants since there was no correlation between *rms* root cytokinin concentration and the respective xylem levels.

n. Strigolactone increases cytokinin levels in the apical root part of pea primary root (0-46 mm) probably through inhibition of CKX enzymatic activity. This regulation seems to be local and is independent of the *RMS2*-mediated feedback signal.

o. Strigolactone was shown to differentially regulate cytokinin concentrations in the apical root part and the lateral root zone site of pea primary root.

p. Cytokinin homeostatic mechanism through alteration of hormone biosynthesis, metabolism and/or degradation, enables compensation for perturbed xylem cytokinin content arriving in the shoot of pea, and seems to be *RMS2*-dependent.

7.10 Future Experiments

Since more than one cytokinin compound is bioactive, and both precursor and some conjugate forms can be rapidly interconverted to these bioactive cytokinins, the establishment of how cytokinin compounds establish gradients at the tissue specific level would be valuable information. Therefore it is suggested to examine whether the tissue specific presence of cytokinin compounds, demonstrated here in pea, is more widely conserved. This could be achieved by quantifying cytokinins across sequential tissues of of *Arabidopsis*. Since in *Arabidopsis* the tissue-specificity of cytokinin-related genes has been extensively examined, a tissue specific analysis of cytokinin endogenous levels could complement our knowledge on gradients within the plant tissues. Also, since the pea transcriptome is now available (http://www.biomedcentral.com/1471-2164/13/104) the distribution of expression of the pea homologues of cytokinin-related genes can now be investigated. Any similarities or differences in gene expression profiles and endogenous levels of cytokinin in the two plant species will facilitate a better understanding on how different cytokinin compounds contribute to the already known functions of the hormone and might also indicate new roles of cytokinin. Furthermore, taking advantage of the available TILLING mutant population in pea (Dalmais *et al.,* 2008) multiple cytokinin mutants can be created to promote genetic studies in pea and to take advantage of the more favorable physiology of pea for example for grafting experiments.

Further investigation can be also conducted into the putative loading site for xylem cytokinins through the apoplast in the lateral root zone where the endodermal Casparian strips are interrupted by the formation of the lateral root primordia. Measurements of endogenous cytokinin levels in the apoplastic and symplastic fluid and in the xylem sap of pea and *Arabidopsis* would allow insights into which route is more likely to correspond to cytokinin xylem concentrations and if this is a conserved trend. Comparison of xylem cytokinins, isolated through the centrifugation method (López-Millán *et al.,* 2001) from whole roots, root parts lacking the lateral root zone and the lateral root zone alone would facilitate identification of the importance of lateral root zone as a cytokinin loading site to the xylem.

The role of cZ-riboside could be investigated by grafting experiments. The double *atipt29* mutant, lacks functional *tRNA-IPT*s and has undetectable levels of cZR and other cZ-cytokinins (Miyawaki *et al.,* 2006), and would be grafted reciprocally with wild type plants. Cytokinin quantification in the shoots, roots, xylem and phloem saps of both grafting

combinations along with the observed phenotypes will provide evidence of cZR role as a systemic signal.

The discussion in Chapter 7.5. led to the hypothesis that excess of cytokinins produced in the stele cells are transported to the columella where they are deactivated through AtUGT and AtCKX enzymes . The importance of cytokinin export from stele cells can be examined by cytokinin quantification in the stele and columella cell populations of the *atabcg14* mutant. This would be achieved by crossing of the mutant with the transgenic cell marker lines *pWOL:GFP* and *M0028:GFP*. The newly developed method described in Chapter 4 can be then used for isolation of the cell populations and quantification of the hormone. Further investigation of the significance of cytokinin degradation in the columella could be achieved by both increasing the antagonism for cytokinin deactivation process and silencing the local enzymes responsible for this process. An *M0028* promoter driven *IPT* expression could be induced in the respective cell population or local treatment of exogenous tZ and IP could be applied to increase the deactivation antagonism between wild type concentrations of cytokinins and artificially provided ones. Cell-specific promoters have been previously used to drive expression of *IPT* genes revealing that ectopic cytokinin biosynthesis affects lateral root initiation but not lateral root development (Laplaze *et al.,* 2007). In parallel, a transgenic line with two inducible RNA-silencing constructs, one concerning the conserved domains between *AtUGT76C2* and *AtUGT85A1* and the other one between *AtCKX4* and *AtCKX5,* driven by *M0028* promoter could specifically reduce cytokinin deactivation process in the columella cell population.

The presence of active receptors in the plasma membrane hypothesized in Chapter 7.6 and the indication of tZ as the only intracellular bioactive cytokinin able to trigger cytokinin response could be further examined with the following experiments. Isolated protoplasts from roots of *TCSn:GFP* line would be treated with free IP and tZ and with the same compounds attached to sepharose beads. Since the beads prevent the attached cytokinin nucleobases from entering the cytosol only outward facing plasma membrane receptors would be activated. Any initiation of cytokinin signalling would be indicated by the fluorescence levels. A similar experiment was performed for gibberellin plasma membrane receptor activation (Hooley *et al.,* 1991). Finally, to confirm the identity of apoplastic cytokinins and check if this is a conserved trend among plant species, cytokinins and CKX activity will be compared in root apoplast and symplast of pea and *Arabidopsis*.

Cytokinin distribution and inferred roles of specific compounds, like cZR in the hormone transport and DZ-glucosylation in the hypocotyl tissue, can be further studied by performing feeding experiments with labelled cytokinins (labelled cZ, tZ, DZ, IP). The labelled compound could be infiltrated into the hypocotyl of the plant entering the xylem sap flow as described in Mader *et al.,* (2003). The labelled products will be quantified over a timecourse in root, shoot, xylem and phloem sap. This kind of experiment will allow simultaneous tracing of the metabolism and transport of cytokinin nucleobases.

Future research on strigolactone-cytokinin crosstalk would provide a better insight into the regulation of cytokinin distribution since *rms1* and *rms2* mutants have oppositely altered xylem cytokinin content. Driven by results discussed in Chapter 7.7.1 it was hypothesized that since absolute levels of root cytokinins were not correlated with for the altered xylem levels, then transport might be the key regulatory component. *ABCG14* was recently identified as a cytokinin efflux carrier tightly associated with tZ loading in the xylem (Zhang *et al.,* 2014.a; Ko *et al.,* 2014). By identifying *AtABCG14* homologs in pea, transcript levels could be tested in *max* and *rms* mutant roots for possible correlation with xylem cytokinin levels in *rms1* and *rms2*. If *AtABCG14* is responsible for altered cytokinin content in *rms* mutants then it would be expected that *AtABCG14* expression would be suppressed in *rms1* (low xylem cytokinin content) and induced in *rms2* (high xylem cytokinin content).

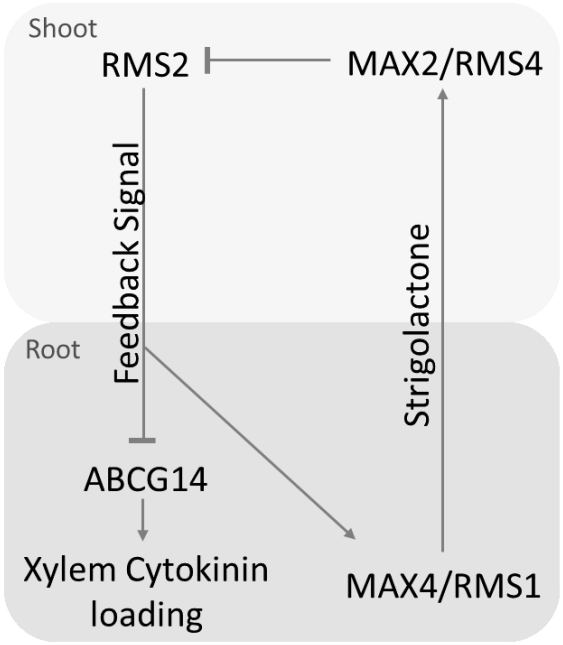

Figure 39 *Hypothesis on how strigolactone regulates xylem cytokinin levels. Strigolactone, biosynthesized by MAX4/RMS1 inhibits the RMS2-dependent basipetal feedback signal though MAX2/RMS4. The inhibitory effect of the RMS2-mediated feedback signal on ABCG14 cytokinin transporter faclitating export of cytokinins from the cells and into the xylem is then restrained.*

The generation of the double mutant *max4abcg14* in *Arabidopsis* and examination of its xylem cytokinin contents would facilitate genetic validation of this hypothesis, shown in

Figure 39 If *AtABCG14* is regulated by strigolactone in the double mutant the *max*4-like branching would be suppressed and the retarded shoot growth phenotype of *atabcg14* (Ko *et al.,* 2014; Zhang *et al.,* 2014.a) would be epistatic. Further examination of *AtABCG14* regulation by strigolactone in the roots could be provided by grafting experiments between *max*4 scion and *max4abcg14* rootstock. Likewise, crosses and respective grafting experiments could be performed with *max*2 insensitive mutant to test whether this regulation occurs through *MAX*2-mediated strigolactone signaling.

Another possibility is that strigolactone affects xylem cytokinins by regulating cambial activity. It was recently shown in *Arabidopsis*, pea and Eucalyptus globulus that strigolactone positively regulates secondary growth (Agusti *et al.,* 2011). It could be possible that impaired vascular activity in strigolactone mutants affects xylem formation and thus xylem cytokinins. This hypothesis could be tested by sectioning roots of *rms1* and *rms2* and comparing their cambial regions for correlation with their respective xylem cytokinin content. The mutant *INTERFASCICULAR FIBER* mutant, *ifl1*, also displayed reduction of cambium activity (Zhong and Ye 2001). Measuring xylem cytokinins in this mutant would provide a strigolactone-independent control experiment.

Examination of cytokinin distribution in *rms1* and *rms2* aerial parts receiving altered content of root-derived cytokinins, implied that cytokinin homeostasis through biosynthesis, metabolism and/or degradation might require *RMS2*. To test this further, expression of cytokinin genes involved in the biosynthesis, metabolism and degradation of the hormone should be examined in *rms2* mutants. There are already two *PsIPT* and *PsCKX* genes published (Vaseva-Gemisheva *et al.,* 2005; Tanaka *et al.,* 2006) but according to the *Arabidopsis* respective gene families having at least 7 members each, more bioinformatic analysis is required especially now that pea transcriptome is available (http://www.biomedcentral.com/1471-2164/13/104). However cytokinin homeostasis may still occur in *rms2* aerial parts through cytokinin perception and/or response. Therefore genes involved in these processes should also be examined in *rms2*. Additionally, cytokinin quantification and examination of respective gene expression, mentioned above, should be examined in *rms1rms2* double mutant.

References

Adrian, A. *et al.,* 2012. The Path from β-Carotene to Carlactone, a Strigolactone-Like Plant Hormone.pdf. Science, 335, pp.1348–1351.

Aguilar-Martínez, J.A., Poza-Carrión, C. & Cubas, P., 2007. *Arabidopsis* BRANCHED1 acts as an integrator of branching signals within axillary buds. The Plant cell, 19(2), pp.458–72.

Agusti, J. *et al.,* 2011. Strigolactone signaling is required for auxin-dependent stimulation of secondary growth in plants. Proceedings of the National Academy of Sciences of the United States of America, 108(50), pp.20242–7.

Akiyama, K. & Hayashi, H., 2006. Strigolactones: chemical signals for fungal symbionts and parasitic weeds in plant roots. Annals of botany, 97(6), pp.925–31.

Aloni, R. *et al.,* 2004. Role of cytokinin in the regulation of root gravitropism. Planta, 220(1), pp.177–82.

Aloni, R. *et al.,* 2005. Root-synthesized cytokinin in *Arabidopsis* is distributed in the shoot by the transpiration stream. Journal of experimental botany, 56(416), pp.1535–44.

Aremu, A.O. *et al.,* 2012. Physiological responses and endogenous cytokinin profiles of tissue-cultured "Williams" bananas in relation to roscovitine and an inhibitor of cytokinin oxidase/dehydrogenase (INCYDE) treatments. Planta, 236(6), pp.1775–90.

Argueso, C.T., Ferreira, F.J. & Kieber, J.J., 2009. Environmental perception avenues: the interaction of cytokinin and environmental response pathways. Plant, cell & environment, 32(9), pp.1147–60.

Argyros, R.D. *et al.,* 2008. Type B response regulators of *Arabidopsis* play key roles in cytokinin signaling and plant development. The Plant cell, 20(8), pp.2102–16.

Arite, T. *et al.,* 2009. D14, a Strigolactone-Insensitive Mutant of Rice, Shows an Accelerated Outgrowth of Tillers. Plant & cell physiology, 50(8), pp.1416–24.

Arite, T. *et al.,* 2007. DWARF10, an RMS1/MAX4/DAD1 ortholog, controls lateral bud outgrowth in rice. The Plant journal : for cell and molecular biology, 51(6), pp.1019–29.

Ashikari, M. *et al.,* 2005. Cytokinin oxidase regulates rice grain production. Science (New York, N.Y.), 309(5735), pp.741–5.

Åstot, C. *et al.,* 2000. An alternative cytokinin biosynthesis pathway. PNAS, 97(26), pp.14778–14783.

Bae, E. *et al.,* 2008. Crystal structure of *Arabidopsis thaliana* cytokinin dehydrogenase. Proteins: Structure, Function, and Bioinformatics, 70(1), pp.303–306.

Bainbridge, K. *et al.,* 2005. Hormonally controlled expression of the *Arabidopsis* MAX4 shoot branching regulatory gene. The Plant journal : for cell and molecular biology, 44(4), pp.569–80.

Bangerth, F., 1994. Rapid communication Response of cytokinin concentration in the xylem exudate of bean (Phaseolus vulgaris L .) plants to decapitation and auxin treatment , and relationship to apical dominance. Planta, 194, pp.439–442.

Bennett, T. & Leyser, O., 2014. Strigolactone signalling: standing on the shoulders of DWARFs. Current opinion in plant biology, 22C, pp.7–13.

Beveridge, C.A., 2000. Long-distance signalling and a mutational analysis of branching in pea. Plant growth, 32, pp.193–203.

Beveridge, Christine Anne Symons, C.M. *et al.,* 1997.a. The rms1 Mutant of Pea Has Elevated Indole-3-Acetic Acid Levels and Reduced Root-Sap Zeatin Riboside Content but I ncreased B ranch i ng Controlled by Graft -TransmissibIe Signal (s). , 115, pp.1251–1258.

Beveridge, C.A. *et al.,* 1997.b. The shoot controls zeatin riboside export from pea roots. Evidence from the branching mutant rms4. The Plant Journal, 11(2), pp.339–345.

Beveridge, C.A., Ross, J.J. & Murfet, C., 1994. Branching Mutant rms-2 in *Pisum sativum '*. Palnt Physiology, pp.953–959.

Bielach, a. *et al.,* 2012. Spatiotemporal Regulation of Lateral Root Organogenesis in *Arabidopsis* by Cytokinin. The Plant Cell, 24(October), pp.1–15.

Bilyeu, K.D. *et al.,* 2001. Molecular and biochemical characterization of a cytokinin oxidase from maize. Plant physiology, 125(1), pp.378–86.

Birnbaum, K. *et al.,* 2003. A gene expression map of the *Arabidopsis* root. Science (New York, N.Y.), 302(5652), pp.1956–60.

Birnbaum, K. *et al.,* 2005. Cell type-specific expression profiling in plants via cell sorting of protoplasts from fluorescent reporter lines. Nature methods, 2(8), pp.615–9.

Bishopp, A., Help, H., *et al.,* 2011.a. A mutually inhibitory interaction between auxin and cytokinin specifies vascular pattern in roots. Current biology : CB, 21(11), pp.917–26.

Bishopp, A., Lehesranta, S., *et al.,* 2011.b. Phloem-transported cytokinin regulates polar auxin transport and maintains vascular pattern in the root meristem. Current biology : CB, 21(11), pp.927–32.

Blagoeva, E. *et al.,* 2003. Cyclin-dependent kinase inhibitor, roscovitine, in combination with exogenous cytokinin, N6-benzyladenine, causes increase of cis-cytokinins in immobilized tobacco cells. Biotechnology letters, 25(6), pp.469–72

Booker, J. *et al.,* 2005. MAX1 encodes a cytochrome P450 family member that acts downstream of MAX3/4 to produce a carotenoid-derived branch-inhibiting hormone. Developmental cell, 8(3), pp.443–9.

Booker, J. *et al.,* 2004. MAX3 / CCD7 Is a Carotenoid Cleavage Dioxygenase Required for the Synthesis of a Novel Plant Signaling Molecule. , 14, pp.1232–1238.

Brady, S.M. *et al.,* 2007. A high-resolution root spatiotemporal map reveals dominant expression patterns. Science (New York, N.Y.), 318(5851), pp.801–6.

Braun, N. *et al.,* 2012. The pea TCP transcription factor PsBRC1 acts downstream of Strigolactones to control shoot branching. Plant physiology, 158(1), pp.225–38. A

Brewer, P.B. *et al.,* 2009. Strigolactone acts downstream of auxin to regulate bud outgrowth in pea and *Arabidopsis*. Plant physiology, 150(1), pp.482–93.

Brunoud, G. *et al.,* 2012. A novel sensor to map auxin response and distribution at high spatio-temporal resolution. Nature, 482(7383), pp.103–6.

Brzobohatý, B. *et al.,* 1993. Release of active cytokinin by a beta-glucosidase localized to the maize root meristem. Science (New York, N.Y.), 262(5136), pp.1051–4.

Bürkle, L. *et al.,* 2003. Transport of cytokinins mediated by purine transporters of the PUP family expressed in phloem, hydathodes, and pollen of *Arabidopsis*. The Plant journal : for cell and molecular biology, 34(1), pp.13–26.

Caesar, K. *et al.,* 2011. Evidence for the localization of the *Arabidopsis* cytokinin receptors AHK3 and AHK4 in the endoplasmic reticulum. Journal of experimental botany, 62(15), pp.5571–80.

Cambridge, A. & Morris, D., 1996. Transfer of exogenous auxin from the phloem to the polar auxin transport pathway in pea (*Pisum sativum* L.). Planta, 199(4), pp.583–588.

Castiglione, M.R., 1998. Immunogold localization of trans-zeatin riboside in embryo and endosperm during early fruit drop of Malus domestica. Biologia Plantarum, 41(4), pp.523–532.

Cedzich, A. *et al.,* 2008. Characterization of cytokinin and adenine transport in *Arabidopsis* cell cultures. Plant physiology, 148(4), pp.1857–67.

Chatfield, S.P. *et al.,* 2000. The hormonal regulation of axillary bud growth in *Arabidopsis*. The Plant journal : for cell and molecular biology, 24(2), pp.159–69.

Collier, M.D. *et al.,* 2003. Regulation of nitrogen uptake by Fagus sylvatica on a whole plant level – interactions between cytokinins and soluble. , 1560, pp.1549–1560.

Corbesier, L. *et al.,* 2003. Cytokinin levels in leaves, leaf exudate and shoot apical meristem of *Arabidopsis thaliana* during floral transition. Journal of experimental botany, 54(392), pp.2511–7.

Coutinho, P.M. *et al.,* 2003. An Evolving Hierarchical Family Classification for Glycosyltransferases. Journal of Molecular Biology, 2836(03), pp.307–317.

Cutcliffe, J.W. *et al.,* 2011. CRFs form protein-protein interactions with each other and with members of the cytokinin signalling pathway in *Arabidopsis* via the CRF domain. Journal of experimental botany, 62(14), pp.4995–5002.

D'Agostino, I.B., Deruère, J. & Kieber, J.J., 2000. Characterization of the response of the *Arabidopsis* response regulator gene family to cytokinin. Plant physiology, 124(4), pp.1706–17.

Dalmais, M. *et al.,* 2008. UTILLdb, a *Pisum sativum* in silico forward and reverse genetics tool. Genome biology, 9(2), p.R43.

Dannel, F., Pfeffer, H. & Marschner, H., 1995. Isolation of Apoplasmic Fluid from Sunflower Leaves and its Use for Studies on Influence of Nitrogen Supply on Apoplasmic pH. Journal of Plant Physiology, 146(3), pp.273–278.

Dinneny, J.R. *et al.,* 2008. Cell identity mediates the response of *Arabidopsis* roots to abiotic stress. Science (New York, N.Y.), 320(5878), pp.942–5.

Dobra, J. *et al.,* 2010. Comparison of hormonal responses to heat, drought and combined stress in tobacco plants with elevated proline content. Journal of plant physiology, 167(16), pp.1360–70.

Dobrev, P.I. & Kamínek, M., 2002. Fast and efficient separation of cytokinins from auxin and abscisic acid and their purification using mixed-mode solid-phase extraction . Journal of chromatography. A, 950(1-2), pp.21–9.

Dodd, I.C. & Beveridge, C. a, 2006. Xylem-borne cytokinins: still in search of a role? Journal of experimental botany, 57(1), pp.1–4.

Dodd, Ian C. *et al.,* 2004. Effects of nitrogen supply on xylem cytokinin delivery , transpiration and leaf expansion of pea genotypes differing in xylem-cytokinin concentration. Functional Plant Biology, 31, pp.903–911.

Dolan, L. *et al.,* 1993. Cellular organisation of the *Arabidopsis thaliana* root. Development (Cambridge, England), 119(1), pp.71–84.

Drummond, R.S.M. *et al.,* 2009. *Petunia hybrida* CAROTENOID CLEAVAGE DIOXYGENASE7 is involved in the production of negative and positive branching signals in petunia. Plant physiology, 151(4), pp.1867–77.

Dun, E. a *et al.,* 2012. Antagonistic action of strigolactone and cytokinin in bud outgrowth control. Plant physiology, 158(1), pp.487–98.

Emery, J.R.N. *et al.,* 1998. cis-Isomers of Cytokinins Predominate in Chickpea Seeds throughout Their Development 1. Plant physiology, 117, pp.1515–1523.

Faiss, M. *et al.,* 1997. Conditional transgenic expression of the ipt gene indicates a function for cytokinins in paracrine signaling in whole tobacco plants.pdf. The Plant Journal, 12(2), pp.401–415.

Ferreira, F.J. & Kieber, J.J., 2005. Cytokinin signaling. Current opinion in plant biology, 8(5), pp.518–25.

Foo, E. *et al.,* 2007. Feedback regulation of xylem cytokinin content is conserved in pea and *Arabidopsis*. Plant physiology, 143(3), pp.1418–28.

Foo, E. *et al.,* 2005. The Branching Gene RAMOSUS1 Mediates Interactions among Two Novel Signals and Auxin in Pea. , 17(February), pp.464–474.

Foo, E., Turnbull, C.G. & Beveridge, C. a, 2001. Long-distance signaling and the control of branching in the rms1 mutant of pea. Plant physiology, 126(1), pp.203–9.

Franco-Zorrilla, J.M. *et al.,* 2002. Mutations at CRE1 impair cytokinin-induced repression of phosphate starvation responses in *Arabidopsis*. The Plant journal : for cell and molecular biology, 32(3), pp.353–60.

Frébort, I. *et al.,* 2011. Evolution of cytokinin biosynthesis and degradation. Journal of experimental botany, 62(8), pp.2431–52.

Frébortová, J. *et al.,* 2004. Catalytic reaction of cytokinin dehydrogenase: preference for quinones as electron acceptors. The Biochemical journal, 380(Pt 1), pp.121–30.

Gajdosová, S. *et al.,* 2011. Distribution, biological activities, metabolism, and the conceivable function of cis-zeatin-type cytokinins in plants. Journal of experimental botany, 62(8), pp.2827–40.

Galuszka, P. *et al.,* 2007. Biochemical Characterization of Cytokinin Oxidases/Dehydrogenases from *Arabidopsis thaliana* Expressed in Nicotiana tabacum L. Journal of Plant Growth Regulation, 26(3), pp.255–267.

Galuszka, P. *et al.,* 2001. Cytokinin oxidase or dehydrogenase? Mechanism of cytokinin degradation in cereals. European journal of biochemistry / FEBS, 268(2), pp.450–61.

Galuszka, P. *et al.,* 2000. Degradation of cytokinins by cytokinin oxidases in plants. , pp.315–327.

Gaudinová, A. *et al.,* 2005. The Involvement of Cytokinin Oxidase/Dehydrogenase and Zeatin Reductase in Regulation of Cytokinin Levels in Pea (*Pisum sativum* L.) Leaves. Journal of Plant Growth Regulation, 24(3), pp.188–200.

Ghanem, M.E. *et al.,* 2011. Root-targeted biotechnology to mediate hormonal signalling and improve crop stress tolerance. Plant cell reports, 30(5), pp.807–23.

Gillissen, B. *et al.,* 2000. A new family of high-affinity transporters for adenine, cytosine, and purine derivatives in *Arabidopsis*. The Plant cell, 12(2), pp.291–300.

Gilroy, S., Hughes, W. a & Trewavas, a J., 1989. A Comparison between Quin-2 and Aequorin as Indicators of Cytoplasmic Calcium Levels in Higher Plant Cell Protoplasts. Plant physiology, 90(2), pp.482–91.

Golovko, A. *et al.,* 2002. Identification of a tRNA isopentenyltransferase gene from *Arabidopsis thaliana*. , pp.161–169.

Gomez-Roldan, V. *et al.,* 2008. Strigolactone inhibition of shoot branching. Nature, 455(7210), pp.189–94.

Gu, R. *et al.,* 2010. Comparative Expression and Phylogenetic Analysis of Maize Cytokinin Dehydrogenase/Oxidase (CKX) Gene Family. Journal of Plant Growth Regulation, 29(4), pp.428–440.

Guan, J.C. *et al.,* 2012. Diverse roles of strigolactone signaling in maize architecture and the uncoupling of a branching-specific subnetwork. Plant physiology, 160(3), pp.1303–17.

Guo, Y. *et al.,* 2013. Smoke-derived karrikin perception by the α/β-hydrolase KAI2 from *Arabidopsis*. Proceedings of the National Academy of Sciences of the United States of America, 110(20), pp.8284–9. A

Ha, S. *et al.,* 2012. Cytokinins: metabolism and function in plant adaptation to environmental stresses. Trends in plant science, 17(3), pp.172–9.

Hamiaux, C. *et al.,* 2012. DAD2 Is an α/β Hydrolase likely to Be Involved in the Perception of the Plant Branching Hormone, Strigolactone. Current Biology, pp.1–5.

Hartung, W., Sauter, A. & Hose, E., 2002. Abscisic acid in the xylem : where does it come from , where does it go to ? , 53(366), pp.27–32.

Havlová, M. *et al.,* 2008. The role of cytokinins in responses to water deficit in tobacco plants over-expressing trans-zeatin O-glucosyltransferase gene under 35S or SAG12 promoters. Plant, cell & environment, 31(3), pp.341–53.

Hecht, S. *et al.,* 2001. Studies on the nonmevalonate pathway to terpenes : The role of the GcpE (IspG) protein. , 98(26), pp.14837–14842.

Heyl, A. *et al.,* 2008. The transcriptional repressor ARR1-SRDX suppresses pleiotropic cytokinin activities in *Arabidopsis*. Plant physiology, 147(3), pp.1380–95.

Heyl, A. & Schmülling, T., 2003. Cytokinin signal perception and transduction. Current Opinion in Plant Biology, 6(5), pp.480–488.

Higuchi, M. *et al.,* 2004. In planta functions of the *Arabidopsis* cytokinin receptor family. PNAS, 101(23), pp.8821–8826.

Hirose, N. *et al.,* 2005. Functional Characterization and Expression Analysis of a Gene , OsENT2 , Encoding an Equilibrative Nucleoside Transporter in Rice Suggest a Function in Cytokinin Transport 1. Plant Physiology, 138(May), pp.196–206.

Hirose, N. *et al.,* 2008. Regulation of cytokinin biosynthesis, compartmentalization and translocation. Journal of experimental botany, 59(1), pp.75–83.

Hooley, R., Beale, M.H. & Smith, S.J., 1991. Gibberellin perception at the plasma membrane of. Planta, 183, pp.274–280.

Hou, B. *et al.,* 2004. N-glucosylation of cytokinins by glycosyltransferases of *Arabidopsis thaliana*. The Journal of biological chemistry, 279(46), pp.47822–32.

Huynh, L.N. *et al.,* 2005. Regulation of flooding tolerance of SAG12:ipt *Arabidopsis* plants by cytokinin. Journal of experimental botany, 56(415), pp.1397–407.

Hwang, I. & Sakakibara, H., 2006. Cytokinin biosynthesis and perception. Physiologia Plantarum, 126(4), pp.528–538.

Hwang, I. & Sheen, J., 2001. Two-component circuitry in *Arabidopsis* cytokinin signal transduction. Nature, 413(6854), pp.383–9.

Hwang, I., Sheen, J. & Müller, B., 2012. Cytokinin signaling networks. Annual review of plant biology, 63, pp.353–80.

Imamura, a *et al.,* 1999. Compilation and characterization of *Arabidopsis thaliana* response regulators implicated in His-Asp phosphorelay signal transduction. Plant & cell physiology, 40(7), pp.733–42.

Imamura, A., Takeshi, Y. & Mizuno, Y., 2001. Cellular localization of the signalling components of *Arabidopsis* His-to-Asp Phosphorely. Bioscience, Biotechnology, and Biochemistry, 65(9), pp.2113–2117.

Inoue, T. *et al.,* 2001. Identi ® cation of CRE1 as a cytokinin receptor from *Arabidopsis*. Nature, 409(February), pp.48–51.

Dello Ioio, R. *et al.,* 2008. A genetic framework for the control of cell division and differentiation in the root meristem. Science (New York, N.Y.), 322(5906), pp.1380–4.

Dello Ioio, R. *et al.,* 2007. Cytokinins determine *Arabidopsis* root-meristem size by controlling cell differentiation. Current biology : CB, 17(8), pp.678–82.

Ishida, K. *et al.,* 2008. Three type-B response regulators, ARR1, ARR10 and ARR12, play essential but redundant roles in cytokinin signal transduction throughout the life cycle of *Arabidopsis thaliana*. Plant & cell physiology, 49(1), pp.47–57.

Ishikawa, S. *et al.,* 2005. Suppression of tiller bud activity in tillering dwarf mutants of rice. Plant & cell physiology, 46(1), pp.79–86.

Jin, S.-H. *et al.,* 2013. Overexpression of glucosyltransferase UGT85A1 influences trans-zeatin homeostasis and trans-zeatin responses likely through O-glucosylation. Planta, 237(4), pp.991–9.

Johnson, X. *et al.,* 2006. Branching genes are conserved across species. Genes controlling a novel signal in pea are coregulated by other long-distance signals. Plant physiology, 142(3), pp.1014–26.

Kagiyama, M. *et al.,* 2013. Structures of D14 and D14L in the strigolactone and karrikin signaling pathways. Genes to cells : devoted to molecular & cellular mechanisms, 18(2), pp.147–60.

Kakimoto, T., 2001. Identification of plant cytokinin biosynthetic enzymes as dimethylallyl diphosphate:ATP/ADP isopentenyltransferases. Plant & cell physiology, 42(7), pp.677–85.

Kakimoto, T., 2003. Perception and signal transduction of cytokinins. Annual review of plant biology, 54, pp.605–27.

Kapulnik, Y. *et al.,* 2011. Strigolactones affect lateral root formation and root-hair elongation in *Arabidopsis*. Planta, 233(1), pp.209–16.

Kasahara, H. *et al.,* 2004. Distinct isoprenoid origins of cis- and trans-zeatin biosyntheses in *Arabidopsis*. The Journal of biological chemistry, 279(14), pp.14049–54.

Kiba, T. *et al.,* 2004. *Arabidopsis* response regulator, ARR22, ectopic expression of which results in phenotypes similar to the wol cytokinin-receptor mutant. Plant & cell physiology, 45(8), pp.1063–77.

Kiba, T. *et al.,* 1999. Differential expression of genes for response regulators in response to cytokinins and nitrate in *Arabidopsis thaliana*. Plant & cell physiology, 40(7), pp.767–71.

Kiba, T. *et al.,* 2013. Side-chain modification of cytokinins controls shoot growth in *Arabidopsis*. Developmental cell, 27(4), pp.452–61.

Kiba, T. *et al.,* 2003. The Type-A Response Regulator , ARR15 , Acts as a Negative Regulator in the Cytokinin-Mediated Signal Transduction in *Arabidopsis thaliana*. , 44(8), pp.868–874.

Kiba, T., Yamada, H. & Mizuno, T., 2002. Characterization of the ARR15 and ARR16 response regulators with special reference to the cytokinin signaling pathway mediated by the AHK4 histidine kinase in roots of *Arabidopsis thaliana*. Plant & cell physiology, 43(9), pp.1059–66.

Kieber, J.J. & Schaller, G.E., 2014. Cytokinins. The *Arabidopsis* book / American Society of Plant Biologists, 12, p.e0168.

Kim, H.J. *et al.,* 2006. Cytokinin-mediated control of leaf longevity by AHK3 through phosphorylation of ARR2 in *Arabidopsis*. Proceedings of the National Academy of Sciences of the United States of America, 103(3), pp.814–9.

Ko, D. *et al.,* 2014. *Arabidopsis* ABCG14 is essential for the root-to-shoot translocation of cytokinin. Proceedings of the National Academy of Sciences of the United States of America, 111(19), pp.7150–5.

Kojima, M. *et al.,* 2009. Highly sensitive and high-throughput analysis of plant hormones using MS-probe modification and liquid chromatography-tandem mass spectrometry: an application for hormone profiling in Oryza sativa. Plant & cell physiology, 50(7), pp.1201–14.

Köllmer, I. *et al.,* 2014b. Overexpression of the cytosolic cytokinin oxidase/dehydrogenase (CKX7) from *Arabidopsis* causes specific changes in root growth and xylem differentiation. The Plant journal : for cell and molecular biology, pp.1–13.

Koltai, H., 2011. Strigolactones are regulators of root development. New Phytologist, 190(3), pp.545–549.

Kopecný, D. *et al.,* 2010. Phenyl- and benzylurea cytokinins as competitive inhibitors of cytokinin oxidase/dehydrogenase: a structural study. Biochimie, 92(8), pp.1052–62.

Kowalska, M. *et al.,* 2010. Vacuolar and cytosolic cytokinin dehydrogenases of *Arabidopsis thaliana*: heterologous expression, purification and properties. Phytochemistry, 71(17-18), pp.1970–8.

Krall, L. *et al.,* 2002. The Tzs protein from Agrobacterium tumefaciens C58 produces zeatin riboside 5 P -phosphate from 4-hydroxy-3-methyl-2- (E) -butenyl diphosphate and AMP. , 527, pp.315–318.

Kretzschmar, T. *et al.,* 2012. A petunia ABC protein controls strigolactone-dependent symbiotic signalling and branching. Nature, 483(7389), pp.341–4.

Kuderová, A. *et al.,* 2008. Effects of conditional IPT-dependent cytokinin overproduction on root architecture of *Arabidopsis* seedlings. Plant & cell physiology, 49(4), pp.570–82.

Kudo, T. *et al.,* 2012. Cytokinin Activity of cis-Zeatin and Phenotypic Alterations Induced by Overexpression of Putative cis-Zeatin-O-glucosyltransferase in Rice. Plant physiology, 160(1), pp.319–31.

Kudo, T., Kiba, T. & Sakakibara, H., 2010. Metabolism and long-distance translocation of cytokinins. Journal of integrative plant biology, 52(1), pp.53–60.

Kurakawa, T. *et al.,* 2007. Direct control of shoot meristem activity by a cytokinin-activating enzyme. Nature, 445(7128), pp.652–5.

Kuroha, T., 2002. A trans-zeatin riboside in root xylem sap negatively regulates adventitious root formation on cucumber hypocotyls. Journal of Experimental Botany, 53(378), pp.2193–2200.

Kuroha, T. *et al.,* 2009. Functional analyses of LONELY GUY cytokinin-activating enzymes reveal the importance of the direct activation pathway in *Arabidopsis*. The Plant cell, 21(10), pp.3152–69.

Laplaze, L. *et al.,* 2007. Cytokinins act directly on lateral root founder cells to inhibit root initiation. The Plant cell, 19(12), pp.3889–900.

Laskey, J.G. *et al.,* 2003. Rate enhancement of cytokinin oxidase / dehydrogenase using 2 , 6-dichloroindophenol as an electron acceptor. , pp.189–196.

Li, G. *et al.,* 2003. Equilibrative nucleoside transporters of *Arabidopsis thaliana*. cDNA cloning, expression pattern, and analysis of transport activities. The Journal of biological chemistry, 278(37), pp.35732–42.

Li, J. *et al.,* 2005. *Arabidopsis* H+-PPase AVP1 regulates auxin-mediated organ development. Science (New York, N.Y.), 310(5745), pp.121–5.

Li, X. *et al.,* 2008. A distinct endosomal Ca2+/Mn2+ pump affects root growth through the secretory process. Plant physiology, 147(4), pp.1675–89.

Lin, H. *et al.,* 2009. DWARF27, an iron-containing protein required for the biosynthesis of strigolactones, regulates rice tiller bud outgrowth. The Plant cell, 21(5), pp.1512–25.

Lindner, A.-C. *et al.,* 2014. Isopentenyltransferase-1 (IPT1) knockout in Physcomitrella together with phylogenetic analyses of IPTs provide insights into evolution of plant cytokinin biosynthesis. Journal of experimental botany, 65(9), pp.2533–43.

Liu, Z., Yuan, B.-F. & Feng, Y.-Q., 2012. Tandem solid phase extraction followed by online trapping-hydrophilic interaction chromatography-tandem mass spectrometry for sensitive detection of endogenous cytokinins in plant tissues. Phytochemical analysis : PCA, 23(6), pp.559–68.

Lohaus, G. *et al.,* 2001. Is the infiltration-centrifugation technique appropriate for the isolation of apoplastic fluid? A critical evaluation with different plant species. Physiologia plantarum, 111(4), pp.457–465.

Lomin, S.N. *et al.,* 2012. Receptor properties and features of cytokinin signaling. Acta naturae, 4(3), pp.31–45.

López-Millán, a F. *et al.,* 2001. Iron deficiency-associated changes in the composition of the leaf apoplastic fluid from field-grown pear (Pyrus communis L.) trees. Journal of experimental botany, 52(360), pp.1489–98.

Mader, J.C., Turnbull, C.G.N. & Emery, R.J.N., 2003. Transport and metabolism of xylem cytokinins during lateral bud release in decapitated chickpea (Cicer arietinum) seedlings. Physiologia Plantarum, 117(1), pp.118–129.

Mähönen, A.P. *et al.,* 2000.a. A novel two-component hybrid molecule regulates vascular morphogenesis of the *Arabidopsis* root. Genes & Development, 14(23), pp.2938–2943.

Mähönen, A.P., Bishopp, A., *et al.,* 2006.a. Cytokinin signaling and its inhibitor AHP6 regulate cell fate during vascular development. Science (New York, N.Y.), 311(5757), pp.94–8. Available at: http://www.ncbi.nlm.nih.gov/pubmed/16400151 [Accessed July 16, 2012].

Mähönen, A.P., Higuchi, M., *et al.,* 2006.b. Cytokinins regulate a bidirectional phosphorelay network in *Arabidopsis*. Current biology : CB, 16(11), pp.1116–22. Available at: http://www.ncbi.nlm.nih.gov/pubmed/16753566 [Accessed September 5, 2014].

Marentes, E. & Grusak, M. a., 1998. Mass determination of low-molecular-weight proteins in phloem sap using matrix-assisted laser desorption/ ionization time-of-flight mass spectrometry. Journal of Experimental Botany, 49(322), pp.903–911.

Martin, R.C. *et al.,* 2001.a. A maize cytokinin gene encoding an O-glucosyltransferase specific to cis-zeatin. Proceedings of the National Academy of Sciences of the United States of America, 98(10), pp.5922–6.

Martin, R.C. *et al.,* 2001.b. DEVELOPMENT OF TRANSGENIC TOBACCO HARBORING A ZEATIN O -GLUCOSYLTRANSFERASE GENE FROM PHASEOLUS. In vitro cell developmental biology-Plant, 37(June), pp.354–360.

Martin, R.C., Mok, M.C. & Mok, D.W., 1999. Isolation of a cytokinin gene, ZOG1, encoding zeatin O-glucosyltransferase from Phaseolus lunatus. Proceedings of the National Academy of Sciences of the United States of America, 96(1), pp.284–9.

Mashiguchi, K. *et al.,* 2009. Feedback-Regulation of Strigolactone Biosynthetic Genes and Strigolactone-Regulated Genes in *Arabidopsis*. Bioscience, Biotechnology, and Biochemistry, 73(11), pp.2460–2465.

Mason, M.G. *et al.,* 2005. Multiple Type-B Response Regulators Mediate Cytokinin Signal Transduction in *Arabidopsis*. , 17(November), pp.3007–3018.

Mason, M.G. *et al.,* 2004. Type-B Response Regulators Display Overlapping Expression Patterns in *Arabidopsis* 1. , 135(June), pp.927–937.

Matsumoto-Kitano, M. *et al.,* 2008. Cytokinins are central regulators of cambial activity. Proceedings of the National Academy of Sciences of the United States of America, 105(50), pp.20027–31.

Mayzlish Gati, E. *et al.,* 2012. Strigolactones Are Involved in Root Response to Low Phosphate Conditions in *Arabidopsis*.,

Medford, J. *et al.,* 1989. Alterations of Endogenous Cytokinins in Transgenic Plants Using a Chimeric lsopentenyl Transferase Gene. , 1,pp. 403-413.

Minakuchi, K. *et al.,* 2010. FINE CULM1 (FC1) works downstream of strigolactones to inhibit the outgrowth of axillary buds in rice. Plant & cell physiology, 51(7), pp.1127–35.

Miyawaki, K. *et al.,* 2006. Roles of *Arabidopsis* ATP/ADP isopentenyltransferases and tRNA isopentenyltransferases in cytokinin biosynthesis. Proceedings of the National Academy of Sciences of the United States of America, 103(44), pp.16598–603.

Miyawaki, K., Matsumoto-Kitano, M. & Kakimoto, T., 2004. Expression of cytokinin biosynthetic isopentenyltransferase genes in *Arabidopsis* : tissue specificity and regulation by auxin, cytokinin, and nitrate. The Plant Journal, 37(1), pp.128–138.

Möhlmann, T. *et al.,* 2001. Characterisation of a concentrative type of adenosine transporter from *Arabidopsis thaliana* (ENT1,At). FEBS letters, 509(3), pp.370–4.

Mok, M.C. *et al.,* 2005. Topolins and Hydroxylated Thidiazuron Derivatives Are Substrates of Cytokinin O-Glucosyltransferase with Position Specificity Related to. Plant physiology, 137(March), pp.1057–1066.

Moreira, S. *et al.,* 2013. AHP6 inhibits cytokinin signaling to regulate the orientation of pericycle cell division during lateral root initiation. PloS one, 8(2), p.e56370.

Morris, S.E. *et al.,* 2001. Mutational analysis of branching in pea. Evidence that Rms1 and Rms5 regulate the same novel signal. Plant physiology, 126(3), pp.1205–13.

Motyka, V. *et al.,* 1994. Changes in Cytokinin Content and Cytokinin Oxidase Activity in Response to Derepression of ipt Cene Transcription in Transgenic Tobacco Calli and Plants , (1 996), pp.1035–1043.

Müller, B. & Sheen, J., 2008. Cytokinin and auxin interplay in root stem-cell specification during early embryogenesis. Nature, 453(7198), pp.1094–1097.

Müller, D. & Leyser, O., 2011. Auxin, cytokinin and the control of shoot branching. Annals of botany, 107(7), pp.1203–12.

Müller, M. & Munné-Bosch, S., 2011. Rapid and sensitive hormonal profiling of complex plant samples by liquid chromatography coupled to electrospray ionization tandem mass spectrometry. Plant methods, 7:37.

Napoli, C., *et al.,* 1996. Highly Branched Phenotype of the Petunia dad1-1 Mutant Is Reversed by Grafting. Plant physiology, 111(1), pp.27–37.

Nelson, D.C. *et al.,* 2011. F-box protein MAX2 has dual roles in karrikin and strigolactone signaling in *Arabidopsis thaliana*. Proceedings of the National Academy of Sciences of the United States of America, 108(21), pp.8897–902.

Nishimura, C. *et al.,* 2004. Histidine Kinase Homologs That Act as Cytokinin Receptors Possess Overlapping Functions in the Regulation of Shoot and Root Growth in *Arabidopsis*. The Plant cell, 16, pp.1365–1377.

Nishiyama, R. *et al.,* 2012. Transcriptome analyses of a salt-tolerant cytokinin-deficient mutant reveal differential regulation of salt stress response by cytokinin deficiency. PloS one, 7(2), p.e32124.

Nongpiur, R. *et al.,* 2012. Cross talk between hormone and stress responses Histidine kinases in plants. Plant Signaling & Behavior, 7(10), pp.1230–1237.

Nordström, A. *et al.,* 2004. Auxin regulation of cytokinin biosynthesis in *Arabidopsis thaliana*: a factor of potential importance for auxin-cytokinin-regulated development. Proceedings of the National Academy of Sciences of the United States of America, 101(21), pp.8039–44.

Novák, O. *et al.,* 2008. Cytokinin profiling in plant tissues using ultra-performance liquid chromatography-electrospray tandem mass spectrometry. Phytochemistry, 69(11), pp.2214–24.

Novák, O. *et al.,* 2003. Quantitative analysis of cytokinins in plants by liquid chromatography–single-quadrupole mass spectrometry. Analytica Chimica Acta, 480(2), pp.207–218.

Ongaro, V. & Leyser, O., 2008. Hormonal control of shoot branching. Journal of experimental botany, 59(1), pp.67–74.

Pencík, A. *et al.,* 2013. Regulation of auxin homeostasis and gradients in *Arabidopsis* roots through the formation of the indole-3-acetic acid catabolite 2-oxindole-3-acetic acid. The Plant cell, 25(10), pp.3858–70.

Pertry, I. *et al.,* 2009. Identification of Rhodococcus fascians cytokinins and their modus operandi to reshape the plant. Proceedings of the National Academy of Sciences of the United States of America, 106(3), pp.929–34.

Petersson, S. V *et al.,* 2009. An auxin gradient and maximum in the *Arabidopsis* root apex shown by high-resolution cell-specific analysis of IAA distribution and synthesis. The Plant cell, 21(6), pp.1659–68.

Petricka, J.J. *et al.,* 2012. The protein expression landscape of the *Arabidopsis* root. Proceedings of the National Academy of Sciences of the United States of America, 109(18), pp.6811–8.

Pineda Rodo, A. *et al.,* 2008. Over-expression of a zeatin O-glucosylation gene in maize leads to growth retardation and tasselseed formation. Journal of experimental botany, 59(10), pp.2673–86.

Punwani, J.A. & Kieber, J.J., 2010. Localization of the *Arabidopsis* histidine phosphotransfer proteins is independent of cytokinin. Plant Signaling & Behavior, 5(7), pp.896–898.

Quesnelle, P.E. & Emery, R.J.N., 2007. cis -Cytokinins that predominate in *Pisum sativum* during early embryogenesis will accelerate embryo growth in vitro. Canadian Journal of Botany, 85, pp.9–103.

Rahayu, Y.S. *et al.,* 2005. Root-derived cytokinins as long-distance signals for NO3-induced stimulation of leaf growth. Journal of experimental botany, 56(414), pp.1143–1152.

Rani, K. *et al.,* 2008. Biosynthetic considerations could assist the structure elucidation of host plant produced rhizosphere signalling compounds (strigolactones) for arbuscular mycorrhizal fungi and parasitic plants. Plant physiology and biochemistry : PPB / Société française de physiologie végétale, 46(7), pp.617–26.

Rappsilber, J., *et al.,* 2003 Stop and Go Extraction Tips for matrix-assisted laser desorption/ionization, nanoelectrospray, and LC/MS sample pretreatment in proteomics. Anal Chem. 75: 663–670.

Rashotte, A.M. *et al.,* 2006. A subset of *Arabidopsis* AP2 transcription factors mediates cytokinin responses in concert with a two-component pathway. Proceedings of the National Academy of Sciences of the United States of America, 103(29), pp.11081–5.

Rashotte, A.M. & Goertzen, L.R., 2010. The CRF domain defines cytokinin response factor proteins in plants. BMC plant biology, 10, p.74.

Rasmussen, A. *et al.,* 2013. Strigolactones fine-tune the root system. Planta, 238(4), pp.615–26.

Rasmussen, A. *et al.,* 2012. Strigolactones suppress adventitious rooting in *Arabidopsis* and pea. Plant physiology, 158(4), pp.1976–87.

Reid, J.B. & Ross, J.J., 2011. Mendel's genes: toward a full molecular characterization. Genetics, 189(1), pp.3–10.

van Rhijn, J.. *et al.,* 2001. Quantitative determination of glycosylated and aglycon isoprenoid cytokinins at sub-picomolar levels by microcolumn liquid chromatography combined with electrospray tandem mass spectrometry. Journal of Chromatography A, 929(1-2), pp.31–42.

Riefler, M. *et al.,* 2006. *Arabidopsis* Cytokinin Receptor Mutants Reveal Functions in Shoot Growth , Leaf Senescence , Seed Size , Germination , Root Development , and Cytokinin Metabolism. , 18, pp.40–54.

Rijavec, T. *et al.,* 2011. Spatial and temporal profiles of cytokinin biosynthesis and accumulation in developing caryopses of maize. Annals of botany, 107(7), pp.1235–45.

Rivero, R.M. *et al.,* 2010. Enhanced cytokinin synthesis in tobacco plants expressing PSARK:IPT prevents the degradation of photosynthetic protein complexes during drought. Plant & cell physiology, 51(11), pp.1929–41.

Rohmer, M. *et al.,* 1999. The discovery of a mevalonate-independent pathway for isoprenoid biosynthesis in bacteria , algae and higher plants . , pp.565–574.

Romanov, G. a *et al.,* 2005. A live cell hormone-binding assay on transgenic bacteria expressing a eukaryotic receptor protein. Analytical biochemistry, 347(1), pp.129–34

Romanov, G. a, Kieber, J.J. & Schmülling, T., 2002. A rapid cytokinin response assay in *Arabidopsis* indicates a role for phospholipase D in cytokinin signalling. FEBS letters, 515(1-3), pp.39–43.

Romanov, G. a, Lomin, S.N. & Schmülling, T., 2006. Biochemical characteristics and ligand-binding properties of *Arabidopsis* cytokinin receptor AHK3 compared to CRE1/AHK4 as revealed by a direct binding assay. Journal of experimental botany, 57(15), pp.4051–8.

Ruyter-Spira, C. *et al.,* 2011. Physiological effects of the synthetic strigolactone analog GR24 on root system architecture in *Arabidopsis*: another belowground role for strigolactones? Plant physiology, 155(2), pp.721–34.

de Saint Germain, A. *et al.,* 2013. Novel insights into strigolactone distribution and signalling. Current opinion in plant biology, 16(5), pp.583–9.

Sakai, H. *et al.,* 2001. ARR1, a transcription factor for genes immediately responsive to cytokinins. Science (New York, N.Y.), 294(5546), pp.1519–21.

Sakakibara, H. *et al.,* 2005. Agrobacterium tumefaciens increases cytokinin production in plastids by modifying the biosynthetic pathway in the host plant. Proceedings of the National Academy of Sciences of the United States of America, 102(28), pp.9972–7.

Sakakibara, H., 2006. Cytokinins: activity, biosynthesis, and translocation. Annual review of plant biology, 57, pp.431–49.

Sakamoto, T. *et al.,* 2006. Ectopic expression of KNOTTED1-like homeobox protein induces expression of cytokinin biosynthesis genes in rice. Plant physiology, 142(1), pp.54–62.

Samuelson, M.E., Eliasson, L. & Larsson, C.M., 1992. Nitrate-regulated growth and cytokinin responses in seminal roots of barley. Plant physiology, 98(1), pp.309–15.

Santner, A. & Estelle, M., 2009. Recent advances and emerging trends in plant hormone signalling. Nature, 459(7250), pp.1071–8.

Sasaki, T. *et al.,* 2014. Shoot-derived cytokinins systemically regulate root nodulation. Nature Communications, 5, p.4983.

Schmitz, R.Y. *et al.,* 1972. Cytokinins: Synthesis and Biological Activity of Geometric and Position Isomers of Zeatin. Plant Physiology, 50(6), pp.702–705.

Schmitz, R.Y. & Skoog, F., 1972. Cytokinins: synthesis and biological activity of geometric and position isomers of zeatin. Plant physiology, 50(6), pp.702–5.

Schwartzenberg, K. von *et al.,* 2007. Cytokinins in the bryophyte Physcomitrella patens: analyses of activity, distribution, and cytokinin oxidase/dehydrogenase overexpression reveal the role of extracellular cytokinins. Plant physiology, 145(3), pp.786–800.

Seto Yoshiya, Kameoka Hiromu, Yamaguchi Shinjiro, K.J., 2012. Recent advances in strigolactone research: chemical and biological aspects. Plant and Cell Physiology, 53(11), pp.1843–53.

Sheen, J., 2013. The cytokinin side chain commands shooting. Developmental cell, 27(4), pp.371–2.

Shimizu-sato, S. & Mori, H., 2001. Control of Outgrowth and Dormancy in Axillary Buds 1. , 127, pp.1405–1413.

Simons, J.L. *et al.,* 2007. Analysis of the DECREASED APICAL DOMINANCE genes of petunia in the control of axillary branching. Plant physiology, 143(2), pp.697–706.

Skoog, F. *et al.,* 1966. Cytokinin Activity : Localization in Transfer RNA Preparations Published by : American Association for the Advancement of Science Stable

Smehilová, M. *et al.,* 2009. Subcellular localization and biochemical comparison of cytosolic and secreted cytokinin dehydrogenase enzymes from maize. Journal of experimental botany, 60(9), pp.2701–12.

Snowden, K.C. *et al.,* 2005. The Decreased apical dominance1 / *Petunia hybrida* CAROTENOID CLEAVAGE DIOXYGENASE8 Gene Affects Branch Production and Plays a Role in Leaf Senescence , Root Growth , and Flower Development. , 17, pp.746–759.

Sorefan, K. *et al.,* 2003. MAX4 and RMS1 are orthologous dioxygenase-like genes that regulate shoot branching in *Arabidopsis* and pea. Genes & development, 17(12), pp.1469–74.

Spanswick, R.M. and Miller, A.G., 1977. Measurements of the Cytoplasmic pH in Nitella translucens. Plant Physiology, 59, pp.664–666.

Spíchal, L., 2012. Cytokinins - recent news and views of evolutionally old molecules. Functional Plant Biology, 39(4), p.267.

Spíchal, L. *et al.,* 2004. Two cytokinin receptors of *Arabidopsis thaliana*, CRE1/AHK4 and AHK3, differ in their ligand specificity in a bacterial assay. Plant & cell physiology, 45(9), pp.1299–305.

Spiess, L.D., 1975. Comparative Activity of Isomers of Zeatin and Ribosyl-Zeatin on Funaria hygrometrica. Plant physiology, 55(3), pp.583–5.

Stanga, J.P. *et al.,* 2013. SUPPRESSOR OF MORE AXILLARY GROWTH2 1 controls seed germination and seedling development in *Arabidopsis*. Plant physiology, 163(1), pp.318–30.

Stirnberg, P., Furner, I.J. & Ottoline Leyser, H.M., 2007. MAX2 participates in an SCF complex which acts locally at the node to suppress shoot branching. The Plant journal : for cell and molecular biology, 50(1), pp.80–94.

Stirnberg, P., van De Sande, K. & Leyser, H.M.O., 2002. MAX1 and MAX2 control shoot lateral branching in *Arabidopsis*. Development (Cambridge, England), 129(5), pp.1131–41.

Stolz, A. *et al.,* 2011. The specificity of cytokinin signalling in *Arabidopsis thaliana* is mediated by differing ligand affinities and expression profiles of the receptors. The Plant journal : for cell and molecular biology, 67(1), pp.157–68.

Sun, J. *et al.,* 2005. *Arabidopsis* SOI33/AtENT8 Gene Encodes a Putative Equilibrative Nucleoside Transporter That Is Involved in Cytokinin Transport In Planta. Journal of Integrative Plant Biology, 47(5), pp.588–603.

Suzuki, T. *et al.,* 2002. An *Arabidopsis* histidine-containing phosphotransfer (HPt) factor implicated in phosphorelay signal transduction: overexpression of AHP2 in plants results in hypersensitiveness to cytokinin. Plant & cell physiology, 43(1), pp.123–9.

Suzuki, T. *et al.,* 1998. Histidine-containing phosphotransfer (HPt) signal transducers implicated in His-to-Asp phosphorelay in *Arabidopsis*. Plant & cell physiology, 39(12), pp.1258–68.

Suzuki, T. *et al.,* 2001. The *Arabidopsis* sensor His-kinase, AHk4, can respond to cytokinins. Plant & cell physiology, 42(2), pp.107–13.

Svačinová, J. *et al.,* 2012. A new approach for cytokinin isolation from *Arabidopsis* tissues using miniaturized purification: pipette tip solid-phase extraction. Plant methods, 8(1), p.17.

Swarup, R. *et al.,* 2005. Root gravitropism requires lateral root cap and epidermal cells for transport and response to a mobile auxin signal. Nature cell biology, 7(11), pp.1057–65

Tajima, Y. *et al.,* 2004. Comparative studies on the type-B response regulators revealing their distinctive properties in the His-to-Asp phosphorelay signal transduction of *Arabidopsis thaliana*. Plant & cell physiology, 45(1), pp.28–39.

Takei, K., Yamaya, T. & Sakakibara, H., 2004.a. *Arabidopsis* CYP735A1 and CYP735A2 encode cytokinin hydroxylases that catalyze the biosynthesis of trans-Zeatin. The Journal of biological chemistry, 279(40), pp.41866–72.

Takei, K., Ueda, N., *et al.,* 2004.b. AtIPT3 is a key determinant of nitrate-dependent cytokinin biosynthesis in *Arabidopsis*. Plant & cell physiology, 45(8), pp.1053–62.

Takei, K. *et al.,* 2002. Multiple routes communicating nitrogen availability from roots to shoots: a signal transduction pathway mediated by cytokinin. Journal of experimental botany, 53(370), pp.971–7.

Takei, K. *et al.,* 2001.a. Nitrogen-Dependent Accumulation of Cytokinins in Root and the Translocation to Leaf : Implication of Cytokinin Species that Induces Gene Expression of Maize Response Regulator. Plant Cell Physiology, 42(1), pp.85–93.

Takei, K., Sakakibara, H. & Sugiyama, T., 2001.b. Identification of genes encoding adenylate isopentenyltransferase, a cytokinin biosynthesis enzyme, in *Arabidopsis thaliana*. The Journal of biological chemistry, 276(28), pp.26405–10.

Tanaka, M. *et al.,* 2006. Auxin controls local cytokinin biosynthesis in the nodal stem in apical dominance. The Plant journal : for cell and molecular biology, 45(6), pp.1028–36.

Tanaka, Y. *et al.,* 2004. Comparative Studies of the AHP Histidine-containing Phosphotransmitters Implicated in His-to-Asp Phosphorelay in *Arabidopsis thaliana*. , 68(2), pp.462–465.

Taylor, J.S. *et al.,* 1990. Cytokinins in the Phloem Sap of White Lupin. Plant physiology, 94, pp.1714–1720.

Tian, F. *et al.,* 2014. A highly selective biosensor with nanomolar sensitivity based on cytokinin dehydrogenase. PloS one, 9(3), p.e90877.

To, J.P.C. *et al.,* 2007. Cytokinin regulates type-A *Arabidopsis* Response Regulator activity and protein stability via two-component phosphorelay. The Plant cell, 19(12), pp.3901–14.

To, J.P.C. *et al.,* 2004. Type-A *Arabidopsis* Response Regulators Are Partially Redundant Negative Regulators of Cytokinin Signaling. , 16(March), pp.658–671.

Tucker, E.B., 1993. Azide treatment enhances cell-to-cell diffusion in staminal hairs of Setcreasea purpurea. , pp.45–49.

Turnbull, C.G.N. *et al.,* 1997. Rapid increases in cytokinin concentration in lateral buds of chickpea (Cicer arietinum L.) during release of apical dominance. Planta, 202(3), pp.271–276.

Ueguchi, C., Sato, S., *et al.,* 2001. The AHK4 gene involved in the cytokinin-signaling pathway as a direct receptor molecule in *Arabidopsis thaliana*. Plant & cell physiology, 42(7), pp.751–5.

Umehara, M. *et al.,* 2008. Inhibition of shoot branching by new terpenoid plant hormones. Nature, 455(7210), pp.195–200..

Vaseva-Gemisheva, I., Lee, D. & Karanov, E., 2005. Response of *Pisum sativum* Cytokinin Oxidase/Dehydrogenase Expression and Specific Activity to Drought Stress and Herbicide Treatments. Plant Growth Regulation, 46(3), pp.199–208.

Veach, Y.K. *et al.,* 2003. O -Glucosylation of cis-Zeatin in Maize . Characterization of Genes , Enzymes , and Endogenous Cytokinins 1. , 131(March), pp.1374–1380.

Vreman, H.J., Thomas, R. & Corse, J., 1978. Cytokinins in tRNA Obtained from Spinacia oleracea L . Leaves and Isolated Chloroplasts1. , 260(1978), pp.296–306.

Vyroubalová, S. *et al.,* 2009. Characterization of new maize genes putatively involved in cytokinin metabolism and their expression during osmotic stress in relation to cytokinin levels. Plant physiology, 151(1), pp.433–47.

Waadt, R. *et al.,* 2014. FRET-based reporters for the direct visualization of abscisic acid concentration changes and distribution in *Arabidopsis*. , pp.1–28.

Wada, H., Matthews, M. a & Shackel, K. a, 2009. Seasonal pattern of apoplastic solute accumulation and loss of cell turgor during ripening of Vitis vinifera fruit under field conditions. Journal of experimental botany, 60(6), pp.1773–81.

Wagner, B.M. & Beck, E., 1993. Cytokinins in the perennial herb Urtica dioica L . as influenced by its nitrogen status. , (Horgan 1992), pp.511–518.

Waldie, T., McCulloch, H. & Leyser, O., 2014. Strigolactones and the control of plant development: lessons from shoot branching. The Plant journal : for cell and molecular biology, 79(4), pp.607–22.

Wang, J. *et al.,* 2013. Glucosyltransferase UGT76C1 finely modulates cytokinin responses via cytokinin N-glucosylation in *Arabidopsis thaliana*. Plant physiology and biochemistry : PPB / Société française de physiologie végétale, 65, pp.9–16.

Wang, J. *et al.,* 2011. N-glucosyltransferase UGT76C2 is involved in cytokinin homeostasis and cytokinin response in *Arabidopsis thaliana*. Plant & cell physiology, 52(12), pp.2200–13.

Waters, M.T., Nelson, D.C., *et al.,* 2012.a. Specialisation within the DWARF14 protein family confers distinct responses to karrikins and strigolactones in *Arabidopsis*. Development (Cambridge, England), 139(7), pp.1285–95.

Waters, M.T., Brewer, P.B., *et al.,* 2012.b. The *Arabidopsis* ortholog of rice DWARF27 acts upstream of MAX1 in the control of plant development by strigolactones. Plant physiology, 159(3), pp.1073–85. A

Werner, T. *et al.,* 2003. Cytokinin-Deficient Transgenic *Arabidopsis* Plants Show Functions of Cytokinins in the Regulation of Shoot and Root Meristem Activity. The Plant Cell, 15, pp.2532–2550.

Werner, T. *et al.,* 2006. New insights into the biology of cytokinin degradation. Plant biology (Stuttgart, Germany), 8(3), pp.371–81.

Werner, T. *et al.,* 2001. Regulation of plant growth by cytokinin. Proceedings of the National Academy of Sciences of the United States of America, 98(18), pp.10487–92.

Werner, T. *et al.,* 2010. Root-specific reduction of cytokinin causes enhanced root growth, drought tolerance, and leaf mineral enrichment in *Arabidopsis* and tobacco. The Plant cell, 22(12), pp.3905–20.

Werner, T. & Schmülling, T., 2009. Cytokinin action in plant development. Current opinion in plant biology, 12(5), pp.527–38.

White, P.J., 2001. The pathways of calcium movement to the xylem. Journal of Experimental Botany, 52(358), pp.891–899.

White, P.J. & Broadley, M.R., 2003. Calcium in plants. Annals of botany, 92(4), pp.487–511

Witzel, K. *et al.,* 2011. Comparative evaluation of extraction methods for apoplastic proteins from maize leaves. Plant methods, 7(1), p.48.

Woo, H.R. *et al.,* 2001. ORE9 , an F-Box Protein That Regulates Leaf Senescence in *Arabidopsis*. , 13(August), pp.1779–1790.

Wormit, A. *et al.,* 2004. Characterization of three novel members of the *Arabidopsis thaliana* equilibrative nucleoside transporter (ENT) family. The Biochemical journal, 383(Pt 1), pp.19–26.

Wulfetange, K. *et al.,* 2011. The cytokinin receptors of *Arabidopsis* are located mainly to the endoplasmic reticulum. Plant physiology, 156(4), pp.1808–18.

Xie, X. *et al.,* 2013. Confirming stereochemical structures of strigolactones produced by rice and tobacco. Molecular plant, 6(1), pp.153–63.

Xie, X., Yoneyama, K. & Yoneyama, K., 2010. The Strigolactone Story. Annual review phytopathology, 48, pp.93–117.

Yamada, H. *et al.,* 2001. The *Arabidopsis* AHK4 histidine kinase is a cytokinin-binding receptor that transduces cytokinin signals across the membrane. Plant & cell physiology, 42(9), pp.1017–23.

Yan, H. *et al.,* 2007. Rice tillering dwarf mutant dwarf3 has increased leaf longevity during darkness-induced senescence or hydrogen peroxide-induced cell death. Genes & Genetic Systems, 82(4), pp.361–366.

Yang, Z.-B. *et al.,* 2012. Physiological and molecular analysis of the interaction between aluminium toxicity and drought stress in common bean (Phaseolus vulgaris). Journal of experimental botany, 63(8), pp.3109–25.

Yevdakova, N. a & von Schwartzenberg, K., 2007. Characterisation of a prokaryote-type tRNA-isopentenyltransferase gene from the moss Physcomitrella patens. Planta, 226(3), pp.683–95.

Yokoyama, A. *et al.,* 2007. Type-B ARR transcription factors, ARR10 and ARR12, are implicated in cytokinin-mediated regulation of protoxylem differentiation in roots of *Arabidopsis thaliana*. Plant & cell physiology, 48(1), pp.84–96.

Yonekura-Sakakibara, K. *et al.,* 2004. Molecular Characterization of Cytokinin-Responsive Histidine Kinases in Maize . Differential Ligand Preferences and Response to cis-Zeatin 1. Plant physiology, 134(April), pp.1654–1661.

Yoneyama, K. *et al.,* 2009. Strigolactones: structures and biological activities. Pest management science, 65(5), pp.467–70.

Young, N.F. *et al.,* 2014. Conditional Auxin Response and Differential Cytokinin Profiles in Shoot Branching Mutants. Plant physiology, 165(4), pp.1723–1736.

Yu, Q. *et al.,* 1999. Extraction of apoplastic sap from plant roots by centrifugation. New Phytol., 143, pp.299–304.

Zalabák, D. *et al.,* 2011. Genetic engineering of cytokinin metabolism: Prospective way to improve agricultural traits of crop plants. Biotechnology advances.

Zalewski, W. *et al.,* 2010. Silencing of the HvCKX1 gene decreases the cytokinin oxidase/dehydrogenase level in barley and leads to higher plant productivity. Journal of experimental botany, 61(6), pp.1839–51.

Zatloukal, M. *et al.,* 2008. Novel potent inhibitors of A. thaliana cytokinin oxidase/dehydrogenase. Bioorganic & medicinal chemistry, 16(20), pp.9268–75.

Zazímalová, E. *et al.,* 2010. Auxin transporters--why so many? Cold Spring Harbor perspectives in biology, 2(3), p.a001552.

Zhang, H. *et al.,* 2001. Novel cytokinins: The predominant forms in mature buds of Pinus radiata. Physiologia plantarum, 112(1), pp.127–134.

Zhang, K. *et al.,* 2014.a. *Arabidopsis* ABCG14 protein controls the acropetal translocation of root-synthesized cytokinins. Nature communications, 5, p.3274.

Zhang, Y. *et al.,* 2014.b. Rice cytochrome P450 MAX1 homologs catalyze distinct steps in strigolactone biosynthesis. Nature chemical biology, 10, 1028–1033

Zhang, X. *et al.,* 2013. Adenine phosphoribosyl transferase 1 is a key enzyme catalyzing cytokinin conversion from nucleobases to nucleotides in *Arabidopsis*. Molecular plant, 6(5), pp.1661–72.

Zhao, J. *et al.,* 2014. DWARF3 participates in an SCF complex and associates with DWARF14 to suppress rice shoot branching. Plant & cell physiology, 55(6), pp.1096–109.

Zhao, L.-H. *et al.,* 2013. Crystal structures of two phytohormone signal-transducing α/β hydrolases: karrikin-signaling KAI2 and strigolactone-signaling DWARF14. Cell research, 23(3), pp.436–9.

Zhong, R. & Ye, Z., 2001. Alteration of Auxin Polar Transport in the *Arabidopsis* ifl1 Mutants 1. , 126(June), pp.549–563.

Zhou, F. *et al.,* 2013. D14-SCF(D3)-dependent degradation of D53 regulates strigolactone signalling. Nature, 504(7480), pp.406–10.

Zou, J. *et al.,* 2006. The rice HIGH-TILLERING DWARF1 encoding an ortholog of *Arabidopsis* MAX3 is required for negative regulation of the outgrowth of axillary buds. The Plant journal : for cell and molecular biology, 48(5), pp.687–98.

Zürcher, E. *et al.,* 2013. A robust and sensitive synthetic sensor to monitor the transcriptional output of the cytokinin signaling network in planta. Plant physiology, 161(March), pp.1066–1075.

Zwanenburg, B. & Pospísil, T., 2013. Structure and activity of strigolactones: new plant hormones with a rich future. Molecular plant, 6(1), pp.38–62.

Appendix

Supplementary Figure 1 Cytokinin Distribution in *GFP*-expressing Cells of Four *Arabidopsis* Lines. (non-normalized data presented as the CK concentration in fmol/100,000 protoplasts). Figure was drawn by Ondřej Novák.

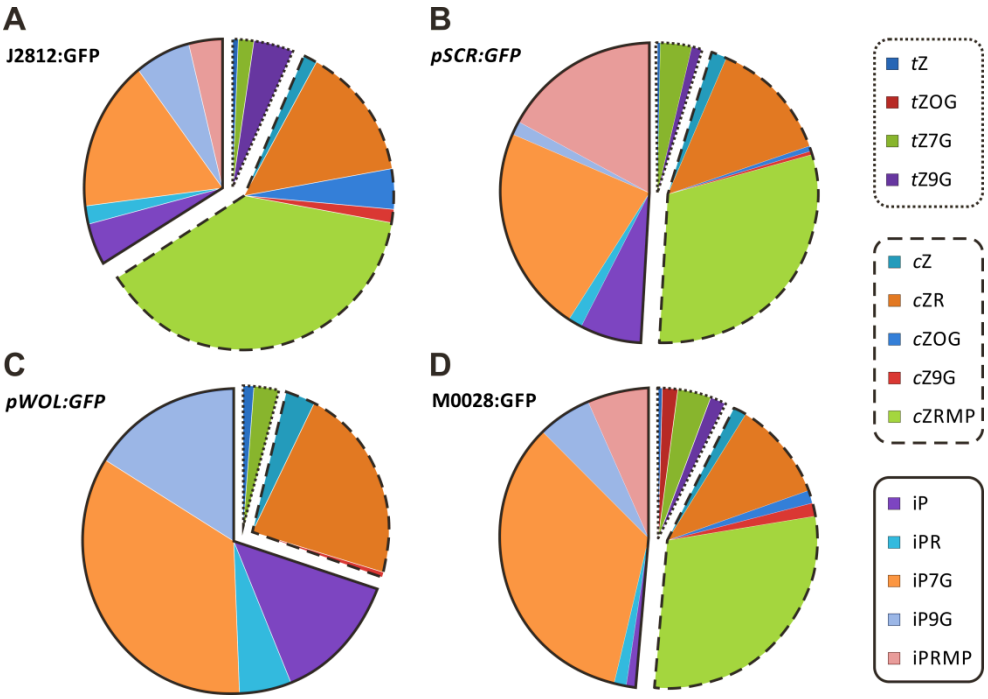

Supplementary Figure 2 Cytokinin Distribution in *GFP* non-expressing Cells of Four *Arabidopsis* lines. (non-normalized data presented as the CK concentration in fmol/100,000 protoplasts). Figure was drawn by Ondřej Novák.

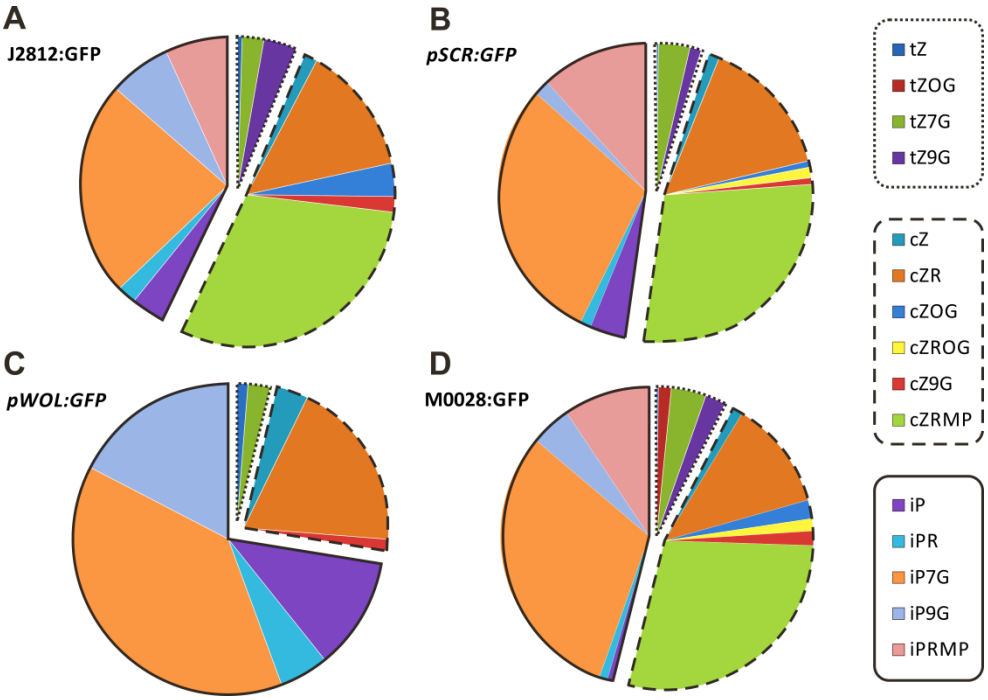

Supplementary Figure 3 Cytokinin Metabolite Levels in Four Different Cell Types Isolated from the *Arabidopsis* Root. The individual cytokinin metabolites detected in the sorted cell lines are presented. The arrows indicate the cytokinin metabolism. The metabolites were quantified in fmol/100,000 protoplasts and the respective ratios were computed in each of the sorted transgenic lines J2812:*GFP* (green), *pWOL:GFP* (red), *pSCR:GFP* (blue) and M0028:*GFP* (yellow). Error bars indicate standard error. The results occurred form 6 biological replicates and for each 2 technical replicates were performed. Figure was drawn by Ondřej Novák.

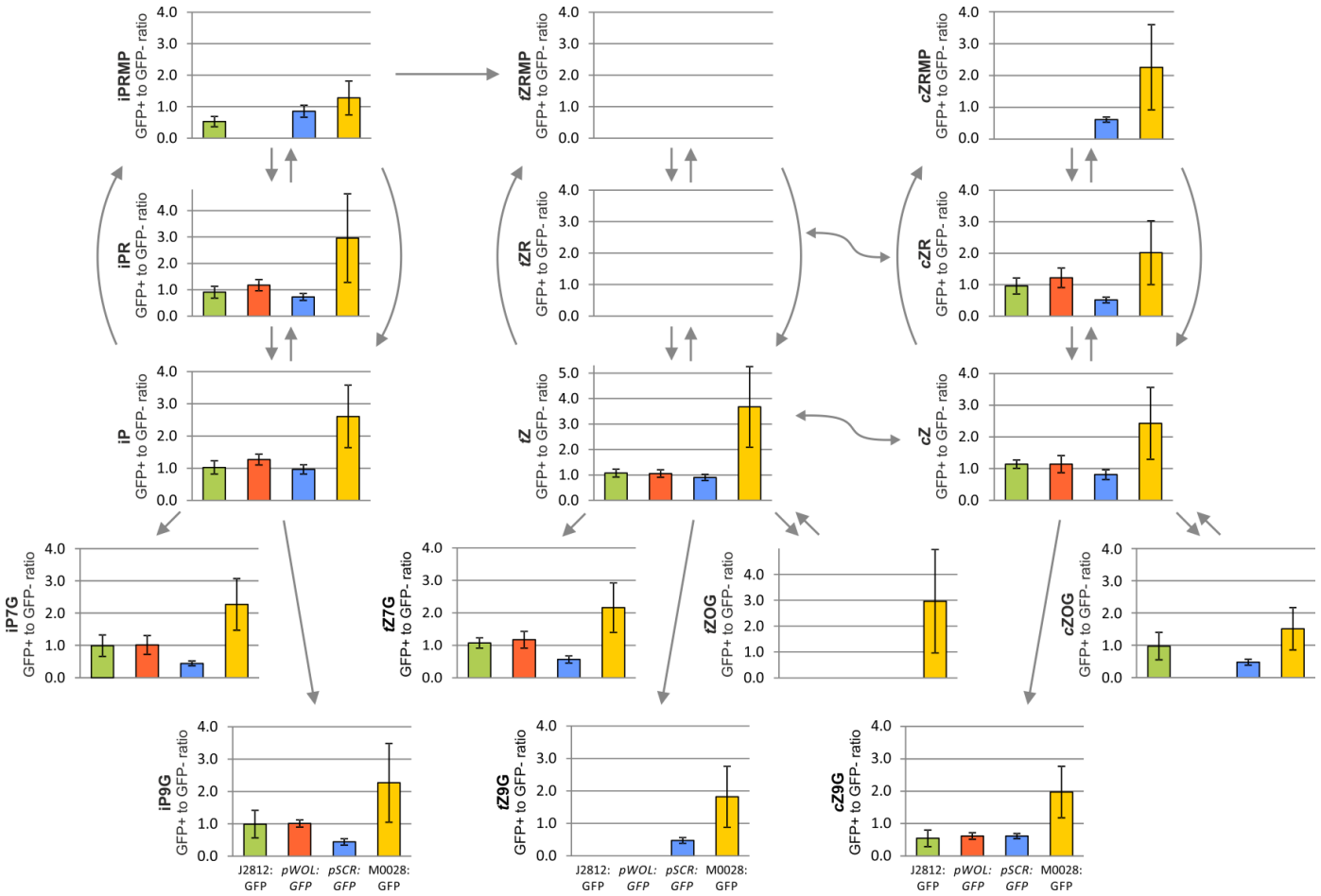

Supplementary Table 1 MS optimized conditions. The precursor and product ions of the studied compounds and optimized collision energies (Fragmentor) are listed. The retention time stability and limits of detection (LOD) are shown for UHPLC-ESI(+)-MS/MS analysis of isoprenoid cytokinins. Conditions in positive ion mode were as follows: drying gas temperature, 200 °C; drying gas flow, 16 l min^{-1}; nebulizer pressure, 35 psi; sheath gas temperature, 375 °C, sheath gas flow, 12 l min^{-1}; capillary, 3400 V; noozle voltage, 0 V; delta iFunnel high/low pressure RF, 150/60 V. Table was constructed by Ondřej Novák.

Compound	MRM	Fragmentor (V)	Collision Energy (V)	Retention time[a] (min)	LOD[b] (fmol)
*t/c*Z	220.1 > 136.1	380	19	12.77 ± 0.03 / 14.65 ± 0.03	0.1
*t/c*ZR	352.2 > 220.1	380	20	17.69 ± 0.04 / 18.74 ± 0.03	0.1
*t*Z7G	382.2 > 220.1	380	21	8.90 ± 0.01	0.1
t/cZ9G	382.2 > 220.1	380	21	10.93 ± 0.04 / 12.09 ± 0.03	0.5 / 0.1
*t/c*ZOG	382.2 > 220.1	380	21 / 18	11.50 ± 0.01 / 12.88 ± 0.01	0.1
*t/c*ZROG	514.2 > 220.1	380	21	16.09 ± 0.01 / 17.22 ± 0.01	1.0
*t/c*ZRMP	432.2 > 382.2	380	21	10.23 ± 0.02 / 14.67 ± 0.02	1.0 / 5.0
DHZ	222.1 > 136.1	380	23	13.74 ± 0.04	0.1
DHZR	354.2 > 222.1	380	22	18.58 ± 0.01	0.01
DHZ7G	384.2 > 222.1	380	23	10.27 ± 0.01 / 10.79 ± 0.01	0.1
DHZ9G	384.2 > 222.1	380	23	11.90 ± 0.04	0.1
DHZOG	384.2 > 222.1	380	21	13.73 ± 0.03	0.1
DHZROG	516.2 > 222.1	380	22	17.94 ± 0.02	1.0
DHZRMP	434.2 > 384.2	380	23	10.92 ± 0.02	1.0
iP	204.1 > 136.1	380	16	23.79 ± 0.02	0.01
iPR	336.2 > 204.1	380	20	24.49 ± 0.02	0.05
iP7G	366.2 > 204.1	380	21	17.33 ± 0.01	0.1
iP9G	366.2 > 204.1	380	22	21.85 ± 0.02	0.1
iPRMP	416.2 > 204.1	380	22	20.66 ± 0.01	1.0

[a] Values are means ± SD (n = 10). [b] Limit of detection, defined as a signal-to-noise ratio of 3:1.

Supplementary Figure 4 Sum of cytokinin compounds concentration (pmol/100.000 protoplasts) in *TCSn:GFP*+ cells.

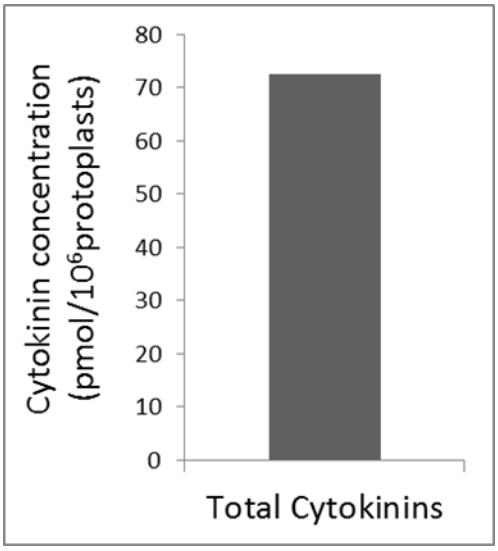

Supplementary Figure 5 Cytokinin concentration (pmol/100.000 protoplasts) in all the sorted cells of *TCSn:GFP* (Sum of *GFP*+ and *GFP*- cells). The cytokinin glucoside forms are the most abundant forms with IP7G and tZ7G predominating. Interestingly cZR was also found to be a prevalent cytokinin form in the root cells even though it was also abundantly found in the apoplast. However cZR was also significantly enriched in the *TCSn:GFP*+ cells.

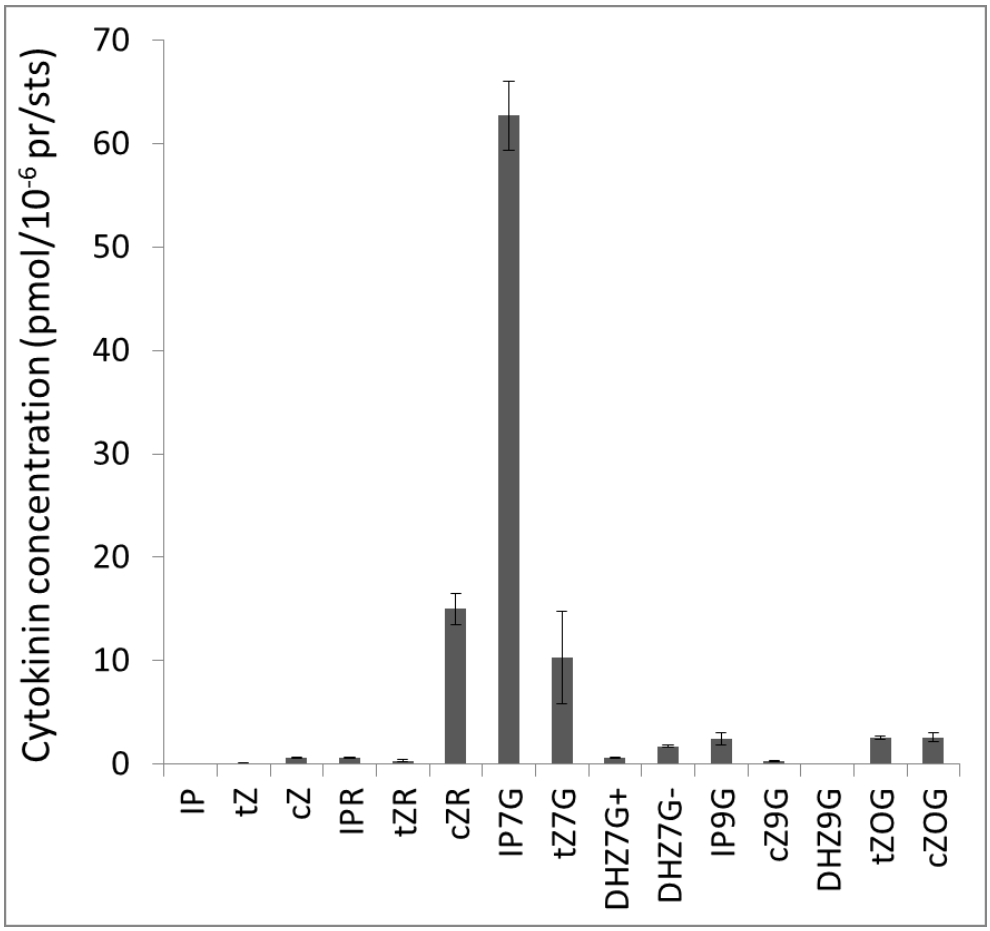

Supplementary Figure 6 Selection process of *GFP*- and *GFP*+ protoplasts from *TCSn:GFP* root tips in FACS. a. Graph of forward (FSC) and side scatter (SSC) representing the sample loaded in the FACS. b. Graph of forward (FSC) and side scatter (SSC) and indication of the cell population initially selected for cell sorting (P1). c. Graph of autofluorescence and green fluorescence indicating further selection of cell populations: P3 population in blue represents the *GFP*+ cells and P2 population in green represents the *GFP*- cells. d. Graph showing the different populations during collection in separate eppendorf tubes.

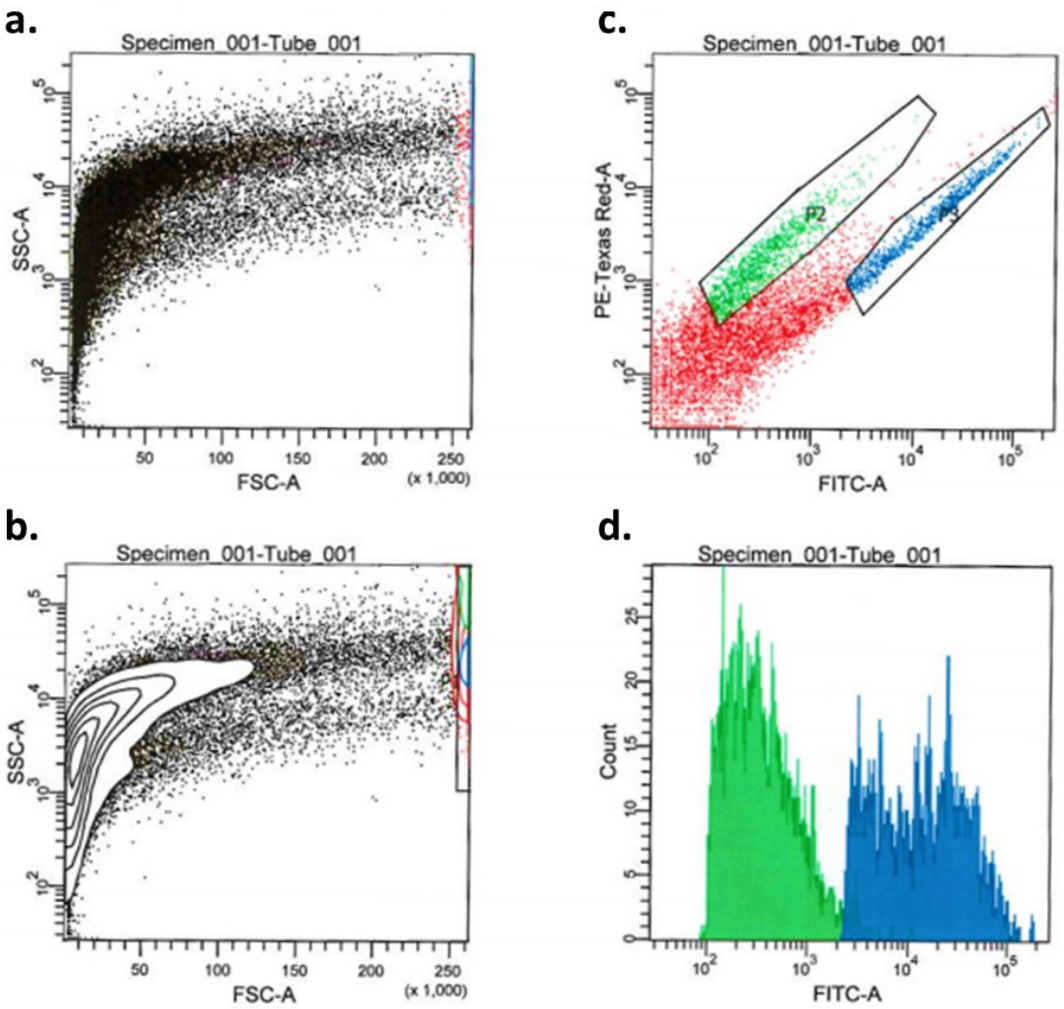

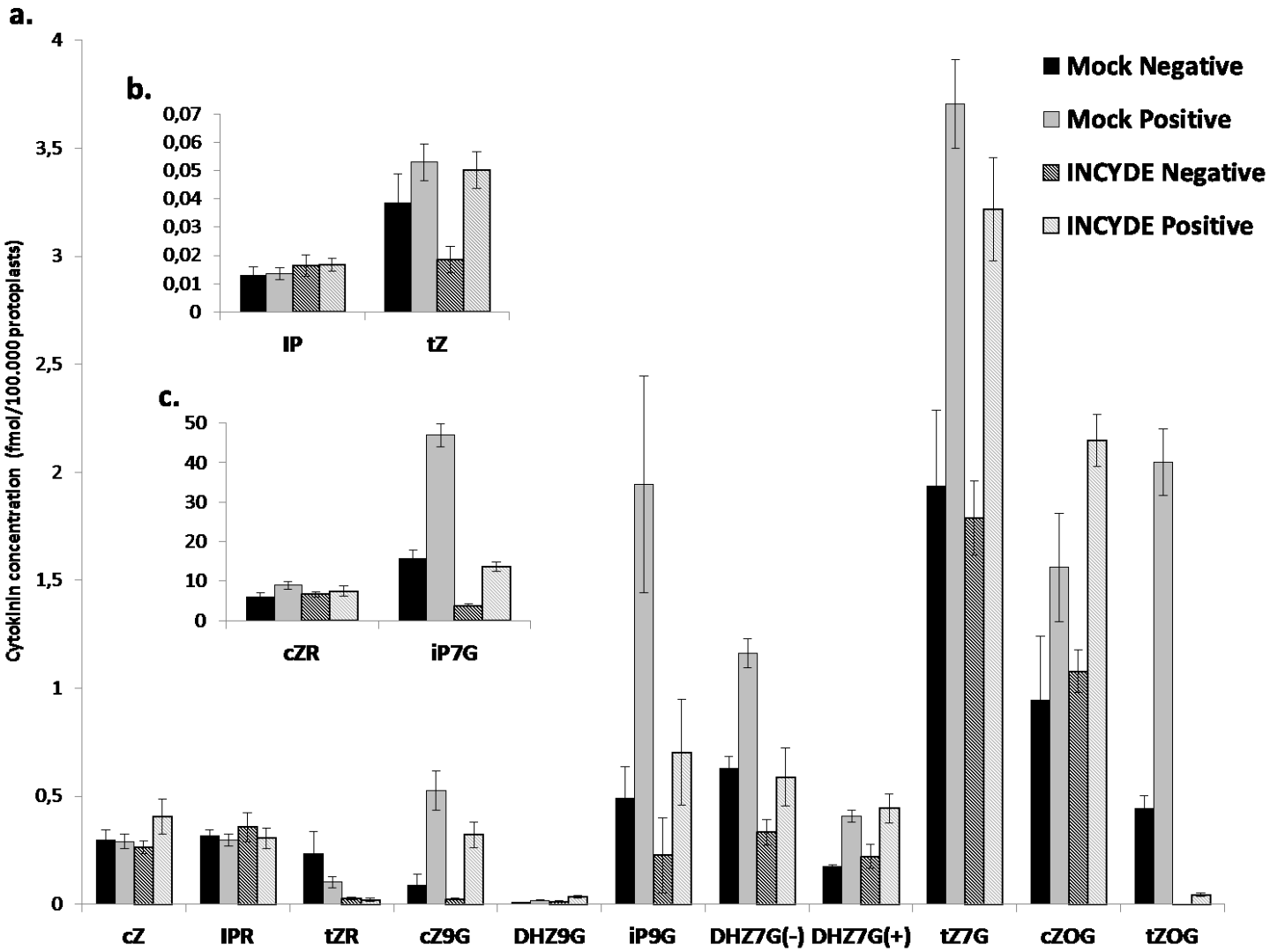

Supplementary Figure 7 Cytokinin concentration (fmol/100.000 protoplasts) in *GFP*+ and *GFP*- cells of *TCSn:GFP* primary roots treated with 20 µM INCYDE or untreated (Mock). Cytokinin compounds are presented in charts **a., b.** and **c.** according to their concentration levels. For each experiment 6-9 biological replicates were performed and 2 technical replicates per sample. The error bars indicate standard error (n=9 for mock and n= for treated samples).

Supplementary Figure 8 Cytokinin response in apoplastic fluid extracted under different centrifuge forces and duration of centrifugation.

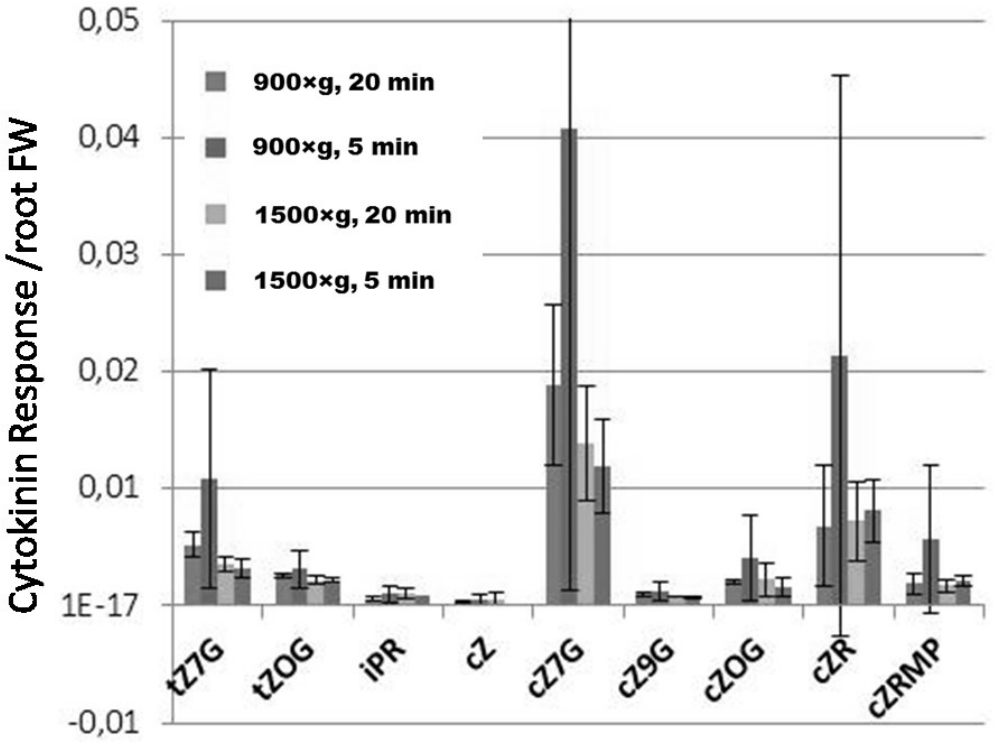

Supplementary Figure 9 Cytokinin concentration (fmol/plant – Log10 scale) in apoplastic and symplastic fluid extracted from the same *Arabidopsis* roots.

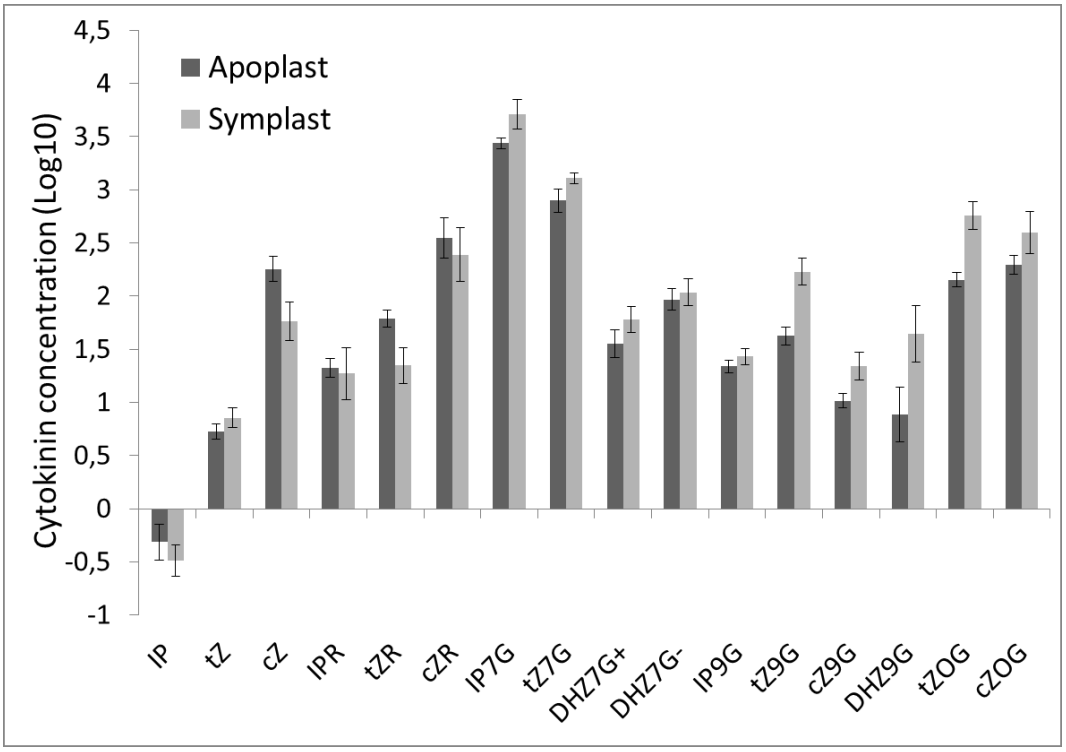

Supplementary Table 2 Cytokinin concentration (fmol/plant) in apoplastic and symplastic fluid extracted from the same *Arabidopsis* roots.

	IP	tZ	cZ	IPR	tZR	cZR	IP7G	tZ7G
Apoplastic Fluid 1	0,251433	4,072186	106,0196	24,7814	77,52171	564,9617	2725,805	956,3819
Apoplastic Fluid 2	0,468674	7,100679	261,2316	27,09332	70,5168	514,4233	3351,708	1069,746
Apoplastic Fluid 3	0,971039	5,203726	209,8973	14,14144	42,34923	146,3025	2242,953	479,8169
Symplastic Fluid 1	0,506886	9,514822	103,8129	34,06933	37,93147	441,7245	8200,184	1548,554
Symplastic Fluid 2	0,397043	8,194957	71,32072	31,26353	27,56899	431,1362	5810,549	1324,419
Symplastic Fluid 3	0,16988	4,694127	26,15993	6,079069	10,43625	77,54437	2785,504	1022,27
Total Fluid 1	0,559359	10,9682	311,681	82,82827	115,7105	944,9431	11356,17	1729,294
Total Fluid 2	0,525568	11,7402	302,0355	79,05788	125,7261	962,0047	12553,17	2398,617
Total Fluid 3	0,631495	7,1269	200,607	35,81274	60,17404	368,4922	8855,074	2319,919

	DHZ7G+	DHZ7G-	IP9G	tZ9G	cZ9G	DHZ9G	tZOG	cZOG
Apoplastic Fluid 1	42,68685	104,1922	26,53383	46,93334	12,04478	14,10322	155,0434	224,2378
Apoplastic Fluid 2	53,20663	127,9091	23,41388	55,3524	12,28231	13,84578	175,8935	254,4182
Apoplastic Fluid 3	19,5027	59,30898	16,83998	28,94599	7,486001	2,364206	105,3894	132,8687
Symplastic Fluid 1	84,25473	153,1869	35,49496	261,5107	34,21798	88,90381	898,8396	768,7439
Symplastic Fluid 2	74,17371	138,381	19,64133	188,3539	24,73532	72,82501	641,229	476,8589
Symplastic Fluid 3	34,42589	60,36988	27,91307	97,99915	12,54445	13,14498	322,7227	165,9593
Total Fluid 1	94,77458	218,8281	85,83101	441,9367	51,31384	124,542	1534,376	1273,451
Total Fluid 2	114,1658	293,1264	94,34477	449,1094	60,7364	90,64858	1470,88	1314,218
Total Fluid 3	70,55955	148,3086	58,93998	280,6135	47,2914	14,72514	706,2661	863,0921

Supplementary Figure 10 Cytokinin quantification in Parvus (wild-ype), rms1 and rms2 **a.** shoot, **b.** first node and internode (1st NI) and **c.** epicotyl. Each sample derived from a pool of at least 3 plants. Cytokinin concentration was calculated in pmol and normalized to the fresh weight (FW) of the plant tissue. The data were further normalized to Parvus cytokinin concentration in each tissue. The error bars represent standard error (n = 3). Statistical analysis was performed using Student's t-test comparing cytokinin concentration between each rms mutant and Parvus.

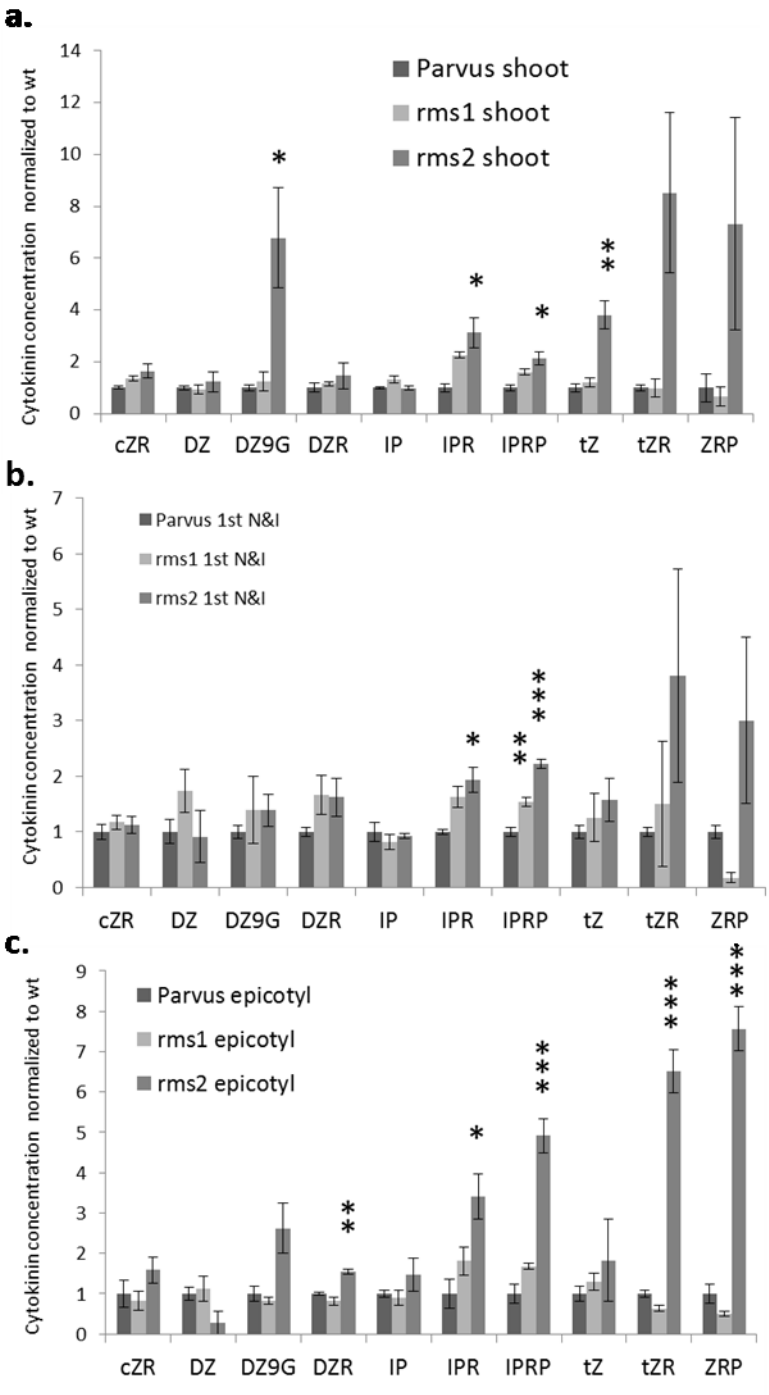

Supplementary Figure 11 Cytokinin quantification in Parvus (wild-ype), rms1 and rms2 **a.** hypocotyl and **b.** root. Each sample derived from a pool of at least 3 plants. Cytokinin concentration was calculated in pmol and normalized to the fresh weight (FW) of the plant tissue. The data were further normalized to Parvus cytokinin concentration in each tissue. The error bars represent standard error (n = 3). Statistical analysis was performed using Student's t-test comparing cytokinin concentration between each rms mutant and Parvus.

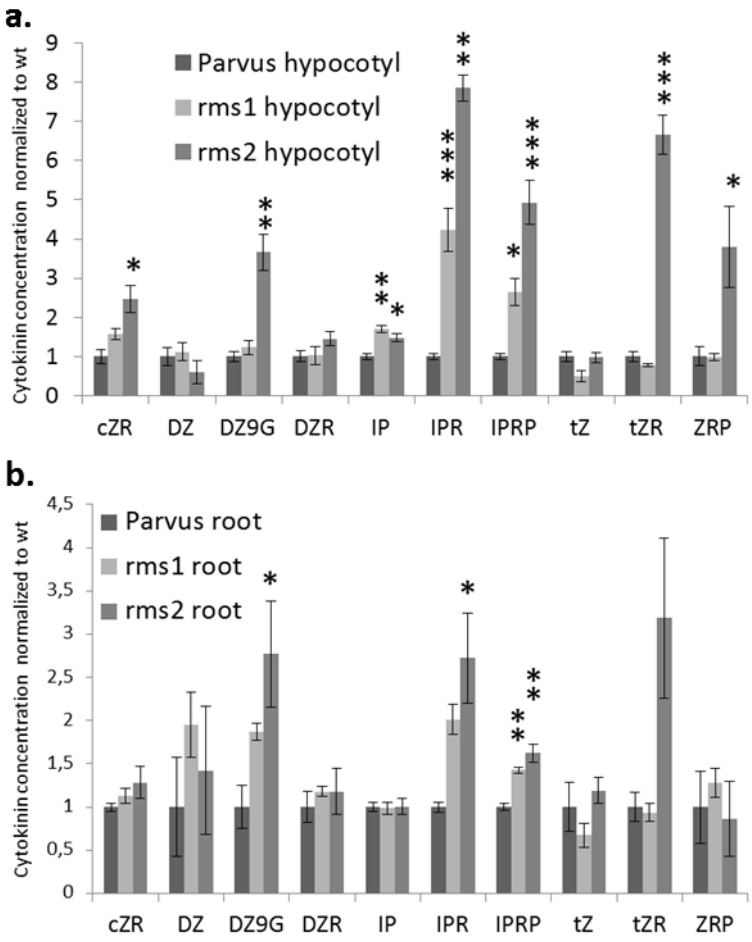

Supplementary Figure 12 Cytokinin quantification in root parts of 7 days old Parvus, rms1 and rms2 seedlings. The 0 mm represents the root cap of the primary root. **a.** DZR and **b.** cZR concentrations are presented. Each sample derived from a pool of 30-50 plants. Cytokinin concentration was calculated in pmol and normalized to the fresh weight (FW) of the plant tissue. The error bars represent standard error (n = 3). The stars indicate statisticallly significant differences of cytokinin concentration between each rms mutant and Parvus by Student's t-test.